UNIVERSIDADE DE LISBOA

INSTITUTO SUPERIOR TÉCNICO

Design of Spectral- and Cost-Efficient High-Capacity Optical Transport Networks

Daniela Aguiar Moniz

Supervisor: Doctor João José de Oliveira Pires

Co-Supervisor: Doctor João Manuel Ferreira Pedro

Thesis approved in public session to obtain the PhD Degree in

Electrical and Computer Engineering

Jury final classification: Pass with Distinction

2022

UNIVERSIDADE DE LISBOA

INSTITUTO SUPERIOR TÉCNICO

Design of Spectral- and Cost-Efficient High-Capacity Optical Transport Networks

Daniela Aguiar Moniz

Supervisor: Doctor João José de Oliveira Pires

Co-Supervisor: Doctor João Manuel Ferreira Pedro

Thesis approved in public session to obtain the PhD Degree in

Electrical and Computer Engineering

Jury final classification: Pass with Distinction

Jury

Chairperson: **Doctor Mário Alexandre Teles de Figueiredo, Instituto Superior Técnico, Universidade de Lisboa**

Members of the Committee:

Doctor Adolfo da Visitação Tregeira Cartaxo, Escola de Tecnologias e Arquitetura, ISCTE-Instituto Universitário de Lisboa

Doctor Paulo Sérgio de Brito André, Instituto Superior Técnico, Universidade de Lisboa

Doctor João Luís da Costa Campos Gonçalves Sobrinho, Instituto Superior Técnico, Universidade de Lisboa

Doctor Amaro Fernandes de Sousa, Universidade de Aveiro

Doctor João José de Oliveira Pires, Instituto Superior Técnico, Universidade de Lisboa

Doctor Fernando Henrique Corte-Real Mira da Silva, Instituto Superior Técnico, Universidade de Lisboa

2022

Acknowledgments

This section is not enough to express my gratitude to all who, throughout my PhD, have helped me, directly or indirectly, to achieve my goals and to accomplish one more step in this long academic career. This way, I hope that these few words could express my profound gratitude.

My deep gratitude goes to Professor João Pires, who expertly guided me throughout this long journey from the supervision of my master to the PhD Thesis. His fruitful counsel and guidance were key to finalizing this work successfully in due time.

To my co-supervisor, Doctor João Pedro, I thank for giving me the opportunity to start this PhD within a collaboration between the academic and industry environments and for providing all the tools and expertise to pursue new ideas and concepts throughout this work. His persistence and mindset always showed the way to explore challenging and innovative subjects.

I would also like to thank Coriant (now Infinera) and Instituto de Telecomunicações for giving me the opportunity to pursue this PhD, providing all the conditions and tools to successfully finalize this journey.

My appreciation also extends to my colleagues in Infinera for receiving me as part of their team, providing the positive atmosphere to develop this work.

Importantly, I would like to thank my friends for showing their support and guidance throughout this time and providing me with such great moments that makes every challenge easier.

Most of all, a big recognition goes to my family for always giving the most important advice and encouragement to fulfil my dreams. Their commitment and resilience set the example on how an excellent human being and professional should be.

Finally, a special appreciation to Gonçalo Nazaré for providing me unfailing support, care and patience and for always pushing me further than I would go on my own with his positive mindset.

Resumo

O expectável crescimento exponencial de tráfego proveniente de diferentes tipos de aplicações e tecnologias define esta década como uma das mais desafiantes para os operadores de redes de transporte óticas, que devem conseguir corresponder a este requisito de tráfego sem um aumento proporcional no seu investimento. Portanto, é essencial para os mesmos procurar diversas estratégias para operar sua infraestrutura perto do ponto ótimo em termos de custo e eficiência. Esta constante procura pelo ponto ótimo de operação de rede leva ao desenvolvimento de novas tecnologias e arquiteturas de rede, tendo como objetivo principal a redução do custo por bit transmitido. Sendo um tópico emergente, a otimização de redes óticas no contexto de planeamento com elevada capacidade foca essencialmente no escalar de uma rede de transporte ótico de modo a transportar mais dados, enquanto simultaneamente se reduz os custos associados.

Nesse sentido, esta tese apresenta múltiplas estratégias de planeamento e algoritmos de otimização para dimensionar uma rede de transporte ótico, a fim de enfrentar os desafios de alta capacidade que estas redes enfrentam atualmente. Os algoritmos de otimização desenvolvidos são responsáveis por obter soluções de encaminhamento, agregação e alocação espectral de modo a transportar todo o tráfego necessário numa arquitetura de transporte ótica pré-definida, tendo em conta os diferentes objetivos de otimização. Estas soluções são obtidas através de desenvolvimento de modelos de programação linear inteira e/ou algoritmos heurísticos dependendo do contexto em estudo.

Inicialmente, é apresentada uma análise multi-objetivo das redes de transporte ótico centrada no dimensionamento dos nós da rede com o objetivo de minimizar tanto os custos de transmissão como os custos de comutação de rede em cenários com arquiteturas de comutação flexíveis. Neste contexto, a otimização destas arquiteturas flexíveis é fundamental para interligar eficazmente o tráfego de clientes e os canais óticos, permitindo reduzir o custo global da rede e transportar mais capacidade.

Outros algoritmos baseados em formulações de programação linear inteira são também apresentados de forma a explorar a próxima geração de interfaces de linha que suportam formatos de modulação e taxas de símbolo de ordens superiores, possibilitadas pelos recentes avanços na eletrónica de alta velocidade e no processamento digital de sinal. Os algoritmos propostos incluem também uma nova estratégia baseada nas capacidades de comutação OTN, de modo a gerir os recursos do espectro desde o início de operação da rede com o objetivo de reduzir os problemas de fragmentação de espectro que surgem com a adoção de uma grelha *Dense Wavelength Division Multiplexing* (DWDM) flexível, que é necessária para suportar a próxima geração de interfaces de linha. A análise tecno-económica desenvolvida no âmbito deste estudo indica que o algoritmo proposto permite alcançar eficiências espectrais mais elevadas e ao mesmo tempo maximizar o tráfego transportado para todos os cenários analisados sem aumentar o custo global da rede.

Além disso, os algoritmos são também adaptados para suportar os requisitos de sobrevivência associados quer à proteção de fibras quer a interfaces óticas de linha, uma vez que uma única falha

poderá causar um impacto considerável na operação de uma rede de transporte ótico, afetando o valor requerido pelo acordo de nível de serviço.

O conjunto de algoritmos de otimização propostos nesta tese estendem-se também aos sistemas multi-banda e multi-fibra que têm de inevitavelmente ser adotados num futuro próximo para fazer face ao elevado aumento de capacidade que estas redes de transporte ótico enfrentam atualmente. Os resultados evidenciam a eficácia da adoção do sistema de transmissão multi-banda C+L em termos do adiamento de instalação de fibra adicional e do aumento de tráfego transportado para a mesma infraestrutura de fibra ótica, em consequência de apenas um pequeno aumento do número de canais óticos utilizados. Além disso, este estudo destaca também o maior número de dimensões de otimização a serem consideradas nestes cenários que requerem o desenvolvimento de algoritmos de encaminhamento e atribuição de recursos mais complexos.

Finalmente, esta tese conclui com um cenário disruptivo baseado nos recentes desenvolvimentos das redes óticas autónomas que permitem a redução das margens dos canais óticos com foco no aumento da capacidade global transportada. Neste contexto, são propostos dois algoritmos de otimização que exploram o provisionamento de margens reduzidas nas redes de transporte ótico com o objetivo de reduzir o seu custo e, ao mesmo tempo, atenuar o risco de perturbação do tráfego devido ao funcionamento demasiado próximo do limite de desempenho ótico.

Palavras-chave:

Comutador Ótico, Interfaces de linha, Otimização multi-objetivo, Planeamento com margens reduzidas, Planeamento multi-banda, Planeamento multi-período, Planeamento multi-fibra, Programação Linear Inteira, Redes de transporte, Redes resilientes

Abstract

The expected exponential growth of traffic from different applications and technologies sets this decade as one of the most challenging ones for optical transport network (OTN) operators, which have to meet this traffic requirement without a proportional increase in revenue. Therefore, network operators must relentlessly pursue ways to operate their infrastructure close to optimality in terms of cost and efficiency. This constant search for optimality drives the industry to develop new technologies and network architectures, having as the key objective the reduction of the cost per bit transmitted. Being an emergent topic, the network optimization in the context of high-capacity planning focuses on how the OTN can scale to transport more data while simultaneously reducing the overall network capital expenditures.

Therefore, the aim of this Thesis is to present multiple planning strategies and optimization algorithms to dimension an optical transport network, addressing the high-capacity challenges that these networks are facing nowadays. The developed optimization frameworks are responsible for providing a routing, grooming and resource allocation solution to transport all the traffic in the predefined optical transport architecture according to the different goals of optimization, which are defined through Integer Linear Programming (ILP) models and/or heuristic algorithms depending on the addressed context.

Initially, a multi-objective analysis of the optical transport networks is presented focusing on the dimensioning of the network nodes with the aim of minimizing both transmission and switching costs of the network in scenarios with flexible switching architectures. In this context, the optimization of these flexible node architectures is key to effectively interconnect the traffic signals and optical channels, allowing to reduce the overall network cost and transport more capacity.

Further algorithms based on ILP formulations are presented to exploit the next-generation of line interfaces, that support higher order modulation formats and symbol rates, enabled by the recent advancements in high-speed electronics and digital signal processing. The proposed algorithms also include a novel strategy based on OTN switching capabilities to manage the spectrum resources from the beginning of network operation in order to cope with the fragmentation problems arising as a result of adopting a flexible Dense Wavelength Division Multiplexing (DWDM) grid, which is required to support the next-generation of line interfaces. The techno-economic analysis presented in this study indicates that the proposed framework enables to reach higher spectral efficiencies and at the same time maximize the carried traffic load for all the analysed scenarios without increasing the overall network cost.

Moreover, the algorithms are extended to support survivability requirements regarding the reliability of fibre links and optical line interfaces, since a single failure can cause a substantial impact in the network operation, affecting the required service level agreement (SLA).

The suite of optimization algorithms proposed in this Thesis also extends to multi-band and multi-fibre systems that have to be inevitably deployed in near future to address the high increase of capacity

faced by optical transport networks today. The simulation results highlight the effectiveness of adopting the C+L-band transmission system in terms of postponing additional fibre deployment and increasing the carried traffic load for the same optical fibre infrastructure with minor augment on the number of optical channels. Moreover, this study also highlights the larger number of optimization dimensions that should be considered in these scenarios, requiring the development of more complex routing and resource assignment algorithms.

Finally, this Thesis concludes with a disruptive scenario based on the recent developments in autonomous optical networks that enable the reduction of optical channels' margins to increase the overall capacity transported. In this context, two different service-provisioning algorithms are proposed to exploit reduced-margin provisioning in optical transport networks with the aim of operating them more cost-effectively and at the same time mitigating the risk of traffic disruption due to operating too close to the performance limit.

Keywords:

Integer Linear Programming, Line Interfaces, Low-Margin Planning, Multi-band Planning, Multi-Fibre Planning, Multi-Objective Optimization, Multi-Period Planning, OTN switch, Survivability, Transport Networks.

Table of Contents

ACKNOWLEDGMENTS ..... **III**

RESUMO ..... **V**

ABSTRACT ..... **VII**

TABLE OF CONTENTS ..... **IX**

LIST OF FIGURES ..... **XII**

LIST OF TABLES ..... **XVI**

LIST OF ACRONYMS ..... **XVII**

LIST OF SYMBOLS ..... **XXII**

CHAPTER 1: INTRODUCTION **1**

1.1 Evolution of Optical Transport Networks 2
1.2 Motivation 5
1.3 Objectives and Thesis Outline 8
1.4 Main Contributions 10

CHAPTER 2: NETWORKING ASPECTS FOR DESIGNING THE NEXT-GENERATION OF OPTICAL TRANSPORT NETWORKS **12**

2.1 Optical Transport Network Concepts 13
2.1.1 Transport Architecture of OTN over DWDM *16*
2.1.2 Optical Impairments and Performance Evaluation *17*
2.1.2.1 Optical Impairments 17
2.1.2.2 System Design 18
A. Evolution Line Interfaces Technology with Coherent Detection 19
2.1.2.3 Optical Performance Evaluation 21
2.1.3 Network Planning and Traffic Modelling *23*
2.1.3.1 Optimization Algorithms for Planning an OTN 23
2.1.3.2 Survivability Design 27
2.1.3.3 Node Architectures 29
2.2 Future Trends of OTN 34
2.3 Chapter Summary 37

CHAPTER 3: NODES DIMENSIONING **38**

3.1 Transmission/Switching CAPEX Trade-off 40
3.2 Multi-objective Genetic Algorithm 42
3.2.1 Genetic Encoding *43*
3.2.2 Population Initialization *44*
3.2.3 Fitness Evaluation *45*

3.2.4 Selection of Surviving Solutions *46*
3.2.5 Crossover *47*
3.2.6 Mutation *48*
3.2.7 Evaluation Engine *50*
3.3 Simulation Results 51
3.3.1 MOGAs Comparison *53*
3.3.2 Complexity of the MOGAs *55*
3.3.3 Performance of the IF-Aware Genetic Algorithm *57*
3.4 Chapter Summary 59

CHAPTER 4: NETWORK PLANNING WITH NEXT-GENERATION OF LINE INTERFACES 61

4.1 Networking Aspects of Using Higher-Symbol Rate Line Interfaces 63
4.2 Spectrum Grid Configurations 64
4.3 Multi-Period Planning Workflow 66
4.3.1 Planning Workflow *67*
4.3.2 ILP Models and Heuristic Algorithm *70*
4.4 Impact of Adopting Next-Generation of Line Interfaces 77
4.4.1 Spectral Consumption *78*
4.4.2 Maximum Carried Traffic Analysis *81*
4.4.3 Line Interfaces Utilization *82*
4.5 Chapter Summary 84

CHAPTER 5: DESIGN STRATEGIES TO TRANSPORT HIGH-CAPACITY TRAFFIC 85

5.1 Capacity Upgrades in Optical Transport Networks 86
5.2 Service-Provisioning Framework Supporting C+L-band Transmission Systems 88
5.2.1 ILP Models *90*
5.2.2 Heuristic Algorithm: Spectrum and fibres assignment *93*
5.3 Impact of Adopting C+L Service-Provisioning Framework 95
5.3.1 Analysis of the Deployment of Single-Mode Optical Fibres *96*
5.3.2 Analysis of the Optical Channels Utilization *98*
5.4 Design of Geographically-Dependent Fibre Upgrade Expenditures with C+L-band Transmission System 101
5.4.1 Multi-Fibre C+L Network Design Framework *101*
5.4.1.1 ILP model 103
5.4.1.2 Heuristic Algorithm: L-band Min Spectrum Assignment 105
5.5 Impact of Adopting Geographically- Dependent Fibre Upgrade Expenditures 106
5.5.1 Network and Traffic Scenario *106*
5.5.2 Simulation Results *108*
5.6 Chapter Summary 110

CHAPTER 6: TECHNO-ECONOMIC EVALUATION OF EXPLOITING AUTONOMOUS OTN 111

6.1 Autonomous Networking 113

6.2 Network Planning and Operation with Reduced Margins 115
6.3 Service-Provisioning Frameworks with Reduced Margins 117
6.3.1 Proactive Service-Provisioning Framework with Reduced Margins 117
6.3.1.1 Multi-period Framework 119
6.3.1.2 Aging modelling and Optical Performance Estimation 122
6.3.1.3 ILP Models 124
6.3.1.4 Results and Discussion 130
A. Aging Impact 131
B. Performance Threshold 132
C. Line Interfaces Requirements 133
D. Mandatory Rerouting Events and Actual Residual Margin Performance 134
6.3.1.5 Discussion of Proactive Service-Provisioning Framework 137
6.3.2 Service-Provisioning Framework Exploiting Low-Margin for Preplanned Optical Shared Restoration Paths 137
6.3.2.1 Multi-period Framework 139
6.3.2.2 ILP Model 141
6.3.2.3 Network Scenario, Results and Discussion 144
6.3.2.4 Discussion of Service-Provisioning Framework Exploiting Low-Margin for Optical Shared Restoration Paths 146
6.4 Comparison of Reduced Margins Provisioning Strategies 147
6.4.1 Reduced Margins Provisioning Strategies 147
6.4.2 Simulation Results and Discussion 150
6.5 Chapter Summary 152
CHAPTER 7: CONCLUSIONS AND FUTURE WORK 154
7.1 Conclusions 155
7.2 Future Work 159
APPENDIXES 161
Appendix A. Optical Performance Model 162
Appendix B. Network Topologies 164
REFERENCES 167

List of Figures

Figure 1.1 Layered telecommunication network and (b) Geographic network hierarchy [2]. 3

Figure 1.2 (a) DWDM fixed grid, (b) superchannel spectral configuration and (c) DWDM flexible grid. .5

Figure 2.1 OTN over DWDM network architecture. 13

Figure 2.2 Transport modes: (a) Opaque, (b) Transparent and (c) Translucent. 14

Figure 2.3 Main concepts of designing a translucent optical transport network: (a) Optical Network, (b) Traffic demand's definition, (c) Optical channels' computation and (d) Transport of the traffic demand (1-4). 15

Figure 2.4 (a) Optical transport module and (b) Segments of the optical multiplex section. 17

Figure 2.5 Constellation diagrams of the (a) 16 QAM and (b) 64 QAM modulation formats. 20

Figure 2.6 Two axes of optical capacity scaling. 21

Figure 2.7 Different margins added to the optical channels' performance estimation [45]. 22

Figure 2.8 Example of optical transport network design including GRSA. 27

Figure 2.9 Survivability mechanisms with (a) dedicated and (b) shared backup resources. 28

Figure 2.10 1+1 dedicated protection or preplanned shared restoration schemes at: (a) ODU layer and (b) OCh layer. 29

Figure 2.11 Architecture of the OADM. 30

Figure 2.12 B&S ROADM-CDC architecture of a three-degree node with a contentionless degree of 2. 31

Figure 2.13 R&S ROADM-CDC architecture of a three-degree node with a contentionless degree of 2. 31

Figure 2.14 (a) Muxponder/Transponder-based and (b) OTN switch-based traffic aggregation. 33

Figure 2.15 OTN switch concept with different client and line interfaces. 33

Figure 2.16 Optical channel provisioning comparison between utilization of additional performance margins at BoL and exploiting smaller margins. 35

Figure 2.17 Schematic of single-mode, multi-mode and multi-core optical fibers. 36

Figure 3.1 Example of conflicting solutions considering the minimization of both line interfaces and OTN switches as objectives. 41

Figure 3.2 Genetic encoding: (a) network topology, (b) possible encodings to meet the traffic demand between the end-nodes 1 and 6, (c) genome structure and (d) algorithm workflow. 44

Figure 3.3 Non-dominated fronts in a multi-objective context. 47

Figure 3.4 Examples of the generation of initial, crossover and mutation solutions utilized in the IF-Aware genetic algorithm. 49

Figure 3.5 Illustration of the (a) hypervolume and (b) convergence rate metrics used for evaluating the performance of genetic algorithms. 52

Figure 3.6 Comparison results of the IF-Aware and Random GA: (a) Non-dominated fronts obtained by both genetic algorithms and (b-c) objectives' space explored by IF-Aware and random genetic algorithm for DT topology with 100 traffic demands and k=1, respectively. 55

Figure 3.7 Comparison between the results of IF-Aware algorithm and ILP model with 50 traffic demands and k=1 for (a) DT and (b) ARPANET topologies. 57

Figure 3.8 Comparison between the Pareto fronts for different values of k with 50 traffic demands for DT topology. 58

Figure 3.9 Pareto fronts with 100 and 200 traffic demands considering k=3 for (a) DT and (b) ARPANET topologies. 59

Figure 4.1 Spectrum configurations: (a) Fixed-grid configuration, (b) Flexi-grid configuration, (c) Virtual grid configuration and (d) example of overprovisioning of spectrum with a virtual grid. 66

Figure 4.2 Multi-period planning workflow. 67

Figure 4.3 Network design example of the computation of the most spectral efficient candidate optical channels using 32 and 64 Gbaud technology. 68

Figure 4.4 Spectrum usage throughout the entire network lifecycle for (a) DT and Unprotected, (b) SBN and Unprotected, (c) DT and OCh protection, (d) SBN and OCh protection, (e) DT and ODU protection and (f) SBN and ODU protection. 79

Figure 4.5 Cumulative number of interfaces used throughout the entire network lifecycle for (a) DT and Unprotected, (b) SBN and Unprotected, (c) DT and OCh protection, (d) SBN and OCh protection, (e) DT and ODU protection and (f) SBN and ODU protection. 83

Figure 5.1 Multi-period C+L-band planning workflow. 90

Figure 5.2 Generation of the combinations ($Comb$) defined in Algorithm 5. 95

Figure 5.3 Evolution of traffic growth per planning period. 96

Figure 5.4 Evolution of the number of fibres deployed along the network lifetime with C and C+L transmission systems for the (a-b) CIF and CIF-SC and (c-d) CIF and NGIF for SBN and IBN network topologies, respectively. 97

Figure 5.5 Illustration of the number of fibres deployed per network link in the SBN topology with C and C+L transmission systems considering CIF and NGIF design scenarios. 99

Figure 5.6 Evolution of the cumulative number of (single- or sub-) optical channels provisioned along the network lifetime with C and C+L bands for (a-b) CIF and CIF-SC and (c-d) CIF and NGIF for SBN and IBN network topologies, respectively. 100

Figure 5.7 Multi-fibre C+L network design framework workflow. 102

Figure 5.8 Example of the best neighbour fit criterium. 106

Figure 5.9 (a) Italy population density and (b) Network physical topology with differentiated fibre upgrade expenditures. 107

Figure 5.10 (a) Total cost of fibre deployed, (b) total number of line interfaces that have to be acquired and (c) Total number of fibres that have to be assigned for the different optimization scenarios. 109

Figure 6.1 Autonomous control loop of an optical network [175]. 113

Figure 6.2 Proposed transport network architecture to provision optical channels with reduced margins. 116

Figure 6.3 Optical channel performance evolution. 117

Figure 6.4 (a) Evolution of the optical channel throughout the network lifecycle and (b) proposed provisioning engine using real-time performance monitoring. 119

Figure 6.5 Workflow of the multi-period Proactive Service-Provisioning framework. 120

Figure 6.6 Examples of the reconfiguration processes involving the mandatorily rerouted traffic demands (a) Reconfiguration of the traffic carried over a single released optical channel. (b) Reconfiguration of traffic carried over two released optical channels. 122

Figure 6.7 Evolution of the number of node-pairs directly connected with each modulation format for (a) SBN and (b) IBN topologies. 131

Figure 6.8 Cumulative number of line interfaces that have to be acquired during the network operation for (a) SBN and ILP-7, (b) SBN and ILP-8, (c) IBN and ILP-7 and (d) IBN and ILP-8. 134

Figure 6.9 Cumulative number of traffic demands that have to be mandatory rerouted when reaching the minimum acceptable performance point for (a) SBN and (b) IBN topologies. 135

Figure 6.10 Average performance residual margin of the deployed optical channels for (a) SBN and (b) IBN topologies. 135

Figure 6.11 Network operation with working and protection/restoration channels in the presence of a network link failure. 138

Figure 6.12 Network operation using the preplanned shared restoration at OCh layer with 3R regenerators. 139

Figure 6.13 Multi-period framework using the optical shared restoration with CoL service-provisioning. 140

Figure 6.14 (a-b) Evolution of the number of 3R regenerators that have to be deployed for regeneration in the backup paths and (c-d) evolution of the total number of interfaces that have to be acquired throughout network operation for both network topologies. 145

Figure 6.15 Multi-period planning workflow for provisioning with reduced margins. 149

Figure 6.16 Line interface savings with respect to conventional EoL planning for both (a) SBN and (b) IBN network topologies. 151

Figure B.1 DT topology. 164

Figure B.2 ARPANET topology (link distances in km). 164

Figure B.3 SBN topology. 165

Figure B.4 IBN topology. 165

List of Tables

Table 1.1 ITU-T frequency bands. 5

Table 2.1 Optical channel formats for the different generations of coherent line interfaces based on [29]. 19

Table 3.1 MOGAs comparison. 54

Table 3.2 Complexity evaluation of MOGAs algorithms. 56

Table 4.1 Maximum Carried Traffic Load 81

Table 5.1 Optical Fibre Parameters 97

Table 6.1 Aging figures utilized per network element. 123

Table 6.2 Number of traffic demands mandatorily rerouted as function of the performance threshold for the IBN network topology. 132

Table 6.3 Main characteristics of the reduced margins service-provisioning strategies 148

Table 6.4 Total traffic interrupted and number of rerouting events 152

Table B.1 Topological characteristics of the reference networks. 166

List of Acronyms

API	Application Programming Interface
ARPANET	Advanced Research Projects Agency Network
ASE	Amplified Spontaneous Emission
B&S	Broadcast-and-select
B2B	Back-to-back
BDM	Band-Division Multiplexing
BER	Bit Error Rate
BoL	Beginning-of-life
BT	British Telecom
CAPEX	Capital expenditures
CD	Chromatic Dispersion
CDC	Colorless, Directionless, Contention-less
CIF	Current generation of line interfaces
CIF-SC	Current generation of line interfaces- superchannel configuration
CoL	Current-state-of-life
CoL-P	Current-state-of-life Provisioning
DCF	Dispersion Compensating Fibre
DCI	Data Center Interconnection
DEMUX	Demultiplexer
DP	Dedicated Protection

DSP	Digital Signal Processing
DSR	Dynamic Source Rerouting
DT	Deutsche Telekom
DWDM	Dense Wavelength Division Multiplexing
EDFA	Erbium-doped Fibre Amplifier
EoL	End-of-life
EoL-P	End-of-life Provisioning
FEC	Forward Error Correction
FL	Fibre Length
FR	Fiber Rent
FWM	Four-wave Mixing
GN	Gaussian Noise
GRSA	Grooming, Routing and Spectrum Assignment
IBN	Italian Backbone network
IF	Interface
ILP	Integer Linear Programming
IP	Internet Protocol
ISRS	Inter-channel Stimulated Raman Scattering
ITU-T	International Telecommunication Union – Telecommunication Standardization Sector
LEAF	Large Effective Area Fibre
LI	Line Interface
MAPP	Minimum Acceptable Performance Point

MCF	Multi-Core Fibre
MOGA	Multi-objective Genetic Algorithm
MUX	Multiplexer
MW	Maintenance Window
NGIF	Next-generation of line interfaces
NLI	Nonlinear Interference
NP	Non-deterministic Polynomial
NSGA	Non-dominated Sorting Genetic Algorithm
OADM	Optical Add/Drop Multiplexer
OAM	Operation, Administration and Maintenance
OCh	Optical Channel
ODU	Optical Data Unit
OEO	Optical-Electrical-Optical
OMS	Optical Multiplex Section
OPEX	Operational Expenditures
OPM	Optical Performance Model
OPU	Optical Payload Unit
OS	OTN Switching
OSNR	Optical Signal-to-Noise Ratio
OTM	Optical Transport Module
OTN	Optical Transport Network
OTS	Optical Transmission Section

OTU	Optical Transport Unit
PAES	Pareto-Archived Evolution Strategy
PMD	Polarization-mode Dispersion
PSR	Preplanned Shared Restoration
QAM	Quadrature amplitude modulation
QoT	Quality-of-transmission
QPSK	Quadrature phase-shift keying
R&S	Route-and-select
RM	Residual Margin
ROADM	Reconfigurable Optical Add/Drop Multiplexer
SBN	Spanish backbone network
SDH	Synchronous Digital Hierarchy
SDM	Spatial-Division Multiplexing
SDN	Software-Defined Networking
SLA	Service level agreement
SM	System Margin
SMF	Single-Mode Fibre
SPEA	Strength-Pareto Evolutionary Algorithm
SR	Shared Restoration
SSMF	Standard Single Mode Fibre
SU	Spectrum utilization
UK	United Kingdom

WDM	Wavelength Division Multiplexing
WSS	Wavelength Selective Switch
XPM	Cross-phase Modulation

List of Symbols

A	Weight parameter used to balance the objectives in the ILP models
B	Weight parameter used to balance the constraints of the ILP models
BW	Bandwidth of the spectral slots
B_{ref}	Reference optical bandwidth
C_d	Bit-rate of each traffic demand $d \in D$
Chr_{sor}	Ordered chromosomes to be assigned
C_l	Bit-rate available per optical channel $l \in L$
$Comb$	Set of network links' combinations presented in E_{block}
$Connector_{loss}$	Connector loss
$Ctrans_l$	Total capacity transported by each optical channel $l \in L$
D	Set of traffic demands
D_b	Set of best-effort rerouted traffic demands
D_h	Set of traffic demands that are carried over the optical channel reaching the MAPP $h \in H$ in previous planning periods
D_m	Set of mandatorily rerouted traffic demands
D_n	Set of new traffic demands
D_r	Set of traffic demands that have to be re-groomed
D_{res}	Set of traffic demands that are carried by an optical channel running out of margin in its restoration path
D_T	Set of traffic demands already assigned in the previous planning periods
E	Set of network links

E_{block}	Set of network links traversed by channels that have been blocked in the assignment process
EV_l	Set of end-nodes of each optical channel $l \in L$
f	Frequency of the optical channel
F	Number of available frequency slots
FE	Fitness Evaluation
$FillThresh$	Threshold value used in the Algorithm 4
F_l	Total number of 12.5 GHz frequency slots allocated to each optical channel $l \in L$
FR_l	Fill ratio of each optical channel $l \in L$
h	Planck's constant
H	Set of optical channels that reached the MAPP.
I_{nodes}	Set of intermediate network nodes where there is traffic switched between different optical channels
I_{sr}	Number of line interfaces available in the inventory with symbol rate $sr \in SR$, $SR = \{32,64\}$
K_e	Total number of fibre kilometres deployed in each network link $e \in E$
L	Generic set of candidate optical channels
L_d	Optical channels' path used to meet each traffic demand $d \in D$
L_e	Set of optical channels that traversed the network link $e \in E$
$L_{i,j}$	Set of available optical channels between source node i and destination node j
$Lreg_v$	Set of optical channels $l \in L$ that required a regenerator at network node $v \in V$ in the restoration channel
$Lreg_v^e$	Set of optical channels $l \in L$ that required a regenerator at network node $v \in V$ in the restoration channel using the network link $e \in E$

L_{sr}	Set of optical channels available per symbol rate $sr \in SR,\ SR = \{32,64\}$
L_T	Set of optical channels already deployed in previous planning periods
L_v	Set of optical channels that passed-through the network node $v \in V$
l_bound	Maximum number of cases considered in Algorithm 5
LZ	Large weight parameter used to balance the constraints of the ILP models
M_l	Maximum number of optical channels $l \in L$ that can be established in the 87.5 GHz slot composition
MK_e	Multiplier factor that differentiates the kilometres of fibre deployed according to the geographical area
$N_{connectors}$	Total number of connectors
N_d	Total number of traffic demands $d \in D$ between the same end-nodes and bit-rate
NF	Amplifier's noise figure
NIF_o	Total number of line interfaces utilized in the offspring ($Offs$) solution
N_{ROADM}	Total number of traversed ROADMs
N_{spans}	Total number of spans
$N_{splices}$	Total number of splices
OC_l	Total number of optical channels $l \in L$ used in previous planning period
$Offs$	Offspring's genome
$OSNR_{B2B}$	The required optical signal to noise ratio in back-to-back
$OSNR_{add}$	Optical signal to noise ratio at the add ROADM node along the path
$OSNR_{drop}$	Optical signal to noise ratio at the drop ROADM node along the path
$OSNR_{int}$	Optical signal to noise ratio at the intermediate ROADM nodes along the path

$OSNR_{tot}$	Optical signal to noise ratio at the end of the path
P	Set of working and protection paths that have to be assigned to each traffic demand $d \in D$
Par	Parent's genome
P_{ASE}	The average amplified spontaneous emission noise level
P_{NLI}	The average nonlinear interference noise level
$pOCh_l$	Flag array that indicates if an optical channel $l \in L$ has the potential to be released
P_{rx}	The average optical signal power
Q_{sr}	Total number of line interfaces already deployed in previous planning periods with symbol rate $sr \in SR$, $SR = \{32,64\}$
RIF	Set of released line interfaces
RIF_h	Set of released line interfaces of the optical channel that reaches the MAPP $h \in H$
RIF_h^v	Set of released line interfaces of the optical channel that reaches the MAPP $h \in H$ using the network node $v \in V$
RIF_v	Set of released line interfaces using the network node $v \in V$
S_d	Total number of 1.25 Gbit/s slots per traffic demand $d \in D$ based on its bit-rate
S_{length}	Span length
S_{loss}	Span loss
$Splice_{loss}$	Splice loss
$Spectrum$	Optical Spectrum defined by the number of network links over the number of available frequency slots in the network
SR	Set of symbol rates, $SR = \{32,64\}$

t	Percentage of chromosomes used to initialize the offspring's genome ($Offs$)
TH_l	Binary array that indicates if an optical channel $l \in L$ is below the performance threshold.
$T_{next-gen}$	The planning period where the next-generation of line interfaces become readily available
$T_{periods}$	Total number of planning periods
V	Set of network nodes
$W_d^{l,p}$	Total number of traffic demands $d \in D_T$ that used the optical channel $l \in L_T$ over the working or protection path ($p \in P$) in the previous planning periods
X_l	Total number of 1.25 Gbit/s slots supported by the optical channel $l \in L$ based on its capacity
Y_h	Total number of traffic demands within the set D_h
Z	Weight parameter used to balance the objectives in the ILP models
$\Pi_e \in \mathbb{N}^0$	Total number of additional fibres deployed per network link $e \in E$
$\Lambda_l \in \mathbb{N}^0$	Total number of single optical channels $l \in L$ utilized
$\Phi_l \in \{0,1\}$	Binary variables that indicate if the number of optical channels $l \in L$ is increasing during the optimization process
$\Omega_h^l \in \{0,1\}$	Binary variables that indicate if at least one of the traffic demands that used the optical channels that reached the MAPP ($h \in H$) in previous planning period is now using the optical channel $l \in L$
$\alpha \in \mathbb{N}^0$	Total number of optical channels below the performance threshold.
α_{atte}	Fibre attenuation parameter
$\beta_{sr} \in \mathbb{N}^0$	Total number of line interfaces that have to be acquired with symbol rate sr, $SR = \{32,64\}$
$\gamma_{sr} \in \mathbb{N}^0$	Total number of released line interfaces with symbol rate sr, $SR = \{32,64\}$

$\delta_l \in \mathbb{N}^0$	Total number of 87.5 GHz frequency slots used to meet $l \in L$
$\varepsilon_l \in \mathbb{N}^0$	Total number of channels deployed per candidate superchannel format $l \in L$
$\zeta_h^l \in \{0,1\}$	Binary variable that indicates if at least one of the traffic demands that used the optical channel selected by variable ξ_h in the previous planning periods is now using optical channel $l \in L$
θ_l	Total number of optical channels used for the candidate channel $l \in L$
$\lambda_{d_{(o,t)}}^{l_{(i,j)},p}$	Number of traffic demands $d \in D$ between source node o and destination node t using the optical channel $l \in L$ with source node i and destination node j over the working or protection path $p \in P$
$\xi_h \in \{0,1\}$	Binary variable that defines the optical channel that reaches the MAPP $h \in H$ whose the carried traffic demands will not reuse the released interfaces from other optical channels that also reach the MAPP
$\pi_l \in [0,1]$	Binary variable that indicates if the number of optical channels $l \in L$ utilized is an odd value
$\rho_l \in \mathbb{N}^0$	Total number of line interfaces reused from the inventory (RIF) for the optical channels $l \in L$
$\rho_l^{ev} \in \mathbb{N}^0$	Total number of line interfaces reused from the inventory RIF for the optical channels $l \in L$ using the end-node $ev \in EV_l$
$\sigma_v^e \in \mathbb{N}^0$	Total number of affected restoration channels with end-node $v \in V$ when the network link $e \in E$ fails
$\tau_l \in \mathbb{N}^0$	Total number of superchannels utilized for the candidate channel $l \in L$
$\psi_v \in \mathbb{N}^0$	Total number of regenerators required per network node $v \in V$
$\Delta \in \mathbb{N}^0$	Total number of channels assigned per superchannel deployed
$\eta \in \mathbb{N}^0$	Total number of network resources acquired
$\Gamma \in \mathbb{N}^0$	Amount of spectrum occupied
$\kappa \in [0,1]$	Weight parameter used to balance the fitness equation

$\nu \in \mathbb{N}^0$	Total cost of fibre deployed per kilometre
ς	Set of channels (single or superchannels) deployed in the optical spectrum
$\varsigma Block$	Set of channels blocked in the assignment process
φ	Total number of 32 Gbaud interfaces used from the inventory
$\chi \in \mathbb{N}^0$	Total number of single channels deployed
ϑ	Total number of 32 Gbaud optical channels decoupled in the 87.5 GHz slots
$\#IFs$	Total number of line interfaces used
$\#OTNSwitches$	Total number of OTN switches used

Chapter 1: Introduction

1.1 Evolution of Optical Transport Networks

The telecommunication network is typically divided in transport and service network layers, as shown in Fig. 1.1 (a). The service network layer is responsible for providing the logical connectivity defined by the traffic, e.g., if two users communicate through the Internet, the generated traffic will be addressed by the Internet Protocol (IP) through the IP routers on the service level, but physically it will be transported across different distances that may span hundreds of kilometres (transport network layer). Additionally, the transport layer represents the technological platform that ensures the transparent routing of various types of traffic, assuming the capabilities of transmission, multiplexing, routing, protection and provisioning of capacity.

From the point of view of geographical scope and capacity to aggregate traffic, telecommunication networks can also be described as a hierarchical model with three layers: core/long-haul, metro/regional and access, as described in Fig. 1.1 (b). In detail, the access network connects the subscribers to their service providers via copper, fibre or wireless connections, which are typically less than 100 km. When the traffic reaches the service providers' premises, the traffic aggregation can be either be defined as metro/regional level, which may cover large metropolitan areas (up to 500 km), or core/long-haul level that may span entire countries or continents over 500 km distances or more [1, 2].

Throughout the years, different types of network transport technologies have been adopted to effectively transport the traffic. In the 1980s, the Synchronous Digital Hierarchy (SDH) became the transport protocol of choice that allows data streams with low bit-rates to be combined into high-rate data streams over fibre optics. However, the need of transporting more capacity in telecommunication networks has shown the limitations of SDH when compared to other technologies, such as optical transport network (OTN) that offers more flexible architectures with reduced transport costs and higher bandwidth transported [3].

The OTN ended up being standardized by International Telecommunication Union – Telecommunication Standardization Sector (ITU-T) through the recommendation G.872 [4] in 1999, including both electrical and optical layer functions to support wavelength division multiplexing (WDM) with the aim of increasing the maximum capacity transported. In detail, the WDM is a transmission technique that increases the bandwidth transported by allowing independently optical channels at different frequencies being transmitted over a single optical fibre, enabling a bidirectional communication as well as multiplication of signal capacity. In this context, the OTN over WDM technology is also called "digital wrapper" since it allows to transport one or more services into a single wavelength independently of the type of traffic, provide the required operation, administration and maintenance (OAM) functionalities and the multiplexing and routing of the traffic in the metro and core networks [5].

In general, this Thesis will focus on OTN over WDM technology in a core component of a transport network, since this multi-layer structure is capable of aggregating and transporting different services onto a single wavelength/optical channel and providing the interwork between electrical and optical technologies, enabling the transmission of several Terabit per second (Tb/s) of data over a single optical fibre and across different distances [4]. In this context, an optical transport network consists of a set of

network nodes connected by optical fibres (network links) supervised by the control/management plane. In OTN/WDM domain, the network nodes are implemented by optical add/drop multiplexers (OADM) which are responsible for optical adding/dropping client signals at each node as well as to provide the capability of expressing wavelengths through a node. The OADMs can be fixed or reconfigurable (ROADMs). The former enables the set of wavelengths to be dropped/added in a fixed way, whereas the latter add/drop can be remotely changed in response to traffic alterations by the control/management plane. Moreover, the optical devices can be combined with electrical switching equipment, which appropriately map the traffic into data containers for suited wavelength transport. More details about the network nodes and links dimensioning are provided in the next chapter.

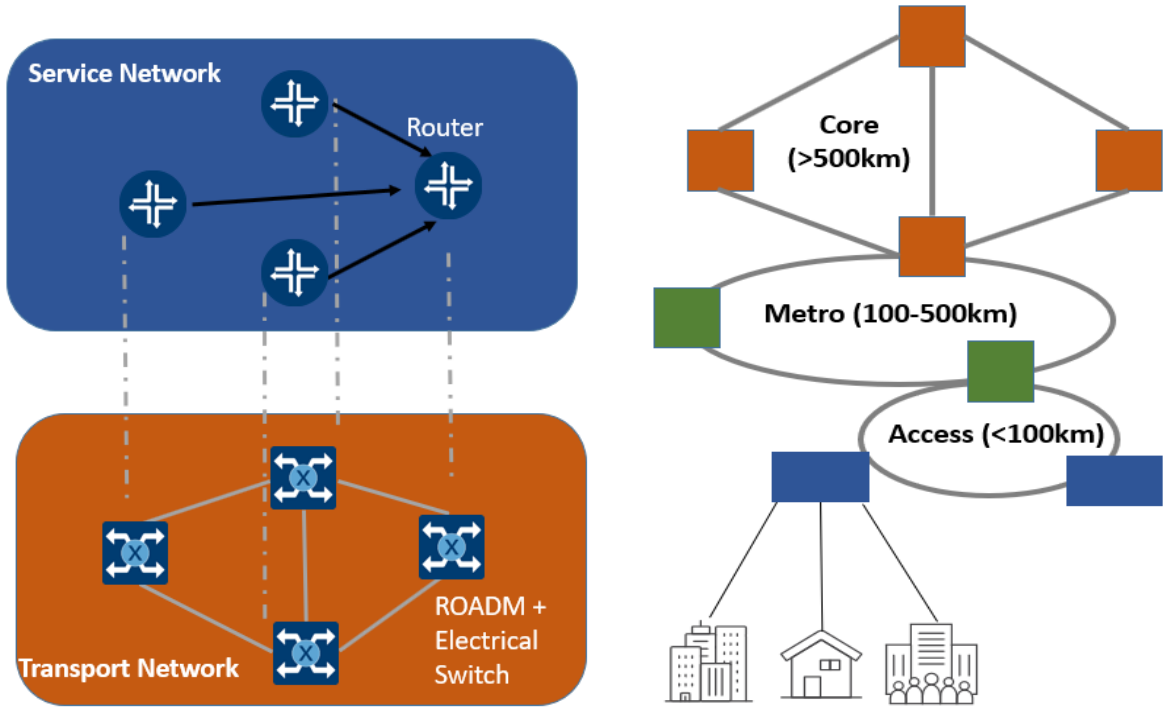

Figure 1.1 Layered telecommunication network and (b) Geographic network hierarchy [2].

The main driver for the evolution of the transport infrastructure resides in the need to increase the capacity supported by the telecommunication network to meet ever-growing bandwidth and service requirements. In this sense, the OTN over WDM transmission system showed to be the most suitable approach to transport high-capacity traffic. Moreover, the increase of transported capacity can be accomplished over time via three strategies: increasing both symbol rate of channels and the number of bits transmitted per symbol as well as the number of channels per optical fibre. In detail, three important technology advancements that empowered these strategies was the development of optical amplifiers (e.g., erbium-doped fibre amplifiers (EDFA)) since it enables the amplification of all channels simultaneously [6], the improvements in coherent detection and digital signal processing (DSP) [7] and/or the introduction of forward error correction (FEC) techniques to improve the signal tolerance to noise [8].

In the first place, the evolution of optical transmission technology led to the appearance of 2.5 Gbit/s, 10 Gbit/s and 40 Gbit/s single-channels based on direct detection modulation formats [9]. Nevertheless, the application of coherent detection to optical systems contributed to the greatest achievement in increasing channel rates, since it enables the use of modulation formats exploiting phase encoding that can increase the number of bits carried per symbol [10]. The development of coherent detection combined with digital signal processing (DSP) technique enabled the transmission of 100 Gbit/s channels [11]. The maturation of this technology [10] also brought new opportunities to effectively scale capacity through the deployment of a single optical channel that can be used to transmit 100, 150 or 200 Gbit/s data signals by increasing the number of bits transmitted per symbol via the use of higher order modulation formats, such as quadrature phase-shift keying (QPSK), 8-quadrature amplitude modulation (QAM) and 16 QAM [12, 13, 14].

Focusing on the quest for increasing the number of channels per optical fibre, early WDM deployments with direct detection featured 16, 32 and 80 optical channels with bit-rate of 2.5 Gbit/s per optical fibre [15]. Later coherent detection has enabled the transmission of 96 channels at 100 Gbit/s over the optical fibre. These WDM systems tightly packing many optical channels in the C-band (1530-1565 nm) of the optical fibre are referred to and standardized by ITU-T [16] as Dense Wavelength Division Multiplexing (DWDM). This transmission system has also been defined as DWDM fixed grid [16] where the central frequency of each optical channel is normalized by ITU-T and the channels' spacing is constant, typically of 50 GHz. Fig. 1.2 (a) exemplifies the central frequencies of DWDW fixed grid with constant channels' spacing of 50 GHz. Note that, the optical fibre is divided into six spectral bands that can be used for the communication systems, as described in Table 1.1 and standardized by ITU-T in [17]. However, the early WDM deployments only utilized the C-band since this spectral band is compatible with the EDFA amplifiers and the channels can be properly transmitted. Nowadays, the L-band is also starting to be commercialized due to the evolution of EDFA amplifiers and the possibility of using the S-band is being researched but only with the appearance of new amplifiers compatible with this band.

Another strategy to improve the capacity of WDM networks consists of using superchannels via the Nyquist-WDM technique [18, 19, 20]. These channels are defined as a logical entity capable of spectrally grouped channels between the same source and destination nodes, as shown in Fig. 1.2 (b). In contrast to typical single-channel transmission defined in Fig. 1.2 (a) by DWDM fixed grid, it can be seen that the use of multiple separate optical channels requires the addition of guard bands on the two sides of the channels to reduce the filtering penalty, whereas in superchannel technology it only adds guard bands on the two sides of the superchannel, which can enable the reduction of the total amount of spectrum utilized and the augment of transmission efficiency.

Through the illustration of Fig. 1.2 (b), it can be seen that the concept of superchannel seems to be incompatible with fixed DWDM grid, because the fixed spacing does not allow the adjustment of superchannel widths. This led the telecommunication industry to propose a novel spectrum configuration design called flexible DWDM grid and standardized by ITU-T in [21]. To support the flexible DWDM grid, it is necessary to introduce the concept of spectral slot where each optical channel can be assigned with

the amount of the contiguous spectral slots according to the needs. In this scenario, the optical bandwidth is divided into 12.5 GHz spectral slots and each optical channel is characterized by its central frequency and the total number of spectral slots (12.5 GHz) assigned, as depicted in Fig. 1.2 (c).

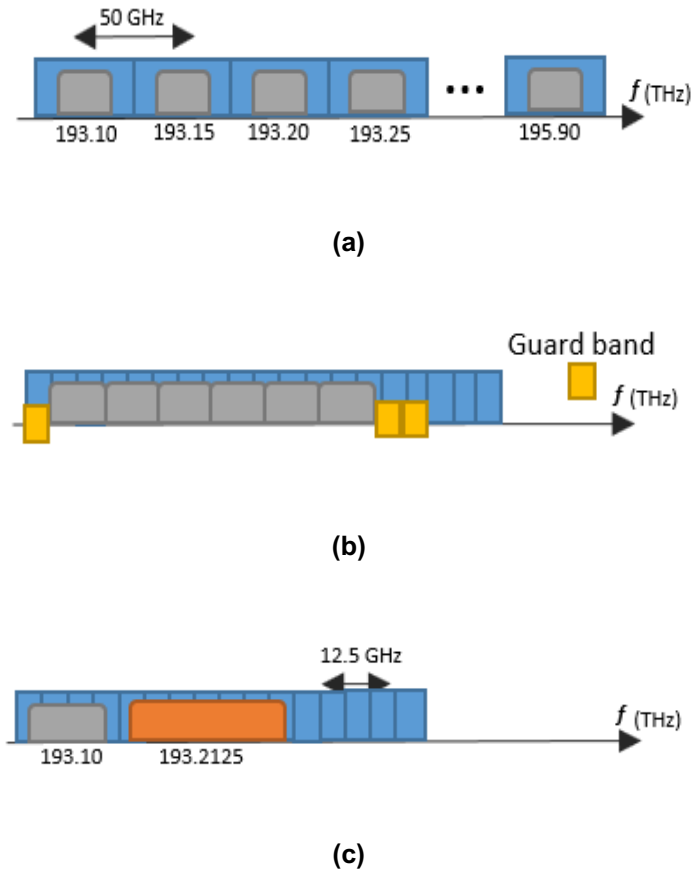

Figure 1.2 (a) DWDM fixed grid, (b) superchannel spectral configuration and (c) DWDM flexible grid.

Table 1.1 ITU-T frequency bands.

Band	Name	Wavelength Range (nm)
O	Original	1260-1360
E	Extended	1360-1460
S	Short	1460-1530
C	Conventional	1530-1565
L	Long	1565-1625
U	Ultra-long	1625-1675

1.2 Motivation

In recent years, telecommunications industry and service provider networks have been evolved in order to cope with the massive explosion of digital traffic (e.g., video streaming, cloud computing, mobile applications) [22]. Moreover, the constant introduction of new packet-based services has made the traffic pattern more unpredictable and bandwidth demanding, which leads the network operators to pursue different ways to maximize the return of their investments in state-of-the-art optical transport networks gear [23]. This relentless search drives the industry to develop new technologies, network architectures and optimization algorithms, having as the key objectives the reduction in the cost per bit transmitted and the transport of maximum capacity possible over the predefined optical infrastructure [24].

Network optimization for designing purposes in OTN has always played an important role for the network operators since the extent of their investments in optical transport networks are directly related to the costs associated with the developed technologies that offer the highest capacity in transport networks. In this context, one of the most important objectives when planning an OTN resides in the

minimization of shorter-term capital expenditures (CAPEX), namely the equipment required to transmit the optical channels (e.g., line interfaces and regenerators) that transport all the traffic demands [25]. Depending on the characteristics of the transmission path, this affects the modulation format deployed per optical channel and consequently the maximum capacity that can be used between two end-nodes of the OTN [26]. In conventional transport planning and operation, the most cost-effective modulation format to deploy between two nodes is the one available that provides enough capacity to transparently support all current traffic between those nodes while minimizing, firstly the number of optical channels deployed and, secondly, the amount of spectrum occupied [27]. Particularly, the maximization of spectral efficiency measured in [bit/s/Hz] (referring to the number of bit/s that can be transmitted for each Hz of the spectral bandwidth) also reveals to be an important goal when optimizing an OTN, given the constraints on the optical fibre's bandwidth that depends directly on the number of spectral bands deployed, as described in 1.1 [28]. These aspects are even more important in this new era associated with the explosion of digital traffic.

One opportunity to increase spectral efficiency in OTN resides in the development of optical transmission technology via the use of coherent detection. Thus, the recent progress in high-speed electronics and better DSP will allow to develop a next-generation of coherent optical line interfaces that will further improve this goal, namely by (i) providing a wider array of modulation formats (e.g., 32 and 64 QAM) and by (ii) approximately doubling the maximum symbol rate (e.g., 64 Gbaud) with still acceptable reach (referring to the maximum distance that a channel can be transmitted without regeneration) [29, 30, 31, 32]. The latter feature is of particular interest to reduce the cost per bit transmitted and attain higher spectral efficiencies. Besides the advantages, the deployment of this new generation of optical line interfaces will inevitably raise planning and dimensioning challenges, one of the major ones being the requirement to evolve to a flexible spectrum grid, since the fixed 50 GHz grid is no longer sufficient support optical channels with symbol rates significantly higher than the typical value used for the current ones (~32 Gbaud).

The adoption of a flexible grid and the co-existence of optical channels that operate at different symbol rates (for example 32 and 64 Gbaud) will potentially increase spectrum fragmentation and reduce the overall network performance, mainly in the presence of dynamic and unpredictable traffic [33, 34, 35]. Particularly relevant to OTN being deployed now and in short-term, the initial set of services will use a generation of optical line interfaces with smaller symbol rate, which means that when the network operator starts to leverage the advantages of the new generation of line interfaces that operate at higher symbol rate, a part of the spectrum resources will already be in use. As a result, the spectrum allocation strategy utilized from the network beginning-of-life will affect the deployment of these new services. Thus, this will require the development of novel network planning algorithms where the evolution in transmission technology is accounted for, such that both capital expenditures and spectral resource usage can be minimized targeting not only the present planning period, but instead the entire network lifecycle.

As mentioned before, the increase of capacity transported in OTN has been possible via the deployment of consecutive generations of optical line interfaces, each superseding the previous by

providing both higher capacity and spectral efficiency. However, this increase of capacity is rapidly approaching the fundamental limits (Shannon limit) imposed by three aspects: 1) the optical signal-to-noise ratio (OSNR) enforces an upper bound on the number of bits that can be transported [36], 2) the distributed non-linearity of conventional single-mode fibres (SMF) [37] and 3) the maximum distance that a channel can be transmitted without regeneration is limited by the gain bandwidth of C-band EDFA optical amplifiers (5 THz) [38]. For these reasons, capacity transported in OTN will be increased mostly via using more spectrum [39]. As a result, network operators will face the prospect of using more spectral bands of the optical fibre (e.g., S- and L-band), installing additional single-mode fibres or deploying novel multi-core/mode fibres. In the short- to medium-term, exploiting C+L band systems and installing additional single-mode fibres are the only commercially available options [40, 41, 42].

In this context, the effectiveness of the deployment of multi-band/fibre systems depends on the adopted transmission technologies and design strategies that can lead to different CAPEX implications. Consequently, it is paramount to develop a network design framework addressing this new environment, particularly in the resource allocation that may have to account both the spectral domain (e.g., optical channel formats of different sizes) and the spatial domain (e.g., multiple fibres). Consequently, the larger number of dimensions to be considered and the optical performance constraints will demand more complex routing and resource assignment algorithms, which may require the development of efficient Integer Linear Programming-based or/and heuristic-based algorithms tailored for these network scenarios.

Another strategy that could be utilized to maximize the return of investment in OTN resides in reassessing the process of provisioning optical channels, which typically assumes large enough performance margins to guarantee the quality-of-transmission (QoT) of the data channel until the network end-of-life (EoL). This is achieved by forecasting, within reasonable bounds, the impact of different effects that deteriorate optical performance, such as aging of components and fibre plants. The resulting conservative approach could inhibit the use of higher order modulation formats of coherent transmission technology [30], which reduces the prospect of increasing capacity per optical channel being provisioned. Conversely, the deployment of optical channels with reduced margins according to the current-state-of-life (CoL) of the network can enable the increase of capacity per channel deployed, allowing to transport more traffic clients over a single optical channel which leads to lower CAPEX [43, 44, 45]. However, this requires the ability to have access to key physical parameters of the network to accurately estimate the current margins of the optical channels and forecast their evolution, which can only be cost-effectively attained when using a platform to monitor in real-time the network parameters [46, 47].

This novel scenario will demand an optimized planning framework that appropriately models the provisioning of services using optical channels with smaller margins while mitigating the impact of events, where the optical channels can have a time-to-live shorter than that the traffic it carries leading to traffic disruption, since the reduction of margins will imply to operate closer to the optical channel performance limit. Thus, the developed routing engine should comprise an optimized model capable of addressing different phases of operation according to the optical channels performance in order to

manage how both existing and new traffic are routed with the objective of optimizing the number of network resources that have to be acquired while guaranteeing a minimum risk of traffic disruption in this dynamic environment.

Being an emergent topic, the optical network optimization in the context of high-capacity set by the massive explosion of digital traffic, focuses on how the optical transport network infrastructure can scale to transport more data while simultaneously reducing the operational and equipment costs. This also involves the deployment of different network node architectures to interconnect the traffic signals and optical channels that influences the overall network cost. Particularly, the deployment of flexible switching configurations may enable savings on the amount of transmission resources required (i.e., optical line interfaces) to accommodate the traffic [48, 49]. However, deploying this switching flexibility entails a premium, which implies that when designing the network multiple and possibly conflicting objectives can co-exist, leading to trade-offs solutions (e.g., minimize transmission CAPEX vs. switching CAPEX).

On the other hand, survivability also plays an important role on the optimization of OTN, namely due to the capacity increase in DWDM channels (up to 600 Gbit/s in next-generation optical channels), since a single fibre failure can cause a substantial impact in the network operation, affecting the required service level agreement (SLA), that is a formal contract between the service provider and users [50]. In this context, the service-provisioning optimization algorithms should also be adapted to address network resilience, allowing to assess the cost and spectrum resource usage implications of considering survivability against different types of failures.

Given the different challenges that the OTN are facing nowadays, it is paramount to develop network optimization frameworks to obtain optimal solutions and, in this regard, the exact mathematical problems that always search for the optimal point, like Integer Linear Programming, should be the first option to be adopted. However, most of the challenges are NP (Non-deterministic Polynomial)-hard problems for being combinatorial problems, making them computationally difficult to be solved via the ILP models and need to be settled via the use of heuristic-based approaches [51].

1.3 Objectives and Thesis Outline

The main goal of the work described in this Thesis consists of the development of different network planning and design frameworks, aiming to provide optimized solutions to address some of the main challenges of dimensioning a high-capacity OTN. This will comprise the development of novel network planning algorithms to exploit the utilization of a wide set of optical channels formats (higher order modulation formats and symbol rates), characterized by different trade-offs between capacity, reach and spectral occupation, but also entail more complex routing and resource allocation algorithms via the deployment of a flexible DWDM grid.

On the other hand, the capacity scaling will demand the exploitation of more spectral bands of the optical fibre or parallel fibres, which require the development of novel network optimization frameworks to address these novel scenarios. In this context, different cost-effective optical switching architectures

are also considered, also requiring the development of suitable routing and resource assignment algorithms, embedding the constraints introduced by such architectures. Finally, this work also addresses the recent trends that emphasize the need of adopting a more autonomous network paradigm in order to operate adaptively to the actual network environment, aiming to augment capacity transported in optical transport network and optimize the overall network costs.

In each case, the developed optimization frameworks will be responsible for providing a grooming, routing and resource allocation solution to transport all the traffic in the predefined optical transport architecture [52, 53]. In general, routing is responsible for choosing the best path for each traffic demand, grooming defines how small traffic units generated by the clients of transport network are grouped into larger data unit (optical channels) and spectrum assignment is responsible for assigning the frequencies to all connections with the aim of optimizing a given objective (More details about these algorithms are presented in the next section). The algorithms proposed throughout this Thesis will be based, when possible, on exact mathematical programming formulations capable of producing optimal solutions, such as Integer Linear Programming models. Alternatively, when scalability limitations prevent the use of these solutions, alternative heuristic algorithms are utilized. Concretely, this work intents to address the following objectives:

- Development of a tool that contemplates the deployment of flexible switching architectures at the network nodes of an OTN.
- Development of a service-provisioning framework exploiting the next-generation of line interfaces with higher order modulation formats and symbol rates, also considering the support of survivability protection schemes.
- Development of network design frameworks modelling the deployment of strategies to transport high-capacity traffic via using more spectrum (e.g., multi-band and multi-fibre systems).
- Development of different frameworks that exploits the advancements in automation and real-time performance monitoring to operate the transport networks with reduced margins, providing a novel routing engine for this environment.
- Perform accurate techno-economic comparisons with other optimization strategies for each objective defined in the context of this study.

The Thesis is structured in six chapters. In detail, Chapter 2 provides an introduction and review of the main concepts associated with an optical transport network that will be applied throughout the developed work. In Chapter 3, a multi-objective framework is presented focusing on node dimensioning with the aim of minimizing both transmission and switching network costs, resulting from addressing more flexible switching architecture scenarios. After observing the impact of deploying flexible node architectures, Chapter 4 describes a detailed techno-economic analysis of adopting the next-generation of optical line interfaces that exploits the use of higher order modulation formats and symbol rate, highlighting the main concepts, spectrum grid configurations, node architecture challenges and the proposed service-provisioning strategy that can optimally cope with the future of optical transport network.

Although the introduction of the next-generation of optical line interfaces will be the choice in near future to increase capacity in OTN (Chapter 4), this could not be sufficient to transport the bandwidth-hungry traffic and so it will inevitably require the implementation of different high-capacity strategies via using more spectrum. These strategies are then analysed in Chapter 5 through the development of different service-provisioning algorithms, addressing multi-band and multi-fibre systems. The final development chapter of this Thesis also focuses on transporting more capacity in OTN but considering a more disruptive approach based on the recent advancements in network automation with the aim of operating an OTN with smaller margins. Hence, Chapter 6 proposes two frameworks that exploit the advancement in real-time monitoring platforms in order to reduce the margins and maximize the optical channel capacity. Finally, the main conclusions and suggestions for future research avenues are presented in Chapter 7.

1.4 Main Contributions

This Thesis proposes different optimization algorithms and methodologies, which addresses some of the main challenges to cost-effectively design the next-generation of optical transport networks. The developed work focuses on how the OTN can scale to provide higher capacity while reducing the cost per bit transported. Furthermore, various comparative techno-economic analyses are performed with the aim of fulfilling the stated objectives. The most relevant accomplishments, along with the publications associated with them, are as follows:

- Development of a multi-objective genetic algorithm that addresses the possible conflicting problem of both minimizing the transmission and switching CAPEX, resulting from the use of more flexible switching architectures at the network nodes of an OTN. Benchmark comparison of the proposed algorithm with other optimization strategies [J1].
- Proposal of a service-provisioning framework based on an ILP model and spectrum management strategy with the aim of exploiting the next-generation of optical channels. The study also considers the support of survivability protection schemes and a comparison study with other spectrum management configurations [J2, C1, C2].
- Study of network design strategies to deploy high-capacity traffic via using more spectrum (multi-band/fibres systems), comparing the effectiveness of the different methods utilized [J3]. Update the multi-fibre system algorithm to consider geographically-dependent fibre upgrade expenditures [C3].
- Development of different frameworks that exploits the recent advancements in real-time performance monitoring and automation networks with the aim of reducing the optical performance margins and increasing the capacity per channel deployed [J4, C4, C5, C6, C7, C8, C9].

Papers in journals

[J1] D. Moniz, J. Pedro, N. Horta and J. Pires, “Multi-objective framework for cost-effective OTN switch placement using NSGA-II with embedded domain knowledge” Applied Soft Computing Journal, vol. 83 (105608), October 2019.

[J2] D. Moniz, J. Pedro and J. Pires, “Network design framework to optimally provision services using higher-symbol rate line interfaces”, IEEE/OSA Journal of Optical Communications and Networking, vol. 11, no. 2, pp. A174-A185, February 2019.

[J3] V. Lopez, B. Zhu, D. Moniz, N. Costa, J. Pedro, X. Xu, A. Kumpera, L. Dardis, J. Rahn and S. Sanders, “Optimized design and challenges for C&L band optical line systems”, IEEE/OSA Journal of Lightwave Technology, vol.38, no. 5, pp. 1080-1091, January 2020.

[J4] D. Moniz, J. Pedro and J. Pires, “Dynamic multi-layer service-provisioning framework operating with reduced performance margins” IEEE/OSA Journal of Optical Communications and Networking, vol. 11, no. 9, pp. C35-C47, September 2019.

Papers in conference proceedings

[C1] D. Moniz, J. Pedro and J. Pires, “Network design framework to spectral- and cost- efficiently exploit next-generation line interfaces” Optical Fiber Communications (OFC), San Diego USA, M1A.4, March 2018.

[C2] D. Moniz, J. Pedro and J. Pires, “Spectral-Efficient Provisioning of Protected Services over DWDM Networks Exploiting High-Symbol Rate Line Interfaces” European Conference on Optical Communication (ECOC), Rome Italy, M1A.4, September 2018.

[C3] D. Moniz, V. Lopez and J. Pedro, “Design Strategies Exploiting C+L-Band in Networks with Geographically-Dependent Fiber Upgrade Expenditures”, Optical Fiber Communications Conference and Exhibition (OFC), San Diego, USA, March 2020.

[C4] D. Moniz, J. Pedro and J. Pires, “Service Provisioning Framework with Dynamic Margin Management for Optical Transport Networks”, Optical Fiber Communications Conference and Exhibition (OFC), San Diego, USA, March 2019.

[C5] J. Pedro, D. Moniz and J. Pires, “Multi-Layer Optimization Framework for Optical Transport Networks with Dynamic Margin Management”, 21st International Conference on Transparent Optical Networks (ICTON), Angers, France, July 2019.

[C6] D. Moniz, J. Pedro and J. Pires, “Multi-Layer Network Optimization Efficiently Exploiting Real-Time Performance Monitoring”, IEEE Global Communications Conference (GLOBECOM), Waikoloa USA, December 2019.

[C7] D. Moniz, J. Pedro and J. Pires, “Network Design Framework Exploiting Low-Margin Provisioning of Optical Shared Restoration Resources”, Optical Fiber Communications Conference and Exhibition (OFC), San Diego, USA, March 2020.

[C8] D. Moniz, J. Pedro and J. Pires, “Design and Operation Strategies for Optical Transport Networks with Reduced Margins Service-Provisioning”, Optical Fiber Communications Conference and Exhibition (OFC), San Diego, USA, March 2020.

[C9] J. Pedro, D. Moniz and J. Pires, “Performance Comparison of Operational Models for MCh Provisioning with Reduced Margins”, 22nd International Conference on Transparent Optical Networks (ICTON), Bari, Italy, July 2020.

Chapter 2: Networking Aspects for Designing the Next-Generation of Optical Transport Networks

The design of an optical transport network involves different types of problems and concepts (e.g., transport, routing, multiplexing, management and survivability of optical channels carrying traffic) that need to be clearly defined before analysing the optimization procedures proposed in this Thesis. Therefore, this chapter details the main concepts and algorithms that have been defined in the literature for effectively designing an OTN, from the architectural and technological subjects to future optical trends.

2.1 Optical Transport Network Concepts

The OTN standard [4] is defined by the concept of multi-layered networks (OTN over DWDM), as depicted in Fig. 2.1. Note that, the main difference between this illustration and the Fig. 1.1 (a) depicted in Chapter 1 resides in the transport network layer of Fig. 1.1 (a) that it is even more detailed here with the aim of highlighting the electrical and optical layers of OTN over DWDM networks. In this context, the signals of the clients (e.g., 1 Gbit/s Ethernet, 10 Gbit/s Ethernet, 100 Gbit/s Ethernet, Fibre channel, etc. [54]) from the service layer (highlighted in Fig. 1.1 (a)) are transported through the combination of the electrical and optical domains. The electrical domain is responsible for aggregating the client signals into the OTN transport signals, whereas the optical domain enables the generation and multiplexing of optical channels over a single optical fibre across different distances [55].

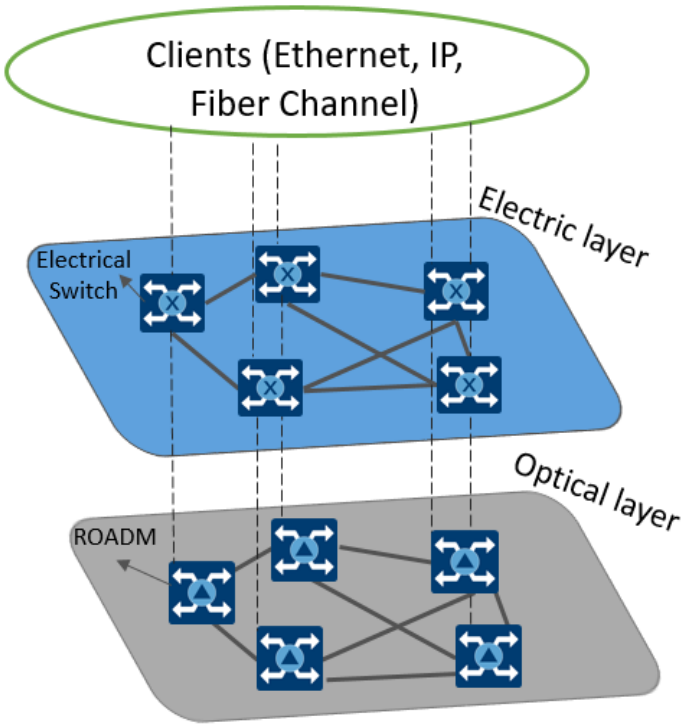

Figure 2.1 OTN over DWDM network architecture.

The combination of the electrical and optical layers at each network node allows for multiple transport modes, such as opaque, transparent and translucent. In an opaque network, the node functions (multiplexing and switching) take place in the electrical domain, which allows the channels to be added/dropped or expressed at each node. However, it requires interfaces capable of performing

optical-electrical-optical (OEO) conversions at each network node. On the other hand, the transparent network only enables the traffic demand to be transmitted end-to-end, bypassing the electrical layer at each intermediate node and working only in the optical domain. Finally, the translucent design combines the transparent and opaque modes, where the channels are selectively added/dropped at some intermediate nodes while expressing through others (depending on the traffic requirements). These different modes influence the transport of traffic as illustrated in Fig. 2.2 for a network topology with four sequential network nodes.

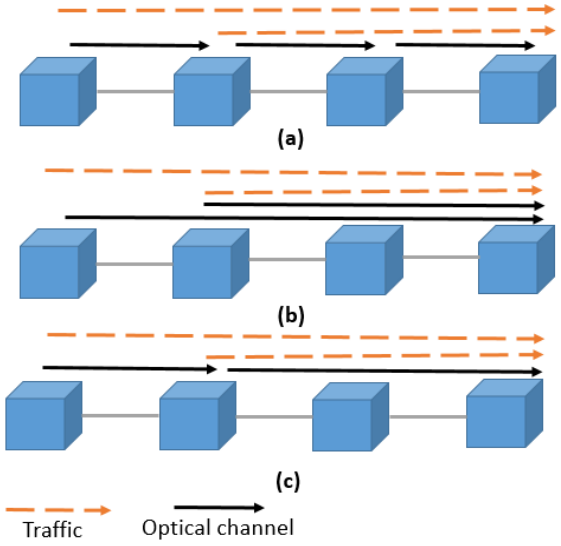

Figure 2.2 Transport modes: (a) Opaque, (b) Transparent and (c) Translucent.

Moreover, the optical networks are composed of network nodes (e.g., ROADMs and electrical switches) connected by network links (optical fibres) used to carry traffic between different distances in an efficient and reliable way. These networks can be defined by the graph $G(V, E)$ where $V = \{v_1, v_2, \dots, v_{|V|}\}$ is the set of network nodes (vertices) and $E = \{e_1, e_2, \dots, e_{|E|}\}$ represents the set of network links (edges). Furthermore, the network links are bidirectional (implemented through a pair of optical fibres, one for each direction) in the sense that the network link that connects v_i to v_j is the same that connects v_j to v_i and each link can be characterized by a cost and a capacity. For the cost, different metrics can be utilized, such as distance, number of hops, latency, among others, whereas the capacity of a link is defined by the number of frequency slots available (F) according to the bandwidth of the optical fibre's bands used for transmission and DWDM grid deployed, as described in Fig. 1.2.

Subsequently, all optical networks have the purpose of transporting different types of traffic demands between their nodes. Each traffic demand is characterized by its pair of source/destination nodes contained in V and its bit-rate measured in Gbit/s that represents the rate at which the bits of data are transferred from one node to another. In this Thesis, the traffic demands are defined by the set $D = \{d_1, d_2, \dots, d_{|D|}\}$ where each traffic demand in D is characterized by its end-nodes and bit-rate.

On the other hand, there are two types of network traffic: static and dynamic. For the static traffic, a set of time-invariant traffic connections are known in advance, and it is typically defined by a traffic matrix

that quantifies the traffic demands between all pairs of origin and destination nodes in an optical network. In this case, the goal of the problem is to accommodate all traffic at the expense of the minimum network resources utilized for transporting the traffic. Regarding the dynamic scenario, the traffic requests arrive over the time and are released throughout the network lifecycle. Therefore, the transport of the traffic is dynamically established by the reuse of the resources available at each moment.

To efficiently transport all the traffic, high-capacity optical channels are used to carry the aggregation of different types of traffic. The optical channels are characterized by the transmission format where each format is represented by the modulation format, symbol rate (measured in Gbaud), the total bit-rate/capacity (measured in Gbit/s), the channel bandwidth and the optical reach. Moreover, the capacity of an optical channel represents the maximum rate that the bits can be transmitted between two network nodes. Each channel can carry different types of traffic and it could happen that only part of the total capacity is occupied called load capacity and the remaining capacity available is designated residual capacity. The channel bandwidth is the amount of spectrum utilized by the format. The optical reach is typically defined by the maximum distance that the format can transmit the channel without having to regenerate the signal. The bit-rate, optical reach and channel bandwidth of the optical channels is conditioned by the modulation format and symbol rate utilized.

In order to illustrate the aforementioned concepts, Figure 2.3 presents a detailed translucent network design example, where the channels are selectively added/dropped at some intermediate nodes while expressing through others. The optical network defined by a graph is depicted in Fig. 2.3 (a) where the cost metrics represent the real distances between the network nodes, whereas the definition of a traffic demand between the network nodes 1 and 4 at 10 Gbit/s is set in Fig. 2.3 (b). The optical channels to transport that traffic demand are defined in Fig. 2.3 (c) with different bit-rates. As mentioned in Chapter 1, the recent transmission technologies support a wider range of optical channels' modulation formats

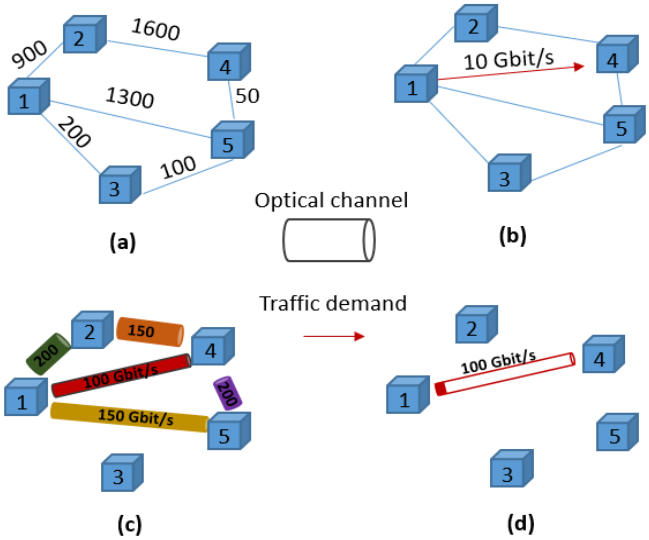

Figure 2.3 Main concepts of designing a translucent optical transport network: (a) Optical Network, (b) Traffic demand's definition, (c) Optical channels' computation and (d) Transport of the traffic demand (1-4).

and symbol rates that lead to different capacities and optical reaches trade-offs. Finally, Figure 2.3 (d) represents an example of the transport of the traffic demand between the network nodes 1 e 4 that uses a direct optical channel via 1-2-4 route with 100 Gbit/s bit-rate, QPSK modulation format and 32 Gbaud symbol rate. Note that, only part of the optical channel's capacity is occupied to transport the traffic demand at 10 Gbit/s and therefore the remaining residual capacity (90 Gbit/s) can be used to transport other traffic demands.

2.1.1 Transport Architecture of OTN over DWDM

The OTN architecture is made up of several components that constitute the hierarchy depicted in Fig. 2.4 (a) for communication between two network nodes. The optical transport module is the structure transported across the nodes and it has two main domains: electrical and optical domain. In the electrical domain, the different signals of the clients are mapped into the Optical Payload Unit (OPU), which is responsible for encapsulating the client-data (e.g., 1, 10, 100 Gbit/s Ethernet, Fibre Channel, etc.) and adding its own overhead that allows the OTN to manage the transport of this data. The OPU is then converted to Optical Data Unit (ODU) through the introduction of the overheads required. Finally, one obtains the Optical Transport Unit (OTU) by adding the corresponding overhead and the FEC field. The FEC works by adding redundant bits at the transmitter side using the Reed-Solomon code, while at the receiver a decoder uses these control bits to detect and correct transmission errors [56]. The transition to optical domain is achieved by modulating an optical source (laser) by the OTU signal, originating the optical channel (OCh). As defined in the previous section, each optical channel corresponds to an optical connection between two nodes of the optical network.

The optical multiplex section (OMS) is responsible for multiplexing the different optical channels and assigning the respective wavelengths, originating a DWDM signal. Note that, the aim of Fig. 2.4 (b) is to illustrate the different segments of the OMS layer. In detail, the optical terminal multiplexer (OTM) is a network element that delimits the OMS section, and it is responsible to multiplex the different wavelengths into an optical fibre via the optical multiplexer (MUX) and also demultiplexes a DWDM signal into individual wavelengths via the optical demultiplexer (DEMUX). In this context, the OTM includes three functional elements: line interfaces, wavelength (de)multiplexers and optical amplifiers, meaning that it can either be composed by line interfaces, a MUX and a pos-amplifier at the transmitter node or by line interfaces, a DEMUX and a pre-amplifier at the receiver node, as described in Fig. 2.4 (b). In detail, the pre-amplifier before the DEMUX compensates the losses of the previous span of the fibre, while the pos-amplifier after the MUX compensates the pass-through losses of the WDM multiplexer.

Another important piece of the OTM is the line interface or transponder, since it maps the client signals into the OPU/ODU/OTU by implementing the aforementioned functions and also generates the optical channels, providing the required OEO capability. The line interface's technology is considered to be among the most expensive devices in a transport network since it is used to transport each optical channel individually. Furthermore, it also allows the change of optical channels' wavelengths by first converting them to electrical domain (OEO functionality) and the monitor of the optical channel's bit error

rate (BER). Finally, the OMS transmission section is also composed by individual optical transmission sections (OTS) that are defined by the optical line amplifiers placed in the middle of the optical fibre, as depicted in Fig. 2.4 (b). Note that the optical line amplifiers are placed in the middle of the optical fibre with periodical breaks of 80-120 km with the objective of amplifying the optical signal without the need to convert it to an electrical signal, defining the different OTS sections. Moreover, the deployment of EDFA technology as an optical line amplifier has enabled the amplification of multiple channels simultaneously.

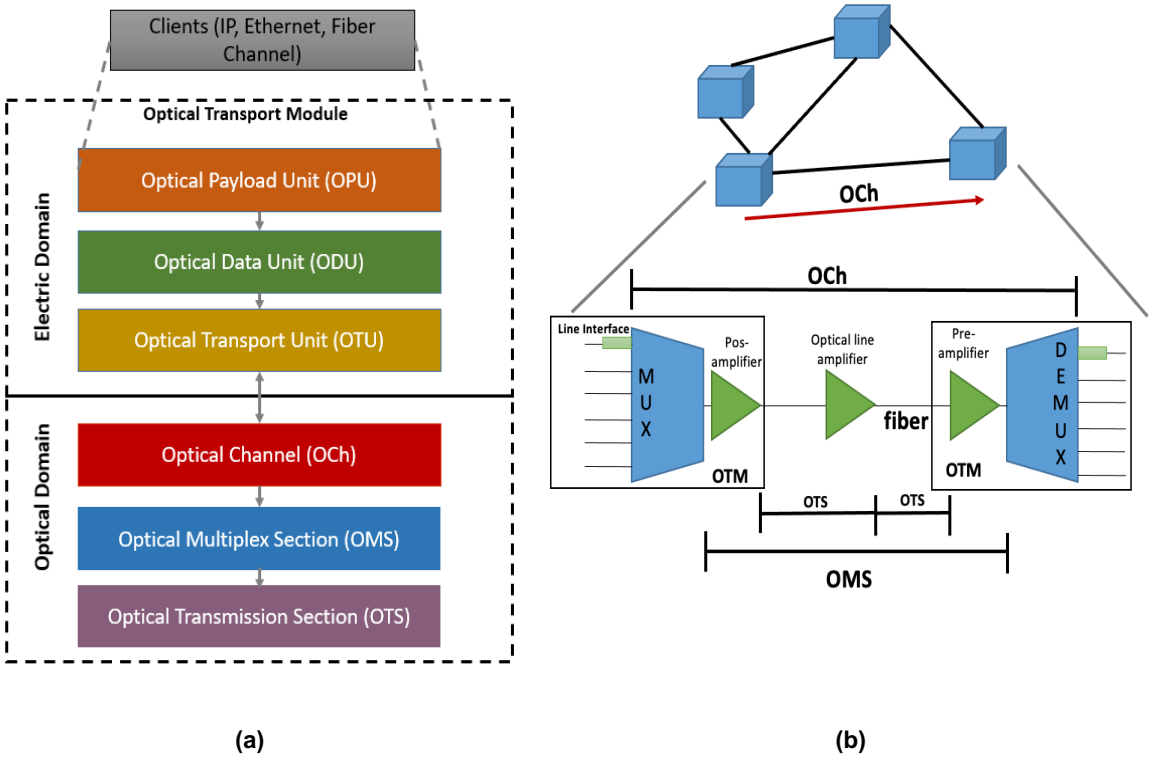

(a) (b)

Figure 2.4 (a) Optical transport module and (b) Segments of the optical multiplex section.

2.1.2 Optical Impairments and Performance Evaluation

The provisioning of optical channels to transport the traffic is one of the key topics when designing an optical transport network, since the transmission of signals over optical channels accumulates a set of impairments that may degrade the quality-of-transmission of these signals and prevent its correct detection at the receiver side of the network nodes.

2.1.2.1 Optical Impairments

As optical channels' transmission involves longer distances and higher bit-rates, the linear effects of the optical fibre like attenuation and dispersion become important limiting factors. Fortunately, the effect of these impairments can be prevented by relying on countermeasures such as using optical amplifiers to compensate for the fibre attenuation and dispersion compensating techniques to overcome the dispersion. However, besides amplifying the signal, optical amplifiers also introduce noise designated as amplified spontaneous emission (ASE) that could affect the transmission of the signal. Therefore, it

is paramount to compute the optical signal-to-noise ratio that is calculated by the ratio of the optical signal power over noise power at the destination node of the channel in order to quantify the impact of noise on the optical signal and guarantee its correct detection at the optical receiver.

On the other hand, the dispersion effect [57, 58] can be compensated in the optical or electric domain. Direct detection systems use dispersion compensation in the optical domain by relying on dispersion compensation techniques, while coherent detection systems compensate for the dispersion in the electric domain through the use of digital signal processing [59].

In the context of DWDM systems that transmit multiple channels simultaneously, the nonlinear effects in the fibre also present a severe limitation. The nonlinear effects arise due to the dependence of the refractive index on the intensity of the applied electric field. One such nonlinearity is the cross-phase modulation (XPM) that arises from the interaction between two signals transmitted over different optical channels on a DWDM system (e.g., one signal influences the variation of phase in the other) [60]. On the other hand, four-wave mixing (FWM) occurs when the light of three different wavelengths is launched into a fibre, giving rise to a new wave [61]. In the context of multi-band transmission system, the main nonlinear effect is the Inter-channel Stimulated Raman Scattering (ISRS), which is responsible for transferring optical power between different channels (from the lower wavelengths to higher ones) due to the Raman effect [62]**.** These nonlinear effects can distort the signal [28, 63, 64] and should be properly addressed when evaluating the performance of a channel.

2.1.2.2 System Design

The transmission characteristics directly influence the design of the whole OTN. An acceptable OSNR level at the optical receiver depends on the receiver sensitivity and the desired system margin, where the receiver sensitivity is defined as the minimum average optical power necessary to achieve a specified BER measured at the optical receiver input. A network is typically designed to perform better than a minimum acceptable level (receiver sensitivity) to account for the different effects that can deteriorate the performance (e.g., aging of network components) that are included in the system margin. Two other important system properties that affect the optical reach (i.e., the maximum distance that a channel can be transmitted without regeneration defined in 2.1) include the spacing between channels in the optical spectrum (closer spacing reduces the optical reach) and the initial launched powers of the optical signals. Increasing the launched powers, increases the optical reach up to a certain point but if the signal power is too high, the nonlinear effects will also have a negative impact on the optical reach, implying that there is an optimum power level, which is system dependent.

Other important design options are the optical signal modulation format and the detection method at the receiver. Over the years, coherent detection has been the approach adopted to achieve higher spectral efficiency while maximizing the OSNR, replacing the direct detection method used in the first generations of optical communications systems. The digital coherent receiver enables the use of a variety of spectral efficient modulation formats, such as QPSK and *M* QAM, and higher symbol rates. On the other hand, digital coherent technology is enabled by fast analog-to-digital converters and advanced signal processing in the electric domain. In addition, the fact that the phase information is

preserved after the detection allows to compensate for the linear transmission impairments, such as CD and PMD, as referred before, via digital signal processing. Note that, the digital signal processing functions (e.g., dispersion compensation) acting on the optical channel can be performed at the electrical stage after detection [7, 65, 66].

A. Evolution Line Interfaces Technology with Coherent Detection

As mentioned in 2.1.1, the line interfaces are responsible for generating the optical channels at different modulation formats and symbol rates. In this context, different generations of optical line interfaces have been developed throughout the years based on the evolution of coherent detection, as depicted in Table 2.1. This table highlights the main characteristics of the optical channels (capacity and optical reach) for the different generations of line interfaces [29]. The optical reach estimation is based on the evolution of the spectral efficiency as a function of the relative reach presented in [67] for each modulation format and symbol rate, assuring the required quality-of-transmission of the channels. Note that, the spectral efficiency of the QPSK modulation format is equal to 2 bit/s/Hz (each carrier phase represents two bits of data), whereas the spectral efficiency of the modulation formats *M* QAM is equal to $\log_2 M$, as described in [68].

Table 2.1 Optical channel formats for the different generations of coherent line interfaces based on [29].

Mod. Format	**1st Gen. (32 Gbaud)**		**2nd Gen. (32 Gbaud)**		**3rd Gen. (64 Gbaud)**	
	Capacity (Gbit/s)	**Reach (km)**	**Capacity (Gbit/s)**	**Reach (km)**	**Capacity (Gbit/s)**	**Reach (km)**
QPSK	100	3600	100	3600	200	3000
8 QAM	-		150	2400	300	2000
16 QAM	-		200	1000	400	850
32 QAM	-		-		500	350
64 QAM	-		-		600	150

In detail, the first generation of line interfaces operating with coherent detection used the QPSK as modulation format, allowing to increase the spectral efficiency, compared to the direct detection, through transmission/reception of channels at 100 Gbit/s over the 50 GHz fixed DWDM grid and using a symbol rate of 32 Gbaud [26]. The novelties of the second generation of line interfaces are the following: 1) better digital signal processing, namely better FEC introduced in the generation OTU layer described in Subsection 2.1.1 and 2) the support of higher-order modulation formats, namely 8 QAM and 16 QAM. As described in Table 2.1, this evolution allows to increase the capacity per optical channel being

deployed, albeit at the expense of reducing the optical reach [12]. Note that, the utilization of higher bit-rates channels increases the impact of ASE noise and nonlinear effects that reduces the maximum distance that a channel can be transmitted without regeneration.

The third generation of line interfaces will bring the following novelties: 1) the provisioning of optical channels with higher modulation formats, up to 64 QAM, 2) better DSP and progress in high-speed electronics that allows to create optical channels with higher symbol rates (64 Gbaud) [69]. This generation will enable lower cost per bit transported by augmenting the capacity per optical line interface via operating at higher symbol rates and/or using higher order modulation formats. For example, it becomes possible to transmit 200 Gbit/s QPSK optical channels over ultra-long-haul networks (previously only 100 Gbit/s optical channels were possible using this modulation format) with minor reach penalty due to operating at higher symbol rate, as shown in Table 2.1. However, the utilization of higher order modulation formats reduces the optical reach due to the accumulation of ASE noise and nonlinear effects, whereas operating at higher symbol rates implies adopting a flexible DWDM grid, since the fixed grid of 50 GHz is no longer sufficient to ensure a reasonable filtering tolerance to transport these channels.

The evolution of line interfaces is associated with the use of higher order modulation formats, particularly *M* QAM. This modulation scheme is obtained through changing the amplitude of two carrier waves with the same frequency and out of phase with each other by 90° (quadrature). These modulation formats can be described by using a constellation diagram, in which the position of the symbols transmitted is shown in a two-dimensional plane with the axes representing the phase of the two carriers (in-phase/quadrature) and the number of bits transmitted per symbol (e.g., 4 and 6 bits per symbol for 16 and 64 QAM, respectively). Figure 2.5 shows the constellation diagram of 16 and 64 QAM modulation schemes. In the 16 QAM, the constellation shows 16 symbols, where each symbol represents 4 bits, while the constellation of the 64 QAM shows 64 symbols, where each symbol represents 6 bits. The Fig.

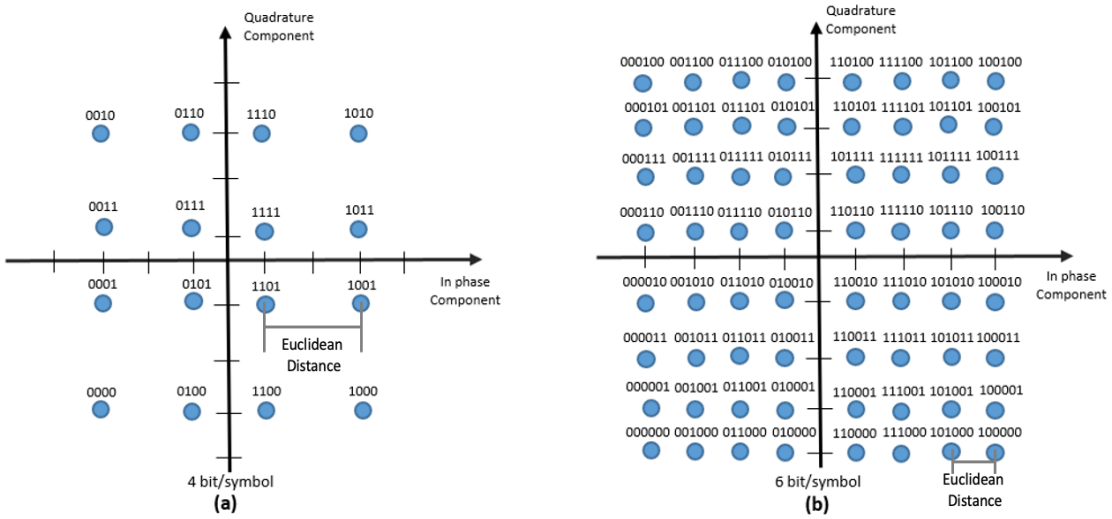

Figure 2.5 Constellation diagrams of the (a) 16 QAM and (b) 64 QAM modulation formats.

2.5 also highlights that the Euclidean distance between the digital symbols reduces significantly when using higher order modulation formats, which become the transmissions less tolerant to ASE noise and nonlinear effects, following the same information provided in Subsection 2.1.2.1.

The following generations of coherent line interfaces are foreseen to be capable of operating at symbol rates of 100 Gbaud or even beyond in future [70]. In order to illustrate the evolution of the consecutive generation of coherent line interfaces, Fig. 2.6 shows the increase of capacity transported via the use of higher order modulation formats (up to 64 QAM) and symbol-rates (up to 100 Gbaud). Prospectively, the use of 100 Gbaud combined with 64 QAM modulation format enables the use of 800 Gbit/s per optical channel being deployed. The capacity of 800 Gbit/s per optical channel being deployed was demonstrated in the study presented in [71].

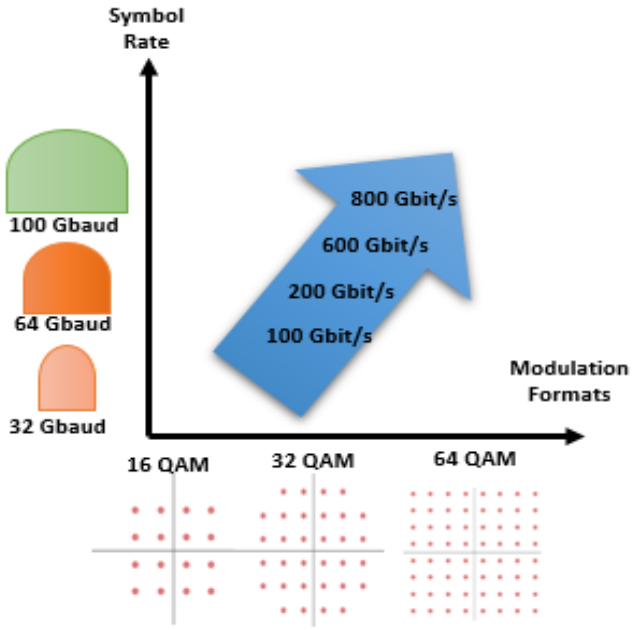

Figure 2.6 Two axes of optical capacity scaling.

2.1.2.3 Optical Performance Evaluation

The performance of an optical channel is usually measured in terms of a quality-of-transmission (QoT) metric like OSNR or BER. In order to estimate these metrics, it is necessary to perform complex and time-consuming computations due to the accumulation of many optical impairments throughout the transmission paths [72] and if possible, a live network trial should be performed in order to analyse the transmission of channels in real conditions [71, 67]. Typically, the models for performance estimation can be classified into two main categories: 1) comprehensive simulation models (e.g., split-step Fourier method [73]) and 2) simplified analytical models (e.g., the Gaussian noise (GN) model [74, 75, 76]). The former can lead to rigorous results, but it relies on complex and time-consuming computations, whereas the simplified models, although not being so complex, can still lead to acceptable results. In order to compensate for the inaccuracies of the simplified models, the network designers typically add an error margin to guarantee the required signal quality during the channel lifetime. At the optical layer, the

margin of an optical channel is defined as the difference between the quality-of-transmission metric of the received signal and the threshold value above which the signal is deemed recoverable error-free.

In each case, it is always necessary to account for different deteriorations of the performance over time and throughout the network operation, such as long-term aging of network elements, interference from newly set up neighbouring channels and sudden failures. Therefore, the optical channels are typically provisioned with high enough margins, carefully chosen to guarantee an acceptable QoT under worst-case scenarios and to ensure that the channel has enough signal quality until the network end-of-life [45]. These margins are divided into three types: design, system and transmission margins, as described in Fig. 2.7. The design margins account for inaccuracies in the optical performance modelling (e.g., GN model), whereas the system margins consider the time-varying network operation conditions like nonlinear effects and network equipment aging (e.g., increasing fibre losses due to splices to repair fibre cuts, degrading amplifier noise factor, etc.). Finally, the transmission margins encompass the transmission channel degradation, i.e., the degradation of the capacity transported by the line interfaces equipment. These margins, measured in dB, are then added to the calculation of QoT metric in order to guarantee that the channel is feasible up to the end of the network operation, where usually 2 dB of margins are set aside in the computation of the optical channels' performance.

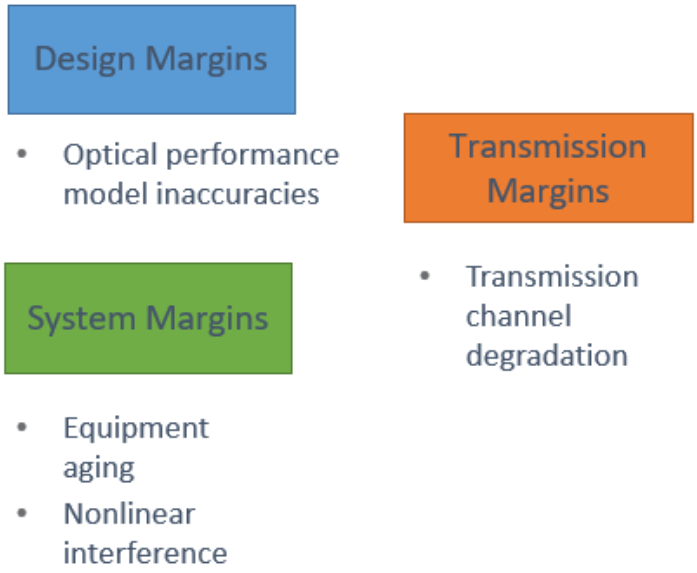

Figure 2.7 Different margins added to the optical channels' performance estimation [45].

In this Thesis' scope, the GN model developed by the author in [29] is fully utilized for the different analyses throughout this work. This model starts by calculating the performance of each optical channel at the end of the path measured in terms of the OSNR metric defined in the formula (A.1) of Appendix A, which considers the OSNR at the add, intermediate, and drop ROADM along the path as well as the OSNR after transmission along the fibre span. Based on this computation, the residual margin of an optical channel is determined by the difference between the OSNR at the end of the path given by the formula (A.1) and the required OSNR in back-to-back operation plus the system margin (defined in Fig. 2.7) to achieve an acceptable channel's performance, as described in Equation (A.5) of Appendix A. Note that, the calculation of the system margin defined in the formula (A.6) includes the 2 dB margins

depicted in Fig. 2.7 and the filtering penalty due to the cascade of WSSs traversed by the optical signal. In this context, the channel is feasible if the residual margin is superior to zero, otherwise it is unfeasible. All details of the computation of the optical channels' residual margin provided by the GN model are presented in Appendix A. Moreover, this computation assumes the impact of ASE noise and nonlinear effects on the performance of the optical channels considering that the dispersion effects are compensated by the coherent receiver at the electric domain.

2.1.3 Network Planning and Traffic Modelling

The planning of an optical transport network is a broad term that addresses a variety of different approaches. These actions can be divided between topological design and capacity planning [77, 78]. The former is responsible for defining the network infrastructure, deciding on the location of switching points (network nodes) and the fibre layout connecting them [77]. Topological optimization is applied for scenarios where no infrastructure is predefined and there is room to decide the placement of nodes and links (greenfield scenario). This type of optimization is usually utilized for access networks that frequently need to be expanded to other regions that did not have the service before [79]. On the other hand, transport networks in the context of brownfield scenarios [80], which are the ones addressed in this Thesis, have typically a predefined network topology by the network operators. For this reason, this work assumes that the physical topology is known in advance, and it is an input parameter of the different optimization frameworks developed.

On the other hand, capacity planning is the process of provisioning the necessary equipment and resources (e.g., line interfaces and spectrum) to ensure that all traffic demands are properly served. In general, the capacity planning involves the routing, traffic grooming and spectrum assignment as the most important procedures [81, 82] to efficiently transport traffic over the feasible high-capacity optical channels. However, in some scenarios both capacity planning and topological design problems are combined with the aim of minimizing the deployment of new fibre rollouts and the number of network resources that have to be acquired to serve the traffic demands, mainly in scenarios where the optical fibres previously deployed are not enough to transport high-capacity traffic.

The network planning problem can be formulated using a single-period or a multi-period approach. The former assumes a static set of traffic demands forecasted in advance, before the capacity planning takes place, while the latter considers a new set of traffic demands at each planning period and must be served according to the resources already deployed in the previous periods to transport the traffic and via available new or idle equipment [83]. The multi-period scenario can also be considered as a dynamic approach if a percentage of traffic demands is removed at the end of each planning period that could result in transport resources being released.

2.1.3.1 Optimization Algorithms for Planning an OTN

Based on the capacity planning process and assuming the single-period or each period of the multi-period approach, the design of the optical transport network starts by commonly receiving as input the network physical topology and the set of traffic demands to be served. As mentioned before, the network

physical topology is typically defined as a graph, representing the network nodes and optical fibres. On the other hand, each entry of the set of traffic demands is mainly defined by the end-nodes and bit-rate.

For each traffic demand, the *k*-shortest paths are computed using the Yen's algorithm [84]. This algorithm operates by computing single-source *k*-shortest loopless paths for a graph with non-negative weights (e.g., real distances of the optical fibres between two network nodes) based on Dijkstra shortest path algorithm. Afterwards, the optical channels are calculated over the predefined shortest paths that allows to generate the final set of candidate paths for each traffic demand. Each candidate path can be established by one optical channel in case of transparent networks or by a set of optical channels, hereafter called optical channels' path (set of optical channels that integrate a certain path) for some translucent and opaque networks. The computation of the feasible optical channels is based on the optical performance model described in Subsection 2.1.2.3. Moreover, the modulation format used between two end-nodes is the one that provides the highest capacity with enough QoT to transport the traffic.

After defining the candidate optical channels for each traffic demand, the design of the optical transport networks relies on Grooming, Routing and Spectrum Assignment (GRSA) as the most important algorithms [82], with the aim of optimizing a given objective (e.g., minimize the number of line interfaces that have to be acquired, the total network cost and/or the total amount of optical spectrum utilized, etc.) [52, 53]. In general, routing is responsible for choosing the best path (set of optical channels) for each traffic demand, grooming defines how small traffic units generated by the traffic demands of the transport network are grouped into the optical channels that are considered to be larger units in terms of capacity [85].

Finally, the spectrum assignment algorithm is a variant of wavelength assignment problem (approach that assigns a single wavelength to each channel used for a fixed DWDM grid) adapted for a flexible DWDM grid [86, 87]. In case of spectrum assignment algorithm, the proper and contiguous number of frequency slots are assigned for each optical channel, guaranteeing that the contiguous spectral slots of different optical channels do not overlap in the same network links and imposing that the same contiguous spectral slots must be allocated in all network links of the optical channel (spectral continuity and contiguity constraints) [88].

The combinatorial optimization problem, like the GRSA problem that chooses the frequency slots and path for each traffic demands, has proven to be a NP-hard problem, which makes the problem computationally difficult to solve, mainly due to the combination of routing and spectrum assignment problems [51]. In order to overcome this complexity, one approach could be the division of the original problem into subproblems, such as aggregating the routing and traffic grooming to be solved as an ILP model in order to obtain a solution closer to optimality and employing a heuristic algorithm for spectrum assignment given its complexity [81].

In this context, the traffic grooming and routing problems can be solved via the use of a node-link or link-path ILP formulation [89, 90]. The former is based on multi-commodity flow routing [89], where the decision variables are the flows (optical channels) associated with each traffic demand. Paths are then

automatically discovered by ensuring the flow conservation between the source and destination nodes of the traffic demands. The link-path approach assumes that for each traffic demand a set of paths between their end-nodes is pre-calculated and the decision variables are associated with the end-to-end paths [90]. In this Thesis, the node-link approach is utilized with the aim of automatically discovering the most suitable set of optical channels to transport the traffic demands without being restricted to the predefined set of paths of the node-link approach. Note that, the work of this Thesis assumes that the network optimization framework receives the set of feasible optical channels as input (Subsection 2.1.2.3) and thus, the node-link seems to be the most suitable approach due to their decision variables being the flows (optical channels) associated with each traffic demand. On the other hand, the most common heuristic algorithms used for spectrum/wavelength assignment subproblem are [51]:

- Graph colouring: This approach, given *m* colours, aims at finding a way of colouring the vertices of a graph such that no two adjacent vertices share the same colour. The graph colouring problem is analogous to spectrum assignment in the sense that each optical channel used could be defined as a graph node and a link should be placed if two channels share the same link in the transport network. Therefore, the feasible graph colouring assignment could produce a spectrum assignment solution for all optical channels [91].
- Random: For each optical channel utilized, a random frequency slot is selected from the set of frequency slots available in all fibre links of the determined channel.
- First-fit: Frequency slots are indexed and searched in a fixed order according to their index number. The assigned frequency slot for a given optical channel is the one with the lowest index from among the candidate frequency slots over all links of the channel.
- Least-used: This algorithm requires access to the global network state in order to determine the frequency slot that is least used in the network. Based on this information, each optical channel is served with the least used frequency slot common to all network links.
- Most-used: In opposition to the previous methodology, the chosen frequency slot is the most used in the network for each optical channel.

Moreover, before applying the spectrum assignment, the optical channels are typically descending in terms of the number of 12.5 GHz frequency slots required (defined in Fig. 1.2 (c)) in order to assign first the channels that require a higher number of frequency slots with the aim of minimizing the spectrum fragmentation inherent of the fact that heterogeneous channel widths increase the misalignment of available spectral slots along the path [34, 92, 93].

To exemplify the different concepts presented before, a network design example is explained in Fig. 2.8, where the procedure starts by receiving as input data: the network topology and the set of traffic demands, described in Fig. 2.8 (a-b). Note that, it is assumed the design of a translucent network in the example of Fig. 2.8, since it is the most common scenario utilized in this Thesis. Routing path computation is performed via the k-shortest path algorithm for each traffic demand. For the sake of simplicity, it is assumed only one traffic demand and k=1 in the example of Fig. 2.8. In this case, it is considered a traffic demand between the network nodes 1 and 6 with a bit-rate of 10 Gbit/s and the shortest path computed is the [1-2-4-6].

Afterwards, the set of feasible candidate optical channels is calculated for each of the shortest paths based on the optical performance model (Fig. 2.8 (c)), e.g., one optical channel can be implemented between the source node 1 and destination node 6 with a capacity of 150 Gbit/s and modulation format of 8 QAM over the shortest path [1-2-4-6]. Therefore, the computation of the candidate optical channels over a given routing path allows determining how the traffic demand can be routed and groomed, as exemplified in Fig. 2.8 (d). For simplicity, this example assumes the utilization of the 2nd generation of line interfaces presented in Table 2.1 of Subsection 2.1.2.2.A that allows the operation of optical channels at 32 Gbaud using the modulation formats from QPSK to 16 QAM.

Finally, the optimization procedure selects the sequence of optical channels to transport the traffic demand with a predefined goal. In this case, the goal is to minimize the number of line interfaces utilized that is identical to the number of optical channels used multiplied by two, since this equipment must be placed in both end-nodes of the channel. In the example of Fig. 2.8, the optimization procedure selects the routing option one of Fig. 2.8 (d) for the traffic demand, i.e., the use of the optical channel 1 of Fig. 2.8 (c) between the network nodes 1 and 6 and requiring only two line interfaces (Fig. 2.8 (e)). Note that, the total number of optical channels between two network nodes is given by the rounded division of the total bit-rates of the traffic demands that the channel transports by the total capacity of the optical channel. See the example of Fig. 2.8, the traffic demand of 10 Gbit/s is routed over the optical channel between the nodes 1 and 6 with a bit-rate of 150 Gbit/s, since the bit-rate of the traffic demand does not exceed the total capacity (150 Gbit/s) of the channel it is only necessary one optical channel.

Finally, the spectrum assignment is presented in Fig. 2.8 (f), by assigning the optical channel 1 to the first spectral slot available in the spectrum of the network links that the channel traverses (1-2, 2-4 and 4-6) based on the first-fit approach. Note that, the use of optical channels that operate at 32 Gbaud allows the utilization of the fixed grid presented in Fig. 1.2 (a) without compromising the filtering penalty due to the cascade of WSSs traversed by the optical signal defined in the formula (A.6) of the optical performance evaluation (Subsection 2.1.2.3).

Although the planning and designing strategy of OTN presented in Fig. 2.8 is the one utilized in the work of this Thesis for the different types of optical networks (transparent, translucent and opaque), there are other approaches that can be applied mainly in the context of transparent networks. The impairment- based routing and spectrum assignment strategy is one example that has led to a large number of research efforts [63, 94, 95]. In detail, the impairment-aware routing algorithm includes the impact of the optical impairments described in 2.1.2.1 into the GRSA algorithm with the aim of selecting the optical paths to transport the traffic demands with minimum impairment effects on their transmission process. To use this approach, one challenge resides on converting the impairments information, especially nonlinearities, to a weight value so that the conventional routing strategies (e.g., Dijkstra's or Yen's algorithms) can be used. Importantly, this procedure was not utilized in this Thesis due to the difficulty of incorporating the different optical impairments into the routing algorithm and the inherent limitation of this approach being only applied for transparent networks. In this sense, the studies presented in this Thesis compute the set of feasible optical channels (considering the accumulation of the optical impairments throughout the transmission paths) before the GRSA algorithm is executed.

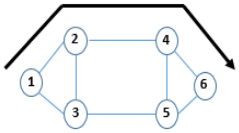

(a)

Demand	Source node	Destination node	Bit-Rate [Gbit/s]	K-shortest paths (links)
1	1	6	10	K=1->[1-2-4-6]

(b)

Optical channels

No.	Source node	Destination node	Bit-Rate [Gbit/s]	Modulation Format	Links
1	1	6	150	8QAM	1-2-4-6
2	1	2	200	16QAM	1-2
3	2	4	200	16QAM	2-4
4	4	6	200	16QAM	4-6
5	1	4	150	8QAM	1-2-4
6	2	6	200	16QAM	2-4-6

(c)

Candidate Paths- Demand 1

Path	Optical Channels Used
1-6	1
1-2|2-6	2 , 6
1-4|4-6	5 , 4
1-2|2-4|4-6	2, 3 , 4

(d)

# Optical Channels	#Line Interfaces
1	2

(e)

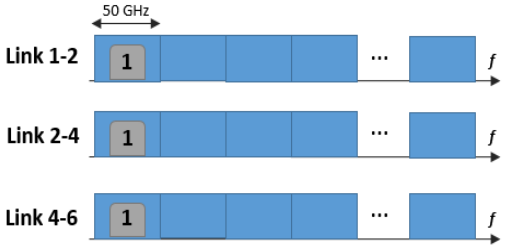

(f)

Figure 2.8 Example of optical transport network design including GRSA.

2.1.3.2 Survivability Design

The requirements for network planning in OTN over DWDM networks include the necessity of ensuring that traffic is resilient to failures in the network, mainly in the presence of high-capacity channels that transport different types of traffic where a single channel failure can cause a substantial impact in the network operation [96, 97]. Therefore, the support of survivability schemes becomes paramount in order to ensure resilience to common failures, such as fibre-cuts and transmission hardware defects [98]. The survivability could be based on protection mechanisms or on restoration procedures. A definition to distinguish them is that protection relies on dedicated or shared backup resources determined in advance, reserved and preconfigured for a particular traffic and which can be quickly triggered to replace working resources in the presence of failures. On the other hand, the restoration mechanism does not utilize dedicated resources and backup paths are only assigned upon recovery from a failure. Additionally, the restoration can be defined as Dynamic Source Rerouting (DSR) if the resources for backup paths are computed after the failure occurs or as Preplanned Shared Restoration (PSR) which ensures that the spare resources are readily available in the network for promptly provisioning backup paths. In this context, if a path fails, the preplanned restoration is provisioned to promptly provide a replacement of the failed working path (i.e., a backup path is computed on demand) [99].

As mentioned earlier, survivability mechanisms can either use dedicated capacity, where spare capacity for each path is exclusively allocated for one protection path, or shared capacity, where spare

capacity can be shared among several connections [100, 101]. This distinction is illustrated in Fig. 2.9, where two working paths are protected by backup paths that share a common link. In the dedicated survivability mechanism, the backup resources (e.g., the spectrum, regenerators or line interfaces assigned to the backup paths) are reserved for a single connection, as shown in Fig. 2.9 (a) where the backup paths use different spectral slots (f_1 and f_2) of the optical spectrum. On the other hand, the shared survivability scheme assumes that the backup resources can be shared among multiple connections under the assumption that the corresponding working paths do not share any network links, as illustrated in Fig. 2.9 (b) where the spectral slot assigned (f_1) is shared between the backup paths. This mechanism considers that two or more connections can share backup resources if their working paths cannot be simultaneously affected by a single link failure since the probability of occurring a failure in two network links at the same time is extremely reduced [102].

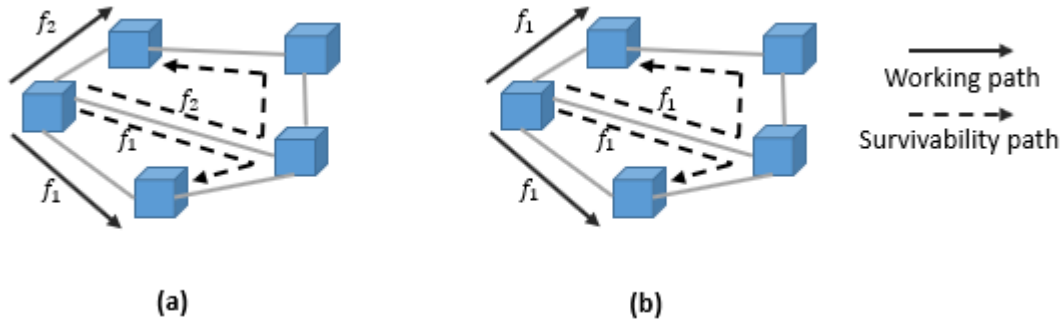

Figure 2.9 Survivability mechanisms with (a) dedicated and (b) shared backup resources.

Moreover, the protection/restoration mechanisms can be done at the electrical level (ODU layer), or at the optical level. In the optical layer, the protection/restoration switching can be done individually for each optical channel (OCh layer) or can take place at the OMS layer by switching all the DWDM signals. In this context, the protection/restoration schemes at ODU and OCh layer can be defined as path protection in the sense that a backup path between the source and destination nodes of the working path is applied (ensuring that the backup and working paths are disjointed) and the failure of the working path is only detected at the termination, whereas the protection/restoration at OMS layer is defined as link protection since only a local backup path between the endpoints of the failed link is used to route the traffic around it. The path protection at either ODU or OCh layer can also be defined as 1+1 or 1:1. The former assumes that the signal is replicated at the beginning of each path and sent over the working and backup paths and when the failure takes place the destination switches onto the alternative path, whereas the latter considers that no traffic is sent over the backup path during the normal operation and when the working path fails both source and destination nodes switches the signal to the backup path via the signalling overhead based on the automatic protection switching (APS) protocol.

In the work presented in this Thesis, 1+1 dedicated protection and preplanned shared restoration mechanisms are used at either ODU or OCh layer, thus Fig. 2.10 represents these survivability schemes. In detail, the use of 1+1 survivability mechanism at ODU layer enforces that the traffic demands are routed through disjoint paths simultaneously via different line interfaces, as shown in Fig.

2.10 (a). On the other hand, the 1+1 survivability mechanism at the OCh layer shares the same line interfaces for both working and protection paths (Fig. 2.10 (b)) and therefore the paths are constrained to use the same spectrum, symbol rate, and modulation format [99]. These survivability constraints have also to be properly addressed in the dimension of capacity planning approach through the GRSA algorithm.

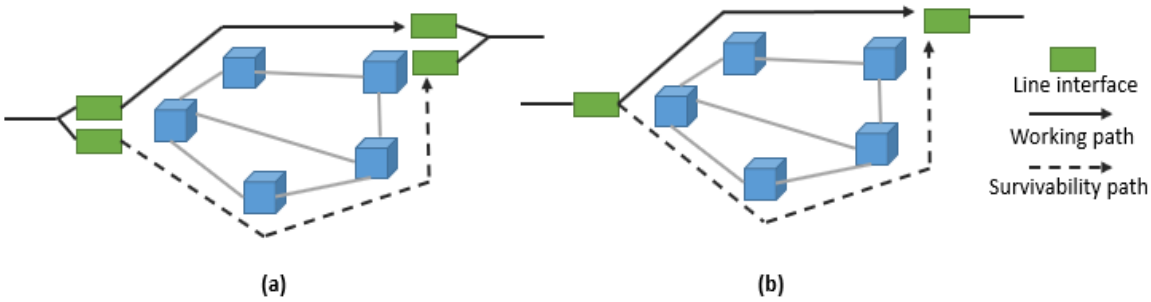

Figure 2.10 1+1 dedicated protection or preplanned shared restoration schemes at: (a) ODU layer and (b) OCh layer.

Moreover, the survivability mechanism (1+1 at ODU layer) described in Fig. 2.10 (a) can also be defined as being client-side protection in the sense that the client signal can be restored in the presence of a line interface failure. On the other hand, the survivability scheme of Fig. 2.10 (b) is considered to be line-side protection since it allows to switch/reroute the optical signal to a different path as result of a link failure but cannot ensure that the service is restored in the event of a link failure [103].

2.1.3.3 Node Architectures

Another important matter in the design of an optical transport network resides in the network node characteristics, which depends on the type of optical network (transparent, translucent and opaque). In general, the transparent network assumes that the traffic's switching within the network takes place exclusively at optical domain, whereas the opaque network assumes the switching at electrical domain, as described in Fig. 2.2. Finally, the translucent network is a combination of both transparent and opaque modes with some nodes switching at electrical domain and others at optical domain.

In this context, one of the most important network elements in the optical domain, as referred before, is the OADM, enabling the addition or drop of channels/wavelengths at each node, but also express the wavelengths through the node at the optical domain, as described in Fig. 2.11. In this example, the channel assigned with the λ_N is expressed through the node, whereas the channels with λ_1 and λ_2 are dropped and added in the node. As mentioned before, the line interface or transponder is responsible for mapping/demapping the client signal into the optical channel, providing the required OEO capability.

Moreover, the OADMs can be fixed or reconfigurable (ROADM). The former assumes that the set of wavelengths which can be dropped/added is fixed, while the latter adds flexibility by supporting dynamic optical channel switching and add/drop operations in response to traffic changes and this can be done remotely and in almost real-time. The reconfigurability of the ROADMs is achieved by using wavelength selective switch (WSS) [104] instead of the MUX/DEMUX blocks utilized for OADM architecture. The WSS is a 1xN bidirectional device that has typically a single input and N output fibres, with the capability

to independently route DWDM channels among the N fibres. The WSS selectively joins the different wavelengths from the various directions and feeds them to the corresponding optical fibre in order to be properly transmitted.

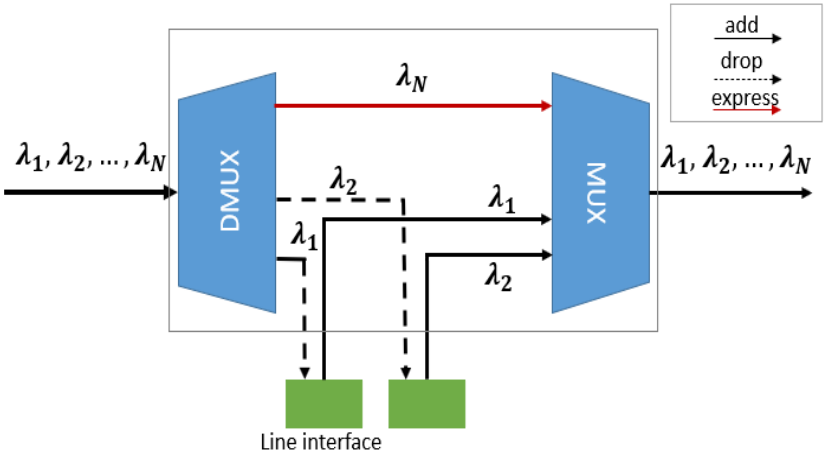

Figure 2.11 Architecture of the OADM.

The ROADM can also be defined as being colourless, directionless and contentionless (ROADM-CDC). In detail, a ROADM is considered colourless if a wavelength can be set under software control plane and it is not fixedly associated with any add/drop section, whereas the directionless feature assumes that any wavelength can be routed to any direction served by the network node by the software control plane. Finally, a contentionless ROADM guarantees that multiple add/drop operations are possible for a given wavelength [105]. The WSS-based ROADMs are typically based on two primary architectures: broadcast-and-select (B&S) and route-and-select (R&S) [106]. The former consists of a passive star coupler (SC) followed by a single WSS per ROADM node, with all signals broadcast onto the splitter output ports and subsequently selected at each WSS input port, whereas the R&S architecture utilizes two WSS per ROADM node. As a result, with this architecture, two stages of WSS are implemented at the input and output of the ROADM.

In this context, Fig. 2.12 and 2.13 depict the B&S and R&S ROADM-CD with a contentionless degree of 2 architectures, respectively. Based on these figures, it can be seen that the ROADM architecture is defined by two types of sections: the fibre port section that connects the ROADM to other ROADMs via the DWDM transmission systems and the add-drop section that connects the ROADM to the local line interfaces. The number of fibre ports defines the ROADM degree that in this example is considered to be equal to three. A three-degree ROADM switches in three directions typically called East, West and North. Moreover, the fibre port section is composed of a star coupler (SC) and WSS in the B&S architecture and by two WSS in the R&S architecture.

In the case of B&S architecture, the SC connects the ingress fibre to all the other fibre ports and to the drop section, whereas the WSS collects signals from the different directions and from the add section and multiplexes them into the outgoing fibre port. On the other hand, the use of WSS and SC at the add-drop section of B&S architecture enables the deployment of the colourless feature, since a tunable transmitter can be used in each SC local port and the receiver can be tuned to any wavelength at the

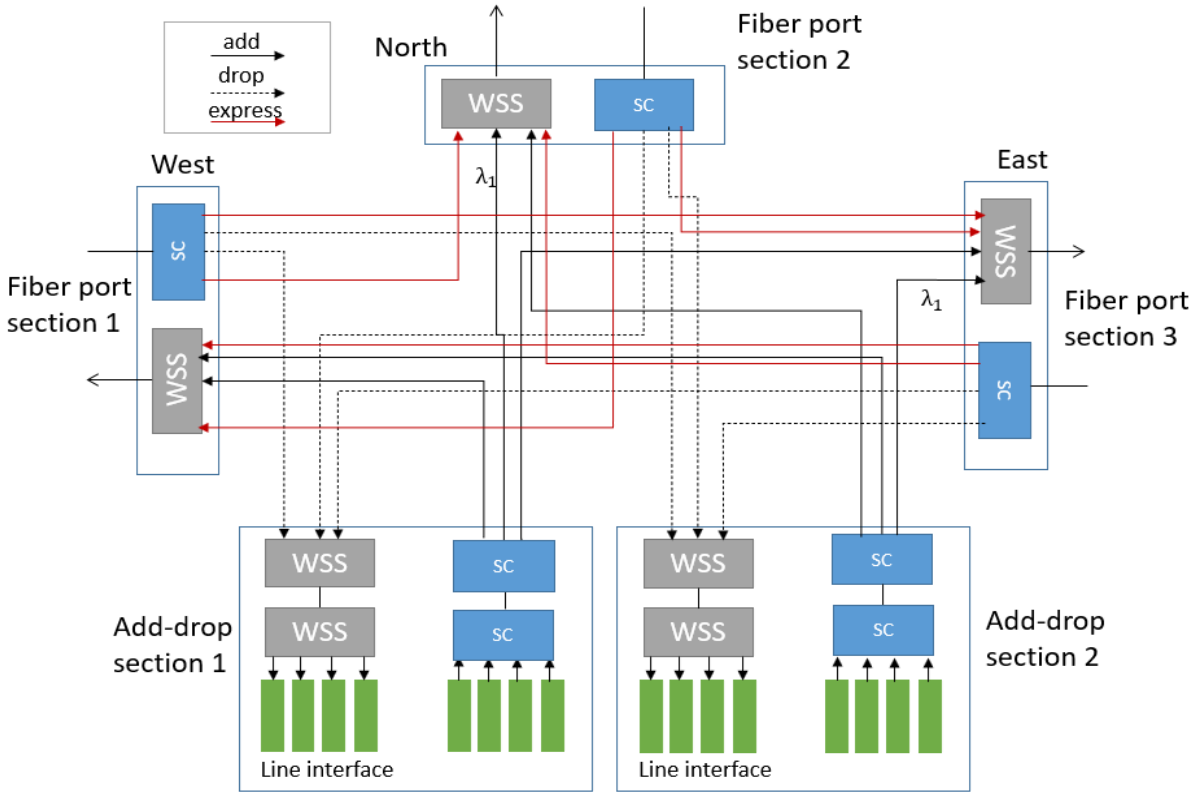

Figure 2.12 B&S ROADM-CDC architecture of a three-degree node with a contentionless degree of 2.

WSS local port. Note that the transmitter and receiver are inside the line interfaces. The fact that the add/drop section is common and shared by all fibre ports sections enables the implementation of the

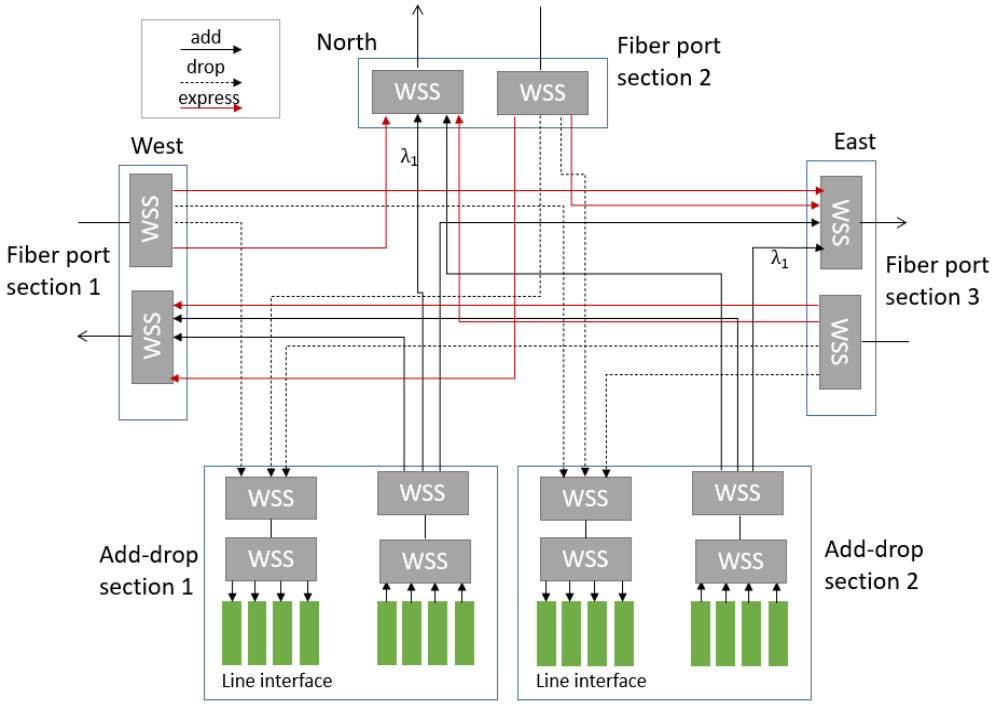

Figure 2.13 R&S ROADM-CDC architecture of a three-degree node with a contentionless degree of 2.

directionless feature where a SC is used to broadcast the added wavelengths to the WSS of each direction and a WSS is used to select the dropped wavelengths. By using two add/drop sections, one can use the same wavelength for two directions (contentionless degree equals to two), as described in Fig. 2.12 with the λ_1. In fact, the contentionless degree can be increased by augmenting the number of add/drop sections. The CD features of the B&S architecture can also be applied for the R&S, but the difference resides in the selection of the optical input signal by a WSS instead of broadcasting the optical input signal at the ROADMs input, as depicted in Fig. 2.13 where the SC blocks of B&S architecture are replaced by WSSs.

In case of translucent nodes, the aforementioned optical node architecture is combined with electrical hardware and switching equipment, which can properly map the signals onto optical channels suited for wavelength transport. On the other hand, the opaque network nodes are solely defined by the electrical hardware. With respect to transport node architecture, two main options are usually available regarding how client traffic signals are aggregated to be transmitted in the same optical channel. The first architecture, depicted in Figure 2.14 (a), assumes each client port (to which a client interface will be connected) to be hardwired to a given line port (i.e., line interface or transponder). This implies that any client signal reaching that client port will always be mapped to the optical channel, generated at the associated line interface, providing the required OEO capabilities. Note that, similar operations to de-map/de-aggregate the client signal will occur when considering the receiver side. The result is designated as a muxponder/transponder-based traffic aggregation [107]. More concretely, the transponder maps one client interface to one line interface (e.g., 100 Gbit/s Ethernet client interface to 100 Gbit/s line interface), whereas the muxponders aggregates/multiplexes the different client interfaces to a single interface (e.g., one to ten 10 Gbit/s Ethernet client interfaces to 100 Gbit/s line interfaces). The key characteristic of the transponder/muxponder approach is that client interfaces are statically mapped to the line interfaces and there is no ability to remotely switch client traffic between different line interfaces. Furthermore, most of the muxponders solutions have a limited range of compatible client interfaces typically 10, 40 and 100 Gbit/s and therefore sometimes it is necessary to resort to stacking of muxponders.

On the other hand, the second architecture, exemplified in Figure 2.14 (b), assumes that the client ports are decoupled from line ports and there is an electrical switch between them, which usually switches at the level of the ODU, known as OTN switch. This architecture is designated as OTN switch-based traffic aggregation. OTN switching provides an alternative to the transponder and muxponder approach, but not replacing the optical layer. The incorporation of an OTN switch enables the ODU client signals to be switched between interfaces, typically via centralized fabrics, mapping any client to any line interfaces and switching pass-through traffic between line interfaces. The centralized switch fabric is the basic topology of how a network is connected to switch the traffic, which is typically based on a switching matrix. Moreover, the operation of changing the optical channel, to which the client signal is mapped, can be triggered remotely without the need of on-site intervention and it is executed very quickly, with minimum disruption of running traffic [108, 49]. This solution offers significant benefits in terms of flexibility and the speed with which services can be provisioned and is also compatible with

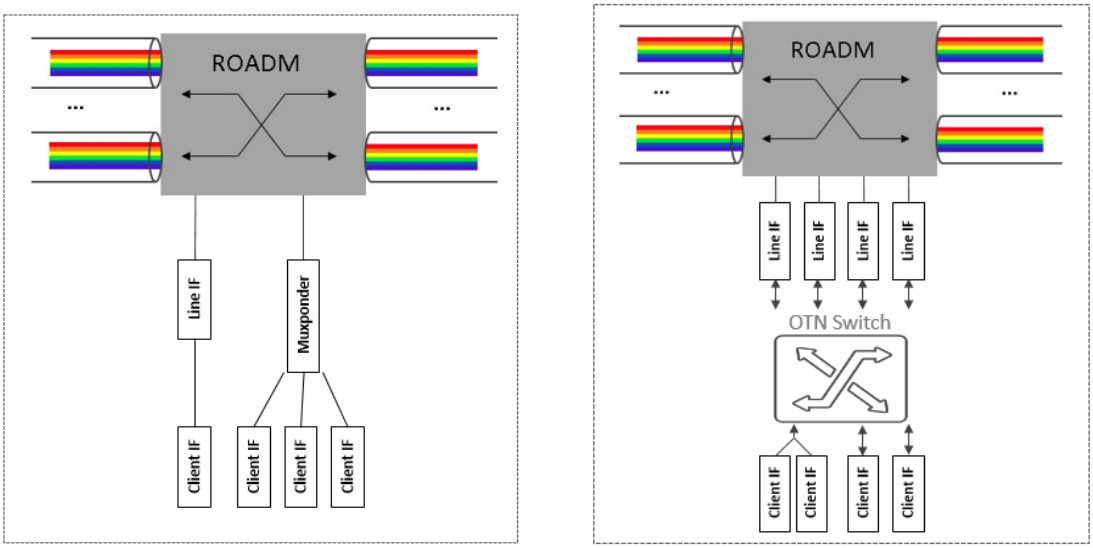

(a) **(b)**

Figure 2.14 (a) Muxponder/Transponder-based and (b) OTN switch-based traffic aggregation.

lower bit-rates traffic (e.g., 1.25 Gbit/s, 1 Gbit/s, Fibre channel, etc.) [109, 110]. In this context, Fig. 2.15 depicts the OTN switch concept where multiple client interfaces (e.g., 10 and 40 Gbit/s) can be switched among the different line interfaces via the centralized switch fabric.

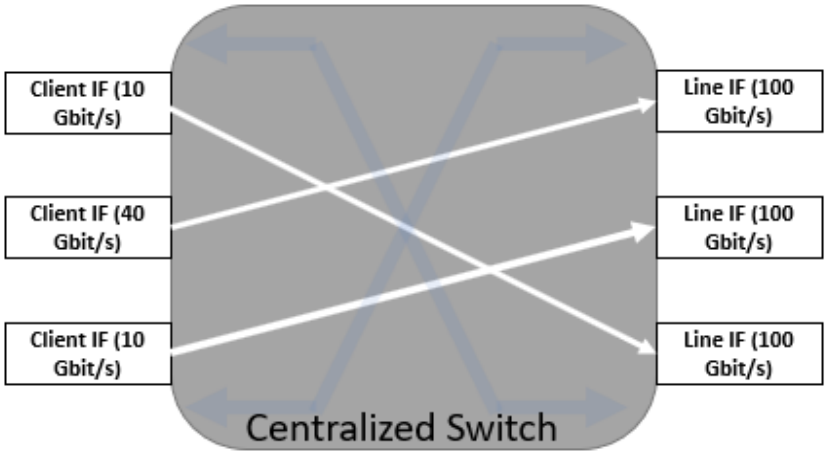

Figure 2.15 OTN switch concept with different client and line interfaces.

The muxponder/transponder-based traffic aggregation has a lower cost, assuming the same number of client and line interfaces deployed, since it avoids the cost of OTN switch deployed in the OTN switch-based traffic aggregation architecture. However, the flexibility of the second architecture means it offers more optimization options for the aggregation of client signals into optical channels, since the clients are no longer tied to specific wavelengths (channels) and it can potentially reduce the number of line interfaces required to transport the traffic [111]. The line interfaces are the most expensive elements of

a transport network due the OEO conversion equipment, thus the savings in terms of reducing these costs is likely to be significantly higher than the incremental cost of adding OTN switching functionality.

2.2 Future Trends of OTN

The recent advancements in OTN highlight the importance of changing the transport networks to become more intelligent and centrally controlled or programmed using software applications. This leads to the concept of Software-Defined Networking (SDN), since the SDN brings the opportunity of decoupling the control plane from a data plane that can be connected through a suitable application programming interface (API). In this context, the control plane can be seen as the network brain of SDN architecture that enables the network to be centrally controlled or programmed using software applications. This helps operators to manage the entire network autonomously and adaptively to complex network environments regardless of the underlying network technology [112]. These automation capabilities and the need to support more dynamic and unpredictable traffic patterns inherent from this new digital era [22] have empowered the concept of operating the network adaptively to the actual network environment, which involves the incorporation of new building blocks within the design process, such as telemetry and trend analytics platforms [113]. More precisely, this evolution allows identifying, predicting and resolving problems before they occur, enabling the reduction of operational (OPEX) and capital expenditures and the simplification of network operations and management.

One of the main advantages of the deployment of a real-time telemetry system is the ability to real-time monitor the key physical parameters of the networks since it allows to improve the optical performance estimation of the existing and new optical channels with current knowledge of the physical parameters of the network [46]. This ability combined with suitable forecasting methods to predict the evolution of performance through trend machine learning analysis [114, 115] paves the way to reduce the margins when provisioning optical channels. These margins are typically large enough to ensure QoT of the channels even considering design inaccuracies and the performance degradation from devices and fibre aging, as described in Subsection 2.1.2.3. In this context, the implementation of real-time monitoring platforms allows to reduce the long-term aging and design margins, since a degradation of components' performance can be detected in real-time and the optical performance estimation is more accurate when using the monitored input parameters [44].

This squeezing of margins will potentially enable the deployment of higher bit-rates using higher order modulation formats allowing to reduce the network cost [43]. See for example Fig. 2.16 in which, an optical channel with the number one, between the network nodes one and two, traversing a distance of 200 km, needs to be provisioned in the optical network to transport the traffic between those nodes. In this context, the typical provisioning approach that considers high enough performance margins described in 2.1.2.3 leads to using 32 QAM in order to guarantee that the channel is feasible until the network end-of-life based on the optical reach values defined in Table 2.1 of Section 2.1.2. This table highlights the maximum distance that an optical channel can be transported for each format considering the use of 2 dB margins depicted in Fig. 2.7 based on the optical performance estimation described in

Subsection 2.1.2.3. However, the evolution of real-time telemetry system allows to confidently predict the residual margin for each format in real-time and a degradation of performance can be detected, as shown in Fig. 2.16, which enables to mitigate some the effects that leads to the use of 2 dB margins in the system margin calculation defined in formula (A.6) of the optical performance estimation model presented in Appendix A. Consequently, the residual margin computation will be less restricted and the 64 QAM modulation can be applied for the optical channel 1.

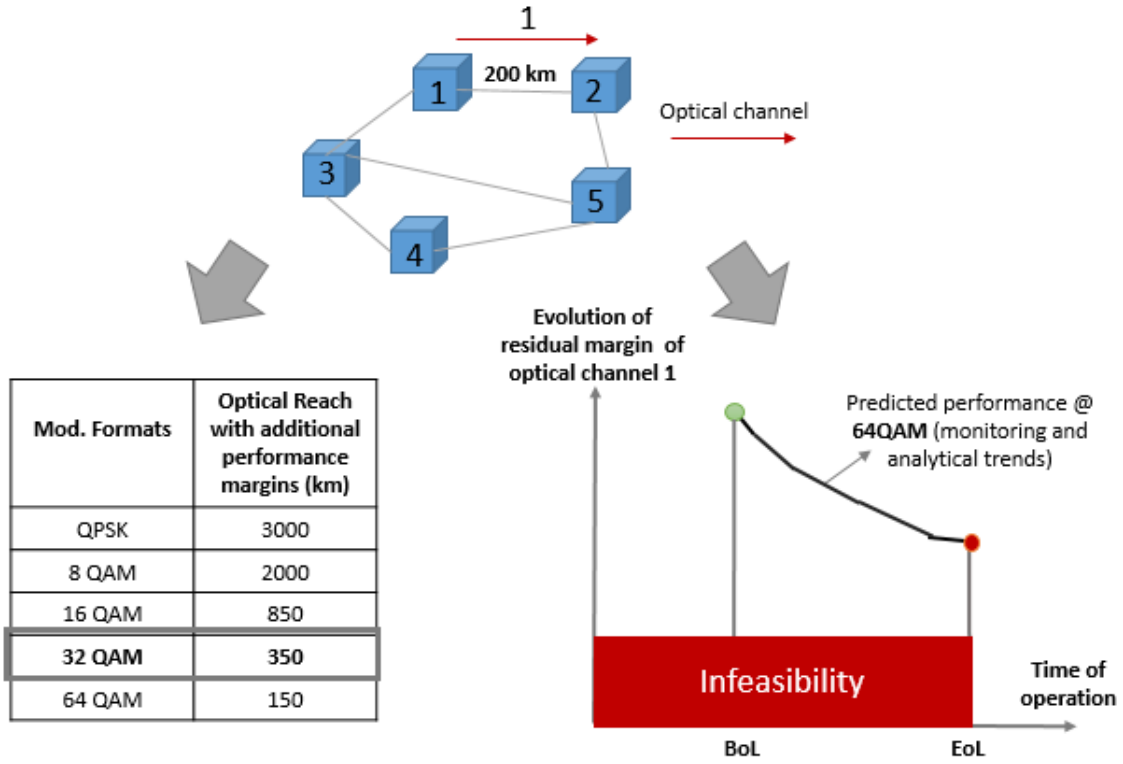

Mod. Formats	Optical Reach with additional performance margins (km)
QPSK	3000
8 QAM	2000
16 QAM	850
32 QAM	**350**
64 QAM	150

Figure 2.16 Optical channel provisioning comparison between utilization of additional performance margins at BoL and exploiting smaller margins.

Although there are clear benefits in shifting to provision optical channels with squeezed performance margins, operating transport networks with current-state-of-life information will require a different level of network vigilance and automation, since a degradation of performance can result in traffic disruption faster than expected. In order to take advantage of this potential to increase capacity in OTN, sophisticated procedures and network design applications (e.g., traffic rerouting, down-grade of modulation format or manual interventions through scheduling a maintenance window) should be investigated with the aim of provisioning channels with reduced margins, while minimizing the probability of traffic disruption due to any channel reaching the minimum acceptable performance limit.

The fact that the internet traffic is expected to continue to accelerate as a result of key events such as the rollout of 5G and massive Internet of Things, will inevitably translate into the need to augment capacity in transport networks. Traditionally, this increase has been possible via the deployment of consecutive generations of optical interfaces, each superseding the previous by providing both higher capacity and spectral efficiency (Subsection 2.1.2.2 A.) or by using more disruptive and innovative strategies to provisioning channels with smaller margins that leads to increase the capacity per optical

channel being deployed, as mentioned before. However, since most deployed optical transport networks operate using DWDM over a spectral window of approximately 4.8 THz in the C-band, the maximum capacity that can be transmitted over these networks is approximately restricted to 38.4 Tb/s/fibre [116, 117, 118].

Consequently, the capacity transported in OTN will be increased mostly via using more spectrum [39] through scaling the actual used technology or applying new ones. In this context, the most viable options to upgrade the available capacity of optical networks are the spatial-division multiplexing (SDM) via the use of multi-core/mode fibre or multi-parallel single-mode fibres and band-division multiplexing (BDM), which enables the transmission over more spectral bands of the optical fibres [119]. Currently, among all SDM solutions, only the multi-parallel SMF is commercially available, relying upon the availability of dark fibres (fibres not utilized that the operator owns in some networks) or the deployment of new ones. This solution is realized by replicating the mature and cost-effective C-band line system technology.

On the other hand, the remaining SDM solutions (multi-core/mode fibres) have high potential to increase transmission capacity in OTN, since by comparison with the single-mode fibre presented in Fig. 2.17, the multi-core fibres have multiple cores that can be employed for signal propagation [120] and the multi-mode fibre enables the transmission of different propagation modes over a larger core diameter when compared to the single-mode fibre' core. However, these solutions require a complete transformation of the optical transport environment, as they require the deployment of new fibres and more specialized equipment (e.g., ROADMs, amplifiers, etc.) [121]. Another key issue in these systems is how to suppress the inter-core crosstalk that arises from unwanted coupling between cores of a homogeneous multi-core fibre and the dispersion between modes in multi-mode fibre. These aspects that lead to high capital expenditures and complex logistics makes the use of these SDM systems less attractive for short- to medium-term applications. Moreover, dedicated multi-core fibres are in research phase and no available commercial solution in the telecommunication is yet available [122].

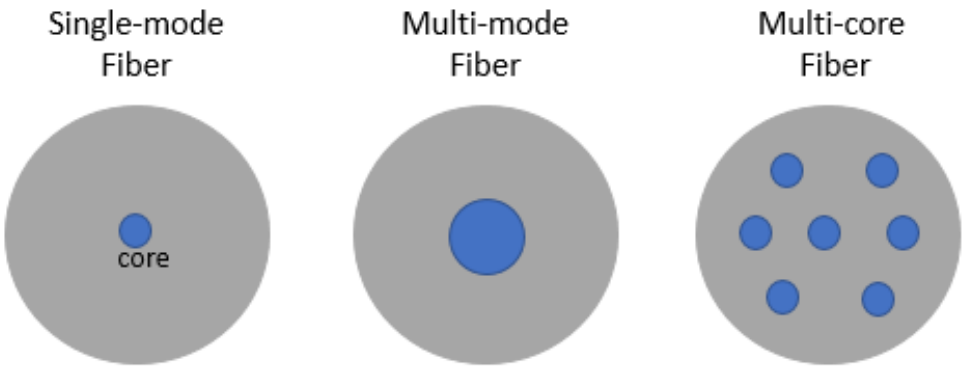

Figure 2.17 Schematic of single-mode, multi-mode and multi-core optical fibers.

On the opposite side, band-division multiplexing can maximize the return of the investment in the already deployed optical transport network infrastructure since it does not require the implementation of additional optical fibres (the BDM can be applied in the standard ITU G.652 single-mode fibres) [123],

being the most viable option to be utilized in short-term to increase the capacity transported in OTN. In this context, several works have evaluated the potential of using multiple spectral bands of optical fibre (from O- to L-band) [124, 125, 126, 127] and there are already available commercial solutions that enable the deploying of C+L transmission systems [128, 129]. These studies have properly addressed the joint multiband power control for BDM systems in order to avoid the impact on the channels' quality of transmission due to using multiple bands of the optical fibre to capacity transmission. Therefore, the BDM system requires the adaptation of the optical network components to support the transmission of data in different spectral bands, such as by designing the optical amplifiers with the best doped material for each spectral band. On the other hand, the optical performance evaluation described in 2.1.2.3 should also be adapted to properly address the impact of transmitting data in different spectral bands (e.g., by updating the noise figure of the optical amplifiers) [40, 41, 124]. Considering the spectral bands available on optical fibre, the next step of the research community seems to point towards the activation of S-band in order to continue increasing the number of channels that can be transported in the single-mode optical fibre [130].

Therefore, the research developments indicate that exploiting C+L-band based on a BDM system and introducing additional single-mode fibres are the only commercially available solutions that could be employed in the near future [41, 42]. In this context, the future investigation efforts should be made in order to provide novel network planning framework which (i) models geographically-dependent fibre upgrade expenditures; (ii) focuses on minimizing both the use of additional fibre and at the same time the number of additional network components required to adopt a C+L-band transmission system, since fibre and equipment investments are costly and strategic activities, mainly the expenditures associated with using additional fibres that can vary significantly, not only from network to network, but also within the same network. For instance, a transport network operator often owns dark fibre in some countries/ regions, while leasing fibre in the remaining ones where it is established. These constraints should all be taken into account when designing network planning frameworks for these different scenarios with the aim of minimizing the total network costs.

2.3 Chapter Summary

This chapter overviews the main networking concepts that serve as a basis for designing the next-generation of optical transport networks, emphasizing how the transport infrastructure can scale to transport more data in order to cope with the massive explosion of high-volume traffic from different applications (e.g., virtual/augmented reality, 5G). The definition of concepts starts by the introduction of the main optical transport network aspects, such as transport and node architecture, performance evaluation, network planning algorithms and survivability design, and finalizes with the description of the future trends of OTN that will be addressed in the context of this Thesis. In each part, the overview is, when possible, complemented with network design examples in order to illustrate the different subjects.

Chapter 3: Nodes Dimensioning

Planning an optical transport network involves the designing and dimensioning of the network nodes and links in order to serve the given traffic demands while minimizing the overall network cost. In a multi-layer network like the one based on the OTN over DWDM configuration, the network nodes must be responsible for functionalities at both electrical and optical layers. A possible solution to implement such nodes relies on using transponders/muxponders (Fig. 2.14 (a)) for the electrical operation together with ROADMs at the optical layer to provide optical switching and flexible add/drop functions. As mentioned before, the muxponders/transponders are responsible for mapping one or more client interfaces to line interfaces. The client/line interfaces will be responsible to receive/transmit individual client signals and aggregate/de-aggregate them into/from an optical channel [4]. Importantly, line interfaces are among the most expensive devices in a transport network. Therefore, minimizing their number is usually the primary objective of transport network design [53]. The utilization of muxponders/transponders is a quite simple approach, but it has a major drawback associated with the fact that the interconnection between client interfaces and line interfaces is fixed and there is no possibility to remotely switch client traffic to another line interface [107].

To overcome this limitation, one can add another network element to the node structure called OTN switch (Fig. 2.14 (b)). This solution supports a wider range of client interfaces and adds much more flexibility at the electrical layer in the sense that one can interconnect any client interface to any line interface, and at the same time switch express traffic between line interfaces. This universal switch architecture has been proposed with the aim of addressing the next-generation of OTN, since it enables the handover of client signals between any pair of line interfaces for attaining more flexibility within the grooming process [48, 49]. As expected, the muxponder/transponder solution has a lower cost, assuming the same number of client and line interfaces deployed, since it avoids the cost of OTN switch. However, the flexibility of using an OTN switch means it offers more options to groom client signals into optical channels, potentially enabling to reduce the number of line interfaces required. Therefore, there are inherent trade-offs to deploying or not OTN switches. Importantly, the extent of the benefits from installing an OTN switch at a given node of the network depend on both the traffic and network properties and, as a result, are difficult to evaluate without performing a complete dimensioning of the network with and without that OTN switch. Moreover, in order to minimize the overall CAPEX, the best network design may comprise OTN switches being deployed at only a subset of the network nodes and not in all of them.

Therefore, the goal of this chapter is to develop a framework that minimizes both the number of line interfaces and OTN switches utilized in the dimensioning of a translucent optical transport network. In this context, the proposed network planning framework addresses this subject as a multi-objective optimization problem to select the most cost-effective network nodes to place OTN switches, while at the same time keeping the number of line interfaces at a minimum value in order to be able to exploit different solutions with diverse trade-offs in terms of the number of line interfaces and OTN switches. The work described in this chapter has one journal publication associated with it [131].

3.1 Transmission/Switching CAPEX Trade-off

In the context of this chapter, the design process of a translucent optical transport network aims primarily at minimizing the CAPEX associated with the number of line interfaces utilized (transmission CAPEX) and to the number of OTN switches to be deployed (Switching CAPEX) since both represent a considerable increase in the capital expenditures, mainly the line interfaces that are among the most expensive devices in these networks. Importantly, the minimization of both objectives (i.e., number of line interfaces and number of OTN switches) can lead to conflicting results, meaning that minimizing one objective does not necessarily mean the other is also being minimized and vice-versa.

In order to illustrate the potential conflict inherent to this optimization problem, Fig. 3.1 shows an example of two different designing solutions that lead to conflicting results. In the example of Fig. 3.1, a set of five 10 Gbit/s traffic demands is to be routed and groomed over the network topology depicted in Fig. 2.8 (a). Two routing and grooming solutions are highlighted in this example. For each one of these solutions, the optical channels utilized by the traffic demands are illustrated as red arrows with the associated total capacities. The computation of the feasible optical channels is based on the optical performance model described in Subsection 2.1.2.3 using the 2nd generation of coherent line interfaces (Table 2.1) which computes the total capacity that each optical channel can support between the nodes of the network topology.

In this context, Solution 1 always selects the direct path to the destination and bypassing the intermediate nodes at optical layer, while solution 2 prefers in some cases to segment the traffic's path along the available intermediate nodes in order to create more room to share the optical channels capacity with other traffic demands and, in this way, improve the channel utilization. For example, the traffic demand 5 between the network nodes 1 and 5 will be served by the optical channels between the nodes 1-3 and 3-5, reusing the optical channels utilized by the traffic demands 3 and 4.

With solution 1, the intermediate nodes do not need to have OTN switches (only require the use of ROADMs that operate at optical layer). Note that, a network node is considered to require an OTN switch if it aggregates/de-aggregates traffic demands for which it is neither the source or destination node, as described in Subsection 2.1.3.3. However, this solution limits the ability to share the optical channels' capacity with other traffic demands, requiring the deployment of ten line interfaces to support five optical channels. Conversely, solution 2 exploits grooming at intermediate nodes to share the capacity of some of the optical channels among multiple traffic demands (three optical channels can be shared among five traffic demands). This allows to enable to reduce the number of line interfaces to six, albeit at the expense of deploying an OTN switch at two of the network nodes. Depending on the relative cost of line interfaces and OTN switches, as well as on other criterium that the network operator wants to set (e.g., network operator restricts the deployment of OTN switches in some network nodes), one solution will be preferable than the other will.

As shown in the example of Fig. 3.1, there is a potential trade-off between saving line interfaces and minimizing the number of nodes with an OTN switch. In this way, one can conclude that the designing of the electrical layer in a translucent OTN can be treated as a multi-objective optimization problem in

the sense that involves the simultaneous resolution of a problem with more than one objective function (i.e., the minimization of the number of the line interfaces and the number of OTN switches), which as seen are conflicting by nature [132]. To face this problem, the work presented in this chapter explores the use of genetic algorithms, more precisely multi-objective genetic algorithms. The goal of applying this approach is not necessarily to find a single solution, but instead a set of solutions of interest, called the Pareto front, that are considered optimal in the sense that it is not possible to find any other solution that improves a given objective without penalizing the other. In particular, genetic algorithms have shown to be capable to exploit vast solution search spaces and capture optimized solutions in complex scenarios [133, 134, 135].

Demand	Source node	Destination node	Bit Rate [Gbit/s]	K-shortest paths (links)
1	3	6	10	K=1->[3-5-6]
2	1	6	10	K=1->[1-2-4-6]
3	1	3	10	K=1->[1-3]
4	3	5	10	K=1->[3-5]
5	1	5	10	K=1->[1-3-5]

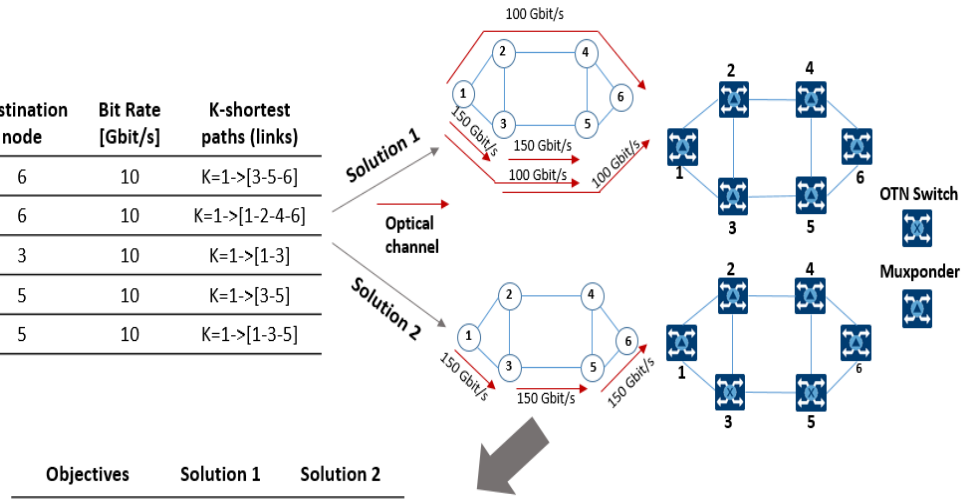

Objectives	Solution 1	Solution 2
# IFs	10	6
#OTNSwitches	0	2

Figure 3.1 Example of conflicting solutions considering the minimization of both line interfaces and OTN switches as objectives.

Although there were several studies in the literature addressing the benefits of introducing the OTN switching technology in the designing of an optical transport network [136, 137, 138] regarding the reduction of CAPEX and network utilization, they have considered a single-objective optimization problem where the relevant equipment cost associated with OTN switches is introduced to the overall network costs or not even adding the OTN switching costs. In detail, [136] analyses the impact of introducing the OTN switches on top of a WDM layer in two reference 100 Gbit/s networks highlighting the benefits in terms of network occupancy and CAPEX associated with the deployment of very-high capacity networks, whereas [137] provides a study that shows how the CAPEX savings of OTN switching over a non-switching architectures vary with the average node degree and the standard deviation of traffic degrees. Furthermore, the study presented in [138] compares the bandwidth effective and relative cost for different WDM transport and switching architectures including the use of OTN switches in the network nodes. By comparison, the study presented in this chapter aims at obtaining the best set of solutions that enables to simultaneously minimize the number of line interfaces and OTN switches required in an optical transport network, allowing the network planner to gain insight on the

range of possible trade-offs in the specific network and traffic scenario being considered, which to the best of our knowledge has not been addressed in literature.

Moreover, the multi-objective genetic algorithms have already been employed to solve different optimization problems in the context of optical transport networks. For example, the authors of [77] have proposed a genetic algorithm with the aim of designing a physical network topology while ensuring survivability and the minimization of transmission cost, whereas a genetic algorithm is proposed in [139] to solve part of the GRSA problem. In detail, the evolutionary algorithm is only used for the routing subproblem, where the multi-objective problem comprises the maximization of the number of transported traffic demands and the minimization of the number of frequency slots utilized. Furthermore, the same authors developed in [140] a multi-objective framework with the aim of maximizing the reliability of the optical network and minimizing the number of switching ports used. In [141], a genetic algorithm is proposed with three objectives: minimizing the number of transceivers, the average propagation delay and maximizing the traffic throughput. On the other hand, a multi-objective genetic algorithm was presented in [142] addressing the trade-off between the spectrum usage and line interfaces cost.

3.2 Multi-objective Genetic Algorithm

As described in the previous section, the optimization design framework developed in this work assumes the use of a multi-objective genetic algorithm (MOGA), which is a heuristic-based approach that exploits the main concepts of natural/biological evolution, e.g., selection, crossover and mutation, with the aim of selecting the most suitable solutions according to the optimization goals as the selection of the surviving individuals in a biological population. The genetic/evolutionary algorithm is a generational process starting by the creation of the initial population of solutions. In each generation, the most qualified solutions are maintained within the optimization process and a set of new solutions are generated through the use of crossover and mutation operators. The algorithm returns the final set of surviving solutions when the maximum run time or a predefined threshold of performance is reached.

Two variants of the genetic algorithm are utilized in this work, one based on the non-dominated sorting genetic algorithm (NSGA-II) as it is originally defined in [143] and a modified implementation of NSGA-II that includes additional modifications related to the addressed problem. In detail, the NSGA-II is used due to its ability to quickly classify the most suitable solutions and preserve diversity within the solutions space that allows to outperform the other multi-objective evolutionary algorithms, such as Strength-Pareto Evolutionary Algorithm (SPEA) [144] and Pareto-Archived Evolution Strategy (PAES) [145], regarding solutions diversity and convergence.

The proposed modified variant of the NSGA-II algorithm embeds in the mutation and crossover operations prior knowledge about the multi-objective problem defined in this study with the aim of increasing the convergence rate. More precisely, the knowledge is focused towards the production of solutions more biased to the minimization of one of the objectives: the number of line interfaces utilized. Noteworthy, this objective can take a wider range of values when compared to the number of OTN switches, which is upper bounded by the number of network nodes, whereas the number of line

interfaces is related to the number of optical channels used to route the different traffic demands, which can assume a wider range of values by comparing with the number of OTN switches, as shown in the example of Fig. 2.8 (c) for only one traffic demand. With the increase of the number of traffic demands, the total number of line interfaces required can dramatically vary along a higher range of values. Since the number of line interfaces can assume a wider range of values motivates the utilization of a more sophisticated process to generate the new solutions that, to a given extent, prevents the algorithm from generating too many solutions that are far from optimality with respect to the reduction of number of line interfaces. This approach still maintains a percentage of solutions completely random in order to preserve diversity within the population.

The proposed variant of the NSGA-II is hereafter designated as IF-Aware genetic algorithm (Interface-Aware genetic algorithm). The main contribution of this algorithm is to embed problem-specific decisions into initialization, mutation and crossover processes in order to increase the convergence of the multi-objective genetic algorithm to properly solve the designing of OTN, such that the overall network cost is minimized. The remaining of this subsection describes the details of the genetic algorithms devised to solve the multi-objective design problem.

3.2.1 Genetic Encoding

The first step consists of the creation of a genetic code that uniquely represents a candidate solution, as the biological genome comprises a set of chromosomes. In this case, the number of traffic demands represents the genome size, where each chromosome in the genome is the traffic demand to be served and its value encodes an integer number, which represents a possible routing/grooming option obtained from the pre-calculated list of candidate paths configurations associated with different concatenations of optical channels along these paths.

Figure 3.2 shows an example of the chromosome encoding for a traffic demand between the end-nodes 1 and 6 for the network topology defined in Fig. 3.2 (a). Three (k=3) different paths have been pre-calculated for the demand using k-shortest path algorithm [84], resulting in the routing options listed in Fig. 3.2 (b) based on the feasible optical channels provided by the optical performance model. Each path option represents the set of optical channels utilized, for example the possible encoding 1 uses a direct optical channel from the network node 1 to 6 following the *k*=1 shortest path (1-2-4-5) and does not require the deployment of OTN switches, whereas the possible encoding 2 uses two optical channels between the network nodes (1-2 and 2-6) also following the *k*=1 shortest path. Note that, the encoding 2 requires the use of OTN switch at network node 2 since it transfers traffic from different optical channels, as described in Subsection 3.1. Moreover, the possible encodings 1-4, 5-8 and 9-16 represent the optical channels' paths (described in 2.1.3.1) over different shortest paths defined in Fig. 3.2 (a). In this example, the demand's chromosome can assume an integer value between 1 and 16 given the possible encodings. The complete encoding comprises the selection of an integer value, which represents a given routing configuration, for every traffic demand, as illustrated in Fig. 3.2 (c). In this example, the genome is represented by N traffic demands where the demand 1 (1-6) has been assigned

with encoding seven and the remaining demands are assigned with random values in order to exemplify a complete genome configuration.

The workflow of the genetic algorithm is shown in Fig. 3.2 (d), highlighting the main steps of the algorithm. The algorithm initially produces a starting population with a set of candidate solutions. In each generation of the algorithm, the solutions are evaluated according to the fitness in each objective and the fittest solutions are selected for the next-generation. These solutions then go through the crossover and mutation operators based on the roulette wheel probabilities. Moreover, the crossover and mutation solutions combined with the fittest ones are preserved within the population for the next generation and the process restarts until the criterion is satisfied. In the end of the algorithm's execution, it returns a list of the most suitable solutions according to the optimization purposes and the preferred network nodes to introduce the OTN switches. All of these steps are explained in the next subsections.

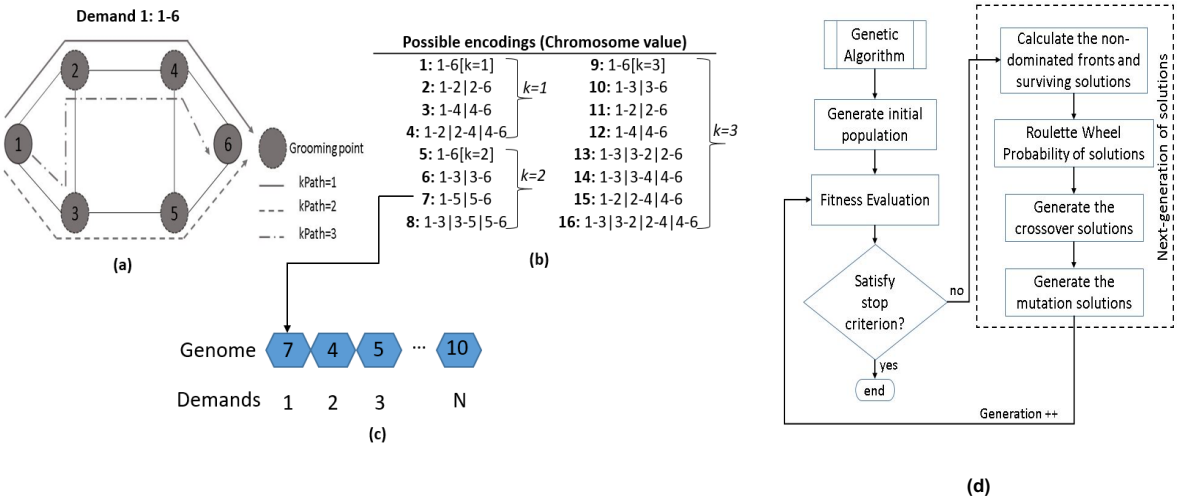

Figure 3.2 Genetic encoding: (a) network topology, (b) possible encodings to meet the traffic demand between the end-nodes 1 and 6, (c) genome structure and (d) algorithm workflow.

3.2.2 Population Initialization

In evolutionary computation, the solutions of the initial population are usually generated at random, as described in [143] for the NSGA-II algorithm. In this work, beyond the use of random initial solutions, also a certain percentage of solutions were adapted in order to improve the IF-Aware genetic algorithm's convergence. As described previously, this adaptation is biased towards the minimization of the number of line interfaces' objective, since it requires a more efficient technique to make more room to produce better solutions in terms of reducing the number of line interfaces.

The generation of these initial adapted solutions for the IF-Aware genetic algorithm is illustrated in Fig. 3.4. Note that, the number of traffic demands that influences the genome size and the integer values assigned for the chromosomes' values at each step are only defined for illustration purposes of the process and therefore the values do not have a particular meaning for the context. The first step of the population initialization involves the creation of the genome composed by a set of chromosomes according to the number of traffic demands defined in the design problem. Afterwards, a small percentage of the traffic demands is assigned with a chromosome value from the list of possible

encodings for each traffic demand at random in order to initialize the process, as shown in step 2 of Fig. 3.4. Based on this partial solution, the algorithm decodes the chromosomes' values already assigned into a set of optical channels' paths as the ones described in Fig. 3.2 (b), which allows to compute the preliminary number of line interfaces utilized for transporting the already assigned traffic demands (step 3 of Fig. 3.4).

Finally, the remaining subset of traffic demands sequentially selects from the list of possible encodings the optical channels' path and consequently its chromosome value that least increases the total number of line interfaces already in use (step 4). These solutions are clearly biased towards the minimization of the number of line interfaces used given the larger solution space that leads to explore values far from the minimum value. It is important to highlight that a percentage of the initial population is generated at random in order to preserve diversity of solutions within the population.

3.2.3 Fitness Evaluation

As previously stated, the goal of the multi-objective framework is to reach the most qualified solutions according to the optimization objectives. Moreover, the genetic algorithm imposes a generational approach, where in each generation a subset of solutions is preserved based on their evaluation function, called fitness. The fitness evaluation is an important measure to describe each solution by a single value that balances both objectives with a predefined weight. In the context of this specific optimization problem, the fitness is calculated through Equation (3.1) where the relative importance of both objectives, number of line interfaces ($\#IFs$) and number of OTN switches ($\#OTNSwitches$), is controlled via the $\kappa \in [0,1]$ parameter. Note that, the objective of the proposed multi-objective is to minimize both the number of line interfaces and OTN switches used and for this reason the preserved solutions are the ones that reduce their fitness value the most.

$$FE = \kappa \times (\#IFs) + (1 - \kappa) \times \#OTNSwitches \tag{3.1}$$

The algorithm for calculating the value of each objective based on a specific genome solution is described as follows:

Algorithm 1 Objectives' Evaluation

INPUT: Genome Solution
Set of Traffic Demands (D)
Set of feasible candidate optical channels (L)

OUTPUT: #IFs, #OTNSwitches

Initialize the arrays $Ctrans$ and I_{nodes}.
for $d \in D$
  Get the corresponding chromosome value and decode the solution into the optical channels' path used to meet the traffic demand L_d.
  for each optical channel l in L_d
    $Ctrans_l$+=C_d
  end for
  add intermediate nodes between channels in L_d to I_{nodes}
end for
for each l in L

11 #IFs+=$ceil(\frac{Ctrans_l}{C_l}) \times 2$
12 ***end for***
13 #OTNSwitches=size(I_{nodes})

The input parameters of the fitness evaluation are the genome solution, the traffic demands set D and the total set of feasible candidate optical channels L, which is calculated based on the optical performance model described in Subsection 2.1.2.3 using the 2nd generation of coherent line interfaces (Table 2.1). The bit-rate of each traffic demand is represented by the variable C_d (measured in Gbit/s) and the optical channels' path used to meet each traffic demand is defined as L_d. The algorithm starts by computing the total capacity transported per optical channel (load capacity) according to the traffic demands that traverse it ($Ctrans_l$) and the intermediate nodes where there are traffic demands switched between different optical channels (I_{nodes}) in order to calculate the number of OTN switches utilized.

Afterwards, the objective values ($\#IFs$ and $\#OTNSwitches$) can be easily calculated. Based on the total capacity of each optical channel (C_l), it is possible to calculate the total number of optical channels required by dividing it through the total bit-rate of the channel. Consequently, the number of line interfaces is identical to the number of optical channels utilized times two since the equipment should be placed at both end-nodes of the channel. On the other hand, the number of OTN switches is identical to the number of different network nodes presented in the I_{nodes} array. The complexity of the fitness evaluation depends on the number of traffic demands and the number of feasible candidate optical channels defined to route the traffic. More precisely, the number of operations is defined by $|D| \times |L_d| + |L|$, which in worst case scenario is characterized by $|D| \times |E| + |E| \times (|E| - 1)$. In worst conditions, the maximum number of optical channels used to carry each traffic demand can be defined by the number of network links ($|E|$) of the network topology that is characterized by a graph $G(V, E)$. On the other hand, the maximum number of candidate optical channels can be the number of possible node-pairs in the network topology ($|V| \times (|V| - 1)$). Therefore, the complexity of the fitness evaluation procedure is considered as $O\big(|D| \times |E| + |V| \times (|V| - 1)\big)$.

3.2.4 Selection of Surviving Solutions

At each generation of the genetic algorithm, it is necessary to evaluate the solutions of the population according to their fitness. In case of multi-objective optimization, the goal becomes finding a set of solutions that cannot be improved on the same objective without deteriorating the quality of the other objective (Pareto front). In order to rank the solutions, the elements of the population are divided into non-dominated fronts based on the concept of dominance relationship proposed by the NSGA-II algorithm [143]. The first front comprises the non-dominated solutions (solutions that cannot be improved on one objective without compromising the quality of the other objective), the second front represents the solutions that are only dominated by the ones in the first one and so forth. Fig. 3.3 provides an example of the different non-dominated fronts, highlighting the dominance relationship between them. Note that, the first non-dominated front is considered to be the Pareto front if all

objectives' space has been analysed and it is not possible to improve a given objective without degrading the other objective's value. The ordering of the non-dominated fronts will allow direct selection of a set of solutions that will be preserved for the population of the next-generation. Within the same front, the solutions with the highest value of crowding distance are the ones to be retained to guarantee diversity, where crowding distance is the average distance with respected to their two neighbours in the same front [143]. The remaining of the next population is generated through crossover and mutation operations.

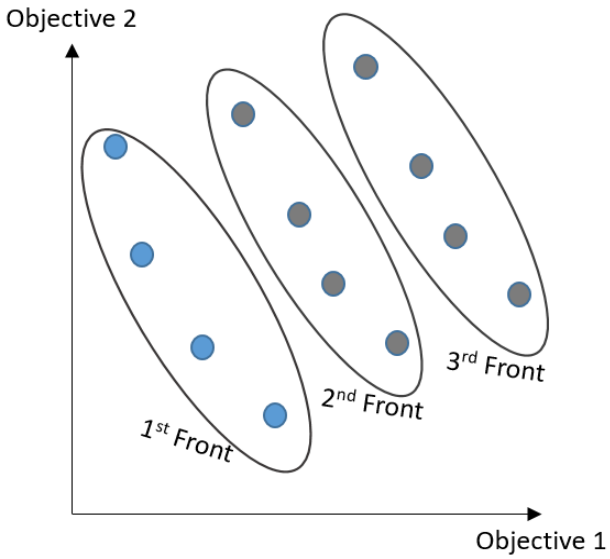

Figure 3.3 Non-dominated fronts in a multi-objective context.

3.2.5 Crossover

The crossover operation involves the combination of two parents to generate new offspring. One of the main purposes of crossover is to attempt to generate better solutions (e.g., when offspring inherits the best part of each parent). In this work, the selection of the parents used for crossover is based on roulette wheel probabilities [146]. This strategy gives a larger range of probability to the best solutions according to their fitness. To generate the combined solutions, two types of crossover are used, the random crossover and the IF-Aware crossover.

The random crossover uses the single-point strategy [134] that first selects two parents for performing crossover and then randomly chooses a crossover point. Two offspring are created by combining the parents at crossover point, one of them inherits the first part of the chromosomes' values from one parent and the second part from the other, whereas the other offspring inherits the two other parts.

On the other hand, the IF-Aware crossover enforces our strategy to improve the algorithm's convergence, which is described in Algorithm 2 and exemplified in Fig. 3.4 through a detailed example. Note that, the number of traffic demands that influences the genome size and the integer values assigned for the chromosomes' values at each step are only defined for illustration purposes of the

process and therefore the values do not have a particular meaning for the context. This algorithm receives as input data the already selected parents for performing the crossover (step 1 of Fig. 3.4), the percentage of chromosomes' values that should be initialized at random and the set of traffic demands defined in the problem. In first place, the algorithm generates at random a percentage of chromosomes' values coming from one of the selected parents, as illustrated in step 2 of Fig. 3.4 of crossover procedure. The chromosomes are generated at random with the objective of initializing the crossover solutions.

Based on this initial selection (step 2 of Fig. 3.4), the partial offspring solutions are decoded into optical channels' paths like the ones presented in Fig. 3.2 (b) and the preliminary number of line interfaces required are computed (step 3 of Fig. 3.4). Afterwards, the offspring that has the smallest preliminary number of line interfaces is selected in order to serve as a bias solution towards the minimization of the total number of line interfaces (Offspring 1 of Fig. 3.4). Thus, the remaining chromosomes of this offspring will sequentially select the chromosome' value that corresponds to optical channels' path from the parent that most minimizes the number of interfaces that have to be used. In the example of Fig. 3.4, the first and third chromosomes' values come from Parent 2 and the fifth from the Parent 1. The order of the chromosomes' values assignment is based on the capacity of the corresponding traffic demand that each chromosome represents in descending order. As a recombination process between two solutions (parents defined in step 1 of Fig. 3.4), the other offspring will be defined by the chromosomes' values of the opposite parent (first and third chromosomes' values come from Parent 1 and the fifth from the Parent 2). Moreover, the global aim is to generate crossover solutions that are partially biased towards the minimization of the number of line interfaces' objective since it can assume a wider range of possible values.

3.2.6 Mutation

By definition, mutation alters one or more chromosomes' values in the genome of the selected parent and usually it involves a random change. The main objective of mutation is to create diversity in the population, enabling it to exploit a wider area of the solutions' search space and potentially escape from the local optimum. In the context of this problem, mutation comprises the modification of the optical channels' path configuration of a random number of traffic demands.

Two types of mutation operations are used in this work. The first consists of changing some chromosomes' values into other encoding values at random. The second type of mutation enforces a more specialized modification by taking into account information about the expected number of line interfaces (IF-Aware Mutation), which is described in Algorithm 3 and illustrated in Fig. 3.4. As mentioned before, the number of traffic demands that influences the genome size and the integer values assigned for the chromosomes' values at each step are only defined for illustration purposes of the process and therefore the values do not have a particular meaning for the context.

Additionally, the first three steps of the algorithm are equivalent to the crossover procedure comprising the parent selection, the generation of the partial solution at random and the calculation of the preliminary number of interfaces used. The difference is in step 4 described in Fig. 3.4, where the

remaining chromosomes of the mutation offspring will sequentially select the chromosome' value that corresponds to optical channels' path from the possible chromosome encodings that most minimizes the number of interfaces that have to be used. The order of the chromosomes' values assignment is based on the capacity of the corresponding traffic demand that each chromosome represents in descending order. In the example of Fig. 3.4, the mutation occurred on the third chromosome varying from the value 9 to 3 and on the fifth chromosome changing from the value 1 to 5. This assignment

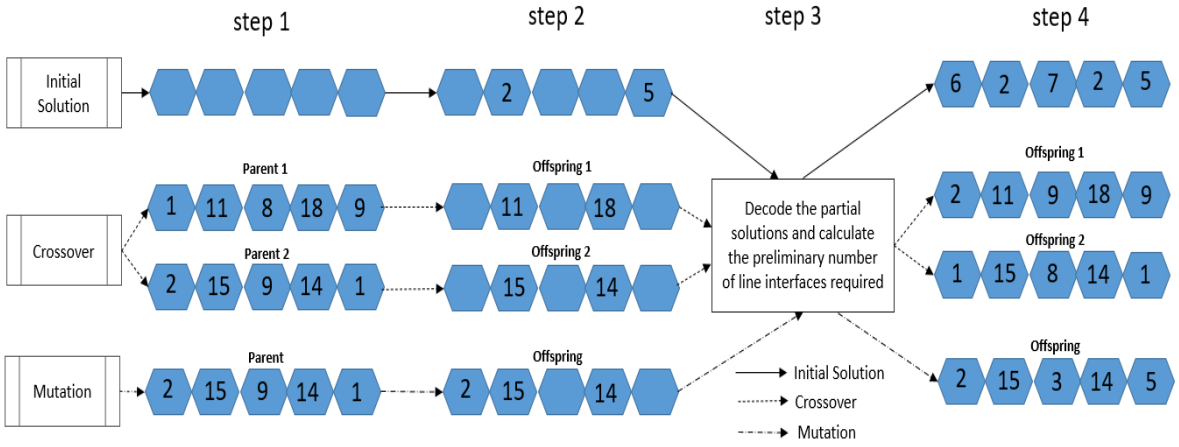

Figure 3.4 Examples of the generation of initial, crossover and mutation solutions utilized in the IF-Aware genetic algorithm.

intentionally produces mutation solutions pre-optimized towards the minimization of the number of line interfaces that have to be used with the goal of improving the performance of the IF-Aware genetic algorithm.

Algorithm 2 *IF-Aware Crossover*

INPUT: Parents genome (Par_1, Par_2)
Percentage of chromosomes to initialize offspring (t)
Set of Traffic demands (D)

OUTPUT: New Offspring $(Offs_1, Offs_2)$

1 Get t of the chromosomes' values randomly from Par_1 to $Offs_1$ and Par_2 to $Offs_2$
2 ***for each*** offspring $(Offs_1, Offs_2)$
3 Decode the partial solutions into optical channels' paths
3 Calculate the preliminary number of line interfaces NIF_o based on values already assigned
5 Select the offspring that has the min(NIF_o) to variable $Offs_s$ and the other to $Offs_r$
6 Sort the chromosomes to be assigned in descending order according to the corresponding bit-rate of the traffic demand $d \in D$ it represents, Chr_{sor}
7 ***for each*** chromosome $\in Chr_{sor}$
8 Choose the chromosome value according to the optical channels' path from the parent (Par_1, Par_2) that most minimizes the increment of the number of line interfaces used NIF_o to offspring $Offs_s$ and assign the other parent value to $Offs_r$

Algorithm 3 IF-Aware Mutation

INPUT: Parent genome (Par)
Percentage of chromosomes to initialize offspring (t)
Set of Traffic demands (D)

OUTPUT: New Offspring $(Offs)$

1 Get t of the chromosomes' values randomly from Par to $Offs$
2 Decode the partial solution of $Offs$ into optical channels' path
2 Calculate the preliminary number of line interfaces NIF_o based on values already assigned
3 Sort the chromosomes to be assigned in descending order according to the corresponding bit-rate of the traffic demand $d \in$ it represents, Chr_{sor}
4 ***for each*** chromosome $\in Chr_{sor}$
5 Select the chromosome value from the list of possible encodings that correspond to the optical channels' path that most minimizes the increment of the number of line interfaces used NIF_o to $Offs$

3.2.7 Evaluation Engine

To evaluate the performance of the evolutionary algorithm, the best (i.e., smallest) number of line interfaces and number of OTN switches are computed independently. For the number of OTN switches, it is a straightforward task since the minimum value corresponds to not deploying any OTN switches and it reduces the benchmark to zero. On the other hand, the smallest number of line interfaces requires a more complex algorithm to retrieve the best solution. For that reason, an integer linear programming model that minimizes the total number of line interfaces required was developed. The ILP model comprises the routing and grooming operations and for the purpose of the study reported in the next section it is solved using the IBM ILOG CPLEX Optimization Studio [147]. The mathematical formulation can be formulated using the following variables and input parameters:

Parameters:

V	Set of network nodes
E	Set of network links
L	Generic set of candidate optical channels
L_e	Set of optical channels that traverse the network link $e \in E$
$L_{i,j}$	Generic set of available optical channels between source node i and destination node j
D	Set of traffic demands
X_l	Total number of 1.25 Gbit/s slots supported by the optical channel $l \in L$ according to its capacity
N_d	Total number of traffic demands between the same end-nodes and bit-rate $d \in D$
S_d	Number of 1.25 Gbit/s slots per traffic demand $d \in D$ according to its bit-rate
F	Number of available frequency slots per network link

Variables:

$\lambda_{d_{(o,t)}}^{l_{(i,j)}} \in \mathbb{N}^0$	Number of traffic demands from type $d \in D$ between source node o and destination node t using optical channel $l \in L$ with source node i and destination node j

$\theta_l \in \mathbb{N}^0$ Number of optical channels used from the format of candidate channel $l \in L$

$\omega \in \mathbb{N}^0$ Total number of line interfaces required

The following formulation describes the ILP model.

$$min\ \omega \tag{3.2}$$

Subject to

$$\sum_{l \in L_{i,j=v}} \lambda_{d_{(o,t)}}^{l_{(i,j)}} - \sum_{l \in L_{i=v,j}} \lambda_{d_{(o,t)}}^{l_{(i,j)}} = \begin{cases} -N_d, & v = o \\ N_d, & v = t \\ 0, & \forall\ v \in V \backslash \{s,t\} \end{cases} \quad \forall d \in D \tag{3.3}$$

$$\sum_{d \in D} S_d \times \lambda_d^l \leq X_l \times \theta_l \qquad \forall l \in L \tag{3.4}$$

$$\sum_{l \in L_e} \theta_l \leq F \qquad \forall e \in E \tag{3.5}$$

$$\sum_{l \in L} 2 \times \theta_l = \omega \tag{3.6}$$

The objective function (3.2) minimizes the number of line interfaces that have to be acquired. Constraints (3.3) ensure the flow conservation for all traffic demands. The optical channels' capacity constraints are set by (3.4). Constraints (3.5) guarantee that the total number of optical channels allocated in the frequency spectrum does not exceed the link capacity. Finally, the constraints (3.6) calculate the total number of line interfaces required to support all the traffic demands. Note that, the number of line interfaces represents the number of optical channels utilized times two since the equipment should be placed in both end-nodes of the channel. The complexity of an ILP model can be determined by the number of variables and constraints used in the creation of the model. In this context, the number of variables is defined by $|D| \times |L| + |L| + 1$, whereas the number of constraints is given by $|D| \times |V| + |L| + |E| + 1$.

3.3 Simulation Results

In this section, the results obtained with the previously described multi-objective genetic algorithms are analysed and the performance of the two evolutionary algorithms (Random and IF-Aware genetic algorithms) is compared. In detail, the NSGA-II was implemented following two different approaches: the first one consists of randomly generating the initial, crossover and mutation solutions, while the second one, called IF-Aware genetic algorithm, gives preference to generating solutions that minimize the number of required line interfaces. The performance study is carried out over two network topologies: The Deutsche Telekom (DT) and Advanced Research Projects Agency Network (ARPANET), which are

depicted in Appendix B. DT is a national backbone network with 12 nodes and 40 network links, whereas ARPANET is a metropolitan sized network with 20 nodes and 64 network links.

For each network scenario, the source and destination nodes of traffic demands are randomly selected and their bit-rates are uniformly distributed between 10 and 100 Gbit/s. For each traffic demand, a set of candidate routing paths is calculated using the *k*-shortest path algorithm, as defined in 2.1.3.1. For each path and using the state-of-art line interfaces operating at 32 Gbaud and supporting modulation formats from QPSK to 16 QAM (2nd generation of line interfaces presented in Table 2.1), the most efficient modulation format is selected between the network nodes along the path based on optical performance evaluation described in 2.1.2.3. Note that, although the 2nd generation of line interfaces is used for analysis purposes, the framework can be applied for all generations of line interfaces. Throughout the different simulation results, the number of traffic demands, k the value of the *k*-shortest paths and the total number of solutions in the population of the genetic algorithms were adapted according to the scenario in analysis. Beyond the possibility to use the OTN switches, the network nodes are also incorporated with CDC-ROADMs for the optical layer, as described in 2.1.3.3.

Furthermore, the performance of the algorithms is measured by the hypervolume and convergence rate metrics. The hypervolume indicator corresponds to the area between all points in the non-dominated front to a reference point (Fig. 3.5 (a)), which represents the worst results that the objectives can assume. This reference point is considered as constant throughout the different generations of the genetic algorithm allowing to obtain the progress of the non-dominated front with respect to this value. On the other hand, it is possible to have an idea of the convergence rate through the Euclidean distance metric between the benchmark point and the closest point to it in the Pareto front, as depicted in Fig. 3.5 (b). In this case, the benchmark point represents the best results that the objectives can assume when calculated independently. These performance metrics are complemented with the aim of properly characterizing the evolution of genetic algorithm where the hypervolume defines the solutions' area

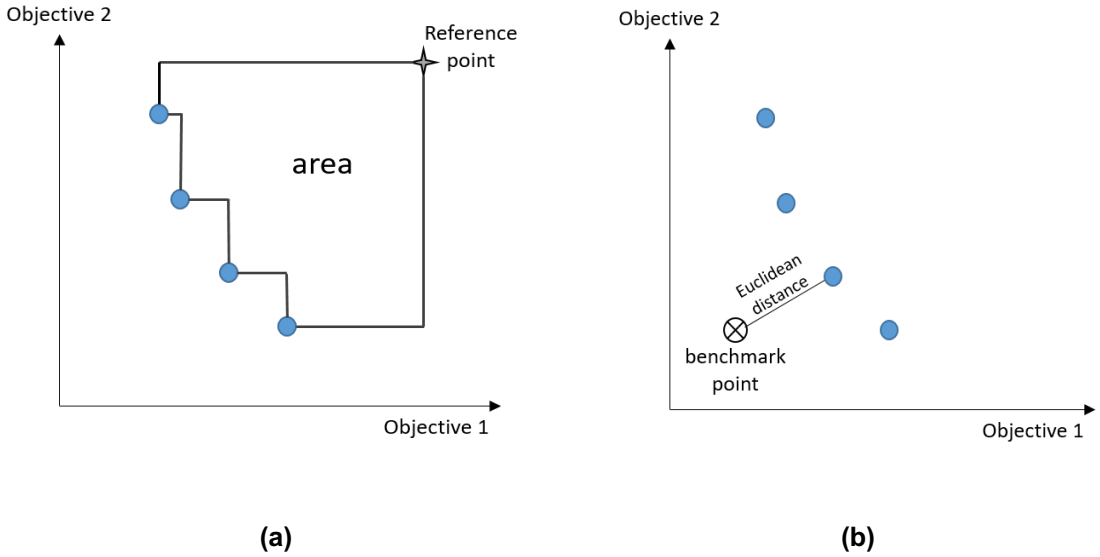

Figure 3.5 Illustration of the (a) hypervolume and (b) convergence rate metrics used for evaluating the performance of genetic algorithms.

explored by the algorithm where (higher hypervolumes leads to better algorithm's performance) and the convergence rate describes the proximity of the non-dominated front to the optimal Pareto front (lower convergence rate leads to better algorithm's performance).

3.3.1 MOGAs Comparison

The first set of simulation results aims at comparing the performance of the Random and IF-Aware genetic algorithms used in this study. The DT network is utilized with different values of *k* and number of traffic demands $|D|$. The study is conducted to measure the evolution of the hypervolumes and convergence rates for different generation runs and network scenarios. In the analysis, it is assumed a population of 120 elements at each generation of the algorithm and κ equal to 0.8 in the fitness Equation (3.1), giving priority to solutions that minimize the number of line interfaces. In each generation of the algorithm, half of the population is maintained according to the non-dominated fronts (Subsection 3.2.4) and the other half is based on the crossover and mutation processes with probability of 0.3 and 0.7, respectively. This assumption increases the number of mutation solutions within the population when compared to crossover approach, since the mutation enables changing just a few chromosomes' values of the already effective solutions in terms of their fitness value with the main goal of producing solutions even more biased towards the minimization of the number of line interfaces. The results are averaged over 30 independent simulation runs (N_{runs}). Table 3.1 shows the average (μ) and the standard deviation (σ) of the hypervolumes and the Euclidean distances for each network scenario with different numbers of generations. The average and standard deviation are calculated through Equations (3.7) and (3.8), respectively. The x_i corresponds to the values of the hypervolume and Euclidean distances in the different simulation runs.

$$\mu = \frac{1}{N_{runs}} \times \sum_{i=1}^{N_{runs}} x_i \tag{3.7}$$

$$\sigma = \sqrt{\frac{1}{N_{runs}} \times \sum_{i=1}^{N_{runs}} (x_i - \mu)^2} \tag{3.8}$$

From the results presented in Table 3.1, it is clear that the use of a customized algorithm, embedding the capability of minimizing one of the objectives during the mutation and crossover processes, will benefit the evolution of the population. To be more concrete, the use of the IF-Aware genetic algorithm enables to reduce on average 52% of the benchmark Euclidean distance that characterizes the convergence rate and to increase on average 56% of the hypervolume analysed when compared to Random genetic algorithm for the different network scenarios addressed in this study. The performance differences are even more noticed with the augment of the number of generations due to the fact that the algorithm has more time to generate optimized solutions with respect to the number of line interfaces. On the other hand, it is also interesting to notice that since the first generation the IF-Aware genetic algorithm achieves the best results, suggesting that the population initialization should not just be

generated at random, instead it requires a more complex initialization that combine both random and expert solutions including prior knowledge about the optimization process.

Moreover, it can be observed that the performance of the Random genetic algorithm tends to degrade when the network scenario becomes more complex. This is exemplified in Table 3.1 for k equal to 3 and 100 traffic demands, where the hypervolume explored by the Random algorithm is on average less 81% of that explored by the IF-Aware algorithm. In addition, the Euclidean distance to the benchmark point is on average 70% greater with the Random algorithm than that with the IF-Aware algorithm. These observations support the need to employ a more sophisticated implementation of the NSGA-II algorithm to solve this specific multi-objective problem. The results of Table 3.1 also highlight that the standard deviation σ of both hypervolume and benchmark Euclidean distance metrics are on average more reduced with the IF-Aware genetic algorithm than with Random genetic algorithm meaning that the results of the proposed algorithm tend to follow the average value μ without higher variations when considered different sets of traffic demands.

The results of Table 3.1 also show that the hypervolumes do not suffer higher variation when increasing the number of generations from 200 to 400, this can be explained by the fact that the algorithm are converging for the Pareto front and the area explored by the algorithm is not increasing at the same rate as the transition between the 1 to 400 generations.

Table 3.1 MOGAs comparison.

Network Scenario				Benchmark Euclidean Distance				Hyper Volume			
Network	$\|D\|$	k	Number of Generations	Random GA		IF-Aware GA		Random GA		IF-Aware GA	
				μ	σ	μ	σ	μ	σ	μ	σ
DT	50	1	1	15.5	3.8	15.4	3.7	14343.4	2879.4	21783.8	3255.9
DT	50	1	200	4.2	2.4	1.3	1.6	27573.3	5257.6	49038.2	2587.6
DT	50	1	400	2.8	1.7	1.1	1.4	28637.2	5304.1	49047	2594
DT	50	3	1	69.9	3.4	37.2	3.7	10549.6	1630.3	17481.2	1550.3
DT	50	3	200	42.2	3.7	10.6	2.6	22692.8	4175.3	61780	539.4
DT	50	3	400	36.8	3.4	9.9	2.8	24131.8	4330.4	61864.7	563.9
DT	100	1	1	43.9	3.5	43.8	4.7	9328.9	1645.9	15618.6	1650.5
DT	100	1	200	23.2	4.7	9.1	2.8	14747.4	3086.8	46320.9	2216.9
DT	100	1	400	20.9	4.0	8.5	2.7	15206.5	2859.7	46396.3	2216.0
DT	100	3	1	126.6	3.7	77.4	5.9	5553	767.2	11445.8	459.5
DT	100	3	200	89	6.1	25.3	5.4	10251.3	1681.5	56228.9	811.4
DT	100	3	400	81.5	7.3	24.5	4.9	10986.8	1883.8	56395.5	795.4

The previous conclusions are reinforced by analysing the results plotted in Fig. 3.6 (a-c), which were obtained after 400 generations for DT network topology with 100 traffic demands and k value equals to one. Fig. 3.6 (a) represents the non-dominated fronts, while Fig. 3.6 (b-c) illustrates the objectives' space (space of solutions) exploited with both IF-Aware and Random genetic algorithms using one of the independent simulations runs, respectively.

Although, it would be expected that the Random algorithm produces a greater spread of the solutions in the objectives' space due to its nature, the IF-Aware genetic algorithm is able to produce more solutions with diversity that explores the whole area of the objectives' space, as shown when comparing the plots of Fig. 3.6 (b-c). The reason for this apparently counterintuitive trend is that the Random algorithm generates multiple solutions that albeit having significantly different chromosomes' values

result in the same objective values (i.e., number of line interfaces and OTN switches). In other words, there is significant redundancy in the solutions space, which cannot be mitigated when using the Random implementation of NSGA-II. Conversely, the IF-Aware algorithm reduces the presence of redundant solutions, ultimately improving both the convergence rate and the hypervolume (results presented in Table 3.1). These conclusions are reinforced through the illustration of non-dominated fronts for both IF-Aware and Random genetic algorithms, as shown in Fig. 3.6 (a). This figure shows the diversity of the solutions in the non-dominated front provided by the proposed algorithm.

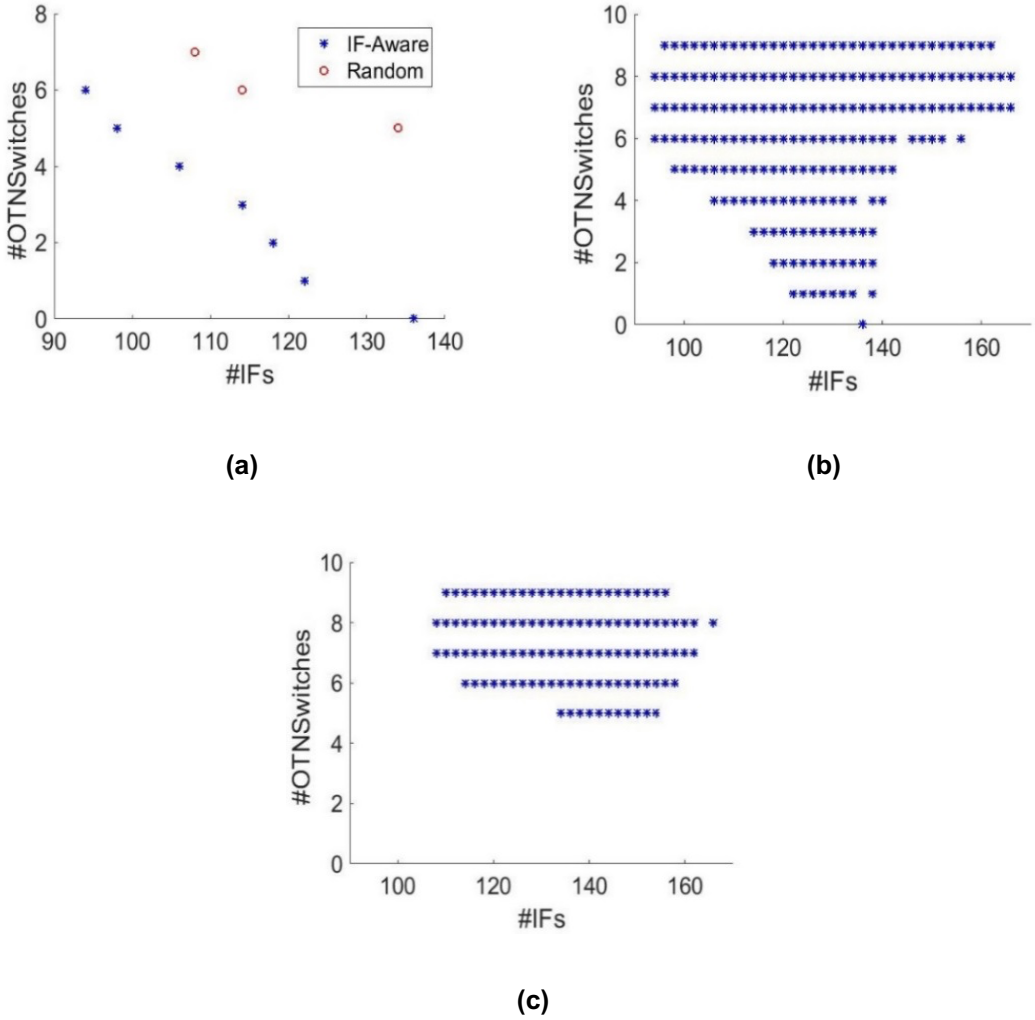

Figure 3.6 Comparison results of the IF-Aware and Random GA: (a) Non-dominated fronts obtained by both genetic algorithms and (b-c) objectives' space explored by IF-Aware and random genetic algorithm for DT topology with 100 traffic demands and k=1, respectively.

3.3.2 Complexity of the MOGAs

This subsection compares the complexity of the Random and IF-Aware genetic algorithms for all the network scenarios considered in this study. The complexity is measured by the average (μ) and standard deviation (σ) of the computation time and the number of evaluations performed until the hypervolume remains constant for at least 60 generations. The total number of evaluations has also taken into account the size of the population evaluated per generation and the total number of generations required that conducts to a constant hypervolume value. Table 3.2 shows, in addition to the computation time of the

algorithms, the total number of paths analysed for all sets of traffic demands, the average number of paths used to route each traffic demand, the number of generations and the size of the population. Note that, the genome size is given by the number of traffic demands, where each chromosome can take an integer value corresponding to a given optical channels' path configuration. All the simulations were solved on a PC with an Intel Xeon CPU E5-2643 V2 with 2 processors of 3.5 GHz and 16 GB of RAM.

The results of Table 3.2 show that the IF-Aware GA tends to be slower than the Random GA due to the fact that the mutation and crossover processes require a more complex algorithms to produce solutions biased towards the number of line interfaces' objective. On the other hand, it can also be seen that the number of generations to keep the hypervolume constant tends to be higher with the proposed genetic algorithm. This can be explained by the fact that the IF-Aware GA is more effective on generating diversified solutions that explores the whole area of the objectives' space that leads to an evolution of the hypervolume metric, whereas the Random GA takes longer time to increase the objectives' space area, as shown in the previous section. Therefore, in most of the network scenarios, the computation time is higher for the IF-Aware algorithm in order to obtain comparable performance results.

In addition, the complexity of IF-Aware genetic algorithm increases with the problem size, which is a function of the number of traffic demands, number of candidate paths per traffic demand and network size. This fact can be seen through the computational time and the number of generations performed to achieve a constant hypervolume. For example, the use of 50 and 100 traffic demands with k=1 in the ARPANET network topology leads to an increment on the number of generations of 62% and on computational time of 75%. On the other hand, an increase of 57% on the number of generations and 58% on the computational time by modifying the k value from 1 to 3 with 100 traffic demands in ARPANET network topology. It is important to notice that parallel computation was not used in this study, but another advantage of genetic algorithms is their suitability for parallelization. For instance, it is possible to subdivide the individuals into subpopulations, where each subpopulation is allocated to a different CPU, defined as the island model [148], which allows to reduce the computational time of Table 3.2.

Table 3.2 Complexity evaluation of MOGAs algorithms.

Network Scenario			Complexity						
			Problem Size			IF-Aware GA		Random GA	
Network	$\|D\|$	k	Average number paths	Total number paths	Size of Population	Number Generations $\mu(\sigma)$	Time [s] $\mu(\sigma)$	Number Generations $\mu(\sigma)$	Time[s] $\mu(\sigma)$
DT	50	1	3.1	153.1	100	113.4(40.3)	1899.5(731.7)	234.4(70.6)	2660.7(855.7)
DT	50	3	14.2	710.1	110	224.3(14.2)	4862.5(271.1)	397.3(137.9)	6252.1(2331.4)
DT	100	1	2.8	275.3	120	247.3(37.7)	9388.9(1555.9)	394.3(112.2)	11483.5(3307.8)
DT	100	3	15.4	1541.3	140	555.7(65.8)	24090.0(9819.6)	507.5(142.2)	21334.5(6401.7)
DT	200	1	2.9	557.3	180	422.1(162.8)	31016.9(5157.4)	311.2(169.4)	17160.3(6932.7)
DT	200	3	16.2	3241.2	200	509.9(249.1)	63175.6(27304.7)	380.8(87.7)	40233.4(7478.1)
ARPANET	50	1	5.1	256.3	100	154.3(33.9)	4087.3(991.3)	249.3(16.5)	8363.7(1021.6)
ARPANET	50	3	30.5	1523.3	110	409.4(206.8)	13088.2(6530.1)	601.2(169.4)	21972.6(16188.9)
ARPANET	100	1	5.6	558.2	120	401.1(143.9)	16567.7(4843.6)	532.7(84.2)	18679.3(3168.5)
ARPANET	100	3	30.2	3023.3	140	750.2(219.6)	40162.9(3485.4)	663.6(167.3)	30616.6(7788.5)
ARPANET	200	1	5.3	1050.3	180	712.3(224.6)	71608.2(14978.1)	655.3(226.2)	57930.2(20804.9)
ARPANET	200	3	31.5	6317.5	200	805.5(327.1)	128464.3(56241.3)	478.6(319.9)	44524.4(27262.7)

3.3.3 Performance of the IF-Aware Genetic Algorithm

Based on the performance advantages of the IF-Aware genetic algorithm presented in the previous sections, it is clear that is the one that should be applied for this multi-objective problem. In this study, the results of the IF-Aware evolutionary algorithm are presented for different network scenarios, considering the DT and ARPANET topologies. The performance analysis starts by comparing the results coming from the genetic algorithm and the benchmark values defined in subsection 3.2.7 for DT and ARPANET scenarios with 50 traffic demands and k=1, which is shown in Fig. 3.7 (a-b), respectively. Note that, this illustration only represents one independent simulation run and the aforementioned ILP returns only one solution that leads to the best value in terms of number of line interfaces but does not take into account the number of OTN switches required.

By observing Fig. 3.7 (a-b), it can be seen that in both networks there are multiple solutions that achieve the minimum number of line interfaces, as determined by the benchmark solution provided by the ILP that has the objective of minimizing the number of line interfaces, but each solution attains this value at the expense of a different number of OTN switches required. In particular, the ILP model returns the solutions that lead to use seventy and ninety line interfaces for DT and ARPANET network topologies, respectively. Using the proposed multi-objective framework, it is possible to obtain a solution that requires the minimum number of line interfaces while using the smallest possible number of OTN switches. Moreover, these results also show how the genetic algorithm is able to return solutions that present other potentially interesting trade-offs between number of line interfaces and number of OTN switches. For instance, if further savings in the number of OTN switches are targeted, it is possible to infer what is in number of additional line interfaces required. This provides evidence that the developed framework can effectively assist a network planner in finding optimal solutions, having insight on the possible trade-offs involved.

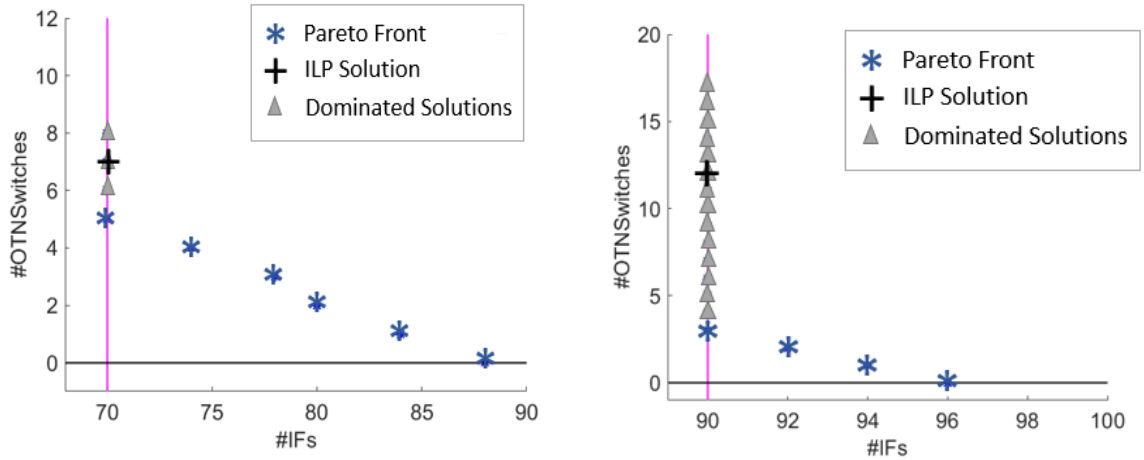

(a) **(b)**

Figure 3.7 Comparison between the results of IF-Aware algorithm and ILP model with 50 traffic demands and k=1 for (a) DT and (b) ARPANET topologies.

The second part of this analysis assesses the non-dominated fronts obtained by the IF-Aware algorithm for different values of k with the same initial network conditions. The results are presented in Fig. 3.8 using the DT topology with 50 traffic demands. This set of results utilizes a different independent simulation run from the one provided in Figure 3.7 in order to present a diversified number of possible non-dominated fronts when changing the set of traffic demands. From the results presented in Fig. 3.8, it can be observed that the non-dominated front shifts to the left and there is an increase in the number of nodes that have to be equipped with OTN switches, when the value of k increases. In fact, there are two consequences from increasing the value of *k*: the first one is that more paths become available for routing each traffic demand, further augmenting the number of possibilities of sharing path segments among different traffic demands. This can lead to better solutions concerning the number of line interfaces. Secondly, since these paths are longer in terms of the number of intermediate nodes traversed, there is more room to choose different nodes to do intermediate grooming which allows to cover almost the entire range of optimization space for the number of OTN switches required.

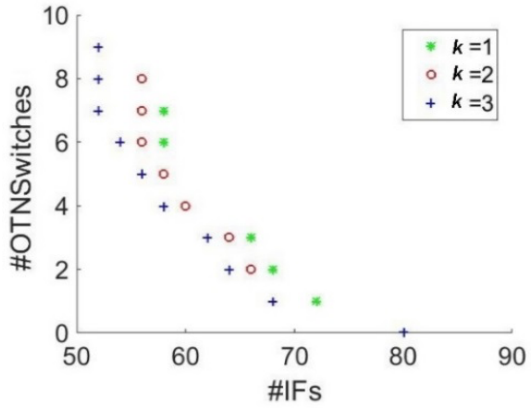

Figure 3.8 Comparison between the Pareto fronts for different values of k with 50 traffic demands for DT topology.

The final part of this analysis is presented in Fig. 3.9 (a-b) by showing the Pareto fronts for both network topologies and different network scenarios. In order to achieve these non-dominated fronts, the evolutionary algorithm was run until the hypervolume remained constant for at least 60 consecutive generations. The plots confirm that it is possible to obtain the optimal Pareto fronts for all the network scenarios, targeting the minimization of the number of the OTN switches and line interfaces. For all the cases, it is possible to find a pool of optimal results in which the most appropriate solution can be chosen according to our optimization scenario. Furthermore, it can also be seen that when the number of traffic demands rises the number of line interfaces and the number of possible nodes to be equipped with OTN switches also increase. Both effects are associated with the need of accommodating more traffic, which directly leads to an increase on the number of line interfaces required and also provides more opportunities for intermediate grooming, increasing the number of OTN switches used.

In the example of DT topology (Fig. 3.9 (a)), the results can help the network planners that the use of a number of OTN switches superior to four does not lead to a considerable gain in the reduction of the number of line interfaces required to transport the traffic demands. Importantly, this assumption can be applied with both 100 and 200 traffic demands. On the other hand, the Pareto fronts presented for

ARPANET (Fig. 3.9 (b)) do not allow to utilize the same approach since an increase on the number of OTN switches will considerably allow to reduce the number of line interfaces for both sets of traffic demands. It can also be seen that probably the stopping criterium (60 consecutive generations with hypervolume constant) could not be the most appropriate criterium for complex scenario like the case of ARPANET with $|D|$ equal to 200 and k equal to 3 since the solutions with the number of OTN switches inferior to ten are not included in the Pareto front.

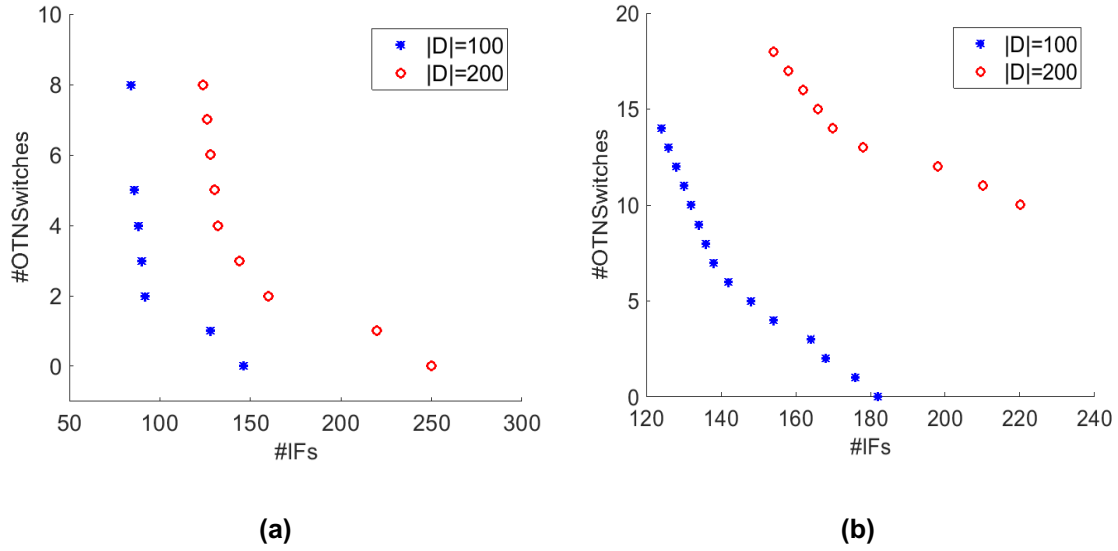

Figure 3.9 Pareto fronts with 100 and 200 traffic demands considering k=3 for (a) DT and (b) ARPANET topologies.

3.4 Chapter Summary

This chapter has focused on node dimensioning in the context of OTN considering the implementation of a more flexible architecture for electrical switching purposes (OTN switch). Particularly, the deployment of flexible switching configurations may enable savings on the amount of transmission resources required to accommodate the traffic. However, deploying this switching flexibility entails a premium, which implies that when designing the network multiple and possibly conflicting objectives can co-exist, leading to trade-off solutions (i.e., minimize transmission CAPEX vs. switching CAPEX). Thereby, the development of proficient procedures to properly dimension an optical transport network is a challenge to network operators.

For this reason, this study has presented a multi-objective network framework with the aim of minimizing both the number of line interfaces and the number of OTN switches required to route all traffic demands in order to reduce the overall capital expenditures. This type of optimization leads to a conflicting problem that can be efficiently handled with an evolutionary algorithm. For that purpose, the NSGA-II was revisited to address this multi-objective problem. However, it was observed that a straightforward implementation of this algorithm cannot efficiently solve this problem. Therefore, an adaptation of NSGA-II embedding problem-specific decisions into the initialization, mutation and crossover processes, called IF-Aware genetic algorithm, was proposed. Through a detailed analysis of

the proposed algorithm, it was shown to substantially improve the effectiveness of using an evolutionary algorithm in this scenario, increasing the diversity and quality of the final solutions, improving the convergence rate and decreasing the computation time when comparing it to a purely random NSGA-II [131].

On the other hand, this study has made it possible to assist the network planner in having insight on the range of possible trade-offs between the number of OTN switches and line interfaces required to design an OTN. For instance, if further savings in the number of OTN switches are targeted it is possible to infer what the impact is in the number of line interfaces and vice-versa.

Chapter 4: Network Planning with Next-Generation of Line Interfaces

Recent trends on optical transport networks emphasize the need of reducing the cost per bit transmitted in order to cope with the higher capacity requirements set by increasingly demanding applications and growth of IP traffic [22]. A key aspect is to exploit the use of each pair of line interfaces deployed per optical channel, since these devices can represent a large share of the total network cost. Therefore, two approaches are paramount to attain the reduction of cost per bit transmitted and the maximization of spectral efficiency: (i) achieve a high fill ratio of the optical channels (the total bit-rate of traffic demands transported by the total capacity available per channel) by optimizing the grooming of traffic demands; and (ii) operate the line interfaces with the higher order modulation formats and symbol rates that allows to increase the optical channels' capacity over a given routing path used to transport the traffic.

Empowered by the aforementioned aspects, the next-generation of coherent line interfaces will be equipped with advanced technologies that allow to operate with modulation formats up 64 QAM and at symbol rates of 64 Gbaud, which are twice the symbol rates of current line interfaces that operate at 32 Gbaud (Subsection 2.1.2.2.A). However, the deployment of these next-generation interfaces will inevitably lead to changes in the design of an optical network, since the fixed grid used up to recently must be replaced by a flexible DWDM grid to meet the expected co-existence of channels that operate at different symbol rates and spectral sizes in order to ensure a reasonable filtering tolerance for both channels. This leads to operational challenges, most notably in terms of managing the mismatch of frequency slots sizes in order to minimize the risk of spectrum fragmentation

In this context, the work of this chapter addresses the foreseen need to plan and provision services in optical transport networks where both current- and next-generation line interfaces co-exist, where the main goals are the minimization of both capital expenditures and spectral resource usage during the network lifetime. In order to proactively mitigate the fragmentation and complexity, the proposed service-provisioning framework described in this chapter includes a novel strategy to manage the spectrum resources from the beginning of network operation, taking advantage of the OTN switch capabilities described in the previous chapter (which assumes the use of OTN switches at each node of the network and thus the multi-objective framework proposed in the previous chapter is not a suitable approach). Moreover, it extends the framework to consider the support of 1+1 dedicated protection schemes at either the ODU and OCh layers (see Fig. 2.10), ensuring that every service provisioned can survive any single link failure.

This chapter is supported by two conferences and one journal publication associated with it. The network design framework for phased service-provisioning with current- and next-generation high symbol rate line interfaces is presented in [149]. On the other hand, the analysis of the proposed framework tailored for provisioning unprotected and protected services in a DWDM network, where both generations of optical line interfaces will co-exist, is performed in [150]. The complete study of the planning with the next-generation of line interfaces is published in [151].

4.1 Networking Aspects of Using Higher-Symbol Rate Line Interfaces

Throughout the years, the developments in digital signal processing combined with coherent detection have brought new opportunities and challenges to OTN over DWDM networks, enabling the deployment of different generation of optical line interfaces by providing both higher capacity and spectral efficiency, as described in Section 2.1.2.2.A [39, 69]. In the previous chapter, one of the objectives of the multi-objective problem consists of the minimization of the number of line interfaces that has assumed the use of interfaces with state-of-the-art electronics operating at 32 Gbaud. These devices have already enabled operation at different modulation formats (QPSK, 8 and 16 QAM) using a single line interface [13], which permit to support bit-rates of 100, 150 and 200 Gbit/s, respectively. As seen, when the spectral efficiency of the modulation schemes increases (by moving from QPSK to 16 QAM), the corresponding bit-rate also augments. However, the optical reach, i.e., the maximum distance that the optical signal can be transmitted with enough quality, decreases significantly (see Table 2.1) [69]. To overcome this limitation, one can rely on high-speed electronics and better DSP with the aim of increasing the symbol rate.

Therefore, the next-generation of line interfaces will further improve the optical line interfaces capabilities, namely by (i) providing a wider array of modulation formats (32 and 64 QAM) and by (ii) approximately doubling the maximum symbol rate (e.g., up to 64 Gbaud) [29, 30, 31, 32]. As a result, these line interfaces can provide (1) higher spectral efficiency and, more importantly, (2) twice the capacity (e.g., 400 Gbit/s vs. 200 Gbit/s using 16 QAM) with still acceptable reach using a single line interface. The capacity and optical reach of the different modulation formats supported by this generation of optical line interfaces are presented in Table 2.1 (3rd generation). As it is seen, they will be key to attain further reductions in the cost per transmitted bit through the augment of capacity per optical channel being deployed with minor optical reach penalties.

Despite the aforementioned advantages, the deployment of the next-generation of line interfaces will inevitably raise planning and operational challenges. In first place, the utilization of 64 Gbaud line interfaces requires wider bandwidths to support the transmitted signals than the 32 Gbaud ones in order to assure a reasonable tolerance to filter cascading in paths traversing many ROADMs [29, 69]. Since the spectral grid of 50 GHz standardized by ITU-T for fixed grid (see the example of Fig. 1.2 (a)) is no longer sufficient to support optical channels with symbol rates significantly higher than 32 Gbaud, the deployment of the next-generation of line interfaces will require the use of at least 75 GHz spectral width to properly transport their channels without impacting their filtering process that result in filtering penalty in the calculation of system margin of the optical performance evaluation described in 2.1.2.3.

In the second place, the co-existing optical channels realized with 32 and 64 Gbaud line interfaces will lead to a mismatch of channel spectral widths in the network operation that inevitably implies the adoption of a flexible grid (see Fig. 1.2 (c)). In this context, the adoption of a flexible grid and the co-existence of optical channels that operate at different symbol rates will potentially increase spectrum fragmentation and reduce the overall network performance, mainly in the presence of dynamic traffic

where the constant setting up and tearing down of traffic stimulates the misaligned of free spectral slots in the different network links that causes problems in the establishment of new optical channels [33, 34]. This deterioration can be further exacerbated by the fact that next-generation line interfaces are still under development, which means that, in the deployments taking place now or in the near future, the provisioning of traffic demands will rely first on the current generation of line interfaces (state-of-the-art electronics operating at 32 Gbaud) and later on when the next-generation of line interfaces become readily available leverage the potential of using the higher-symbol rate capabilities in the network operation. Consequently, the way in which the network is originally planned can also have an impact on its future performance.

Some studies have addressed the aforementioned networking challenges inherent in starting to operate with different symbol-rates [26, 152, 153]. More precisely, the study presented in [26] analyses the practical aspects of deploying the next-generation of optical line interfaces in DWDM spectral grid, whereas the work proposed in [152] highlights the benefits of adopting the 64 Gbaud line interfaces with regards to the augmentation of the transported traffic. On the other hand, [153] details a network simulation setup that compares the use of mixing the 50 GHz and 75 GHz spectral slots and only 75 GHz spectral slots to meet both the 32 Gbaud and 64 Gbaud line interfaces technologies. The results indicate that the use of flexible grid with 50 GHz and 75 GHz spectral slots, even dividing the spectrum into two parts: one for the 50 GHz frequency slots and the other part for 75 GHz, is only advantageous in increasing the network capacity if the exchanged traffic does not exceed the 200 Gbit/s, otherwise the use of only 75 GHz frequency slots to meet both types of line interfaces is more beneficial even with the overprovisioning of spectrum when the 32 Gbaud optical channels are assigned to 75 GHz frequency slots, emphasizing the impact of spectrum fragmentation with flexible grid in the network performance.

The aforementioned studies underline that it is paramount to develop an efficient network planning framework to be applied during the entire lifecycle of the transport network, taking into account the different types of line interfaces deployed and aiming at optimizing the long-term usage of spectrum resources from the beginning of the network operation in order to reduce the complexity and proactively mitigate spectrum fragmentation. Thus, the work presented in this chapter proposes a network design framework where this evolution in line interface technology is accounted for, such that the network costs and spectral resource usage can be minimized through the proposal of a novel spectrum management strategy. Moreover, in the view of the relevance of ensuring failure survivability in transport networks, the framework is also extended to support the dedicated protection.

4.2 Spectrum Grid Configurations

This section describes the strategy for managing the optical spectrum adopted in this study. For the sake of simplicity but without loss of generality, it is assumed that the current optical line interfaces operate at 32 Gbaud and the next generation of interfaces will operate at twice the symbol rate value of current ones (64 Gbaud) [29]. Figure 4.1 shows different options for allocating a spectrum to a set of predefined optical channels between the network nodes A-F, B-E and C-F. Note that, this example

assumes a translucent optical network with six nodes considering the use of ROADM and OTN switching technologies. Furthermore, it highlights the spectrum state on link C-E.

Through the illustration, it can be seen that the 50 GHz frequency slots of the fixed grid represented in Fig. 4.1 (a) are not sufficient to allocate higher-symbol rate channels (64 Gbaud) for two reasons. In first place, increasing the symbol rate results in a proportional increase in the spectral width of the channel and secondly, it is also necessary to ensure a reasonable tolerance to filter cascading in paths traversing many ROADMs [29, 69]. For these reasons, the adoption of a flexible grid (defined in Fig. 4.1 (b)) becomes a solution to accommodate both types of optical channels. Although some studies proposed in the literature [152, 153] assume the 75 GHz spectral width to carry the 64 Gbaud optical channels, since it is considered that the use of 75 GHz can comply with terrestrial meshed WDM networks thanks to advanced spectral engineering of optical filtering [152], this study assumes that the 64 Gbaud optical channels are allocated to 87.5 GHz frequency slots, which is the next multiple value of the network granularity (12.5 GHz) that can be applied in the context of flexible grid (see Fig. 1.2 (c)) with the aim of completely mitigating the possible penalty of the filtering process. In this context, the flexible grid configuration for this scenario is illustrated in Fig. 4.1 (b), making it possible to freely mix frequency slots of 50 GHz and 87.5 GHz. However, this scenario is more prone to spectrum fragmentation since the mismatch of channel spectral widths increases the misalignment of the available slots along the optical paths in the presence of traffic dynamics [35], which are expected to be present when considering the entire lifecycle of the network.

In order to mitigate the aforementioned problem, a different spectrum configuration is proposed in this work that assumes that a virtual grid of 87.5 GHz frequency slots and a specific spectrum allocation policy are set from the start of the network operation, as shown in Fig. 4.1 (c). Particularly, each 87.5 GHz frequency slot can be allocated to a single optical channel at 32 Gbaud or 64 Gbaud or to two optical channels at 32 Gbaud between the same end-nodes. This assumption deliberately restricts the frequency slot size to a common single value, making it possible to keep the spectrum management as simple as the management of a fixed grid. The key advantage of using a virtual grid is that it is intrinsically less predisposed to fragmentation, as it prevents the misalignment of different frequency slots, consequently reducing the need to perform a spectrum defragmentation procedure. Note that, this strategy follows the same approach considered in [34] to group the same channels in routing and spectrum assignment algorithm (even using different segments of the spectrum to provision the various types of channels), but in this scenario, each 87.5 GHz can be optimized to allocate different types of optical channels in same spectral slot and maintaining the concept of fixed grid. However, it also means that there is an overprovisioning of the spectrum when only a single 32 Gbaud optical channel is employed between the same end-nodes, as shown in Fig. 4.1 (d). The proposed optimization framework presented in the next section takes into account this drawback and tries to minimize it along the network's lifecycle.

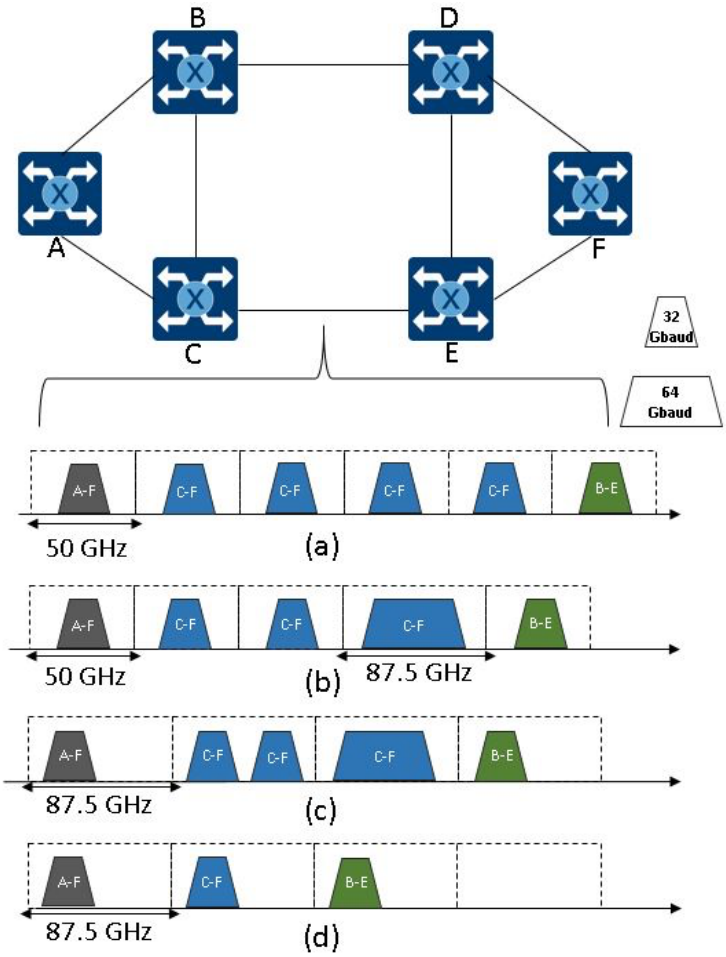

Figure 4.1 Spectrum configurations: (a) Fixed-grid configuration, (b) Flexi-grid configuration, (c) Virtual grid configuration and (d) example of overprovisioning of spectrum with a virtual grid.

4.3 Multi-Period Planning Workflow

The proposed framework is customized to optimize the co-existence of optical channels that operate at different symbol rates (32 Gbaud and 64 Gbaud) through the use of the 87.5 GHz virtual grid and is supported in an incremental multi-period planning approach [83], where the traffic is introduced per planning period and must be served according to optical channels already deployed in previous planning periods and via new optical channels or released line interfaces equipment. At each planning period, a percentage of the active traffic is removed that could result in line interfaces being released (idle equipment). Particularly, the framework considers a realistic scenario where in the first periods of network operation only 32 Gbaud line interfaces are deployed, whereas at a latter period when next-generation line interfaces become readily available ($T_{next-gen}$), the network operator only acquires 64 Gbaud line interfaces and reuses 32 Gbaud line interfaces that are released via the percentage of removed traffic at each planning period. The optimization is conducted with the aim of minimizing the total number of interfaces required and the spectral resource usage throughout the entire network lifetime. Note that the former is directly related to CAPEX, whereas the latter determines how much capacity can be carried over the network up to having to invest in new fibre rollout/lease. In contrast to

the problem described in the previous chapter, this multi-objective problem will not lead to conflicting results, meaning that minimizing one objective necessarily means that the other is also being minimized and vice-versa. Therefore, the minimization of both objectives can be combined through an ILP model.

In the network design, it is assumed that all nodes are equipped with OTN switches and ROADMs (characterized in Fig. 2.14 (b)) [49, 154]. Although the introduction of OTN switches increments the overall network cost (as described in the previous chapter), this technology plays an important role in this network planning strategy in order to effectively optimize the spectrum resource usage since the traffic can be switched between different optical channels remotely. The remainder of this section details the complete workflow and the algorithms proposed.

4.3.1 Planning Workflow

The complete flowchart of the planning workflow is described in Fig. 4.2. The workflow receives as input the network physical topology, the total number of periods ($T_{periods}$), and the planning period where the next-generation of line interfaces (IFs) become available ($T_{next-gen}$). The modulation formats considered in this work and the corresponding reach and bit-rate are shown in Table 2.1 for 2nd (32 Gbaud) and 3rd generation (64 Gbaud) that correspond to current- and next-generation of line interfaces, respectively. Note that the technology for supporting the higher-order modulation formats, 32 QAM and 64 QAM, are only available with the next-generation of line interfaces and that the reach figures of 64 Gbaud optical channels assume a penalty when compared to 32 Gbaud optical channels using the same modulation format since it is considered that the transmission of channels operating at higher symbol rates suffers a greater impact from the optical impairments. On the other hand, the use of 64 Gbaud also allows to double the total capacity available per optical channel for the same modulation format when compared to the 32 Gbaud technology (Subsection 2.1.2.1).

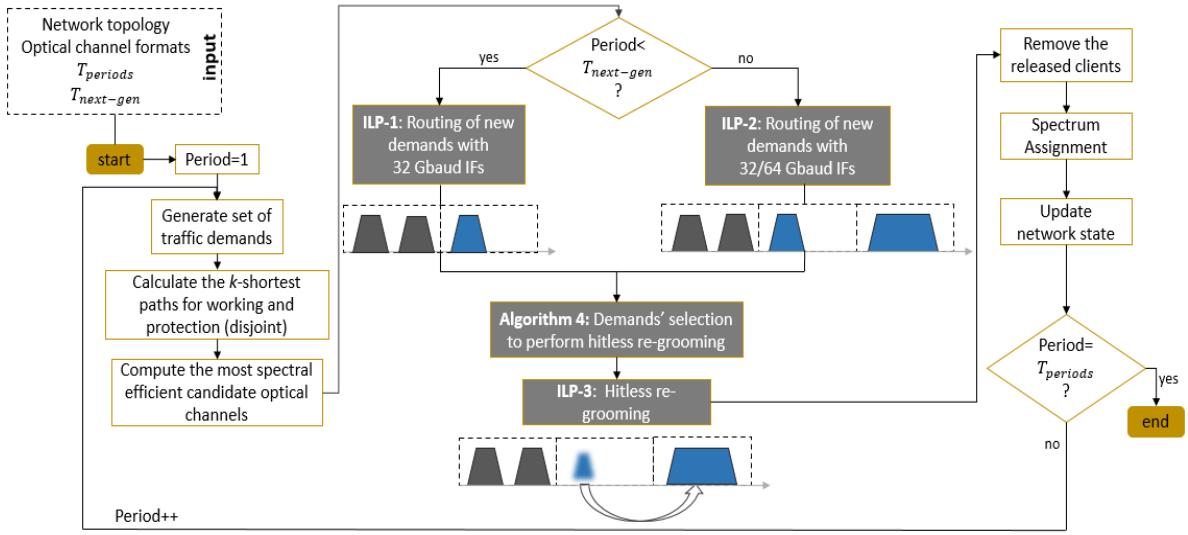

Figure 4.2 Multi-period planning workflow.

The optimization is carried out per planning period, i.e., knowing the set of traffic demands of the current planning period and the network state but not knowing the parameters of the next planning

periods. For each traffic demand, a set of candidate routing paths is first computed based on the *k*-shortest path algorithm. In case of survivability being considered in the design problem, the *k*-shortest path algorithm also includes the computation of the paths for working and the ones for protection, ensuring the disjointness between both paths. For each routing path and using the reach figures of Table 2.1, the most spectrally efficient modulation format that does not require intermediate 3R regeneration between nodes along the path is assessed considering total length of the path and the optical performance evaluation presented in 2.1.2.3. This is performed only for a symbol rate of 32 Gbaud up to $T_{next-gen}$ and for both 32 Gbaud and 64 Gbaud afterwards. The result of this step is a list of the most spectrally efficient candidate optical channels over the pre-computed paths.

In this context, Fig. 4.3 presents a network design example of the calculation of the most spectral efficient candidate optical channels for both current and next-generation of line interfaces. The network physical topology and the set of traffic demands utilized is illustrated in Fig. 4.3 (a) and (b), respectively. For the sake of simplicity, it is assumed one traffic demand at 10 Gbit/s between the network nodes A and F and k=1 for the computation of the k-shortest path algorithm without considering the survivability of the network only for illustration purposes. Based on the shortest path, the most spectral efficient candidate optical channel (the modulation format that provides the highest feasible bit-rate) between the different network nodes along the path according to the total length is assessed. The feasibility of the modulation formats follows the optical reach defined in Table 2.1 for each generation of line interfaces technology. Note that, the optical reach of Table 2.1 is considered to be the maximum distance that format can be transmitted with the sufficient quality-of-transmission that enables the reception of the data at the receiver based on the optical performance evaluation presented in 2.1.2.3. In this example, the set of candidate optical channels are shown in Fig. 4.3 (c) and (d) for both 32 and 64 Gbaud

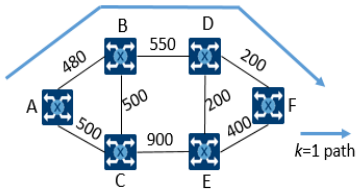

(a)

Demand	Source node	Destination node	Bit Rate [Gbit/s]	K-shortest paths (links)
1	A	F	10	K=1->[A-B-D-F]

(b)

Optical channels @ 32 Gbaud

Source node	Destination node	Capacity [Gbit/s]	Modulation Format	Links
A	B	200	16 QAM	A-B
B	D	200	16 QAM	B-D
D	F	200	16 QAM	D-F
A	D	150	8 QAM	A-B-D
B	F	200	16 QAM	B-D-F
A	F	150	8 QAM	A-B-D-F

(c)

Optical channels @64 Gbaud

Source node	Destination node	Capacity [Gbit/s]	Modulation Format	Links
A	B	400	16 QAM	A-B
B	D	400	16 QAM	B-D
D	F	500	32 QAM	D-F
A	D	300	8 QAM	A-B-D
B	F	400	16 QAM	B-D-F
A	F	300	8 QAM	A-B-D-F

(d)

Figure 4.3 Network design example of the computation of the most spectral efficient candidate optical channels using 32 and 64 Gbaud technology.

technology. Note that, these sets of candidate optical channels are then incorporated into the optimization process in order to select the set of optical channels that integrate a certain path (optical channels' path) to meet each traffic demand.

The optimization process described in Fig. 4.2 is then divided into two phases, according to whether the planning period precedes $T_{next-gen}$ or not. Until that period, the algorithm ILP-1 performs the optimization only with current line interface technology (32 Gbaud). It serves the new traffic demands re-using as much as possible the optical channels already deployed in the previous planning periods (with enough available capacity) and the line interfaces that have been released at each planning period of the network due to the removed traffic considered in a multi-period context (described in Subsection 2.1.3) with the aim of minimizing the number of new line interfaces that have to be acquired. Moreover, the ILP-1 also has the objective of reducing the number of single 32 Gbaud channels on an 87.5 GHz frequency slot without increasing the overall network cost aiming at minimizing the overprovisioning of the spectrum described in Fig. 4.1 (d).

Conversely, when the algorithm reaches the planning period $T_{next-gen}$, the ILP-2 algorithm is employed instead. This algorithm reuses 32 Gbaud optical channels already deployed in the previous planning periods when they have enough available capacity to accommodate the new traffic demands and reuses the released 32 Gbaud line interfaces to create new optical channels, but only if this enables pairing two 32 Gbaud channels on the same 87.5 GHz frequency slots in order to mitigate the overprovisioning of spectrum described in Fig. 4.1 (d). Otherwise, the algorithm creates a new optical channel at 64 Gbaud. It is noteworthy that after $T_{next-gen}$, the framework prevents the allocation of free 87.5 GHz frequency slots to single 32 Gbaud optical channel between the same end-nodes, thereby giving preference to configurations that make a more efficient utilization of the spectrum.

After routing the new traffic demands, the optimization is complemented by performing a hitless re-grooming procedure that makes possible to maintain the optical channel fill ratio (the total bit-rate of traffic demands transported over the total capacity available per channel) at higher levels aiming at exploiting as much as possible the capacity provided by each optical channel deployed and potentially releasing underutilized line interfaces, which allows to optimize the spectrum and even reutilize the released line interfaces for the next planning periods. This procedure makes use of the OTN switching [49] capabilities that allow us to shift the traffic demands between optical channels. Note that, the ILP-3 model is preceded by a heuristic algorithm (Algorithm 4) that optimizes the selection of the traffic demands to perform the hitless re-grooming process. In order to reduce the complexity of the ILPs and ensure the workflow is scalable, spectrum assignment is performed subsequently, using the first-fit algorithm.

At the end of each planning period, the amount of spectrum used and the number of line interfaces deployed from both symbol rates are calculated. The sequential ILPs have different, yet complementary, roles in the optimization process. Their combined effect aims at proactively maintaining as many as possible frequency slots available for the upcoming and more cost-effective 64 Gbaud line interfaces without compromising CAPEX in each planning period. Consequently, it aims to meet the long-term

expectation of the network operator of sustaining more traffic load with the same fibre infrastructure without having to incur additional spending when compared to neglecting this goal and focusing solely on minimizing CAPEX at each planning period.

4.3.2 ILP Models and Heuristic Algorithm

This subsection introduces the three ILP models referred to in Fig. 4.2. The ILP models require the following variables and input parameters.

Parameters:

V	Set of network nodes
E	Set of network links
SR	Set of symbol rates, $SR = \{32,64\}$
L	Generic set of candidate optical channels with both types of symbol rates $sr \in SR$ (as described in the example of Fig. 4.3)
L_{sr}	Set of optical channels available per symbol rate $sr \in SR,\ SR = \{32,64\}$
L_e	Set of optical channels that traverse the network link $e \in E$
$L_{i,j}$	Generic set of available optical channels between source node i and destination node j
L_T	Set of optical channels already deployed in previous planning periods
D	Set of new traffic demands
D_T	Set of traffic demands already allocated in the previous planning periods
D_r	Set of traffic demands that have to be re-groomed
P	Set of working and protection paths that have to be assigned to traffic demand $d \in D$
X_l	Total number of 1.25 Gbit/s slots supported by the optical channel $l \in L$ according to its capacity
N_d	Total number of traffic demands between the same end-nodes and bit-rate $d \in D$

S_d	Total number of 1.25 Gbit/s slots per traffic demand $d \in D$ according to its bit-rate
$W_d^{l,p}$	Total number of traffic demands from type $d \in D_T$ that use the optical channel $l \in L_T$ over working and protection path $p \in P$ in the previous planning periods
F	Total number of available 87.5 GHz frequency slots (virtual grid) per network link
I_{sr}	Number of line interfaces available in inventory with symbol rate $sr \in SR$
Q_{sr}	Total number of line interfaces already deployed in previous planning periods with symbol rate $sr \in SR$
M_l	Maximum number of optical channels from type $l \in L$ that can be established for the 87.5 GHz frequency slot composition
B	Weight parameter used to balance the constraints of the ILP model
A, Z	Weight parameter used to balance the objectives of the ILP model

Variables:

$\lambda_{d_{(o,t)}}^{l_{(i,j)},p} \in \mathbb{N}^0$	Number of traffic demands from type $d \in D$ between source node o and destination node t using optical channel $l \in L$ with source node i and destination node j over working or protection path $p \in P$
$\theta_l \in \mathbb{N}^0$	Number of optical channels required for the candidate format $l \in L$
$\delta_l \in \mathbb{N}^0$	Number of frequency slots of 87.5 GHz (virtual grid) used to meet $l \in L$
$\pi_l \in [0,1]$	Binary variable that indicates if the number of optical channels from the format $l \in L$ is an odd number
ϑ	Total number of single 32 Gbaud optical channels allocated in the 87.5 GHz frequency slots (as the ones illustrated in Fig. 4.1 (d))
$\beta_{sr} \in \mathbb{N}^0$	Total number of line interfaces that have to be acquired with symbol rate sr, $SR = \{32,64\}$
$\gamma_{sr} \in \mathbb{N}^0$	Total number of line interfaces released with symbol rate sr, $SR = \{32,64\}$
φ	Total number of 32 Gbaud interfaces used from inventory (set of released interfaces in the previous planning periods via the removed traffic)

$\omega \in \mathbb{N}^0$ Total number of line interfaces required

The following formulation describes the ILP-1 model, which is responsible for routing the new demands when only the 32 Gbaud line interfaces are available:

$$min\ (\beta_{sr=32} + \frac{\vartheta}{|L_{sr=32}|}) \tag{4.1}$$

subject to

$$\lambda_d^{l,p} = W_d^{l,p} \quad \forall d \in D_T, \forall l \in L_T, \forall p \in P \tag{4.2}$$

$$\sum_{l \in L_{i,j=v}} \lambda_{d_{(o,t)}}^{l_{(i,j)},p} - \sum_{l \in L_{i=v,j}} \lambda_{d_{(o,t)}}^{l_{(i,j)},p} = \begin{cases} -N_d, & v = o \\ N_d, & v = t \\ 0, & \forall v \in V \backslash \{o,t\} \end{cases} \quad \forall d \in D, \forall p \in P \tag{4.3}$$

$$\sum_{p \in P} \sum_{d \in D} S_d \times \lambda_d^{l,p} \leq X_l \times \theta_l \qquad \forall l \in L_{sr=32} \tag{4.4}$$

$$\frac{1}{2} \times \theta_l \leq \delta_l \leq \frac{1}{2} \times \theta_l + 1 \qquad \forall l \in L_{sr=32} \tag{4.5}$$

$$\sum_{l \in L_e} \delta_l \leq F \qquad \forall e \in E \tag{4.6}$$

$$\delta_l - \frac{1}{2} \times \theta_l \leq \pi_l \qquad \forall l \in L_{sr=32} \tag{4.7}$$

$$\sum_{l \in L_{sr=32}} \pi_l = \vartheta \tag{4.8}$$

$$\sum_{l \in L_{sr=32}} 2 \times \theta_l - Q_{sr=32} - I_{sr=32} = \beta_{sr=32} \tag{4.9}$$

The objective function (4.1) consists of minimizing the number of 32 Gbaud line interfaces that have to be acquired (primary objective) and also gives priority to obtain a solution with the higher number of 87.5 GHz frequency slots allocated to two optical channels operating at 32 Gbaud (secondary objective) in order to avoid the overprovisioning of spectrum described in Fig. 4.1 (d). Note that, the variable ϑ indicates the number of 87.5 GHz frequency slots allocated with only one optical channel operating at 32 Gbaud, since the global optimization of the ILP model searches for the minimum, implicitly it is maximizing the number of 87.5 GHz frequency slots allocated to two 32 Gbaud optical channels that avoids the overprovisioning of spectrum. Moreover, this is achieved without increasing the number of line interfaces (additional capital expenditures) since it is ensured that the secondary objective is within the range of $[0,1]$ by normalizing it by the total number of candidate optical channels operating at 32 Gbaud in contrast with the primary objective that is an integer number.

Constraints (4.2) impose that the traffic demands already deployed in previous planning periods maintain the same optical channels' path and (4.3) select the optical channels' path to meet each traffic

demand, ensuring the general flow conservation along the path for all traffic demands. The total number of optical channels utilized are computed on constraints (4.4) according to the total traffic transported and the capacity of the channel. According to the number of optical channels deployed, the constraints (4.5) calculate the number of 87.5 GHz slots used. This computation has to take into account the fact that each 87.5 GHz frequency slot can include one or two channels operating at 32 Gbaud symbol rate and thus the number of optical channels used should be divided by two. The constraints (4.6) guarantee that the total number of allocated frequency slots of 87.5 GHz does not exceed the link capacity.

The constraints (4.7) and (4.8) compute the total number of single optical channels at 32 Gbaud symbol rate allocated on the 87.5 GHz frequency slots. To put it more concretely, the constraints (4.7) are based on the number of 87.5 GHz frequency slots utilized and the total number of optical channels used divided by two. The Equation described in (4.7) is equal to zero when the number of 32 Gbaud channels allocated to 87.5 GHz frequency slots is even otherwise it superior to zero, allowing to determine by a binary variable if the number of optical channels deployed is an odd value per candidate channel $l \in L$. These constraints are complemented by summing all the binary variables in order to calculate the total number of single optical channels operating at 32 Gbaud symbol rate on the 87.5 GHz frequency slots, as detailed in (4.8). Finally, the total number of 32 Gbaud interfaces that have to be acquired is defined by (4.9). In case of this ILP model, the number of variables is defined by $|D| \times |L| \times |P| + 3 \times |L| + 2$, whereas the number of constraints is given by $|D_T| \times |L_T| \times |P| + |D| \times |V| \times |P| + 3 \times |L_{sr=32}| + |E| + 2$.

The ILP-2 formulation is described below. This model is responsible for routing the new demands when both 32 and 64 Gbaud line interfaces are utilized:

$$\min\ (\beta_{sr=64} + A \times \varphi) \begin{cases} A = \frac{1}{1+I_{sr=32}} & I_{sr=32} = 0 \\ A = \frac{1}{I_{sr=32}} & I_{sr=32} > 0 \end{cases} \tag{4.10}$$

subject to

(4.2), (4.3), (4.6) from the definition of ILP-1

$$\sum_{d \in D} \sum_{p \in P} S_d \times \lambda_d^{l,p} \leq X_l \times \theta_l \qquad \forall l \in L \tag{4.11}$$

$$B \times \theta_l \leq \delta_l \leq B \times \theta_l + 1 \quad \begin{cases} B = \frac{1}{2}\ \forall l \in L_{sr=32} \\ B = 1\ \forall l \in L_{sr=64} \end{cases} \tag{4.12}$$

$$\sum_{l \in L_{sr=32}} \theta_l \leq \frac{Q_{sr=32}}{2} + \frac{I_{sr=32}}{2} \tag{4.13}$$

$$\theta_l \leq M_l \qquad \forall l \in L_{sr=32} \tag{4.14}$$

$$\sum_{l \in L_{sr=64}} 2 \times \theta_l - Q_{sr=64} - I_{sr=64} = \beta_{sr=64} \tag{4.15}$$

$$\sum_{l \in L_{sr=32}} 2 \times \theta_l - Q_{sr=32} = \varphi \tag{4.16}$$

The objective function (4.10) minimizes the number of 64 Gbaud line interfaces that have to be acquired (first term) and has a secondary objective to minimize the number of 32 Gbaud line interfaces utilized from the inventory (line interfaces that are released in the previous planning periods) that originate single 32 Gbaud optical channels in the 87.5 GHz frequency slots with the aim of reducing the overprovisioning of spectrum. The A value is used for normalizing the secondary objective according to the number of interfaces presented in the inventory and it also considers the possibility of the inventory not having any line interfaces. The constraints (4.2), (4.3) and (4.6) are the same as those introduced for the ILP-1 model. The constraints (4.11) compute the total number of optical channels utilized according to the total traffic transported and the capacity of the channels. Moreover, the calculation of the 87.5 GHz slots used is set by (4.12) and it depends on the symbol rate of the optical channels. Note that each 87.5 GHz frequency slot can include one or two 32 Gbaud optical channels or one optical channel at 64 Gbaud, so constraints (4.12) should consider these different scenarios.

The constraints (4.13) and (4.14) enforce that the number of existing 32 Gbaud line interfaces is maintained, according to the inventory and the previously deployed line interfaces, whereas constraints (4.15) and (4.16) compute the number of 64 Gbaud line interfaces that have to be acquired and the number of 32 Gbaud interfaces used from the inventory list, respectively. Note that, this formulation is always implicitly exploiting the in-service optical channels already deployed in previous planning periods and as a second option, it is constantly reusing the line interfaces present in the inventory before introducing new 64 Gbaud line interfaces. The reutilization of idle 32 Gbaud line interfaces is restricted to adding optical channels to frequency slots where a single optical channel is already present, which gradually contributes to mitigate spectrum overprovisioning. In case of this ILP model, the number of variables is defined by $|D| \times |L| \times |P| + 2 \times |L| + 2$, whereas the number of constraints is given by $|D_T| \times |L_T| \times |P| + |D| \times |V| \times |P| + 2 \times |L| + |L_{sr=32}| + |E| + 3$.

Finally, the ILP-3 model aims to perform a hitless re-grooming process in order to exploit as much as possible the capacity provided by each optical channel deployed and potentially releasing underutilized line interfaces that can be reused in the next planning periods via the use of OTN switches that allows to shift traffic demands between optical channels. The mathematical formulation is as follows:

$$\max \left(\gamma_{sr=32} + Z \times \gamma_{sr=64}\right) \{Z < 1 \tag{4.17}$$

subject to

$$\sum_{l \in L_{i,j=v}} \lambda_{d_{(o,t)}}^{l_{(i,j)},p} - \sum_{l \in L_{i=v,j}} \lambda_{d_{(o,t)}}^{l_{(i,j)},p} = \begin{cases} -N_d, & v = o \\ N_d, & v = t \\ 0, & \forall v \in V \backslash \{o,t\} \end{cases} \quad \forall d \in D_r, \forall p \in P \tag{4.18}$$

(4.2), (4.6) from the definition of ILP-1

(4.11), (4.12) from the definition of ILP-2

$$\sum_{l \in L} \theta_l \leq \frac{Q_{sr=32}}{2} + \frac{Q_{sr=64}}{2} \tag{4.19}$$

$$Q_{sr=32} - \sum_{l \in L_{sr=32}} 2 \times \theta_l = \gamma_{sr=32} \tag{4.20}$$

$$Q_{sr=64} - \sum_{l \in L_{sr=64}} 2 \times \theta_l = \gamma_{sr=64} \tag{4.21}$$

The objective function (4.17) maximizes the number of released line interfaces through the re-grooming process. This process seeks to reallocate already routed traffic demands to other existing optical channels in order to maximize the number of optical channels that become empty and, as a result, maximize the number of released line interfaces. The implementation of OTN switches in the network nodes plays an important role in this model, since it allows to switch the client signals from one line interface to another, which is the main characteristic of the re-grooming process. The main goal of this model is to optimize the grooming process and minimize the capital expenditures associated with the number of line interfaces with the aim of this minimization could offset the cost of the OTN switches. Note that, although there is a cost of OTN switches (as highlighted in previous chapter), it is considered to be residual when compared to the line interface cost which are among the most expensive equipment in the optical network [109].

The number of released line interfaces from different symbol rates is balanced by parameter Z in the objective function defined in (4.17), where $Z < 1$ in order to give priority to releasing the 32 Gbaud line interfaces such that in the long-term the overprovisioning of 87.5 GHz frequency slots is mitigated. Although most of the constraints are already defined in the previous models, the main difference in this formulation is the definition of the set of candidate traffic demands D_r that should be re-groomed to another path. The constraints (4.18) are only applied to the subset of traffic demands D_r in this model. Moreover, the constraints (4.19) ensure that the number of optical channels is not incremented during the re-grooming process. Finally, the constraints (4.20) and (4.21) compute the number of released 32 and 64 Gbaud line interfaces, respectively. In case of this ILP model, the number of variables is defined by $|D| \times |L| \times |P| + 2 \times |L| + 1$, whereas the number of constraints is given by $|D_T| \times |L_T| \times |P| + |D_r| \times |V| \times |P| + 2 \times |L| + |E| + 3$. Moreover, the selection of the traffic demands for performing the re-grooming process is described by the pseudocode in Algorithm 4.

Algorithm 4: Demands' selection to perform re-grooming

Input: Total set of optical channels used from the variable θ_l of the ILPs
Total set of traffic demands ($D_T \cup D$)
FillThresh

1 Initialize an empty list, pOCh, which will indicate the optical channels with potential to be released.
2 ***for*** each $l \in \theta_l$
3 Calculate the optical channel fill ratio (FR_l)
4 ***if*** l operates at 32 Gbaud symbol rate

5 ***if*** l is single in the 87.5 GHz frequency slot
6 Set pOCh(l)=1
7 ***else***
8 Set pOCh(l)=0
9 ***end if***
10 ***else***
11 ***if*** $FR_l < FillThresh$
12 Set pOCh(l)=1
13 ***else***
14 Set pOCh(l)=0
15 ***end if***
16 ***end if***
17 ***for*** each $d \in (D_T \cup D)$
18 Get the set of optical channels used to transport d based on variable $\lambda_d^{l,p}$ of the ILPs, L_d
19 Count the number of optical channels in traffic demand's routing path (L_d) with pOCh=1, $counter$
20 ***if*** $\frac{counter}{|L_d|} \geq FillThresh$
21 add d to D_r list
22 **return** D_r

The algorithm starts by evaluating the established optical channels in terms of their potential to be released. This potential is measured according to the channels that carried the lowest number of traffic demands since it augments the probability of the traffic being successfully rerouted to other channels. On the other hand, the single channels operating at 32 Gbaud symbol rate in the 87.5 GHz frequency slots are also considered to be potential channels to be released, since their release will benefit the spectrum utilization by mitigating the overprovisioning of spectrum.

In this context, the algorithm considers that the 32 Gbaud channel is a potential candidate to be released if it represents a single channel in an 87.5 GHz slot. On the other hand, the 64 Gbaud channel is set as candidate to be released if its optical channel fill ratio (the total bit-rate of transported traffic demands over the total capacity available of the channel) is below the minimum threshold ($FillThresh$), which is a predefined input variable. After analysing the established optical channels, the algorithm chooses the traffic demands to perform the re-grooming process, which are the ones that are routed over the highest percentage (above a predefined threshold) of optical channels with potential to be released. The main idea is to select only the traffic demands that will allow to release the maximum number of optical channels, based on the aforementioned criterium of potential channels to be released. After the selection of the traffic demands to be re-groomed (D_r), the ILP model (ILP-3) tries to change their optical channels' path and maintains the other demands' paths through the constraints already defined in previous formulations.

The support of the dedicated protection schemes (defined in the Fig. 2.10) to ensure the survivability of the different traffic demands is not explicitly defined in the previous ILP models, except in the definition of the variable P in order to assign disjoint working and protection paths to each traffic demand in the 1+1 dedicated ODU protection scheme. The implementation of the specific survivability scheme is essentially defined before the ILPs' procedure. In the case of 1+1 protection at the ODU level, it is

basically enforced that the traffic demands are duplicated and routed through disjoint paths, whereas in the case of protection at the OCh level, each new optical channel will instead consist of both a working and a protection optical channel using the same line interface, which are constrained to be disjoint, use the same spectrum, symbol rate and modulation format (described in Subsection 2.1.3.2).

4.4 Impact of Adopting Next-Generation of Line Interfaces

In order to assess the impact of adopting the next-generation of line interfaces, three different design scenarios are considered for the purpose of evaluating and comparing the performance of the proposed network design framework. The first scenario (VirtualGrid) corresponds to the proposed workflow with the incorporation of the 87.5 GHz virtual grid from the beginning of the network lifecycle, whereas the second one assumes the existence of a flexible grid with both 50/87.5 GHz frequency slots (FlexiGrid). The third scenario assumes that only the 32 Gbaud interfaces remain operational and, in this case, the 50 GHz fixed grid is sufficient to provision these types of optical channels (FixedGrid). The analysis considers two reference transport networks illustrated in Fig. B.1 and B.2 of Appendix B: the DT network and Telefónica Spanish backbone network (SBN). Both network topologies were defined in the scope of the FP7 IDEALIST project by the abovementioned network operators [155].

For both networks, it was assumed that 30% of all node-pairs exchange traffic selected at random. The traffic demands were randomly generated with 60% and 40% of traffic being ODU2 (10 Gbit/s) and ODU4 (100 Gbit/s), respectively. For each node-pair, it was considered all the grooming possibilities along its shortest path, both for working and protection paths. The allowed channel formats are described in Table 2.1 for the 2nd and 3rd generation of optical line interfaces. For each candidate optical channel, the modulation format with the highest feasible bit-rate is chosen according to its symbol rate.

Each design scenario was evaluated with 20 planning periods, which considers the highest traffic growth profile in the first ten planning periods of the network operation with a traffic increase of 30% and the remaining ones with a traffic growth of 10%. At the end of each period, 5% of the traffic demands were removed from the network. This traffic profile was chosen with the objective of deliberately stressing the network to assess the maximum carried traffic load before service blocking starts to occur with the predefined network infrastructure. Note that, this growth profile is on average similar to the forecasted value per year by Cisco [22].

The results are averaged over 20 independent simulation runs. The ILP models were solved using the CPLEX solver platform [147] running on a PC with an Intel® Xeon® E5-2690 v2 3 GHz processor and 48 GB of RAM. The complexity of ILP models (variables and constraints) is mainly defined by the number of traffic demands deployed per planning period (D) and the total number of candidate optical channels calculated to meet the traffic (L) for both working and protection paths. Nevertheless, on average the simulation run, for 20 planning periods, takes approximately 6 minutes for DT topology and 25 minutes for SBN, although it depends on the traffic growth profile and the pattern of the protection schemes required per traffic demand.

For both VirtualGrid and FlexiGrid, it was assumed that the 64 Gbaud line interfaces would become available from the third period onwards. Also, it was considered that each fibre link would use the C-band with capacity to accommodate 54 slots of 87.5 GHz or 96 frequency slots of 50 GHz. In the proposed workflow, the parameter Z was defined as 0.7 in the ILP-3 in order to give priority for releasing the 32 Gbaud line interfaces but still promote the release of 64 Gbaud line interfaces and a $FillThresh$ of 0.6 in the Algorithm 4 with the aim of making room to re-groom the largest number traffic demands focusing on the release of the largest number of line interfaces that can be re-used in the next planning periods.

The analysis of the planning with the next-generation of optical line interfaces is mainly divided into three sets of results. The first part of the study consists of the evaluation of the spectrum usage throughout the entire network lifecycle for all the design scenarios (virtual, fixed- and flexible-grid). The second set of results is intrinsically associated with the first one, since the network is deliberately stressed in order to assess the maximum carried traffic load before blocking starts to occur, which is directly influenced by the efficiency of the spectrum management and allocation policies. The final part of this section assesses the cumulative number of line interfaces that have to be acquired along all planning periods, with the aim of comparing the expected overall cost associated with the employment of the different design strategies.

4.4.1 Spectral Consumption

The first set of results is presented in Figure 4.4 for both DT and SBN topologies. The figures depict the spectrum utilization (SU) along the different planning periods considering the traffic demands completely unprotected and protected with ODU or OCh 1+1 dedicated protection schemes. The spectrum utilization is calculated through the Equation (4.22) by the sum of the number of 87.5 GHz frequency slots utilized for all network links that includes the spectrum utilized for working and protection paths.

$$SU = (\sum_{e \in E} \sum_{l \in L_e} 87.5 \times \delta_l)/1000 \ (THz) \tag{4.22}$$

The results show that despite the initial overprovisioning of spectrum with VirtualGrid due to the use of 87.5 GHz frequency slots to allocate only the 32 Gbaud interfaces, the adoption of the proposed design framework allows to spectrally recover from this initial disadvantage and in the mid-term outperform the other strategies in both networks and for all survivability schemes considered. This highlights the importance of tailoring the resource allocation decisions at the early stage of network operation to account for the next-generation of line interfaces (64 Gbaud).

Furthermore, it can also be observed that the ODU protection scenario is the one where VirtualGrid is able to recover and provide a reduced spectrum usage faster, whereas the opposite occurs in the OCh protection scenario. This behaviour can be explained by the fact that the OCh protection scheme is constrained by the need of maintaining the same spectral allocation for both working and protection paths, which reduces the ability of releasing line interfaces from underutilized optical channels via hitless

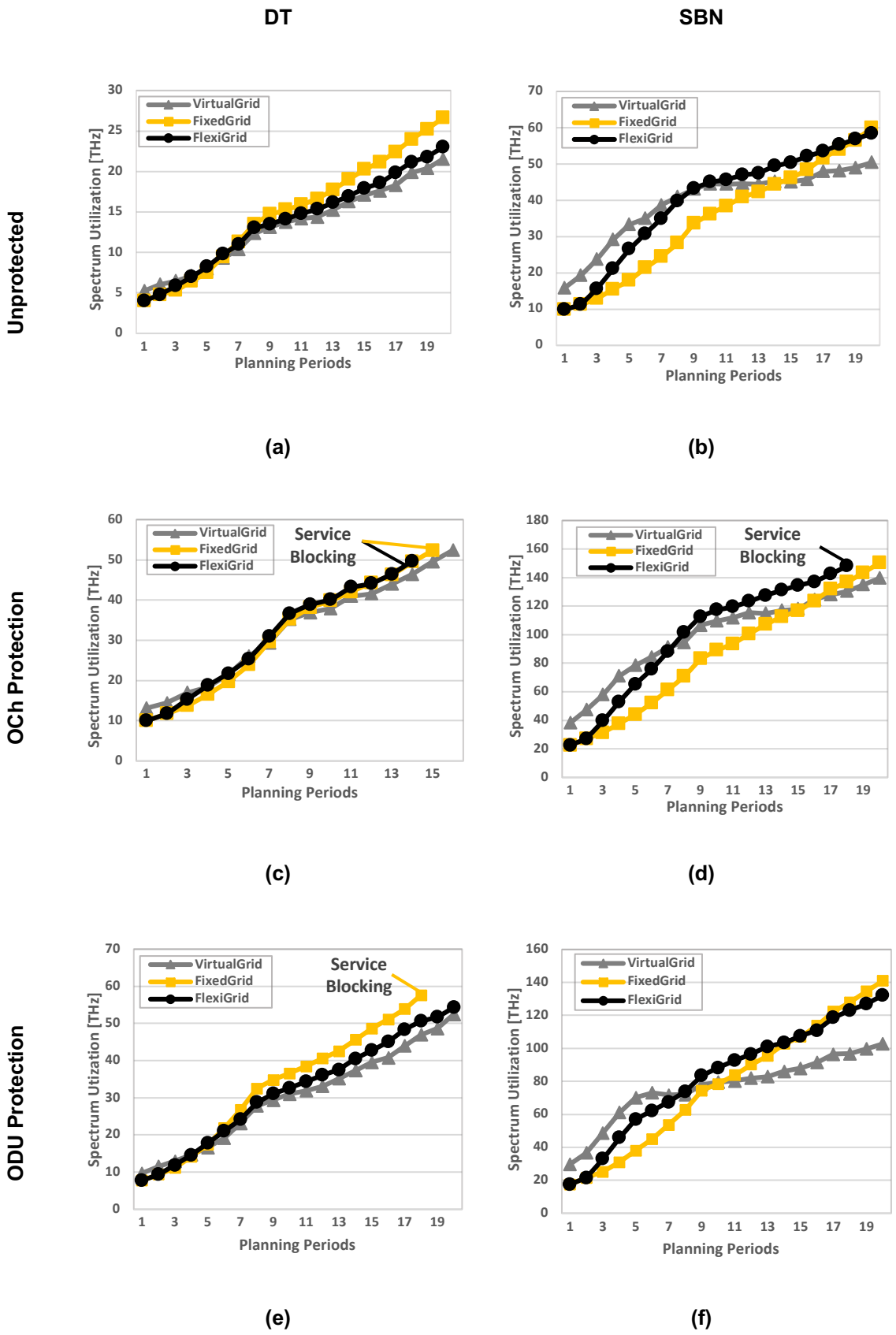

Figure 4.4 Spectrum usage throughout the entire network lifecycle for (a) DT and Unprotected, (b) SBN and Unprotected, (c) DT and OCh protection, (d) SBN and OCh protection, (e) DT and ODU protection and (f) SBN and ODU protection.

re-grooming. Conversely, in the ODU protection scenario it is possible to independently re-groom the

working and protection ODU since the paths use different line interfaces as described in Fig. 2.10 (a), facilitating the task of ILP-3. Moreover, the fact that the support of protection effectively means increasing the amount of traffic being carried in the network, justifies why VirtualGrid also attains an earlier turnaround in the spectrum usage in the case of ODU protection scenario than in the absence of protection.

When comparing the results obtained with both network topologies, it can be seen that DT enables VirtualGrid to achieve an earlier turnaround in spectrum consumption, whereas SBN allows this strategy to attain a higher reduction in spectrum consumption towards the end of the network life-cycle although at the expense of a much higher spectrum overprovisioning in the earlier periods. The latter observation is particularly relevant, since it highlights that in a larger and more complex network topology the spectrum management policy has a more pronounced impact and that the proposed approach can be paramount to attain long-term spectral savings in these networks.

The limitations of spectral allocation with the OCh protection scheme are even more noticeable when employing the FlexiGrid strategy, since it is not able to provide additional capacity from the 14th planning period in DT and from 18th planning period in SBN without blocking some traffic demands. This situation can be explained by the misalignment of the available frequency slots along the optical channels which results in deterioration of the network performance due to the fragmentation problems, essentially in network scenarios such as OCh protection scheme that required the same spectrum allocation for both working and protection paths. On the other hand, the FixedGrid design has the opposite trend: in the beginning of network operation, it is the one that has the smallest spectrum usage, but the fact that it cannot explore higher symbol rate optical channels leads to increasing the number of 50 GHz frequency slots used, eventually exhausting network capacity, as shown in Fig. 4.4 (e).

In the unprotected scenario all traffic demands can be accommodated up to the end of the network life-cycle, enabling computation of the final spectral gain. Hence, it can be seen that VirtualGrid enables to reduce the spectrum usage by up to 19% in DT and 16% in SBN, when comparing with FixedGrid and particularly the combined effect of using the virtual grid and the customized framework allows to save more 6.4% of spectrum usage than the FlexiGrid for DT and 13.73% for SBN.

When comparing the spectral utilization with the different protection schemes, it can be seen that in general the ODU protection scheme leads to a more reduced spectrum utilization than the OCh protection scheme for all the planning periods and spectral configurations (e.g., the OCh protection scheme requires on average more 28.2% of spectrum utilization than the ODU protection scheme for the VirtualGrid scenario in the last planning period of the network). This is due to the fact that the OCh protection scheme demands the use of the same modulation format for both working and protection paths that could lead to a reduction in the maximum capacity used for working paths since the protection paths are on average longer and the feasible modulation format could be different from the one which only considers the working path independently from the protection path such as the ODU protection scheme.

Overall, it is clear that the joint effect of using the VirtualGrid design with the customized optimization framework proposed in this work leads to a more efficient spectrum usage in case of considering the medium/long-term network operation.

4.4.2 Maximum Carried Traffic Analysis

The second part of the analysis translates the spectral-savings, shown in Fig. 4.4 and discussed in the previous subsection, into the average maximum carried traffic load for each network topology without incurring blocking limitation, i.e., it is the computation of the total bit-rates of traffic demands transported in the network. In this context, the maximum carried traffic load is calculated based on the carried traffic load in the planning period before the one that the service blocking starts to occur. This justifies the traffic growth profile used in this work, since it reduces the traffic growth towards the end of the network operation in order to determine more precisely the maximum carried traffic load transported without having traffic blocking. These results aim to show the effectiveness of each network design approach in extending the lifetime of the network before having to upgrade the infrastructure to transport more traffic.

Table 4.1 represents the maximum carried traffic load for all the scenarios previously described. The results indicate that VirtualGrid is the strategy that allows to maximize the carried traffic load for all the analysed scenarios. Moreover, the gain is more exacerbated for unprotected and ODU 1+1 dedicated protection cases. As for the unprotected scenario, it shows an increase in the maximum carried traffic of up to 7% and 18% for DT and 7% and 20% for SBN, when comparing with FlexiGrid and FixedGrid, respectively. In the ODU 1+1 dedicated protection scenario, it shows an increase of around 11% and 22% for DT and 16% and 22% for SBN.

Finally, in the case of OCh 1+1 dedicated protection, the behaviour is slightly different mainly due to the spectrum assignment constraints which prevent attaining higher spectral gains. Note that, this protection scheme is constrained by the need of maintaining the same spectral allocation and modulation format for both working and protection paths that reduces the proficiency of releasing line interfaces via the hitless re-grooming and the use of the higher order modulation formats available when

Table 4.1 Maximum Carried Traffic Load

Design Scenario	**Max. Carried traffic load [Tb/s]**					
	w/o Protection		**ODU Protection**		**OCh Protection**	
	DT	**SBN**	**DT**	**SBN**	**DT**	**SBN**
VirtualGrid	95.1	166.4	43.6	83.3	35.9	63.8
FixedGrid	78.2	133.6	34.2	65.3	34.0	62.8
FlexiGrid	88.7	154.3	38.9	70.1	31.9	54.3

deploying the next-generation of line interfaces. Another important aspect to point out is the performance of FlexiGrid for OCh protection, which reveals to be worse than the one with FixedGrid for both network topologies, which is attributed mainly due to the combined effect of spectral fragmentation with FlexiGrid and the more demanding spectral allocation from having to use the same spectrum for both working and protection optical channels. From the results of Table 4.1, it can also be seen that the use of protection schemes reduces on average the maximum carried traffic load per network (e.g., the use of ODU protection scheme reduces on average the maximum carried traffic load by 54% when compared to the scenario without protection for VirtualGrid in the DT network topology).

4.4.3 Line Interfaces Utilization

The last part of the analysis focuses on the cumulative number of 32 and 64 Gbaud line interfaces employed during the network lifetime. The obtained results are depicted in Fig. 4.5, which shows the evolution of the number of line interfaces for both topologies and different protection schemes. These results are relevant to understand the possible CAPEX implications of adopting each spectral management strategy. Beyond the spectral efficiency gains already mentioned, the VirtualGrid strategy is also able to maintain the cumulative number of line interfaces acquired at lower levels, being the strategy that achieves the smallest number of cumulative line interfaces for almost all planning periods, never surpassing the number of line interfaces required by the other strategies.

When comparing VirtualGrid with FixedGrid, it can be observed that the former enables line interface savings of between 0-39%, 0-32% and 0-37% in DT and 0-37%, 0-30% and 0-36% in SBN for unprotected, OCh and ODU protection schemes scenarios, respectively. These savings are a natural consequence of being able to exploit next-generation line interfaces. Nevertheless, the key finding is that when comparing VirtualGrid and FlexiGrid, which can both take advantage of these line interfaces, the savings provided by the former ranges between 0-3%, 0-3% and 0-1% in DT and 0-9%, 0-7% and 0-9% in SBN. These results are a consequence of the re-grooming process at the end of each planning period, which is promoted by the proposed network design framework. Moreover, it can be observed that the line interfaces savings increases when using a larger network topology (SBN), which can be explained by the fact that the number of optical channels and line interfaces utilized is higher since the network links are on average longer and to guarantee the QoT of the channels used to meet the traffic, it is necessary to use multiple channels to reach the destination node or use channels with lower order modulation formats. This also augments the probability of successfully rerouting the traffic to other optical channels.

This clearly shows that the proposed framework can extend the network lifetime (smaller spectrum usage, higher maximum carried traffic load) while not requiring more line interfaces and, in some cases, even saving some of them mainly in larger network topologies. Moreover, the aforementioned savings provided by VirtualGrid overcome, to some extent, the initial equipment investment of the implementation of OTN switches in the network nodes that allows effective management of the line interfaces and spectrum utilization. It is also important to highlight that the cost of OTN switches is residual when compared to the line interfaces equipment [109]. In this context, the increase of maximum

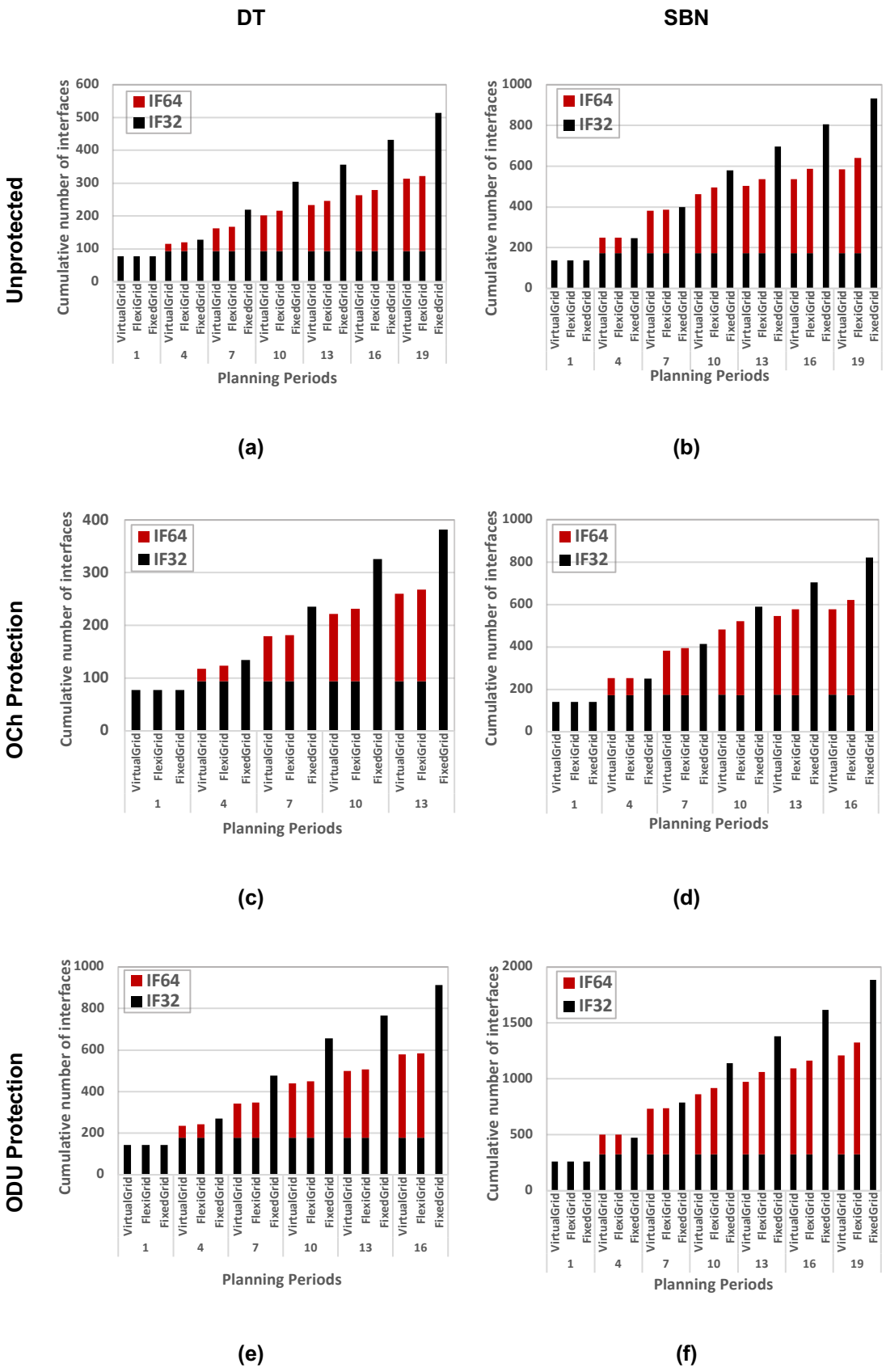

Figure 4.5 Cumulative number of interfaces used throughout the entire network lifecycle for (a) DT and Unprotected, (b) SBN and Unprotected, (c) DT and OCh protection, (d) SBN and OCh protection, (e) DT and ODU protection and (f) SBN and ODU protection.

carried traffic load achieved by the proposed framework in the different network topology enables to

avoid or at least postpone the expensive addition of new fibres to support the remaining traffic, which may involve high capital expenditures investments.

4.5 Chapter Summary

The need to increase spectral efficiency and reduce the cost per bit transmitted has led to the development of next-generation line interfaces that enables the use of higher order modulation formats and symbol-rates. The deployment of these next-generation interfaces will inevitably change the design of the optical network, since the fixed 50 GHz grid used up to recently must be replaced by a flexible DWDM grid. However, the expected co-existence of optical channels that operate at different symbol rates can lead to operational challenges, most notably in terms of managing the mismatch of frequency slot sizes in order to minimize the risk of spectrum fragmentation. Note that, the management of a flexible grid in the controller software and network management systems is more challenging than the management of a fixed grid that maintains constant the set of frequency slots and the spacing between optical channels. On the other hand, the planning challenges resulting from the use of a flexible grid to transport channels with different spectral sizes should not be overlooked, since the spectrum fragmentation limitations can hamper the expected network improvements from the use of higher order modulation formats and higher symbol rates via the deployment of the next-generation of line interfaces.

Consequently, this chapter has presented a network design framework to exploit the next-generation of optical line interfaces capable of operating at higher symbol rates and supporting a wider array of modulation formats, and the utilization of OTN switching technology. The proposed multi-period framework comprises a custom virtual 87.5 GHz grid and a two-stage optimization procedure based on ILP models with the aim of efficiently managing the spectral resource usage and minimizing the hardware cost associated with the number of line interfaces acquired throughout the entire network lifecycle. Moreover, the use of a customized 87.5 GHz virtual grid maintains the spectrum management as simple as the management of the fixed grid. On the other hand, the framework is tailored for the likely and realistic scenario that next-generation of line interfaces become available at later stages of network operation, which means there is a first stage of operation only with 32 Gbaud line interfaces and a second stage of operation with the coexistence of both current- (32 Gbaud) and next-generation (64 Gbaud) line interfaces.

The network simulation results show that the use of proposed framework to provision services in the described network scenario enables to reach higher spectral efficiencies throughout the later stages of the network lifetime without incurring spectrum fragmentation limitations and maintaining the spectral management complexity at lower levels. This efficient management also allows to maximize the carried traffic load for all the analysed results, which shows the effectiveness of this framework to postpone expensive fibre rollouts/lease. Importantly, this is possible without having to increase the number of line interfaces that have to be acquired and, in some cases, even enabling to slightly reduce this number [149, 150, 151].

Chapter 5: Design Strategies to Transport High-Capacity Traffic

In past decades, the cost per bit transmitted in optical transport networks has been reduced with the increase of the number of DWDM channels deployed as well as by the augment of the capacity transported and spectral efficiency on the basic premise of using the C-band of a single mode fibre [156]. This augment has been possible thanks to the development of novel switching architectures and technologies that offers more options to groom the client signals into optical channels potentially enabling to reduce the number of channels utilized (Chapter 3), and via the deployment of consecutive generation of optical line interfaces, each surpassing the previous by providing higher spectral efficiency and capacity (Chapter 4). However, forecasts suggest that these developments will not be sufficient to cope with current growth of transport network traffic demands, which include the imminent deployment of 5G services, the constant growth of IP traffic [157], the data centre interconnections, etc [22].

As seen in Chapter 2, in order to address this increase demand for capacity, different solutions can be envisaged [119], like the use of a band-division multiplexing system over the standard single-mode fibre (ITU G.652) [123] by exploiting spectral bands beyond the C-band (e.g., S, L or O spectral bands) [124] and/or via the utilization of spatial division multiplexing through the deployment of multiple parallel single-mode fibres (multi-fibre system) or by introducing novel multi-core/mode fibres [120]. In this context, the aim of this chapter is to analyse the main advantages and shortcomings of the approaches that the research community indicate to be the most promising ones to be applied in short- to medium-term (BDM and multi-fibre system) to transport high-capacity traffic and highlight the implications in terms of network design algorithms, network costs and technology availability. Moreover, this chapter describes two service-provisioning frameworks that include the impact of using the BDM and multi-fibre transmission systems with regards the overall optical transport network costs, providing a critical assessment of the usual approach utilized until now to optimize the network that focuses only on the minimization of the number of line interfaces for designing the future OTN scenarios.

This chapter is supported by one conference and one journal publication associated with it. A network design framework exploiting the benefits of using a multi-band design strategy is presented in [158]. On the other hand, the optimization problem associated with the adoption of both multi-band and multi-fibre transmission systems on the dimensioning of an optical transport network is described in [159], highlighting the different CAPEX implications.

5.1 Capacity Upgrades in Optical Transport Networks

Internet traffic has been constantly increasing for decades and currently there are forecasts that point out for a yearly traffic growth of 26% [22]. This will inevitably lead to the need to augment capacity in transport networks. Throughout the years, the development of coherent detection combined with DSP has been the principal solution implemented to increase capacity and spectral efficiency in OTN via the deployment of consecutive generations of optical line interfaces [26], as described in Table 2.1.

However, the maximum capacity transported is rapidly approaching the fundamental limits (Shannon limit). Shannon [36] showed that there is a maximum transmitted capacity sent over any communication channel in the presence of noise, without incurring transmission errors. This theoretical capacity is defined in the Equation (5.1) over an optical fibre [38], where C represents the maximum capacity

(measured in Gbit/s), F defines the total number of frequency slots available in the optical fibre's spectrum, BW is the bandwidth of the frequency slots which is assumed to be equal to 12.5 GHz and $OSNR$ characterizes the optical signal-to-noise ratio that is defined in 2.1.2.3.

$$C = BW \times F \times log_2(1 + OSNR) \quad (5.1)$$

Following the Equation (5.1), the increase of capacity through the development of different generations of line interfaces (via the augmentation of OSNR) has reduced the gap to the Shannon limit, meaning that the efforts that can be made in the future to increase the OSNR in OTN will only result in a logarithmic return in terms of capacity (smaller gains) [38, 156, 160]. In general, the fundamental limits dictate that only minor capacity improvements are to be expected in the future with development of technologies that focus only on increasing the OSNR and thus the total capacity transported will only be dramatically augmented via using more spectrum, namely by increasing the variable F of (5.1).

In order to overcome the capacity exhausting in the C-band of the current fibre infrastructures, several approaches have been proposed in literature via using more optical fibre spectrum [39]. One possibility resides in the use of a band-division multiplexing system which allows transmitting data beyond the C-band with the aim of maximizing the return of investment on the already deployed optical infrastructure. Moreover, the BDM transmission system can be assumed as a pay-as-you-grow strategy, meaning that the operators can install the additional bands only when needed. The use of a BDM transmission system by widening the spectral bands utilized for transmission will linearly impact the total system capacity, as defined in Equation (5.1) through the variable F. However, this scenario will raise operational and design challenges, one of them resides in the incorporation of an optical fibre that is low-loss across the entire optical spectrum utilized. In this context, the study presented in [127] had successfully demonstrated the deployment of 5-band (O, E, S, C and L) WDM transmission system over the commercially available SMF (ITU G.652 fibre) [123] and confirmed the increase of capacity transported in OTN via BDM system.

Furthermore, the components of the optical network should also be adapted to support this new BDM environment. In detail, the transceiver at the coherent receiver must be tunable over the entire spectrum, which can be done using for example silicon photonic integrated circuits [161]. On the other hand, the optical amplifiers must be designed to utilize the best doped material for each band. In this context, [125] proposes the different amplifiers' materials that should be utilized according to each spectral band. The optical performance evaluation described in Section 2.1.2.3 of Chapter 2 will also need to be updated in order to properly address the impact of transmitting a channel at different spectral bands, e.g., by updating the noise figure of the amplifiers utilized at each band.

Another option to increase capacity in transport networks relies on the introduction of multiple parallel single-mode fibres (multi-fibre transmission system) [162]. This can be accomplished by installing several parallel systems over new fibres or by lighting up existing dark fibre that the operators often own in some networks, replicating the mature and cost-effective C-band line system technology. For this reason, it can be implemented in the short-term since it does not require any further adaptation of the

technology already in use. With the introduction of the multi-fibre transmission system, the maximum capacity transported (5.1) will be multiplied by the number of additional fibres considered. However, this is a costly solution due to the multiplication of the network components and the deployment or renting of additional optical fibre pairs.

Although the SDM and multi-fibre transmission systems seem to be the mid-term solutions to deal with such augment of capacity in transport networks due to their capabilities to adapt to the current optical fibre infrastructure, for the research community the only evident long-term solution to extend the capacity of optical communication systems relies on the deployment of multi-core/mode fibres [119, 120, 121, 163] defined in Section 2.2. The deployment of these novel fibres allows to establish multiple spatially distinguishable transmission paths through a single fibre, which enables to increase the maximum capacity transported defined in (5.1) by the number of different transmission modes/cores considered in these fibres. However, the deployment of SDM via the use of novel multi-core/mode fibres requires a complete transformation of the optical transport ecosystem, leading to high capital expenditures and complex logistics. Moreover, dedicated standards for multi-core fibres have not yet been finalized and there is not any available commercial solution. Therefore, these types of technologies need to be further developed and it is unlikely to be ready for deployment in the next few years.

In this context, the research developments indicate that exploiting C+L-band based on a BDM system and introducing additional single-mode fibres are the only commercially available solutions that could be employed in the near future [40, 41, 42]. Although there are several studies addressing the general aspects of adopting the BDM transmission systems, it remains to be developed a global network design framework that addresses the different CAPEX and performance effects of adopting these strategies (e.g., extra expenditures with amplifiers in L-band). On the other hand, the fact that the multi-fibre system is expensive (due to renting of fibres or local legislation in some networks), the network operators have to rely on effective optimization algorithms to exploit the available fibre assets as much as possible in order to minimize the network costs [164]. Consequently, this chapter proposes two network design frameworks that considers the aforementioned strategies to increase capacity in OTN (C+L-band and multi-fibre systems), taking into account the different CAPEX and technology implications of adopting each strategy.

5.2 Service-Provisioning Framework Supporting C+L-band Transmission Systems

As mentioned in the previous section, the need to support massive bandwidth growth will lead to the deployment of C+L-band systems with the aim of expanding the optical transmission to L spectral band. By the fact that the BDM being a novel concept in optical transport networks, the proposed framework is designed to consider different generations of coherent line interfaces and technologies in order to be compatible with all optical networks. Moreover, the adaption of a service-provisioning framework to support different design approaches also allows to compare the impact of moving from the single-band to multi-band transmission in diverse scenarios.

In detail, three different design approaches are addressed in this framework, the first design scenario considers the use of current state-of-the-art line interfaces (CIF), operating at 32 Gbaud, allocated over the 50 GHz frequency slots and using QPSK, 8 and 16 QAM modulation formats (2nd generation of Table 2.1). The second one assumes the use of next-generation of line interfaces (NGIF) operating at 64 Gbaud and supporting modulation formats ranging from QPSK up to 64 QAM (3rd generation of Table 2.1), where each channel is allocated over 75 GHz frequency slots. The utilization of an optical network operating only at 64 Gbaud optical channels instead of the coexistence of both 32 and 64 Gbaud (Chapter 4) allows reducing the frequency slots from 87.5 to 75 GHz without compromising the filtering tolerance.

Finally, the last scenario assumes the deployment of state-of-the-art line interfaces but considers a flexible grid enabling the superchannel configuration described in Fig. 1.2 (b), with up to six subchannels allocated over 225 GHz frequency slots and supporting QPSK, 8 and 16 QAM modulation formats (CIF-SC), achieving a total capacity of 600, 900 and 1200 Gbit/s, respectively. The 225 GHz is calculated by assuming that each channel operating at 16 QAM (the highest order modulation format considered in this scenario) will require a minimum of 37.5 GHz frequency slot without affecting the filtering tolerance. This study also uses the superchannel concept for the purpose of contemplating different design strategies to optimize the spectrum usage with C+L-band scenario.

The main objective of the proposed service-provisioning framework is the minimization of the number of single optical channels used in case of CIF and NGIF scenarios and the number of subchannels deployed within the superchannels in the CIF-SC strategy. When the C+L-band reaches the limit of transported capacity, single-mode fibres are introduced to meet the remaining traffic (multi-fibre transmission system). In this case, the number of additional fibre-pairs deployed are also minimized as a secondary objective. The flowchart of the planning workflow is depicted in Fig. 5.1.

In detail, the framework assumes an incremental multi-period scenario which receives as input the network topology and the set of optical channel's modulation formats considered per design strategy (CIF, NGIF and CIF-SC). The optimization is carried out per planning period, i.e., knowing the set of traffic demands of the current planning period and the network state but not knowing the parameters of the next planning periods. For each traffic demand, a set of candidate routing paths is first computed based on the *k*-shortest path algorithm. Based on each routing path and the optical performance model presented in Subsection 2.1.2.3, the most spectrally efficient modulation format that does not require intermediate 3R regeneration between two nodes of the path is assessed, computing the set of candidate optical channels to meet the traffic demands. In this case, it is considered directly the optical performance model presented in Appendix A and described in 2.1.2.3 since it is necessary to calculate quality-of-transmission of each channel (via the calculation of the residual margin presented in A.5 Equation of Appendix A) adapted to each BDM scenario (the transmission in both C and L spectral bands), i.e., changing the optical amplifiers' noise figure (NF variable defined in formula A.3 of Appendix A) from 6 to 7 dB for C- and L-band amplifiers, respectively. Although these noise figures are higher than the typical values of today EDFAs, they were considered here in order to provide a worst-case scenario analysis. In case of C+L-band transmission, and to guarantee that an optical channel is feasible without

3R in both C- and L-bands, the worst residual margin (obtained in L-band) is utilized. In this type of transmission despite ISRS may impact the performance of both bands [62], it has been neglected in this analysis because the optical performance model used through this work does not take this impairment into account. Note that this model, which is described in Appendix A, was fully developed by the author in [29] that made it available for the different analysis throughout this Thesis.

Afterwards, an ILP model, adapted to each design strategy, is used to minimize the number of channels deployed through the selection of the best path for each traffic demand. In order to balance optimality and complexity, the spectrum and fibres assignment is performed through a heuristic algorithm that aims to minimize the number of fibres deployed according to the routing and grooming solution provided by the ILP.

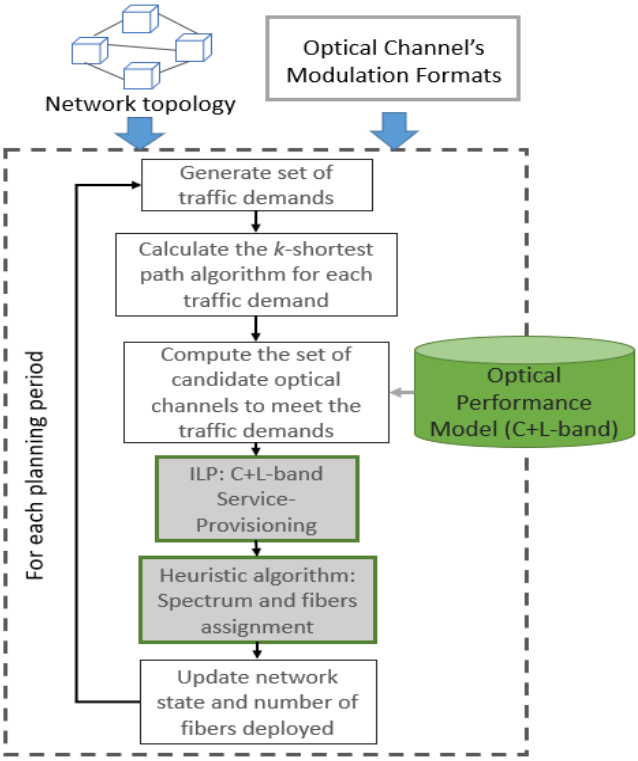

Figure 5.1 Multi-period C+L-band planning workflow.

5.2.1 ILP Models

This subsection introduces the ILP model indicated in Figure 5.1. Two variants of the ILP are considered: i) one that minimizes the number of single optical channels used in the CIF and NGIF scenarios (ILP-4) and ii) another one that minimizes the total number of channels deployed within the superchannels in the CIF-SC approach (ILP-5). Both ILP models use the following parameters and variables.

Parameters:

V Set of network nodes

E	Set of network links
L	Generic set of candidate channels formats that depends on the scenario: single optical channels or superchannels.
L_e	Set of channels that traverse the network link $e \in E$
$L_{i,j}$	Generic set of available channels between source node i and destination node j
L_T	Set of channels already deployed in previous planning periods
D	Set of traffic demands
D_T	Set of traffic demands already allocated in the previous planning periods
X_l	Total number of 1.25 Gbit/s slots supported by the channel/superchannel $l \in L$, which depends on the total capacity supported by each channel
N_d	Total number of traffic demands between the same end-nodes and bit-rate $d \in D$
W_d^l	Total number of traffic demands $d \in D_T$ that use the channel $l \in L_T$
S_d	Number of 1.25 Gbit/s slots per traffic demand $d \in D$ according to its bit-rate
F	Number of available (12.5 GHz) frequency slots per network link
F_l	Number of 12.5 GHz frequency slots allocated to each channel $l \in L$
C_d	Bit-rate of each traffic demand $d \in D$
C_l	Bit-rate available per channel assigned within the superchannel configuration $l \in L$

Variables:

$\lambda_{d_{(o,t)}}^{l_{(i,j)}} \in \mathbb{N}^0$	Number of traffic demands from type $d \in D$ between source node o and destination node t using channel $l \in L$ with source node i and destination node j
$\varepsilon_l \in \mathbb{N}^0$	Number of channels deployed per superchannel of the candidate format $l \in L$
$\tau_l \in \mathbb{N}^0$	Total number of superchannels utilized per candidate format $l \in L$

$\Delta \in \mathbb{N}^0$	Total number of channels assigned for each superchannel deployed
$\Lambda_l \in \mathbb{N}^0$	Number of single optical channels required per candidate format $l \in L$
$\chi \in \mathbb{N}^0$	Total number of single channels that have to be deployed

The following formulation describes the ILP-4 model, which has the objective of minimizing the number of single optical channels deployed for the CIF and NGIF scenarios.

$$min\ \chi \tag{5.2}$$

subject to

$$\lambda_d^l = W_d^l \quad \forall d \in D_T, \forall l \in L_T \tag{5.3}$$

$$\sum_{l \in L_{i,j=v}} \lambda_{d_{(o,t)}}^{l_{(i,j)}} - \sum_{l \in L_{i=v,j}} \lambda_{d_{(o,t)}}^{l_{(i,j)}} = \begin{cases} -N_d, & v = o \\ N_d, & v = t \\ 0, & \forall v \in V \backslash \{o,t\} \end{cases} \quad \forall d \in D \tag{5.4}$$

$$\sum_{d \in D} S_d \times \lambda_d^l \leq X_l \times \Lambda_l \qquad \forall l \in L \tag{5.5}$$

$$\sum_{l \in L_e} F_l \times \Lambda_l \leq F \qquad \forall e \in E \tag{5.6}$$

$$\sum_{l \in L} \Lambda_l = \chi \tag{5.7}$$

The objective function (5.2) consists of minimizing the total number of optical channels. Constraints (5.3) impose that the traffic demands already deployed in previous planning periods are kept in the same channels and (5.4) select the optical channels' path to meet each traffic demand, ensuring the general flow conservation along the routing path for all traffic demands. The total number of optical channels utilized per candidate format are computed on constraints (5.5) according to the total traffic transported and the capacity of the channel and (5.6), guaranteeing that the total number of frequency slots used does not exceed the link capacity that depends on the number of spectral bands utilized. Note that, the difference between the CIF and NGIF scenarios resides in the definition of the candidate channels formats L and the number of 12.5 GHz frequency slots required to allocate each channel (F_l), which depends on the scenario defined by the input parameter (optical channel's modulation formats) of the algorithm, as depicted in Fig. 5.1. Finally, constraint (5.7) calculates the total number of optical channels that have to be provisioned to meet the set of traffic demands. In case of this ILP model, the number of variables is defined by $|D| \times |L| + |L| + 1$, whereas the number of constraints is given by $|D_T| \times |L_T| + |D| \times |V| + |L| + |E| + 1$.

The ILP-5 focuses on the minimization of the total number of channels assigned per superchannels deployed in the CIF-SC scenario:

$$min\ \Delta \tag{5.8}$$

subject to

(5.3-5.4) from the definition of ILP-4

$$\sum_{d \in D} S_d \times \lambda_d^l \leq X_l \times \tau_l \qquad \forall l \in L \tag{5.9}$$

$$\sum_{l \in L_e} F_l \times \tau_l \leq F \qquad \forall e \in E \tag{5.10}$$

$$\sum_{d \in D} C_d \times \lambda_d^l \leq C_l \times \varepsilon_l \qquad \forall l \in L \tag{5.11}$$

$$\sum_{l \in L} \varepsilon_l = \Delta \tag{5.12}$$

The ILP-5 model requires using different variables to represent the number of superchannels and channels deployed within the superchannels. The ILP-5 has the objective function of minimizing the number of channels assigned within the superchannels (5.8), which implicitly also minimizes the number of superchannels utilized, since they can be composed of up to six channels between the same end-nodes and modulation format. The constraints (5.3) and (5.4) are the same as those introduced for the ILP-4. The constraints (5.9) calculate the number of superchannels deployed per candidate format based on the total capacity supported by each superchannel, whereas (5.10) ensures that the total number of frequency slots used per superchannel configuration does not exceed the link capacity. The number of channels assigned per superchannel format is defined by constraints (5.11) and finally the total number of channels assigned for all superchannels deployed is computed in constraint (5.12). In case of this ILP model, the number of variables is defined by $|D| \times |L| + 2 \times |L| + 1$, whereas the number of constraints is given by $|D_T| \times |L_T| + |D| \times |V| + 2 \times |L| + |E| + 1$.

5.2.2 Heuristic Algorithm: Spectrum and fibres assignment

The ILP model is complemented by a heuristic algorithm that performs the spectrum and fibres assignment according to the total number of single channels utilized in CIF and NGIF scenarios and superchannels deployed in the CIF-SC approach given by the ILP model. The algorithm is described by the pseudocode in Algorithm 5.

Algorithm 5: Spectrum and fibres assignment

Input: **List** ς of channels to be deployed (depends on the scenario: single channels Λ_l or superchannels τ_l from the ILP models)
Spectrum (Optical Spectrum defined by the number of network links over the number of available frequency slots $E \times F$),
l_bound (maximum number of network links to consider)

1 Initialize an empty list, ςBlock, which will indicate the number of channels blocked during the assignment process.

2 ***for*** each channel in ς
3 Search for *freq* (frequency slot), the first available one for all network links traversed by the channel in the *Spectrum* with the already deployed optical fibre infrastructure
4 ***if*** there is no available *freq*
5 Add channel to ςBlock list
endif
end for
6 ***if*** ςBlock is not empty
7 Get the network links that are traversed by the channels assigned to ςBlock in descending order of the number of unavailable frequencies in *Spectrum*, E_{block}
8 ***if*** length(E_{block})> l_bound
9 Limit the network links in E_{block} to l_bound
endif
10 Generate the set of possible zero and one's combinations ($Comb$) of the network links in E_{block} (each combination represents the addition of a fibre in the selected links)
11 Sorting the $Comb$ in ascending order of the number of fibres introduced
12 ***for*** each combination in $Comb$
13 Check if it enables to assign all the channels included in ςBlock list
14 ***if*** the combination is successful
15 Update the number of fibres deployed
16 **Exit**
endif
end for
17 ***if*** none of the combinations is successful
18 Select the combination that has the lowest number of channels still to be assigned in ςBlock and add fibres to the network links that their fibres' number have not been updated yet
endif
endif
19 **return** (updated *Specrum* and number of fibres deployed)

The algorithm starts by trying to assign the channels utilized (single channels for CIF and NGIF scenarios and superchannels for CIF-SC approach) to the available spectrum. In case of unavailability of spectrum to assign all the channels, a set of zero and one's combinations of the most demanding network links are computed ($Comb$). These combinations will indicate the network links that require the addition of a new single-mode fibre in order to successfully transport all the traffic. In order to reduce the complexity of the heuristic algorithm, a maximum number of network links l_bound is considered in the generation of the combinations, which is received as an input parameter. The generation of the combinations is exemplified in Fig. 5.2 for a network topology with four nodes. In this example, the network links A-D and B-C have reached the exhaustion of the spectrum (could in C or C+L spectral band depending on the scenario considered) that originated the blocking of some traffic demands (E_{block} in Algorithm 5) and therefore the introduction of single-mode fibres in these network links is required. With the aim of reducing the number of fibres added to the network, a set of zero and one's combinations of the most demanding network links is computed where each combination represents the addition of a

fibre to the selected links, as exemplified in Fig. 5.2. For example, the combination 1 of Fig. 5.2 indicates the addition of a single-mode fibre in the network link B-C, the combination 2 represents the addition of a single-mode fibre in the network link A-D and the combination 3 means the additional of single-mode fibres in both network links

Afterwards, the algorithm tries to assign the blocked channels to one of the combinations ($Comb$). Note that, the combinations are sorted in the ascending order of the number of fibres introduced in order to select the configuration that requires the lowest number of fibres (if more than one combination has the same number of fibres introduced, the first is picked). In the case that the number of combinations is reduced due to the complexity of the heuristic algorithm, it can happen that none of the combinations allows successful allocation of all channels. In this context, the algorithm selects the combination with lowest number of channels still to be assigned and sequentially deploys fibres in the network links that their fibres' number have not been updated yet and are traversed by channels that could not be assigned in the first instance. Finally, the algorithm returns the updated spectrum and set of new fibres that have to be set up.

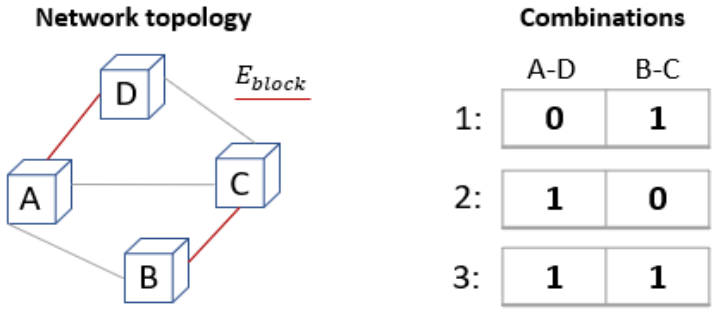

Figure 5.2 Generation of the combinations ($Comb$) defined in Algorithm 5.

5.3 Impact of Adopting C+L Service-Provisioning Framework

In order to properly evaluate the benefits of moving from a single-band (C-band) to a multi-band transmission system (C+L-band) provided by the proposed service-provisioning framework described in the previous section, three design approaches (CIF, CIF-SC and NGIF) were considered through a detailed simulation analysis using the SBN and the Italian Backbone Network (IBN), which are illustrated in Fig. B.3 and B.4 of Appendix B. Both defined by Telefónica and Telecom Italy, respectively, in the scope of the FP7 IDEALIST project [155]. The SBN topology has 30 transparent nodes interconnected by 56 network links using standard single mode fibre (SSMF) fibre spans, whereas the IBN has 44 transparent nodes interconnected by 71 network links using SSMF and large effective area fibre (LEAF) fibre spans. In both network topologies, the fibres deployed were defined by the network operators in [155].

The simulation assumes a 10-year network lifetime with six months between planning periods, 100 and 200 Gbit/s traffic demands between 13% of the node-pairs (randomly generated) with a traffic growth of 26% per year, following the forecast provided by [22]. The evolution of the traffic growth is

depicted in Figure 5.3 and it assumes the same percentage of the traffic rates at each planning period. For each traffic demand, it was considered all candidate optical channels possibilities over the three shortest routing paths calculated by the k-shortest path algorithm, as described in Fig. 5.1. The simulation results are averaged over 20 independent runs.

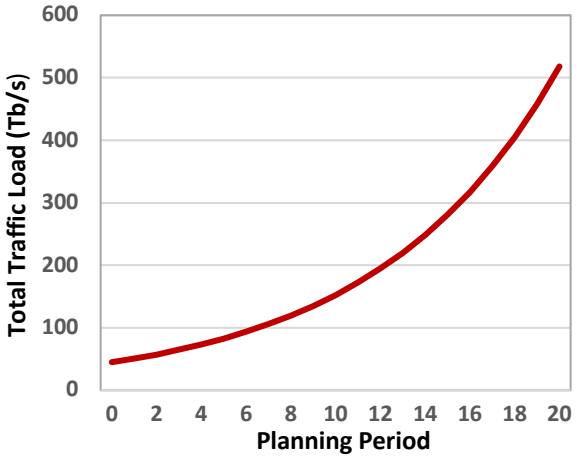

Figure 5.3 Evolution of traffic growth per planning period.

The analysis of the proposed service-provisioning framework is mainly divided into two sets of results. First, the number of fibres that have to be deployed with C-band and C+L-band transmission systems considering the three different design approaches is assessed. Note that, when the capacity is exhausted, the algorithm assumes the deployment of additional optical fibres to transport the remaining data. Afterwards, the number of channels utilized to satisfy all traffic demands along the different planning periods is evaluated, allowing to compare the expected line interfaces count when considering different design approaches. Note that the C-band transmission is used as a comparison benchmark for highlighting the benefits of adopting a multi-band transmission system.

As mentioned before, the evaluation of optical channels' performance utilized to compute the set of candidate channels described in Fig. 5.1 is based on the optical performance model presented in Appendix A. Both C- and L-bands are modelled as having a total bandwidth of 4.8 THz, which corresponds a F equal to 384 frequency slots of 12.5 GHz in each band. The use of different types of fibres (SSMF and LEAF) in the IBN network topology will also have an impact on the optical performance model since the nonlinear coefficient, the attenuation and dispersion parameters are different, as depicted in Table 5.1. This information is received as input of the optical performance model.

5.3.1 Analysis of the Deployment of Single-Mode Optical Fibres

The first set of results is presented in Fig. 5.4 for both SBN and IBN network topologies. The figures depicted the total number of fibres deployed for all network links given by the Algorithm 5 of the proposed multi-period framework. In detail, Fig. 5.4 (a-b) depicts the optical fibre count in SBN and IBN, respectively, when current state-of-the-art line interfaces are used in a CIF and in a CIF-SC configuration, whereas Fig. 5.4 (c-d) focuses on the comparison of the state-of-the-art with the next-generation of line interfaces for both network topologies.

Table 5.1 Optical Fibre Parameters

Fibre Type	Attenuation Parameter	Dispersion Parameter	Nonlinear Coefficient
SSMF	0.21 dB/km	17 ps/nm/km	1.3 1/W/km
LEAF	0.22 dB/km	3.8 ps/nm/km	1.5 1/W/km

The analysis of Fig. 5.4 (a) shows that moving from C-band to C+L-band transmission allows the use of the initial fibres' infrastructure deployed by the network operators for each network link (56 in SBN and 71 in IBN) for 6 more planning periods (3 years), which postpones the additional fibre deployment. Taking into account the 26% yearly increase of traffic, this translates into an increase of the carried traffic load of around 100% for the same optical fibre infrastructure. Fig. 5.4 (a) also shows that there is a clear

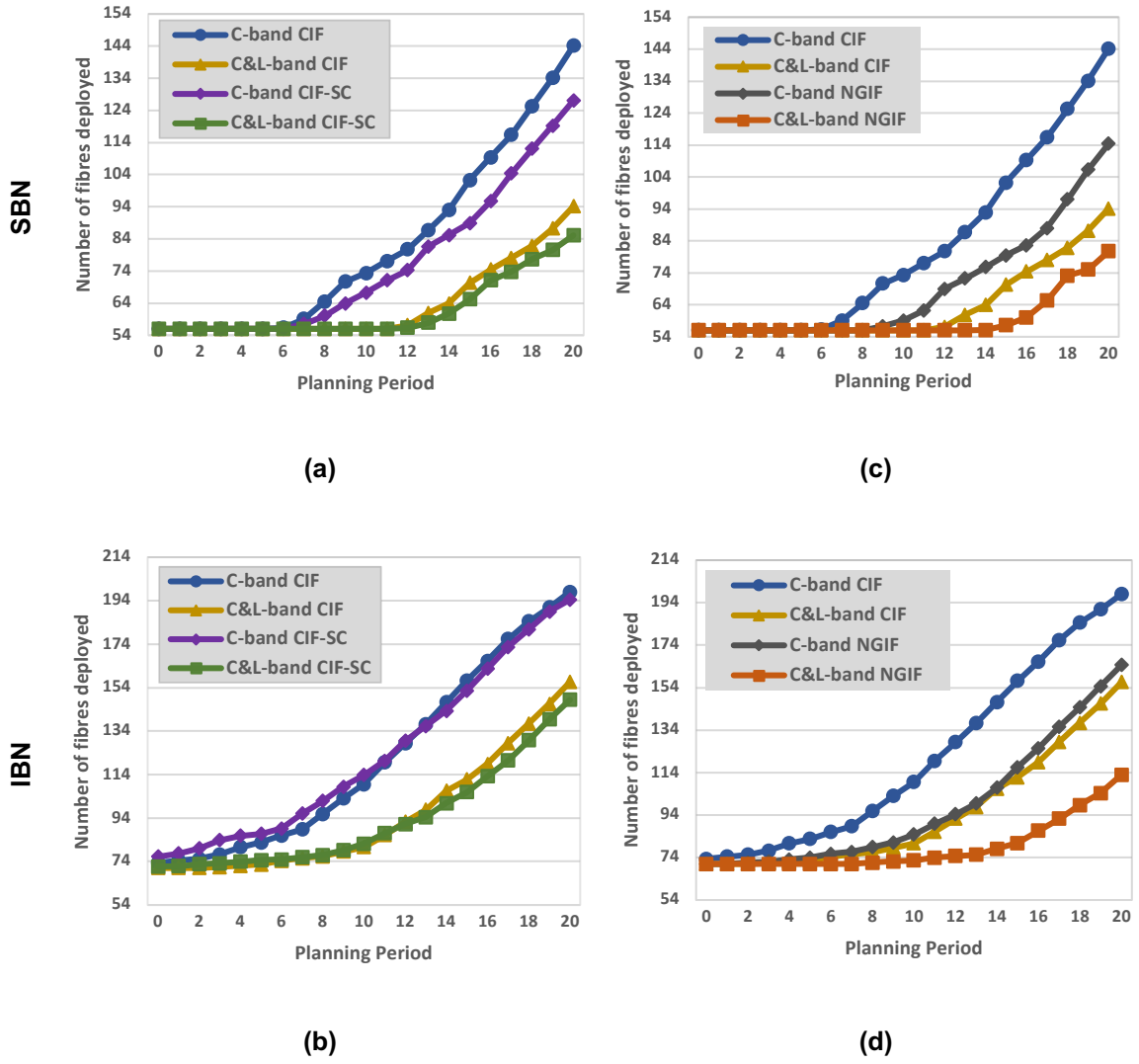

Figure 5.4 Evolution of the number of fibres deployed along the network lifetime with C and C+L transmission systems for the (a-b) CIF and CIF-SC and (c-d) CIF and NGIF for SBN and IBN network topologies, respectively.

benefit from deploying state-of-art line interfaces using a superchannel configuration, since it allows further reducing the optical fibres count (both for C- and C+L-band systems).

Additionally, Fig. 5.4 (c) highlights that the next-generation of line interfaces will further postpone the investment in the optical fibre infrastructure. Using NGIF enables savings of about 21% and 15% in the optical fibre count when compared to the CIF scenario for C- and C+L transmission systems, respectively. When considering a larger network such as the IBN, it can be seen that it leads to similar trends. However, the benefits provided by the superchannel configuration scenario (CIF-SC) are mitigated, as shown in Fig. 5.4 (b). This is a consequence of reserving larger portion of spectrum (225 GHz for ensuring the minimum filtering tolerance) in a network for allocating six channels that can only be used by channels that share the same end-nodes, which cannot be effectively utilized in larger network like IBN where the channels deployed can have a larger number of possible directions (end-nodes). As a result, earlier spectrum exhaustion in some links will lead to the need to route channels over longer and less spectral efficient paths, which can offset the improved spectral efficiency of this configuration when compared to that of single channel configuration (CIF or NGIF).

On the other hand, it can also be seen that the use of larger networks like IBN also enables the increase of the savings in the number of fibres deployed when comparing the NGIF with CIF for C+L-band transmission system (Fig. 5.4 (d)). This can be explained by the fact that the channels in IBN traverse on average longer network links which reduces the performance of these channels and this reduction of performance can have more impact on CIF since it supports modulation formats and symbol rate that provides lower capacity per optical channel being deployed.

In order to illustrate the benefit of adopting the C+L-band transmission system combined with the deployment of NGIF design strategy, Fig. 5.5 depicts the number of fibres deployed per network link in the SBN topology for the same scenarios presented in Fig. 5.4 (c) but considering only the last planning period and one of the simulations runs of the pool of 20 utilized in this study. This illustration helps to visualize the spread of extra fibres in the network, highlighting the most loaded links for the different scenarios. The resulting observation emphasizes the benefit of using next-generation line interfaces combined with a C+L-band transmission system.

5.3.2 Analysis of the Optical Channels Utilization

The last set of results focuses on the number of optical channels (single channels in CIF and NGIF scenarios and subchannels assigned to superchannels in CIF-SC approach) that have to be deployed in the network obtained by the ILP model of the proposed service-provisioning framework described in Fig. 5.1, which are directly associated with the line interfaces count and, ultimately, to CAPEX implications. Figures 5.6 (a-b) and (c-d) depict the number of optical channels required to carry all traffic demands throughout the network lifecycle considering the C- and C+L-band transmission scenarios and comparing the CIF with the CIF-SC and the CIF with the NGIF strategies, respectively.

Figure 5.6 shows that there is a minor increase in the number of optical channels used when moving from the C- to the C+L-band transmission system resulting from a slight degradation of optical

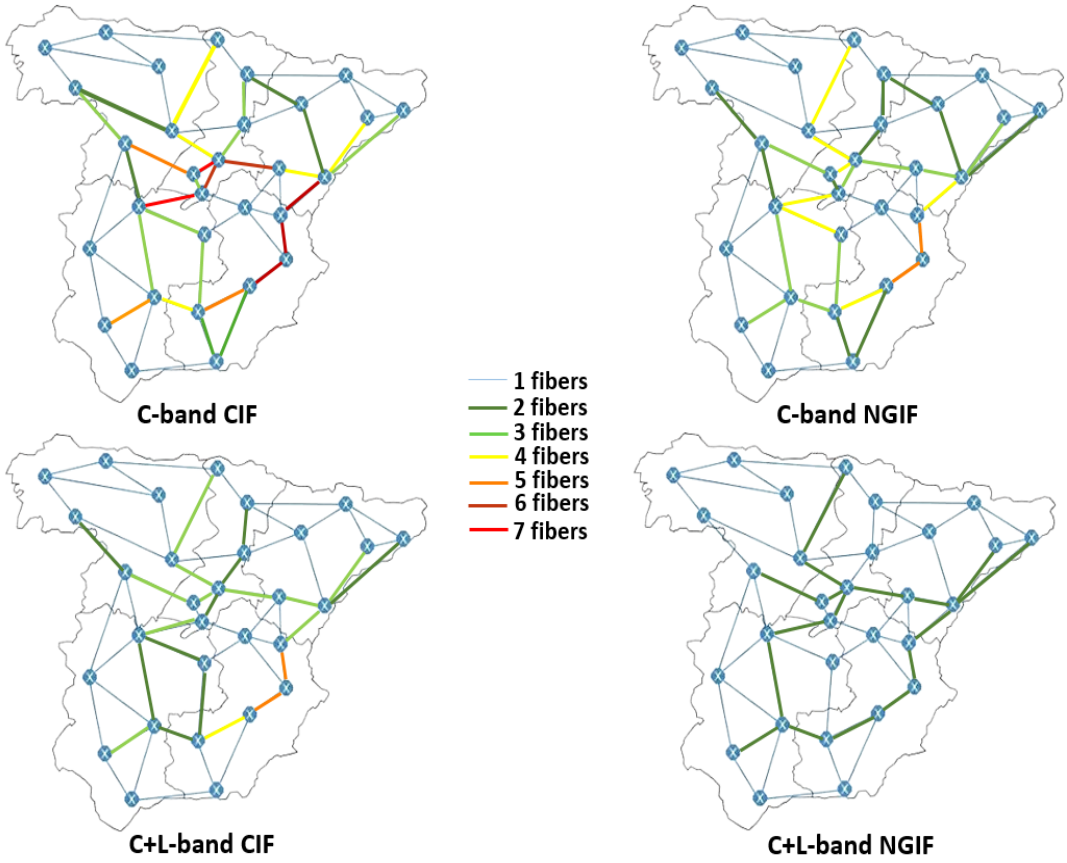

Figure 5.5 Illustration of the number of fibers deployed per network link in the SBN topology with C and C+L transmission systems considering CIF and NGIF design scenarios.

performance in L-band with respect to C-band, thus occasionally preventing the use of higher order modulation formats in some of the longer optical channels. Due to the fact that the channels are on average longer in IBN, it can also be seen that moving from SBN to IBN simulation results, the degradation of channels' performance of using C versus C+L-band transmission systems also slightly increases. Another key finding is that, when comparing the state-of-art line interfaces with single-carrier and superchannel configuration approaches, both attain almost the same number of channels for both network topologies. However, the use of superchannels with up to six subchannels allocated over 225 GHz enables a more effective management of the spectrum, leading to the reduction of the number of fibres that have to be deployed (as shown in Fig. 5.4 (a-b)), mainly for SBN topology.

The most significant savings in the number of optical channels deployed results mainly from using the next-generation line interfaces (for both C- and C+L-band transmission systems). These savings are a consequence of using higher order modulation formats (up to 64 QAM) and higher symbol rates, which increase the maximum total capacity supported per optical channel being deployed. When comparing the NGIF and CIF in a C+L-band transmission scenario, the former is able to reduce the number of channels provisioned by up to 60%. Importantly, these savings are possible without compromising the spectral efficiency, since using the next-generation of line interfaces is also the strategy that enables attaining the minimum number of fibres, as shown in Fig. 5.4 (c-d). Although the next-generation of line interfaces will be more expensive than the current-generation of line interfaces in the beginning of

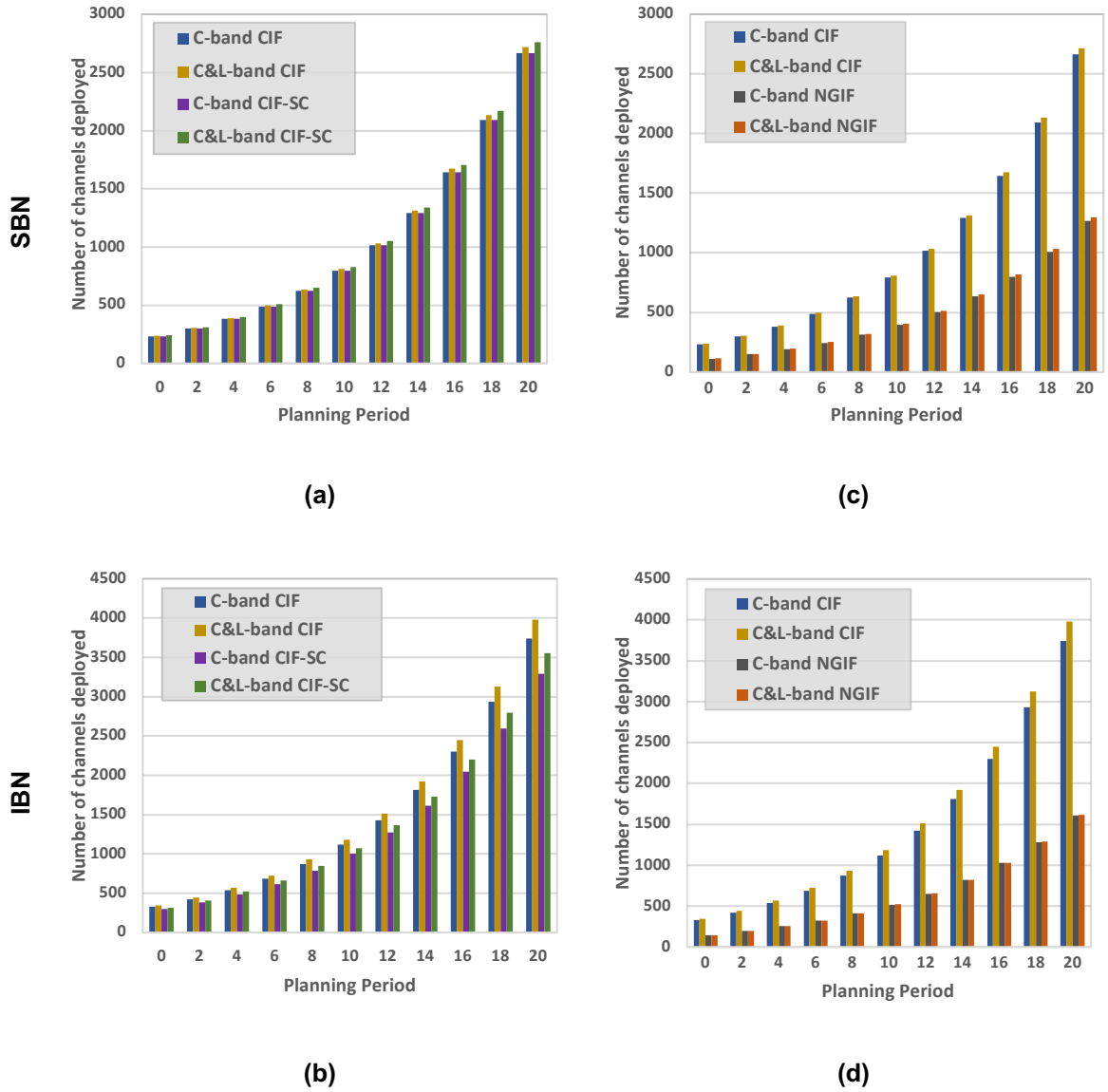

Figure 5.6 Evolution of the cumulative number of (single- or sub-) optical channels provisioned along the network lifetime with C and C+L bands for (a-b) CIF and CIF-SC and (c-d) CIF and NGIF for SBN and IBN network topologies, respectively.

operation due to being a novel technology, the benefits provided by deploying them in terms of line interface count and spectrum utilization (postponing expensive fibre rollouts/lease) will overcome this initial cost difference, as described in this study and in Chapter 4. It is also important to notice that the cost of the next-generation line interfaces will also suffer from cost depreciation over the time of operation.

This study highlights even more the spectral and cost benefits of deploying the next-generation of line interfaces to cope with the massive bandwidth increment already analysed in the previous chapter, even with the utilization of C+L-band transmission system, which allows to avoid or at least postpone the CAPEX investment of deploying additional fibre-pairs between two regions. In this context, the C+L system has shown to be the most suitable and mature technology to effectively extend existing fibre capacity using the same optical infrastructure [158].

5.4 Design of Geographically-Dependent Fibre Upgrade Expenditures with C+L-band Transmission System

The potential benefits of deploying the C+L-band transmission system and ultimately the utilization of multi-band system in extending capacity with the already deployed optical infrastructure will eventually not be enough to meet the forecasted bandwidth growth, at which point additional fibres are mandatory to be used, as shown in Fig. 5.5 of the previous study. In this context, the expenditures associated with adding additional fibres can vary significantly, not only from network to network, but also within the same network. For instance, a transport network operator often owns dark fibre (an unused fibre between two network links that can be used for optical transmission) in some countries/regions, while in other regions the lease of fibre to another network operator is mandatory. Therefore, in some cases using an additional fibre is possible at a reasonable cost and with a moderate time to activate the fibre to be utilized as a transmission system, whereas in others it can be a very expensive and lengthy process, if not impossible at all, e.g., due to shortage of dark fibre in a duct (pipeline where the fibre is installed to provide mechanical protection [165]) or as a consequence of licensing or regulatory aspects.

Therefore, this study presents a network planning framework capable of modelling C+L-band transmission system combined with geographically-dependent fibre upgrade expenditures, which can be customized in terms of giving preference to minimize the number of additional fibres introduced versus the number of line interfaces utilized. Moreover, it also includes the minimization of the number of L-band transmission systems utilized, using the C+L-band system on a per need basis. Particularly, the optical network can be deployed, so that initially only the C-band is available but the network elements are prepared to accommodate the L-band subsystems without the need to overhaul these elements or disrupt traffic reducing, when possible, the use of ROADMs or L-band optical amplifiers utilized when the L-bands are not in use [126]. In general, this complete framework considers the different CAPEX implications of adopting this next-generation of optical transport networks, taking advantage of the benefits of C+L-band for transporting high-capacity traffic, as described in the previous study.

5.4.1 Multi-Fibre C+L Network Design Framework

As mentioned before, the need to support massive bandwidth growth will lead to the deployment of C+L-band systems in the short-term (all the advantages of adopting this technology are presented in the previous section), particularly in congested links where introducing new fibres is very expensive. Moreover, the deployment of optical networks is being prepared to support both bands on a per need basis (i.e., by introducing L-band when needed and without affecting running traffic). This demands a customized service-provisioning framework to optimize the deployment of L-band transmission system, postponing the extra expenditures with L-band amplifiers.

However, the exploitation of the C+L-band transmission system will eventually not be enough to transport all the traffic, leading to the need to install/lease new fibres. Moreover, geographically-dependent fibre upgrade expenditures also need to be taken into account when determining how to

cost-effectively scale fibre capacity. Consequently, a robust service-provisioning framework must model all these requirements, so that the design solution obtained has the lowest network cost. This can be achieved by optimally selecting in which links extra fibres are to be added, based on their specific costs and on fine-tuning the solution, so that a minimum number of L-band transmission system has to be deployed in both existing and new fibres.

In this context, the service-provisioning framework described in this study is developed with the aim of modelling geographically-dependent fibre upgrade expenditures in a multi-fibre environment while at the same time minimizing the number of L-band transmission systems in the C+L approach. Moreover, the framework is also customizable in terms of giving preference to use additional fibres versus line interfaces. The flowchart of the planning workflow is presented in Fig. 5.7.

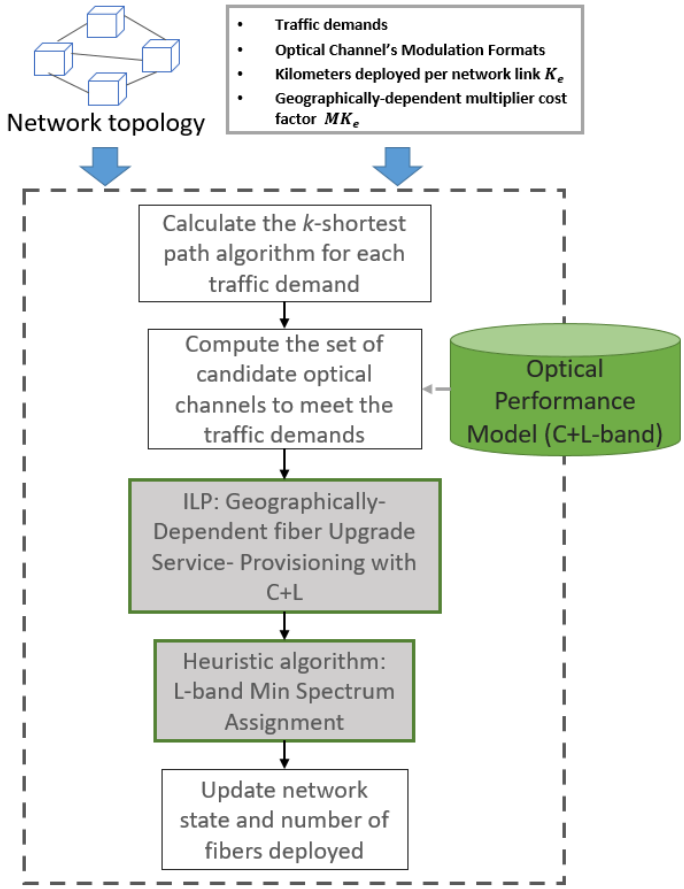

Figure 5.7 Multi-fibre C+L network design framework workflow.

In detail, the proposed framework assumes a single-period optimization approach, which receives as input the network topology, the sets of traffic demands, the modulation formats of optical channels, the total number of optical fibre's kilometres deployed per network link K_e and a multiplier factor that differentiates the kilometres of fibre deployed according to the geographical region MK_e (both utilized in the ILP model). For each traffic demand, a set of candidate routing paths is first computed based on the *k*-shortest path algorithm. Based on each routing path and the optical performance model presented in Section 2.1.2.3, the most spectrally efficient modulation format that does not require intermediate 3R regeneration between two nodes of the path is assessed, computing the set of candidate optical

channels to meet the traffic demands. The optical performance model is also adapted to consider the transmission at both C and L spectral bands.

Afterwards, it combines an integer linear programming model with a heuristic algorithm in order to balance optimality and scalability. The ILP model, designated hereafter as ILP-6, has the objective of routing and grooming traffic demands with the goal of minimizing the total cost with fibre deployment, taking into account the differentiated fibre upgrade costs, and having as an extra objective to minimize the number of line interfaces that have to be acquired. Note that the ILP model is executed under the assumption that both C- and L-band become available whenever a new fibre is deployed.

Based on the resulting grooming, routing and fibre assignment solution, the heuristic algorithm assigns spectrum to the optical channels utilized in the context of L-band Min Spectrum Assignment, so that the deployment of L-band transmission systems is minimized. In detail, this algorithm gives priority to use the C-band by choosing the frequency that avoids having frequencies available only in a short amount of network links, which would otherwise lead to an increased impact of the spectrum continuity constraint and the need to use a wider set of frequencies.

5.4.1.1 ILP model

This subsection introduces the ILP model presented in Fig. 5.7 (ILP-6). This model uses the following variables and parameters:

Parameters:

V	Set of network nodes
E	Set of network links
L	Generic set of candidate optical channels.
L_e	Set of optical channels that traverse the network link $e \in E$
$L_{i,j}$	Generic set of available optical channels between source node i and destination node j
D	Set of traffic demands
S_d	Number of 1.25 Gbit/s slots per traffic demand $d \in D$ according to its bit-rate
X_l	Total number of 1.25 Gbit/s slots supported by the optical channel $l \in L$, which depends on the total capacity of the channel
N_d	Total number of traffic demands between the same end-nodes and bit-rate $d \in D$

F	Number of available (12.5 GHz) frequency slots per network link
F_l	Number of 12.5 GHz frequency slots allocated to optical channel $l \in L$
K_e	Total number of fibre's kilometres deployed in each network link $e \in E$
MK_e	Multiplier factor that differentiates the kilometres of fibre deployed according to the geographical area
Z	Weight value to balance the objectives in the ILP model

Variables:

$\lambda_{d_{(o,t)}}^{l_{(i,j)}} \in \mathbb{N}^0$	Number of traffic demands from type $d \in D$ between source node o and destination node t using optical channel $l \in L$ with source node i and destination node j
$\theta_l \in \mathbb{N}^0$	Number of optical channels required from the format of candidate channel $l \in L$
$\Pi_e \in \mathbb{N}^0$	Total number of additional fibres deployed per network link $e \in E$
$\omega \in \mathbb{N}^0$	Total number of line interfaces that have to be acquired
$\nu \in \mathbb{N}^0$	Total cost associated with the fibres' deployment

The following formulation describes the ILP-6 model, which is responsible for service-provisioning with geographically-dependent fibre upgrade expenditures:

$$min\ (\nu + \frac{\omega}{Z}) \tag{5.13}$$

subject to

$$\sum_{l \in L_{i,j=v}} \lambda_{d_{(o,t)}}^{l_{(i,j)}} - \sum_{l \in L_{i=v,j}} \lambda_{d_{(o,t)}}^{l_{(i,j)}} = \begin{cases} -N_d, & v = o \\ N_d, & v = t \\ 0, & \forall v \in V \backslash \{o,t\} \end{cases} \quad \forall d \in D \tag{5.14}$$

$$\sum_{d \in D} S_d \times \lambda_d^l \leq X_l \times \theta_l \qquad \forall l \in L \tag{5.15}$$

$$\sum_{l \in L} 2 \times \theta_l = \omega \tag{5.16}$$

$$\sum_{l \in L_e} F_l \times \theta_l \leq F \times \Pi_e \qquad \forall e \in E \tag{5.17}$$

$$\sum_{e \in E} K_e \times MK_e \times \Pi_e = \nu \tag{5.18}$$

The objective function (5.13) consists of minimizing the total cost associated with the number of fibres deployed and also has a secondary objective to minimize the total number of line interfaces that have to be acquired. Constraints (5.14) select the optical channels' path to meet each traffic demand, ensuring the general flow conservation along the routing path for all traffic demands. The total number of optical channels utilized per candidate format are computed on constraints (5.15) according to the total traffic transported and the capacity of the channel. Constraint (5.16) calculate the total number of line interfaces that have to be acquired, and (5.17) calculate the number of fibres deployed per network link, guaranteeing that the total number of frequency slots used does not exceed the link capacity per fibre deployed. Finally, constraint (5.18) computes the total cost associated with the fibres' deployment, which is calculated by multiplying the number of additional fibres introduced in the network by the total number of kilometres of the each fibre and the geographically-dependent multiplier cost factor that is predefined according to each fibre' location (representing the total cost per kilometre of fibre deployed). In case of this ILP model, the number of variables is defined by $|D| \times |L| + |L| + |E| + 2$, whereas the number of constraints is given by $|D| \times |V| + |L| + |E| + 2$.

5.4.1.2 Heuristic Algorithm: L-band Min Spectrum Assignment

The ILP model is complemented by a heuristic algorithm that performs the customized spectrum assignment (L-band Min Spectrum Assignment) according to the total number of optical channels and fibres that have to be deployed given by the ILP model with the aim of minimizing the L-band transmission systems utilized. The algorithm is described by the pseudocode in Algorithm 6.

Algorithm 6: L-band Min Spectrum Assignment

Input: **List $\boldsymbol{\varsigma}$** of optical channels that have to be deployed based on the variable θ_l of the ILP-6
Spectrum (Optical Spectrum defined by the number of network links, number of fibres deployed per network link and the number of available frequency slots per network link $\Lambda_e \times E \times F$)

1 **While $\boldsymbol{\varsigma}$** is not empty
2 From the $\boldsymbol{\varsigma}$ list select the optical channel that has an available frequency in spectrum (giving priority to C-band) with the highest score in terms of the following priorities:
1. Best neighbour fit: the frequency already in use for the largest number of adjacent network links of the optical channel' path
2. Relative capacity loss: the frequency that can accommodate the largest number of future channels in their available network links

Assign the channel to the selected frequency of *Spectrum* and remove channel from $\boldsymbol{\varsigma}$
4 **return** *Spectrum*

The algorithm has the objective of assigning the optical channels deployed to the available spectrum. Giving priority to C-band, it selects the frequency for each channel that provides the best neighbour fit in terms of adjacent network links already in use by other optical channels in order to avoid possible

fragmentation of spectrum throughout the different frequencies. In the example of Fig. 5.8, the optical channels 1 (between nodes A and D) and 2 (between the nodes A and C) are already assigned to the frequency f_1 of the $Spectrum$ described at right of the Fig. 5.8. This illustration represents the $Spectrum$ as a matrix between the number of network links and the number of frequency slots available assuming that all network links have only one bi-directional single-mode fibre deployed and the numbers in the matrix represent the number of optical channels assigned to each frequency. In this case, the algorithm will also select the f_1 to the optical channel 3 (between the nodes A and B) since it is the one that is in use by the largest number of adjacent links of the network link traversed by the optical channel 3, this will provide a better compaction of the spectrum that reduces the spread of channels assignment over the different frequency slots allowing to mitigate at some extent the spectrum fragmentation.

If multiple frequencies have the same number of adjacent links already in use, the previous criterium is also combined with the relative capacity loss approach described in Algorithm 6 that selects the frequency capable of accommodating the largest number of optical channels presented in list $\boldsymbol{\varsigma}$, i.e., the frequency that has the highest number of frequency slots available in the network links of the channels still to be assigned in list $\boldsymbol{\varsigma}$. In general, the developed algorithm aims at promoting spectrum compacting actions in order to minimize the use of L-band transmission system.

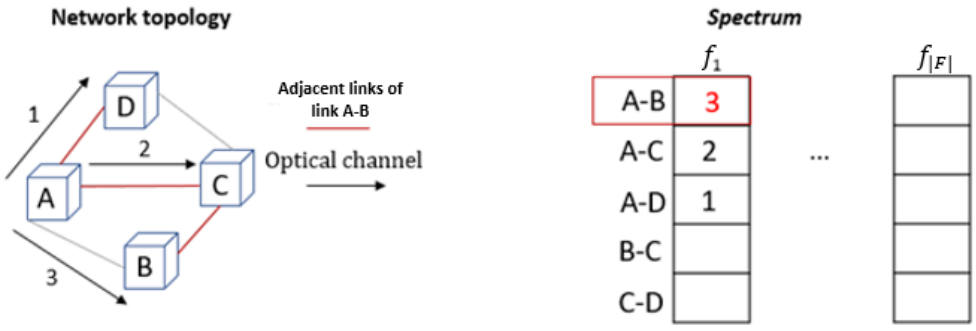

Figure 5.8 Example of the best neighbour fit criterium.

5.5 Impact of Adopting Geographically- Dependent Fibre Upgrade Expenditures

5.5.1 Network and Traffic Scenario

The optical transport network operators are present in several countries and in some of them the operation comprises multiple optical networks in different segments, e.g., metro and core (Fig. 1.1). This means that the need for capacity upgrades is not uniform. Moreover, each country has its own situation and the position in such market varies from operator to operator. Therefore, fibre cost is a key parameter and one of the main reasons to consider rolling out C+L-band transmission systems. Moreover, relative fibre abundancy is realistic in countries where the operator is incumbent, which is the case of Telefónica in Spain, British Telecom (BT) in United Kingdom (UK), Deutsche Telecom in Germany or Altice in Portugal. However, there are scenarios where the leasing of fibre from third-party companies is the only

available solution in some regions/countries (e.g., Telefónica operations in UK), which is a major operational expenditure. In addition, aspects such as legislation promoting the efficient utilization of fibre, like the fibre tax utilized for example in UK [166], also need to be taken into account when designing an OTN in a multi-fibre transmission system.

This work assumes a scenario where the operator is not incumbent in the country and optimizing fibre usage is mandatory. Particularly, the operator is running the national Italian backbone network (IBN) and the cost of upgrading the infrastructure by adding additional fibres is not the same across the entire country: links in more densely populated areas are a premium resource (designated hereafter premium links), e.g., due to increased competition and higher traffic growth. The IBN was selected as it is a larger network capable of spreading the premium links over different regions. For modelling purposes, the population density map of Italy shown in Fig. 5.9 (a) was used to identify 20 bidirectional links that have a fibre rental cost much higher than the remaining ones [167]. Figure 5.9 (b) illustrates the IBN network topology defined in Appendix B with 44-node, 71-link physical topology and the location of premium links.

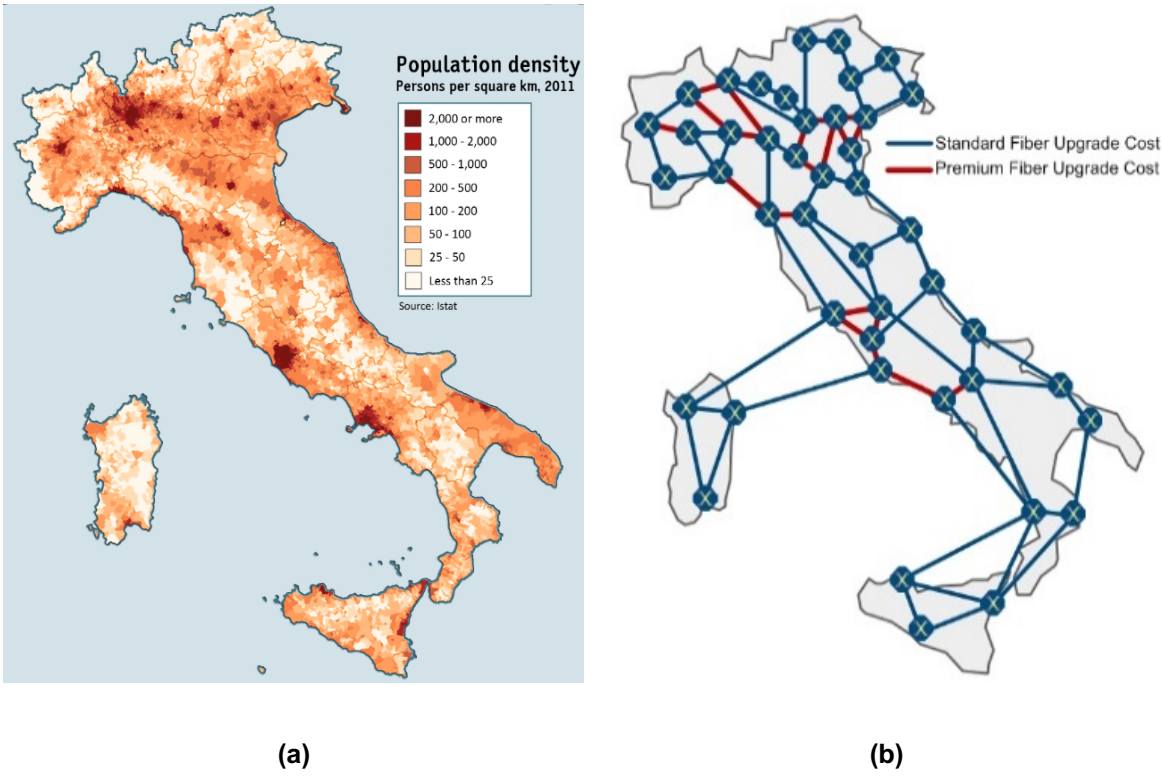

(a) **(b)**

Figure 5.9 (a) Italy population density and (b) Network physical topology with differentiated fibre upgrade expenditures.

In this context, the simulation analysis assumes four design scenarios: (i) the proposed framework considering the differentiated fibre rent (FR) cost with C+L-band (Min FR-C+L); (ii) assuming the simple minimization of fibre length (FL), i.e., without geographical-dependences (Min FL-C+L); (iii) primarily minimizing line interface (LI) count and minimizing the fibre cost as a secondary objective, basically changing the order of the objectives utilized in (i) (Min LI-C+L) and (iv) using the proposed framework but restricted to only C-band (Min FR-C). For simplicity, it is assumed premium links have a 100 times higher upgrade cost per km (MK_e) than the standard links defined in Fig. 5.9 (b).

As utilized in previous study (Subsection 5.2), the evaluation of optical channels' performance utilized to compute the set of candidate channels described in Fig. 5.7 is based on the optical performance model presented in Appendix A, using the optical amplifiers' noise figure of 6 and 7 dB for C- and L-band amplifiers, respectively. In case of C+L-band transmission, and to guarantee that an optical channel is feasible without 3R in both C- and L-bands, the worse residual margin (obtained in L-band) is considered. Both C- and L-bands are modelled as having a total bandwidth of 4.8 THz, which corresponds a F equal to 384 frequency slots of 12.5 GHz in each spectral band.

As in Subsection 5.3, this study also considers the use of the next-generation of line interfaces operating at 64 Gbaud and supporting modulation formats from QPSK and 64 QAM [39]. The study comprises five different optimization runs with different sets of traffic demands considering an increase of 26% traffic load between consecutive runs, following the yearly growth forecast provided by Cisco in [22], where the first run assumes a 150 Tbit/s of total amount of traffic load carried. The sets of traffic demands are randomly generated between 20% of the node-pairs of the IBN topology with bit-rates of 100, 200 and 400 Gbit/s, assuming the same percentage of the traffic rates.

5.5.2 Simulation Results

This section describes the results obtained through the application of the proposed service-provisioning framework presented in Fig. 5.7. The analysis starts by presenting in Figure 5.10 (a) the plot of the total cost with fibres installed based on the total number of kilometres deployed and fibre rent cost, whereas Fig. 5.10 (b) depicts the total number of line interfaces that have to be acquired, both as a function of the total amount of traffic load carried. Figure 5.10 (c), on the other hand, shows the total number of fibres (premium and standard network links) deployed for the different optimization runs.

As can be seen, being aware of geographically-dependent fibre upgrade expenditures, Min FR-C+L minimizes fibre cost (the total cost per kilometre of fibre deployed in each location) by reducing the number of fibres deployed in the regions with highest population density (premium links). Moreover, this can be achieved without compromising the number of line interfaces that have to be acquired when compared to the scenario that does not take into account this geographical-dependence, as visible in Fig. 5.10 (b). Importantly, the deployment of C+L-band comparing to C-band scenario is critical to postpone any fibre rollout until at least 190 Tb/s of carried traffic load, as shown in Fig. 5.10 (a-c) when comparing Min FR-C+L with Min FR-C, i.e., there was already an increment in the number of fibres deployed with a traffic load of 150 Gbit/s for the Min FR-C scenario, In addition, the latter strategy also requires deploying more line interfaces (e.g., as a consequence of using longer paths to avoid deploying even more fibres).

As expected, the number of line interfaces deployed is the minimum when this is the main optimization objective (Min LI-C+L). Nevertheless, this can only be accomplished by deploying significantly more fibres in both standard and premium links, as can be seen in both Fig. 5.10 (a) and (c). Note that, the minimizing of the fibre cost is only considered as a secondary objective, the oppositive of the Min FR-C+L. In this context, both Min LI-C+L and Min FR-C+L design scenarios should be considered by the network planners when designing an OTN in order to understand the potential

impact/trade-off of assuming the minimization of fibre cost or line interfaces as primary objective, since these costs are among the most expensive ones when planning a transport network. See the example of the carried traffic load of 390 Tbit/s, the use of the Min LI-C+L leads to a reduction of the number of line interface by up to 2500 when comparing to the Min FR-C+L scenario, while increasing the total cost of fibres of around 170 000. Depending on operational and the real costs context at the time of planning, one solution could be better than the other in terms of providing the most robust alternative for the network operator.

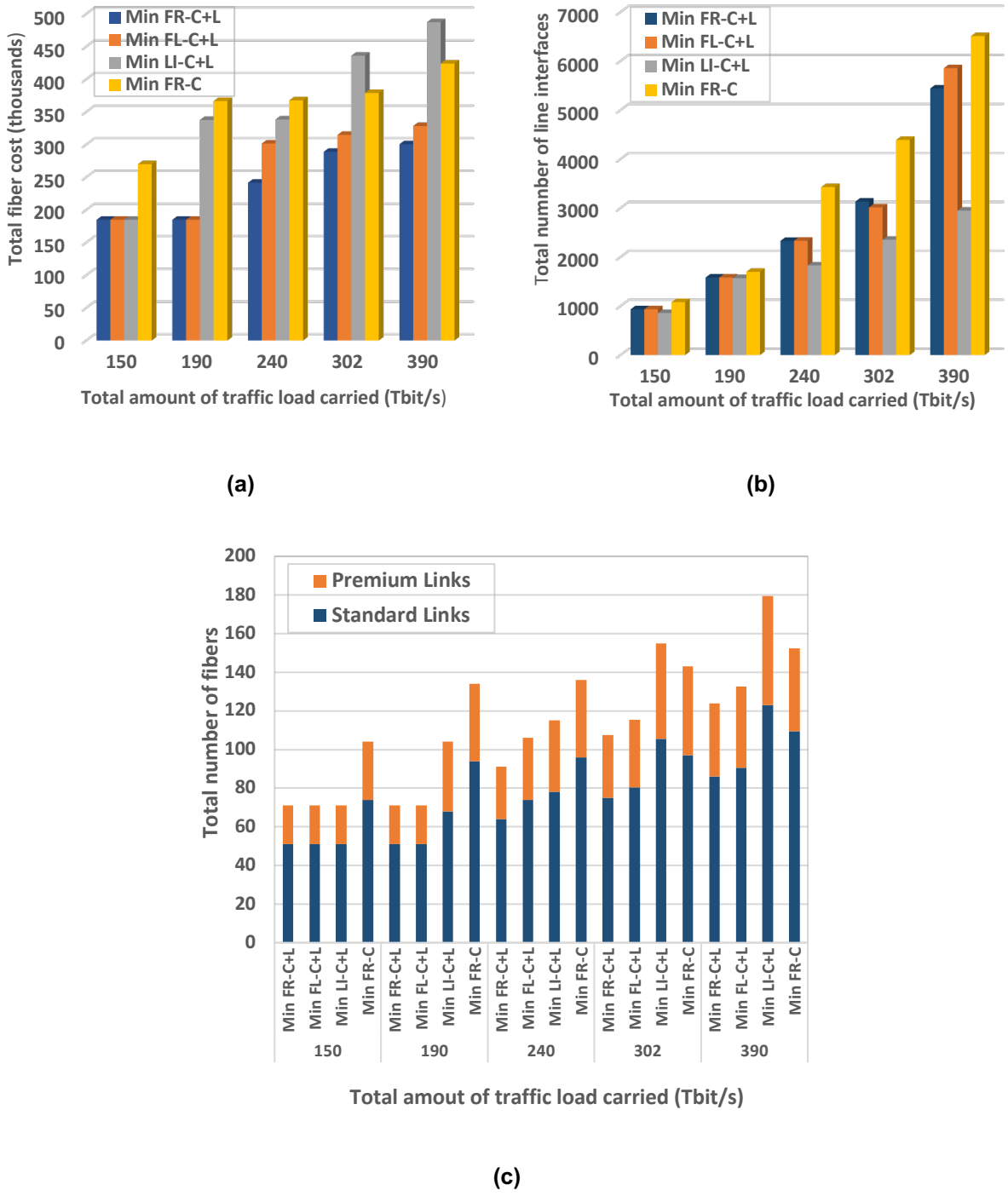

Figure 5.10 (a) Total cost of fibre deployed, (b) total number of line interfaces that have to be acquired and (c) Total number of fibres that have to be assigned for the different optimization scenarios.

In general, this study provides evidence that the usual approach of focusing primarily on minimizing line interface count is ill-suited for future transport network scenarios where C+L-band and multi-fibre deployments are an increasingly important part of the design [159]. Moreover, the adoption of the next-generation of optical transport networks will change the way the network is optimized until now in order to account for the different CAPEX implications that this study has highlighted.

5.6 Chapter Summary

Although next-generation of line interfaces will permit to exploit higher order modulation formats (e.g., 32 QAM, 64 QAM) and higher symbol rates (e.g., above 60 Gbaud), it seems inevitable that the exclusive use of C-band is not enough to sustain future capacity requirements of metro and core networks. Consequently, it is foreseen that either using more spectral bands of the same fibre (e.g., the L band) and/or resorting to multi-fibre transmission system will be needed.

Therefore, this chapter analyses the challenges of adopting these technologies and the necessity to modify the optimization process that has been utilized until now to minimize the total network costs. The first study of this chapter (Sections 5.2-5.3) highlights the effectiveness of adopting the C+L-band transmission system in terms of postponing additional fibre deployment and increasing the carried traffic load for the same optical fibre infrastructure with minor augment on the number of optical channels acquired resulting from a slight degradation of optical performance in L-band with respect to C-band.

On the other hand, the second part of the chapter (Section 5.4-5.5) presents a network planning framework capable of modelling C+L-band transmission system combined with geographically-dependent fibre upgrade expenditures, which can be customized in terms of giving preference to minimize the number of additional fibres introduced versus the number of line interfaces utilized. This can be achieved by optimally selecting in which links extra fibres are to be added, based on their specific costs and on fine-tuning the solution, so that a minimum number of L-band transmission system has to be deployed in both existing and new fibres. Simulation results over a reference transport network highlight the savings that can be realized by optimizing the usage of L-band and carefully selecting the fibre links to be upgraded without compromising the number of line interfaces that have to be acquired.

Chapter 6: Techno-Economic Evaluation of Exploiting Autonomous OTN

The constant pursuit of ways to reduce costs in optical transport networks leads to the need of exploiting the concept of self-driving network aiming at operating it more autonomously and adaptively to the actual network conditions. This inevitably demands the incorporation of new building blocks within the design process, such as real-time telemetry platforms [113]. The capability provided by the real-time performance monitoring platform is a key enabler to provision optical channels with smaller margins instead of adopting the more conservative practice that assumes large enough performance margins to accommodate the different effects that can degrade the optical channel performance (e.g., aging of network devices and fibre plant), as detailed in Subsection 2.2. This squeezing of margins will potentially enable the deployment of higher data-rates per optical channel being deployed through the use of higher order modulation formats, allowing to reduce the overall network cost.

In this context, the main goal of this chapter is to discuss the implications of provisioning channels with smaller margins regarding the optical transport architecture and network design algorithms, since the adoption of squeezed performance margins increases the probability of an optical channel becoming infeasible before end-of-network operation. Furthermore, different provisioning strategies have been proposed within this chapter with the aim of balancing the risk of operating too close to the performance limit with the capacity increase from using more spectral efficient modulation formats. The first strategy consists of using the OTN switching technology in order to reroute the traffic demands whenever the optical channel becomes close to the performance limit and has to be torn down. On the other hand, the other proposed service-provisioning framework restricts the utilization of reduced margins only to shared restoration paths, which exploits the fact that restoration paths are usually active only during the time strictly necessary to fix the source of failures and, consequently, margins such as the ones used to account for device or fibre plant aging are not required without impacting the network operation.

The last part of this chapter focuses on comparing the foreseeable network design frameworks for provisioning optical channels with reduced margins in a transport network, accounting for aspects such as the node architecture, the protection/restoration mechanism, and the flexibility to schedule maintenance windows (periods of time defined in advance by network planners for the sake of changing, upgrading or repairing the optical network that could cause traffic disruption). This assessment is complemented with the application of a simulation setup capable of comparing the excepted performance of the different provisioning strategies.

The work described in this chapter is supported by one journal and six conference publications associated with it. The proposed framework that exploits the reduced performance margins by proactively diverting the traffic demands from optical channels that are reaching the performance limit through the deployment of OTN switches is addressed in [168, 169, 170, 171], whereas the network design framework that exploits the real-time performance monitoring to cost-effectively operate shared restoration paths with reduced margins is presented in [172]. Finally, the comparative analysis of the different service-provisioning frameworks is described in [173, 174].

6.1 Autonomous Networking

The optical transport landscape is changing mainly due to the exponential bandwidth growth mentioned in the previous chapters but also by the appearance of new 5G applications, such as augmented and virtual reality and autonomous vehicles, which implies the need for new requirements in terms of low latency and real-time response. In this context, beyond the aim of operating the optical infrastructure at the highest possible capacity, several studies [113, 114, 175] have discussed the concept of adopting a self-driving optical network that highlights the need to drive for a more agile and autonomous approach, which will allow to simplify network management and reduce overall network costs (operational and capital expenditures).

In detail, the concept of autonomous network will not only allow to cope and adapt to unforeseen events but also to improve and adjust itself to meet the challenges of the actual and future network conditions with little or even without human intervention, where the control decisions must be made with an appropriate knowledge of the current state and supported by a learning process to improve the network performance with the acquired experience. The main concept of an autonomous optical network is presented in Fig. 6.1 based on [176]. Basically, the data corresponding to the current state of the network gathered from the monitoring platform is utilized by an analysis process that understands and derives its environment. The decision of how to act is taken based on the knowledge of the global state of network with an estimate of the likely effect of potential actions and the most promising ones are implemented in Decide & Act stage. This is a continuous process coordinated by the control and management plan (through the SDN controllers described in 2.2) that adapts the optical network in order to automatize certain optimization procedures (e.g., automated service activation, network restoration and resource optimization [177]). With the evolution of this concept, several commercial solutions have been developed in the optical network industry [177, 178, 179, 180].

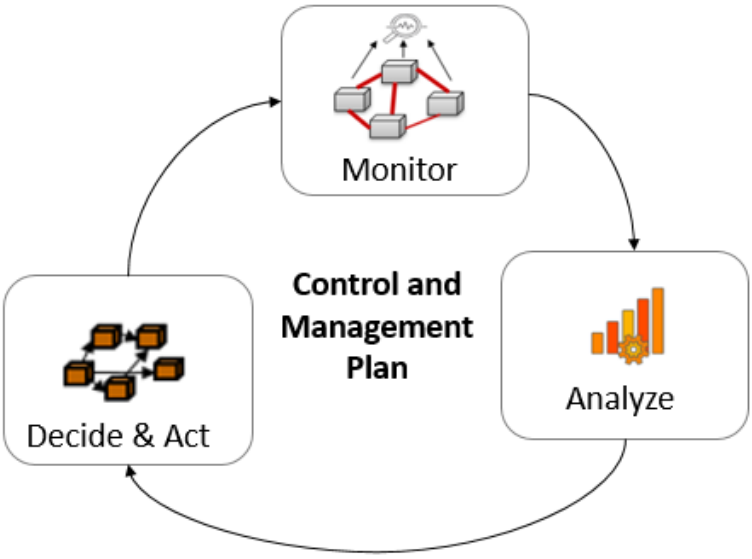

Figure 6.1 Autonomous control loop of an optical network [176].

The ingredients provided by the concept of autonomous network will enable to use the real-time monitoring platform to continuously carry out the prediction of the current state-of-life performance of an established optical channel and also leverage the learning process to forecast the optical channels' performance evolution along the network operation, in turn enabling to develop a network design framework that optimizes the network resources adaptively to the actual and forecasted performance conditions. Importantly, understanding the real-time state of optical performance and confidently estimating its evolution will allow to challenge the established practice of designing optical channels to be uninterrupted until the network end-of-life (EoL), which entails using high margins to accommodate the different effects that can degrade performance and/or limit the estimation accuracy, as described in Fig. 2.7 of Section 2.1.2.3. Apart from guaranteeing the sufficient quality-of-transmission of the deployed optical channels until their EoL, the utilization of this conservative approach can potentially prevent the use of higher order modulation formats that decreases the capacity per channel being provisioned which can result in an increase of the network cost.

In this context, several studies [43, 44, 45, 114, 181, 182] have started to investigate the effect of adopting smaller margins in the provisioning of optical channels when designing an OTN. In detail, the works presented in [43, 181] models the optical channels' performance degradation along the network lifecycle in order to highlight the cost savings of adopting the provisioning with reduced margins when compared to the traditional EoL-based approach that assumes additional performance margins to guarantee that the channels are feasible until the network EoL. [44] details an analysis of the different margins required for optical channels' provisioning and identifies which ones have greater potential to be reduced. Moreover, it also provides a generic overview of key challenges that the network operators have to successfully address in order to exploit a reduced margin-based design.

On the other hand, the work in [45] proposes a multi-period planning framework that uses an aging model to provision channels with minimum margins, assessing the main benefits of adopting this strategy instead of the EoL provisioning approach that considers high performance margins. The authors in [182] investigate the impact of extracting the different performance margins in the design of a sample backbone network, highlighting how the network can benefit from the extracted margins. Additionally, the work presented in [114] proposes a complete network design solution toward autonomous optical networks, detailing the different components depicted in Fig. 6.1. Importantly, this work is the only one presented in literature that considered the fact that adopting smaller margins increases the probability of an optical channel becoming infeasible before the end-of-network operation, potentially resulting in service disruption of the traffic demands it carries. However, the algorithm proposed by the authors in [114] considers the addition of new line interfaces to restore the optical channels that have run out of margin, which results in a temporarily disruption of the traffic demands that are carried over those channels.

In this context, the proposed network planning frameworks and operation with reduced margins presented in this chapter aims at avoiding the aforementioned traffic disruption, ensuring that (i) it is possible to switch (in up to the millisecond range) traffic demands between different optical channels and (ii) the network planning framework appropriately models the critical aspects, with the overall goal

of being able to proactively react to a degradation of the optical channels' performance in order to mitigate disruption of live traffic.

6.2 Network Planning and Operation with Reduced Margins

The performance of an optical channel set up in an optical network, measured in terms of the quality-of-transmission, can vary significantly along its lifecycle, i.e., between the time it is created and the time it is torn down. Several factors can impact the performance of an established optical channel, including the fast or slow variation of the optical impairments due to the variation of the number of optical channels loaded in the network (see Section 2.1.2.1), the long-term aging of the network elements and fibre spans traversed (statistical variations of optical components characteristics) and other unexpected performance degradation factors [44], as described in Subsection 2.1.2.3. Moreover, at the planning stage of an optical network, performance estimation is usually based on expected (i.e., not based on the current values presented in the network) characteristics of the fibre spans, amplifiers and other devices in the signal path and typically assuming simplified optical performance models with limited accuracies (see Section 2.1.2.3)

In order to ensure the error-free-transmission, safety margins are typically assigned at BoL to meet the required service level agreement until the network EoL [44, 46]. These margins are used to accommodate different effects that can impact the optical channels' performance, such as performance model inaccuracies (design margins), transmission channel degradation (transmission margins) and components aging (system margins), as seen in Fig. 2.7. Although the use of high-performance margins can guarantee an error-free operation over the channels' lifetime, it can also hamper the utilization of higher capacity optical channel formats by, for example, preventing the use of a higher-order modulation format, which could be viable with smaller margins, as depicted in Fig. 2.16. Conversely, the use of reduced margins unlocks the potential of advanced coherent modulation formats that enables the maximization of the capacity per optical channel being deployed, thereby reducing the overall network costs.

In this context, developments in next-generation of coherent interfaces [183], real-time performance monitoring and advanced SDN controllers (described in Subsection 2.2) set the stage to incorporate the use of reduced margins in the planning process. Based on the concept of autonomous network described in the previous subsection, the transport network architecture utilized in this study to provision optical channels with reduced margins is presented in Fig. 6.2. In detail, this network architecture uses the real-time monitoring platforms to have access to key physical parameters of the network and the performance of the optical channels already deployed in the network (equivalent to the monitor block of Fig. 6.1). The collected information is fed to a module that embeds (1) an optical performance model to estimate the performance of candidate but yet unestablished optical channels and (2) a forecast method that predicts the evolution of optical channels' performance (analyse process described in Fig. 6.1) based on trend analysis algorithms (e.g., machine learning). Combined, these functionalities can be exploited to fine tune the margins of optical channels (Fig. 2.7) to be established in the future, further contributing to optimize the process. For instance, the system margins can be reduced, since a slower

degradation of the optical components characteristics (aging) can be detected or predicted. On the other hand, the acquisition of more accurate input parameters for optical performance modelling provided by real-time monitoring platforms will also have effect on the decrease of the design margins that accounts for the inaccuracy of the OPM. Afterwards, the performance information coming from the Performance Trend Analysis block defined in Fig. 6.2 is fed to a margin-aware provisioning framework (equivalent of decide & act stage of Fig. 6.1), which leverages this information, mainly to (1) provision optical channels with margins as low as possible while guaranteeing a minimum level of robustness to performance degradations in the short-term and (2) optimally schedule any required rerouting of traffic demands between optical channels, whenever a channel is tagged as being in a critical condition (i.e. near the performance limit).

Furthermore, the control and management plane (SDN controller of Fig. 6.2) will play an important role in the operation of OTN with reduced margins by managing the monitored data, coordinating and deploying the actions provided by the margin-aware framework, and detecting an optical channel degradation of performance since a faster than expected degradation of performance can cause traffic disruption. In order to manage this risk, the transport architecture defined in Fig. 6.2 should be fully automated and act before the performance degrades bellow an acceptable level, following the same concept defined in Fig. 6.1. Importantly, the entire workflow is designed to allow learning from past decisions and continuously adapt with the aim of optimizing resource usage, while managing the risk of traffic disruption.

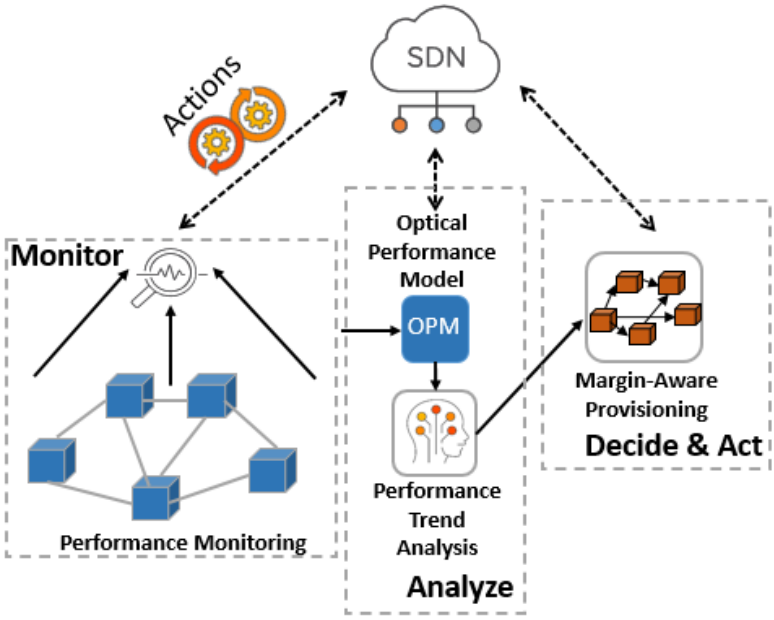

Figure 6.2 Proposed transport network architecture to provision optical channels with reduced margins.

Note that, performance monitoring and trend analysis defined in Fig. 6.2 can assist in a timely identification of optical channels reaching a critical condition. However, in general, it is not possible to exactly predict that the actual performance of an optical channel may evolve differently from what was forecasted by the performance trend analysis at the BoL of the optical channel. For instance, Figure 6.3

illustrates two different performance degradation profiles, assuming the optical channel was set up to carry a traffic demand during a specific time interval. As can be seen, if the actual performance evolution is according to profile 2, the optical channel EoL time (in terms of performance) exceeds the end time of the traffic demand being carried. In this case, there is no traffic disruption or need for reconfiguration. Conversely, if performance evolution follows profile 1, the optical channel EoL time precedes the end time of the traffic demand, which can result in service disruption if the rerouting process is not performed in time. This highlights the importance of a fully automated network architecture able to continuously learn from past decisions and adapt according to the actual network conditions.

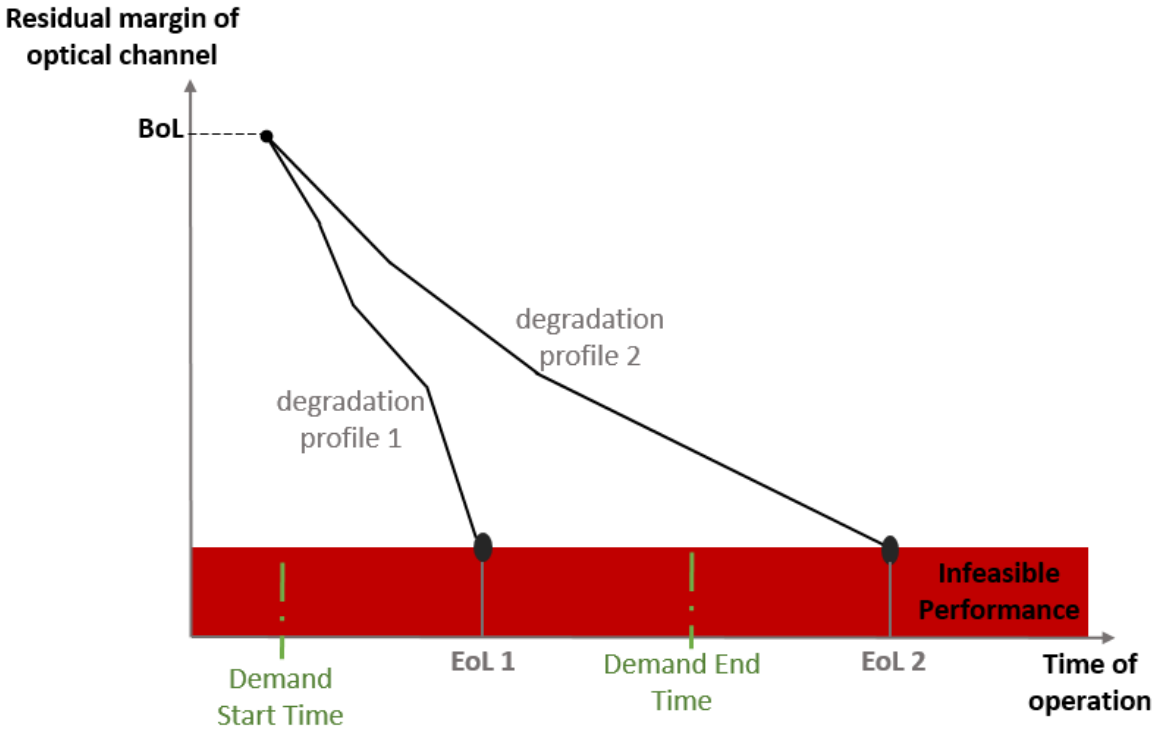

Figure 6.3 Optical channel performance evolution.

6.3 Service-Provisioning Frameworks with Reduced Margins

Using the transport network architecture illustrated in Fig. 6.2 of the previous section, two different service-provisioning strategies (the Proactive Service-Provisioning Framework and the Service-Provisioning Framework for Optical Shared Restoration Paths) have been proposed in the context of this chapter with the aim of exploiting the benefits from starting to deploy optical channels over the optical transport network with smaller margins while minimizing the risk of operating too close to the performance limit. Moreover, the proposed frameworks can directly be applied to the Margin-Aware Provisioning block presented in the illustration of the transport network architecture (Fig. 6.2).

6.3.1 Proactive Service-Provisioning Framework with Reduced Margins

The first service-provisioning framework proposes a routing engine assuming that it has accessed to the current performance of the optical channels already deployed in the network (given by the

combination of the performance monitoring and the optical performance model defined in Fig. 6.2) and the estimated performance of the candidate but yet unestablished optical channels over the time of network operation (provided by the performance trend analysis block of Fig. 6.2). This enables a routing action to be taken before the performance degrades below an acceptable level that could be defined as an alert, as illustrated in Fig. 6.4 (a). This proactive action, when timely triggered, can avoid disruption of the traffic carried over the degraded optical channel. Therefore, the proposed multi-period framework aims at increasing the capacity per provisioned optical channel through the use of reduced margins and also to proactively and effectively reroute the traffic demands carried over optical channels approaching the minimum acceptable performance point (MAPP). The rerouting of traffic is ensured through the use of OTN (electrical) switches in addition to ROADM within the network nodes, enabling to shift traffic between optical channels remotely without disruption of the traffic via the use of SDN controllers (Section 2.2) [49], as defined in the Subsection 2.1.3.3.

In this context, the provisioning engine comprises three phases of operation according to the assignment of a threshold above the MAPP, as illustrated in Fig. 6.4 (b). In this study, this threshold is assumed to be manually assigned with a value close to the MAPP but it can also be dynamically adapted according to the actual network conditions. In the first phase, an optical channel is assumed to be in the green admission state, which means that the optical performance is far from this threshold, so that the channel can accept new traffic demands, and no rerouting of the already carried demands is required. When the performance values lie between the predefined performance threshold and the MAPP (yellow admission state), the optical channel is no longer eligible to receive new traffic demands, and the rerouting of the carried traffic demands to other optical channels via the use of OTN switches is encouraged in a best-effort way (i.e., no additional line interfaces are acquired to accomplish this objective).

Moreover, this proactive best-effort rerouting increases the likelihood that optical channels reaching the MAPP are gradually emptied of traffic in advance of having to be mandatorily torn down, utilizing the optical channels already deployed to carry the remaining traffic. Particularly, the proposed scheme can benefit resource usage by (i) enabling the proactive search for available capacity in other optical channels, improving the overall fill ratio of the established channels, and (ii) allowing a quicker emptying of optical channels close to the MAPP, releasing their line interfaces, which can be used to create new optical channels in the next planning periods of the network operation. Finally, the process is changed to red admission state, when the optical channel reaches the MAPP and the carried traffic demands have to be mandatorily rerouted to other optical channels already assigned in the network, by downgrading the modulation format of the optical channel or via using new optical channels to transport the traffic.

In order to properly adopt the proposed provisioning engine, it is necessary to define a suitable transport node architecture. In this case, it is assumed that the network nodes are equipped with ROADMs and OTN switches, as shown in Fig. 2.14 (b). By having an OTN switch providing the interconnection between client and line signals, it is possible to remotely switch client signals from one

optical channel to another (assuming the latter has been set up) without disruption of the live traffic [108]. This is a key requirement to efficiently support the proposed provisioning engine.

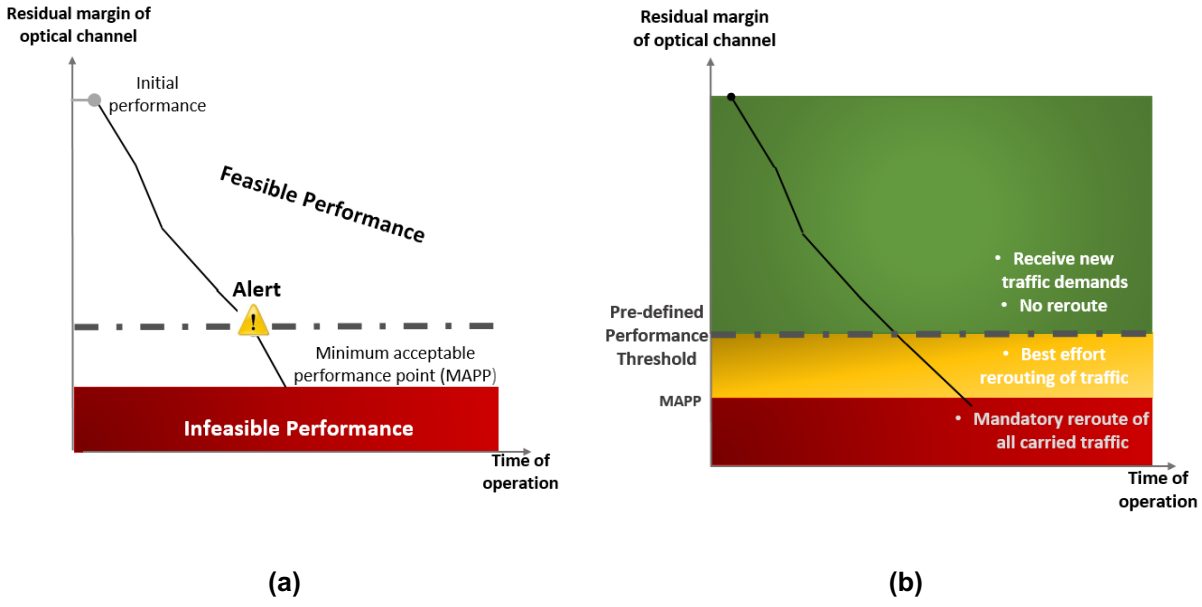

Figure 6.4 (a) Evolution of the optical channel throughout the network lifecycle and (b) proposed provisioning engine using real-time performance monitoring.

6.3.1.1 Multi-period Framework

The proposed framework is customized to operate the OTN with current-state-of-life (CoL) margins based on the information provided by the performance monitoring and trend analysis platforms shown in Fig. 6.2 where the performance's information is constantly obtained in real-time, while acting proactively to minimize the number of rerouting events. Therefore, the optimization is conducted with the aim of minimizing the number of line interfaces that have to be acquired but minimizing, to a certain extent, the number of optical channels deployed that operate too close to the MAPP. Note that, the former is directly related to CAPEX, whereas the latter intends to mitigate the risk associated with having optical channels with very low margin during the network operation (i.e., channel failing due to steeper than expected performance degradation due to fast variation of the optical impairments).

The developed framework assumes an incremental multi-period scenario [83] that considers the new traffic demands to be routed within the current planning period. At each planning period, a percentage of the active traffic is removed, making capacity available in the optical channels over which these traffic demands were routed or even releasing line interfaces (when an optical channel becomes empty). The remainder of this section presents the workflow of the multi-period framework as well as the ILP and aging models used within the optimization process.

The complete flowchart of the planning workflow is described in Fig. 6.5 considering as input the network topology. The optimization is carried out per planning period receiving, i.e., knowing the set of traffic demands of the current planning period and the network state, but not knowing the parameters of the next planning periods. For each traffic demand, a set of candidate routing paths is first computed

based on the *k*-shortest path algorithm. Based on each routing path, the most spectrally efficient modulation format that does not require intermediate 3R regeneration between two nodes of the path is assessed based on the estimated performance provided by the performance monitoring block that will be emulated through an aging model in this study (more details are presented in next section). This allows to compute the set of candidate optical channels to meet the traffic demands. On the other hand, the performance of the already provisioned optical channels are also updated according to the aging performance model that combined with the definition of the manual performance threshold value allows to calculate the sets of traffic demands that need to be best-effort (D_b) and mandatorily rerouted (D_m), as illustrated in Fig. 6.4 (b).

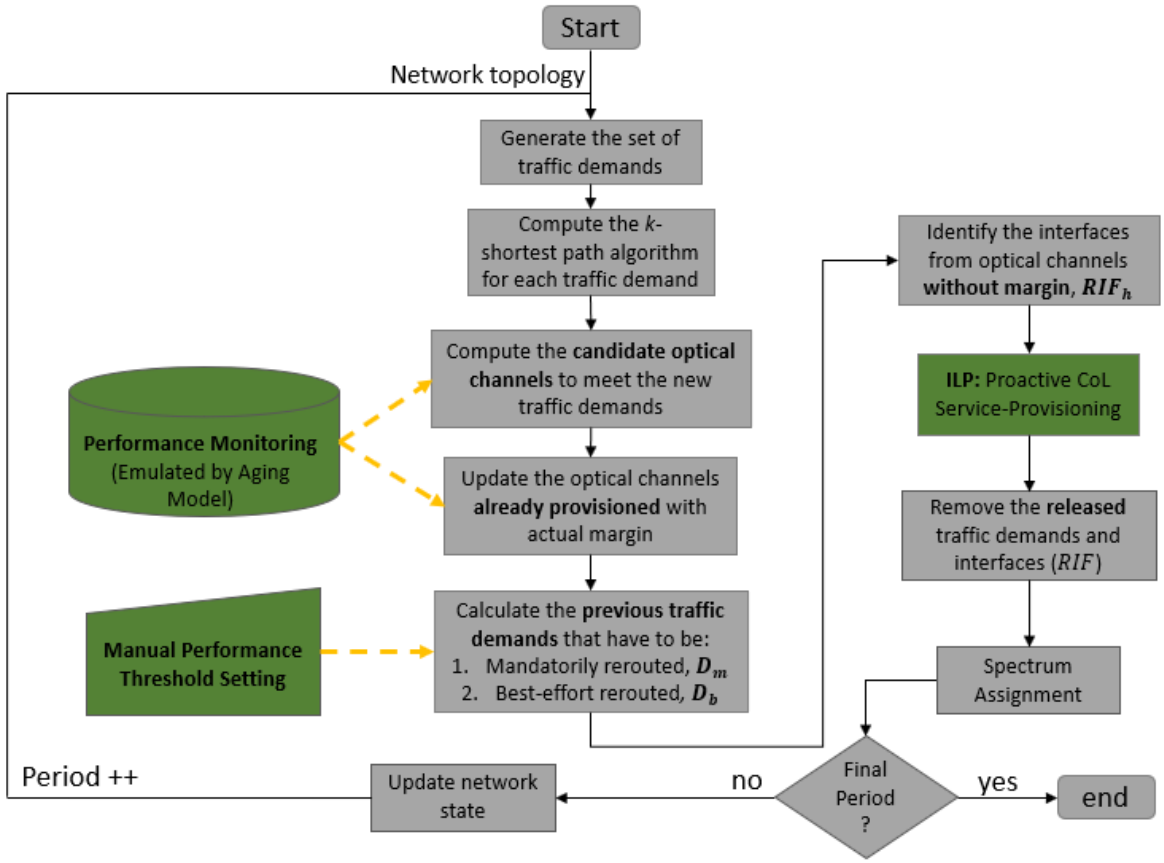

Figure 6.5 Workflow of the multi-period Proactive Service-Provisioning framework.

Before starting the optimization process, it is necessary to identify the interfaces from the optical channels that are reaching the infeasible performance region based on the performance monitoring emulated by the aging model (RIF_h) in order to ensure a hitless reconfiguration of the carried traffic demands via the OTN switches. Afterwards, the ILP model is executed as part of the service-provisioning process, receiving as input the set of pre-calculated parameters (D_m, D_b and RIF_h). In detail, it serves the new traffic demands reusing as much as possible the available capacity of the in-service optical channels and the idle line interfaces with the aim of, primarily, minimizing the number of additional line interfaces that have to be acquired and, secondarily, minimizing the use of optical channels that lie between the predefined performance threshold and the MAPP. As referenced previously, the best-effort traffic demands are rerouted in the current planning period only if there is enough capacity in the already

deployed optical channels or if idle line interfaces can be used, otherwise the reconfiguration is not performed.

From the point of view of designing the ILP model, the most challenging constraints are applied to the mandatorily rerouted traffic demands, since this traffic has to be re-groomed without (i) using the original optical channel that reaches the MAPP and (ii) resorting to the line interfaces used by this specific optical channel. Note that, these constraints are required due to the fact that the traffic demands that are being rerouted must be switched between two active optical channels in order to ensure a hitless reconfiguration via the OTN switches. The optical channel reaching the MAPP can be effectively torn down only after all the traffic demands it carries are rerouted. Therefore, the mandatorily rerouted traffic can be re-groomed via the in-service optical channels with available capacity or idle equipment released in previous/current planning periods, provided that it ensures hitless reconfiguration of the traffic, unless there are no available resources, in which case, extra line interfaces must be acquired to set up new optical channels.

Figures 6.6 (a-b) exemplify two reconfigurations associated with the mandatorily rerouted traffic in a network topology with three nodes equipped with ROADMs and OTN switches and assuming the transport of traffic demands between the different network nodes (A-C, A-B and B-C). In Fig. 6.6 (a), the traffic demands between the network nodes A and C carried over optical channel OCh 1, which reaches the MAPP, can be rerouted via the capacity available in optical channels OCh 2 and 3, whereas the reconfiguration possibility of using a new optical channel (OCh 4'), between the end-nodes A and C, that reuses the grey coloured line interfaces released by OCh 1 is not possible, since the OCh 1 that initially uses the grey coloured line interfaces is still active when the reconfiguration is performed and it is not possible to set up a new optical channel at the same line interfaces guaranteeing the successful reroute of the traffic between the both channels, which leads to a disruption of the carried traffic.

On the other hand, when having two (or more) optical channels reaching the MAPP within the same planning period, the ILP model also has to guarantee that the carried traffic will not be switched through the use of new optical channels reusing the line interfaces released by another optical channel reaching the MAPP, as described in Fig. 6.6 (b). In this example, the OCh 1 and OCh 2 reached the MAPP and the reconfiguration possibility of replacing each channel by adding a new one between the same nodes (OCh 4' and OCh 5') that reuses the line interfaces released by each other (grey and blue coloured line interfaces) will result in a contention of the traffic if both reconfigurations via the OTN switch take place since it is necessary to ensure that the traffic demands are rerouted between two line interfaces and due to the fact that the reconfigurations of Fig. 6.6 (b) are between the same interfaces leads to a collision of traffic that results in traffic disruption.

As a result, if there are multiple optical channels reaching the MAPP at the same time, the ILP must guarantee that there are a set of traffic demands from one of those optical channels that will not reuse any of the line interfaces released by the other optical channels reaching the MAPP. This ensures that the remaining reconfigurations of the traffic demands from the other optical channels reaching the MAPP can smoothly and sequentially take place between two line interfaces without traffic disruption, since the line interfaces released by the selected optical channel that will not reuse any of the line interfaces

released by the other optical channels reaching the MAPP are always there given that its reconfiguration already takes place.

Afterwards, a percentage of the traffic demands is removed due to the use of a multi-period scenario, and the released line interfaces are registered as idle equipment that can be used in the next planning periods. Note that, the idle equipment can be restricted to the same network node where the equipment was originally installed, or, if accepted by the network operator, it can be reused at any network node. This means that the network operator agrees that the line interfaces can be transferred between network nodes and planning periods, assuming that there is enough time to reallocate the equipment between planning periods. Both scenarios are considered and can have different impacts on the efficiency of the proposed framework. In order to reduce the complexity of the ILP, the spectrum assignment is performed subsequently, using the first-fit algorithm, as described in Fig. 6.5.

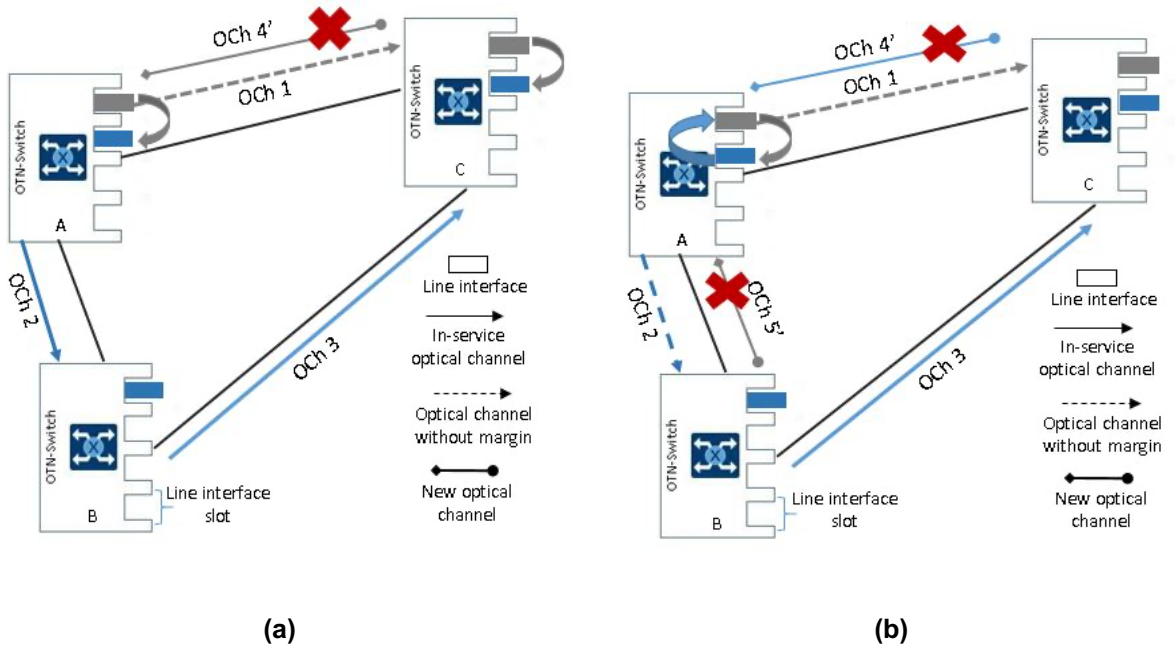

Figure 6.6 Examples of the reconfiguration processes involving the mandatorily rerouted traffic demands (a) Reconfiguration of the traffic carried over a single released optical channel. (b) Reconfiguration of traffic carried over two released optical channels.

6.3.1.2 Aging modelling and Optical Performance Estimation

The proposed service-provisioning framework, described in Fig. 6.5, assumes the access to a performance monitoring platform, which allows the prediction of the performance of each optical channel throughout the network lifecycle, in order to be able to set up new optical channels with reduced margins and proactively divert the traffic demands from these optical channels when they are approaching the MAPP. In this study, the evolution of the optical channels' performance, measured in residual margin described in 2.1.2.3, is emulated based on the progressive impact of the aging in the network elements along the different planning periods. Particularly, it assumes that line interfaces, optical switches, optical amplifiers, and fibre plant are the network elements that most deteriorate performance over the operational time of a transport network. Therefore, the model considers an increase in the attenuation

coefficient of the optical fibre (α_{atte}) over the different planning periods (e.g., in order to account for events such as repairing fibres due to unexpected cuts), as well as an increase in the noise figure of the EDFAs (NF) as a result of aging. In the case of line interfaces, the aging model comprises a progressive degradation of the required back-to-back OSNR ($OSNR_{B2B}$), while in the case of optical switches it accounts for an increase of the WSSs' filtering power penalties presented in the ROADMs ($P_{filt,fm}$). Notably, these figures are modulation format dependent.

In this context, Table 6.1 provides a detailed description of the BoL values and the yearly aging variation figures for the different network elements. The BoL values for the required back-to-back OSNR and filtering power penalties as a function of the number of WSSs traversed are the same as defined in [29], whereas the increase in the filtering penalty per year is the same as given in [43], assuming an increase of 10% of the BoL value of WSS filtering power penalty measured in dB per year. In the case of yearly aging in the required back-to-back OSNR, it is assumed that the higher-order modulation formats will have lower tolerance to impairments in general (components and transmission), which is translated into an increment of 0.01 dB per modulation format starting with the value of 0.05 dB for QPSK, which is the same described in [29]. In addition, the yearly increase in fibre attenuation is based on [98], while the impact of aging in the EDFAs' noise figure is described in [184].

Table 6.1 Aging figures utilized per network element.

Network Element		**BoL Value**	**Yearly Aging**
Fibre Attenuation Coefficient (α_{atte})		SSMF 0.21 dB/km LEAF 0.22 dB/km	0.002 dB/km
EDFA Noise Figure (NF)		4.5 dB	0.1 dB
Line interface required back-to-back OSNR ($OSNR_{B2B}$)	**QPSK**	14 dB	0.05 dB
	8 QAM	18 dB	0.06 dB
	16 QAM	21 dB	0.07 dB
	32 QAM	25 dB	0.08 dB
	64 QAM	30 dB	0.09 dB
WSS filtering power penalty ($P_{filt,fm}$) [dB]	**QPSK**	As defined in [29]	+10%
	8 QAM	As defined in [29]	+10%
	16 QAM	As defined in [29]	+10%
	32 QAM	As defined in [29]	+10%
	64 QAM	As defined in [29]	+10%

The values of Table 6.1 are then incorporated into the optical performance estimation model described in Appendix A without considering the 2 dB of Equation (A.6) since this aging model emulates the operation with reduced margins, enabling the assessment of the optical channels' performance, measured in OSNR, for the different planning periods according to the variation of the yearly aging

values. Note that, Table 6.1 also highlights the different symbols of the parameters utilized in Appendix A. Furthermore, a full-loaded system is assumed when computing the impact of non-linear fibre interference in each fibre span and the optical fibre parameters used in the OPM are presented in Table 5.1.

With the knowledge of the optical channels' performance evolution along the different planning periods, the optical channels below the performance threshold (TH_l), the optical channels running without margin (H) and the associated line interfaces (RIF_h) can be calculated. On the other hand, the traffic demands that have to be mandatorily (D_m) and best-effort rerouted (D_b) according to the state of operation of the traversed optical channels described in Fig. 6.4 (b) can also be computed. All input parameters of the ILP model detailed in the next section, as depicted in the workflow of Fig. 6.5.

6.3.1.3 ILP Models

This subsection introduces the ILP model referred to in Fig. 6.5. Two variants of the ILP model are considered, one that allows the released equipment to be reused at any network node (ILP-7) and another that restricts the reuse of idle equipment to the same network node where the equipment was originally installed (ILP-8). Hence, the framework is compliant with both equipment management policies. Both ILP models require the following variables and input parameters:

Parameters:

V	Set of network nodes
E	Set of network links
L	Generic set of candidate optical channels.
L_e	Set of optical channels that traverse the network link $e \in E$
L_v	Set of optical channels that pass-through the network node $v \in V$
L_T	Set of optical channels already deployed in previous planning periods
$L_{i,j}$	Generic set of available optical channels between source node i and destination node j
D	Set of traffic demands
D_T	Set of traffic demands already allocated in the previous planning periods
D_n	Set of new traffic demands in the current planning period

D_m	Set of mandatorily rerouted traffic demands
D_b	Set of best-effort rerouted traffic demands
S_d	Number of 1.25 Gbit/s slots used to aggregate $d \in D$ into an optical channel
X_l	Total number of 1.25 Gbit/s slots supported by the optical channel $l \in L$, which depends on the bit-rate of the channel
N_d	Total number of traffic demands from type $d \in D$
W_d^l	Total number of traffic demands from type $d \in D_T$ that use the optical channel $l \in L_T$ in the previous planning periods
F	Number of available (12.5 GHz) frequency slots per network link
F_l	Number of 12.5 GHz frequency slots allocated to optical channels $l \in L$
OC_l	Total number of optical channels $l \in L$ used in the previous planning periods
TH_l	Binary array that indicates if an optical channel $l \in L$ is below the performance threshold.
H	Set of optical channels that reach the MAPP.
RIF	Set of released line interfaces
RIF_h	Set of released line interfaces from optical channel that reaches the MAPP $h \in H$
RIF_h^v	Set of released line interfaces from the optical channel that reaches the MAPP $h \in H$ using the network node $v \in V$
RIF_v	Set of released line interfaces using the network node $v \in V$
D_h	Set of traffic demands that are carried over the optical channel that reaches the MAPP $h \in H$ in previous planning periods
Y_h	Total number of traffic demands within the set D_h
EV_l	Set of the end-nodes of each optical channel $l \in L$

Z	Weight value to balance the objectives in the ILPs
LZ	Large weight parameter used to balance the constraints

Variables:

$\lambda_{d_{(o,t)}}^{l_{(i,j)}} \in \mathbb{N}^0$	Number of traffic demands from type $d \in D$ between source node o and destination node t using optical channel $l \in L$ with source node i and destination node j
$\theta_l \in \mathbb{N}^0$	Number of optical channels required from the format of the candidate channel $l \in L$
$\Omega_h^l \in \{0,1\}$	Binary variable that indicates if at least one of the traffic demands that used the optical channel that reaches the MAPP $h \in H$ in previous planning period is now using the optical channel $l \in L$
$\xi_h \in \{0,1\}$	Binary variable that indicates the optical channel that reaches the MAPP $h \in H$ in which the carried traffic demands will not reuse the released interfaces from other optical channels that also reach the MAPP
$\zeta_h^l \in \{0,1\}$	Binary variable that indicates if at least one of the traffic demands that used the optical channel selected by variable ξ_h in the previous planning periods is now using optical channel $l \in L$
$\Phi_l \in \{0,1\}$	Binary variables that point out if the number of optical channels $l \in L$ is increasing during the optimization process
$\rho_l \in \mathbb{N}^0$	Total number of line interfaces reused from inventory of release line interfaces (RIF) for optical channel $l \in L$
$\rho_l^{ev} \in \mathbb{N}^0$	Total number of line interfaces reused from inventory RIF for optical channel $l \in L$ using the end-node $ev \in EV_l$
$\omega \in \mathbb{N}^0$	Total number of line interfaces that have to be acquired
$\alpha \in \mathbb{N}^0$	Total number of optical channels below the performance threshold.

The following formulation described the ILP-7 model, which exploits the ability to reuse idle equipment at any network node:

$$min\ (\omega + \frac{\alpha}{Z}) \tag{6.1}$$

subject to

$$\lambda_d^l = W_d^l \quad \forall d \in D_T \backslash (D_m, D_b), \forall l \in L_T \tag{6.2}$$

$$\sum_{l \in L_{i,j=v}} \lambda_{d_{(o,t)}}^{l_{(i,j)}} - \sum_{l \in L_{i=v,j}} \lambda_{d_{(o,t)}}^{l_{(i,j)}} = \begin{cases} -N_d, & v = o \\ N_d, & v = t \\ 0, & \forall v \in V \backslash \{o, t\} \end{cases} \quad \forall d \in D_n, D_b, D_m \tag{6.3}$$

$$\sum_{d \in D} S_d \times \lambda_d^l \leq X_l \times \theta_l \quad \forall l \in L \tag{6.4}$$

$$\sum_{l \in L_e} F_l \times \theta_l \leq F \qquad \forall e \in E \tag{6.5}$$

$$\sum_{d \in D_h} \lambda_d^l \leq Y_h \times \Omega_h^l \leq \frac{1}{2} + \sum_{d \in D_h} Y_h \times \lambda_d^l \quad \forall h \in H, \forall l \in L \tag{6.6}$$

$$\sum_{h \in H} \xi_h = 1 \tag{6.7}$$

$$\zeta_h^l \leq \xi_h \qquad \forall h \in H, \forall l \in L \tag{6.8}$$

$$\zeta_h^l \leq \Omega_h^l \qquad \forall h \in H, \forall l \in L \tag{6.9}$$

$$\zeta_h^l \geq \Omega_h^l + \xi_h - 1 \qquad \forall h \in H, \forall l \in L \tag{6.10}$$

$$1 - LZ \times (1 - \Phi_l) \leq (2 \times \theta_l - 2 \times OC_l) \leq LZ \times \Phi_l \qquad \forall l \in L \tag{6.11}$$

$$\rho_l \geq 0 \qquad \forall l \in L \tag{6.12}$$

$$\rho_l \leq LZ \times (1 - \Phi_l) + (2 \times \theta_l - 2 \times OC_l) \quad \forall l \in L \tag{6.13}$$

$$\rho_l \leq LZ \times \Phi_l \qquad \forall l \in L \tag{6.14}$$

$$\rho_l \leq RIF - \sum_{h \in H} RIF_h \times \Omega_h^l - \sum_{h \in H} (\sum_{h' \in H \backslash h} RIF_{h'}) \times \zeta_h^l \quad \forall l \in L \tag{6.15}$$

$$\sum_{l \in L} \rho_l \leq RIF \tag{6.16}$$

$$\sum_{l \in L} TH_l \times \theta_l = \alpha \tag{6.17}$$

$$\sum_{l \in L} 2 \times \theta_l - \rho_l = \omega \tag{6.18}$$

The objective function (6.1) consists of minimizing the number of line interfaces that have to be acquired and also gives priority to obtain a solution with the minimum number of optical channels close to the MAPP. Constraints (6.2) impose that the traffic demands already deployed in previous planning periods and that do not need to be rerouted are kept in the same optical channels and (6.3) ensure the general flow conservation for all traffic demands. The optical channel capacity restrictions are set by constraints (6.4) and (6.5) guarantee that the total number of frequency slots used does not exceed the link capacity. Constraints (6.6) calculate the new optical channels of the traffic demands that were routed over optical channels reaching the MAPP, where the different parcels of the Equation (6.6) ensure that the variable Ω_h^l is set to one if at least one of the traffic demands ($d \in D_h$) uses the optical channel $l \in L$. Additionally, the $\frac{1}{2}$ of the equation guarantees that the variable Ω_h^l is set to zero if none of the traffic demands ($d \in D_h$) use the optical channel $l \in L$ and the ($\frac{1}{2} + \sum_{d \in D_h} Y_h \times \lambda_d^l$) parcel is utilized to ensure that the Ω_h^l is set to one when there is at least one traffic demands ($d \in D_h$) using the optical channel $l \in L$.

Constraint (6.7) selects one optical channel from the poll of ones that reach the MAPP, in which the carried traffic demands will not reuse none of line interfaces released by the other optical channels that also reach the minimum acceptable performance point, as illustrated in Fig. 6.6 (b). The constraint (6.7) is complemented by constraints (6.8-6.10) that indicate the new optical channels of the traffic demands that are carried over the optical channel selected in constraint (6.7). Both Ω_h^l and ζ_h^l variables will then be utilized to restrict the number of line interfaces reused from the inventory. In order to properly calculate the total number of line interfaces reused from the inventory per optical channel, the constraints (6.11) compute a set of binary variables that specify per optical channel if its value is increasing during the optimization process. These constraints identify the number of line interfaces that have to be acquired and the ones eligible to reuse from the inventory. Note that, the number of optical channels can decrease due to the re-grooming of best-effort rerouted traffic demands. The constraints (6.12-6.15) compute the number of line interfaces reused from the inventory per type of optical channel. In detail, constraints (6.12) ensure that the values cannot be negative, whereas constraints (6.13-6.14) guarantee that the reuse is only eligible for the optical channels that increase their number, i.e., these constraints ensure that only the optical channels that increase their number during the optimization can utilize the interfaces from the inventory.

Finally, constraints (6.15) limit the reuse to the number of interfaces available in inventory. If the variables (Ω_h^l , ζ_h^l) are active, the number of interfaces available in inventory will be reduced according to the restrictions to ensure a hitless rerouting of the traffic. The activation of Ω_h^l will imply the removal of the interfaces released due to its original optical channel reaching the MAPP (see Fig. 6.6 (a)), while the activation of ζ_h^l requires the removal of all interfaces released by the other optical channels reaching the MAPP (see Fig. 6.6 (b)). Constraints (6.16) ensure that the total number of line interfaces reused from inventory does not exceed the total number of available ones. Finally, constraints (6.17) and (6.18) compute the total number of optical channels deployed close to the limit of performance and the total number of line interfaces that have to be acquired, respectively. In this ILP model, the number of

variables is defined by $|D| \times |L| + 3 \times |L| + 2 \times |H| \times |L| + |H| + 2$, whereas the number of constraints is given by $|D_T| \times |L_T| + \left|D_{n,b,m}\right| \times |V| + 6 \times |L| + 4 \times |L| \times |H| + |E| + 4$.

The ILP-8 model has the same objective function as ILP-7, but it includes specific constraints to only reuse the idle equipment within the same network node where the equipment was originally installed in order to avoid equipment reallocations. The mathematical formulation is as follows:

(6.1) from the definition of ILP-7

subject to

(6.2-6.11) from the definition of ILP-7

$$\rho_l^{ev} \geq 0 \qquad \forall l \in L, \forall ev \in EV_l \tag{6.19}$$

$$\rho_l^{ev} \leq LZ \times (1 - \Phi_l) + (\theta_l - OC_l) \qquad \forall l \in L, \forall ev \in EV_l \tag{6.20}$$

$$\rho_l^{ev} \leq LZ \times \Phi_l \qquad \forall l \in L, \forall ev \in EV_l \tag{6.21}$$

$$\rho_l^{ev} \leq |RIF_{v=ev}| - \sum_{h \in H} RIF_h^{v=ev} \times \Omega_h^l - \sum_{h \in H} \left(\sum_{h' \in H \setminus h} RIF_{h'}^{v=ev} \right) \times \zeta_h^l \qquad \forall l \in L, \forall ev \in EV_l \tag{6.22}$$

$$\sum_{l \in L_v} \rho_l^{ev=v} \leq |RIF_v| \qquad \forall v \in V \tag{6.23}$$

$$\sum_{l \in L} \sum_{ev \in EV_l} \rho_l^{ev} \leq |RIF| \tag{6.24}$$

(6.17) from the definition of ILP-7

$$\sum_{l \in L} \sum_{ev \in EV_l} \theta_l - \rho_l^{ev} = \omega \tag{6.25}$$

The ILP-8 model has to split the variable ρ_l from ILP-7 per end-node of each optical channel in order to limit the reuse of line interfaces from inventory to a specific network node. This implicitly requires the adaptation of constraints (6.12-6.15) used in ILP-7 to (6.19-6.22). On the other hand, the constraints (6.23-6.24) ensure that the total number of line interfaces reused does not exceed the total number of line interfaces available per network node, whereas constraints (6.25) compute the total number of line interfaces that have to be acquired according to the number of line interfaces reused from inventory per end-node. The remaining constraints are the same as those introduced for ILP-7. In case of the ILP-8, the number of variables is defined by $|D| \times |L| + 2 \times |L| + 2 \times |H| \times |L| + |H| + |L| \times |L| + 2$, whereas the number of constraints is given by $|D_T| \times |L_T| + \left|D_{n,b,m}\right| \times |V| + 2 \times |L| + 4 \times |L| \times |H| + |E| + 4 \times |L| \times |L| + |V| + 4$.

6.3.1.4 Results and Discussion

In order to properly benchmark the performance of the proposed proactive service-provisioning framework (CoL-P Proact), that operates the optical network with reduced margins (provided by the proposed aging model) described in Fig. 6.5 of Subsection 6.3.1.1, two alternative design scenarios are considered. The first alternative scenario also assumes a provisioning framework with smaller margins but it is reactive to a performance degradation (CoL-P React), that is, traffic demands are only rerouted when it becomes mandatory (i.e., the optical channel that carries them reaches the MAPP). This scenario does not consider the proposed provision engine presented in Fig. 6.4 (b). Finally, the second alternative scenario adopts the conventional provisioning with additional performance margins detailed in Subsection 2.1.2.3, where optical channels are always set up with a total 3 dB margins to address the combination of the design, system and transmission margins that accounts for performance degradations during the entire network operation (EoL-P). The analysis considers two reference transport networks illustrated in Appendix B: the Telefónica SBN and the Telecom Italia IBN topologies. Both network topologies were defined in the scope of the FP7 IDEALIST project by the abovementioned network operators [155].

This study follows the characteristics of the network topologies defined in IDEALIST project [155] that considers the use of SSMF fibre spans for both topologies, while the IBN also utilizes LEAF fibres in some of the fibre spans. It is assumed that each ROADM node has a route-and-select express layer and a colourless add/drop layer, described in 2.1.3.3. Additionally, next-generation line interfaces (Table 2.1) operating at 64 Gbaud and supporting modulation formats from QPSK to 64 QAM are used. Each optical channel is allocated a 75 GHz frequency slot and it is assumed the support of 64 channels per network link (F_{max}). The simulation also assumes a 10-year network lifecycle with 6 months between consecutive planning periods and 100/200/400 Gbit/s traffic demands randomly generated between 25% of the node-pairs with a traffic growth of 20% for each planning period, assuming the same percentage of the traffic rates at each planning period. At the end of each planning period, 10% of the traffic demands are removed from the network. The traffic demands are routed over one of the available grooming possibilities along the three shortest routing paths between their end-nodes. According to the current performance of the optical channel and the margins imposed by the adopted provisioning framework, the modulation format enabling the highest capacity is chosen.

The simulation results are averaged over 20 independent simulation runs. The ILP models were solved using the CPLEX solver platform [147] running on a PC with an Intel® Xeon® E5-2690 v2 3 GHz processor and 48GB of RAM. Additionally, the weight value (Z) of the ILPs is defined by the maximum number of optical channels that can be deployed according to the number of frequency slots available per network link in order to balance the objectives in the ILP's objective function. In this case, Z equals the total number of candidate optical channels ($|L|$) multiplied by the number of channels that each network link can support (F_{max}). Nevertheless, on average the simulation run, for 20 planning periods, takes approximately 14 hours for SBN topology and 18 hours for IBN, although it depends on the traffic growth profile. The increase of the computational time is due to the utilization of challenging constraints to ensure that the mandatorily rerouted traffic demands are reconfigured without disruption.

The analysis is mainly divided into four sets of results. The first part of the study consists in the evaluation of the aging impact for each network topology throughout the entire network lifecycle, whereas the second set of results focuses on the impact of using different values of the performance threshold on the effectiveness of the proposed service-provisioning framework. The third set of results assesses the cumulative number of line interfaces that have to be acquired along the different planning periods with the aim of comparing the expected overall cost associated with each service-provisioning strategy. The final set of results analyses the influence of using different approaches to exploit smaller margins regarding the optical performance.

A. Aging Impact

Before analysing the cost savings of operating an OTN with current margins, it is important to assess first the impact of the described aging model on the possible usage of each modulation format between the network node-pairs. On one hand, this helps to understand the potential of increasing network capacity (e.g., at BoL) through the use of higher-order modulation formats, which can enable the postponing of line interface acquisition. On the other hand, it can also highlight that, for some of the node-pairs, that low-margin provisioning strategy results in an optical channel that will become infeasible later on.

Therefore, the first set of results is presented in Fig. 6.7 (a-b) for SBN and IBN topologies, respectively. The figures depict the number of node-pairs that can be directly connected, i.e., for which there is at least one routing path over which it is possible to set up an optical channel using a given modulation format for both CoL and EoL scenarios, as a function of the planning period. Note that, the EoL scenario assumes a total of 3 dB margins to set up a connection, whereas the CoL assumes the operation with reduced margins emulated by the progressive impact of the aging in the elements of the network (Subsection 6.3.1.2) over the different planning periods.

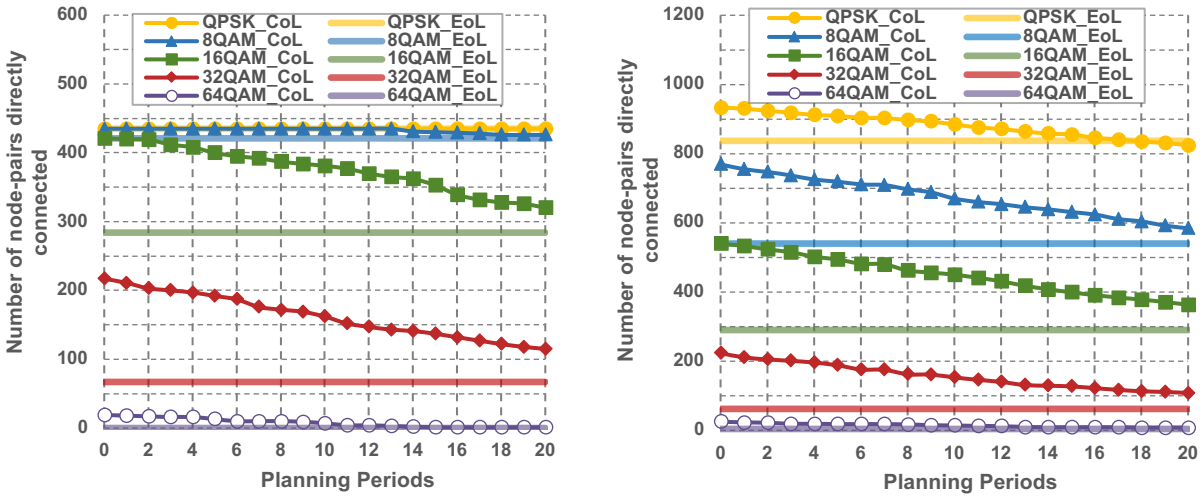

(a) SBN **(b) IBN**

Figure 6.7 Evolution of the number of node-pairs directly connected with each modulation format for (a) SBN and (b) IBN topologies.

The results show a gradual decrease in the number of node-pairs directly connected as a result of the network elements aging for the CoL scenario, which means, for example, that there is room to use more spectral efficient modulation formats in the beginning of the network operation allowing to increase the overall capacity transported when operating with the just enough margins. On the opposite side, the use of conservative EoL approach leads to a smaller number of node-pairs directly connected due to assuming high performance margins to guarantee that the channel is feasible until the network EoL. In the case of the SBN topology, the decrease of performance is only significant for the higher order modulation formats due to the smaller size of the network topology when compared to IBN. As expected, it can also be seen that higher order modulation formats are more affected from the performance degradation associated with the aging of the devices. This is a consequence of the aging model used that intends to capture the lower tolerance of these formats to some of the performance impairments, e.g., the required back-to-back OSNR and WSS filtering cascading as shown in Table 6.1 of the aging modelling subsection.

B. Performance Threshold

In order to determine the most effective performance threshold that should be setting for the proposed service-provisioning framework, Table 6.2 depicts the impact of the CoL-P Proact performance threshold in the cumulative number of mandatorily rerouted traffic demands due to performance limitations for the IBN network topology. This study assumes a performance threshold value between 0.5 and 2 dB. Note that, it was only used values until 2 dB of provisioning margin beyond the MAPP, since this value should be reduced enough in order to avoid the augment of best-effort rerouting events not necessary for the purpose of this study.

Table 6.2 Number of traffic demands mandatorily rerouted as function of the performance threshold for the IBN network topology.

Performance Threshold (dB)	**Cumulative number of traffic demands mandatorily rerouted**		
	CoL-P Proact	**CoL-P React**	**EoL-P**
0.5	53.2	203.2	0
1.0	43.1	203.2	0
1.5	40.6	203.2	0
2.0	39.4	203.2	0

As expected, enforcing a smaller performance threshold will result in an increase in the number of mandatorily rerouting events, since the proposed framework in some cases could not have the enough time to best-effort reroute the traffic demands from the optical channels that are reaching the performance limit, resulting in mandatorily rerouting events, as illustrated in Fig. 6.4 (b). Nevertheless, even with a margin of only 0.5 dB, it still requires only 26% of traffic demands rerouting events, when compared to CoL-P React that does not consider the proactive provisioning engine proposed in this study and assumes the rerouting of the traffic when it becomes mandatory. Based on these results, the

2 dB performance threshold is the value that creates more room to reduce the number of traffic demands that have to be mandatorily rerouted due to reaching the MAPP, while still improving resource usage throughout the network lifecycle due to the reconfiguration processes [168]. Note that, the EoL-P approach does not have any traffic demand being mandatorily rerouted, since it assumes a total of 3 dB margins which is typically the value considered to ensure that the optical channels are feasible until the network EoL.

C. Line Interfaces Requirements

The second part of the analysis focuses on the CAPEX implications of using the three different provisioning strategies throughout the network lifetime. The obtained results are depicted in Fig. 6.8, which shows the evolution of the number of line interfaces that have to be acquired for both topologies considering the two novel ILP models (ILP-7 and -8) which as seen before have different degrees of freedom to reutilize the line interfaces from the inventory. Note that ILP-7 allows the released line interfaces to be reused at any network node, whereas ILP-8 limits the reuse of the released line interfaces to the same network node, where the equipment was originally placed.

As can be seen, there is a clear benefit from starting to operate an OTN with reduced performance margins, since it allows the decrease of the overall network cost. When comparing CoL-P Proact with EoL-P, it can be observed that the former enables line interface savings between 22% for both ILPs in the SBN topology and between 32% for ILP-7 and 29% for ILP-8 in the IBN. First, this provides clear evidence that by provisioning optical channels with reduced margins, it is possible to attain substantial reductions in CAPEX. Secondly, the extent of line interface savings is directly related to the impact of the aging model. For instance, the larger CAPEX savings obtained with IBN, when compared to SBN, is a consequence of the fact that in the former network, optical performance is more impacted by aging for all modulation formats, as already observed in Fig. 6.7. This can be explained by the fact that optical channels are on average longer in IBN which impacts their performance, resulting in a higher decrease of performance emulated by the aging model for the different modulation formats.

Another key finding is that, when comparing the proposed proactive framework (CoL-P Proact) with a more conventional reactive framework (CoL-P React), the former is shown to be more effective than the latter in minimizing the number of line interfaces, and this becomes more evident at later planning periods. This is due to the fact that CoL-P Proact constantly attempts to best-effort reroute the traffic demands, before the traversed optical channels have to be torn down, due to insufficient QoT, which allows the release of a higher number of line interfaces that can be reused in the next planning periods.

Conversely, the reactive approach performs these tasks only when it becomes inevitable in terms of performance, hence reducing the probability of finding rerouting options that avoid acquiring new line interfaces. In the last planning period, the savings enabled by the proactive approach compared to the CoL-P React reach 6% and 9% when using ILP-7 with the SBN and IBN topologies, respectively. These savings are around 4% in both topologies when using ILP-8. These results highlight that the benefit of using CoL-P Proact instead of CoL-P React is smaller when the network operator enforces the policy of

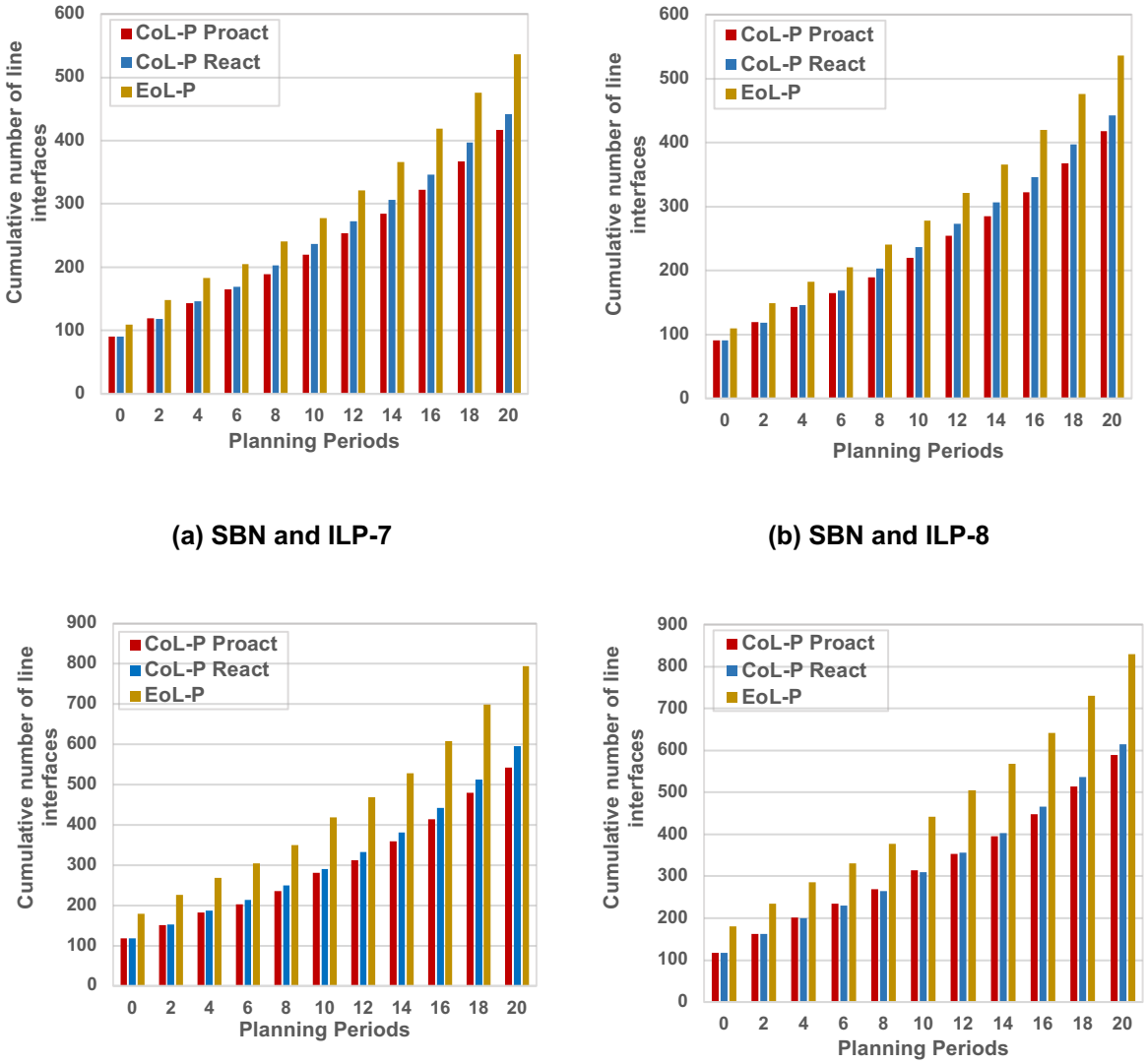

Figure 6.8 Cumulative number of line interfaces that have to be acquired during the network operation for (a) SBN and ILP-7, (b) SBN and ILP-8, (c) IBN and ILP-7 and (d) IBN and ILP-8.

restricting the reutilization of line interfaces to the original node where it was installed. This is an expected outcome, since CoL-P Proact provides a more gradual release of line interfaces, in view of including best-effort rerouting, which is better exploited when line interfaces can be immediately reused at any network node. It can also be observed that the relative impact of restricting line interface reutilization to the original node of deployment is more pronounced in larger network topologies. This follows from the fact that in the IBN there is a larger number of node-pairs that are the source/destination of optical channels, and as a result, there are more candidate nodes to benefit from a line interface that has been released elsewhere in the network.

D. Mandatory Rerouting Events and Actual Residual Margin Performance

In addition to the CAPEX savings, which have been shown to support the adoption of the proposed provisioning framework, it is also paramount to analyse the impact of exploiting smaller performance

margins in other key performance metrics. Particularly, two relevant metrics are (i) the number of traffic demands that have to be mandatorily rerouted when the optical channel that carries them reaches the MAPP and (ii) the average residual margin of the optical channels deployed provided by the optical performance model described in Subsection 6.3.1.2. The evolution of both metrics as a function of the different planning periods are plotted in Fig. 6.9 and 6.10, respectively. All the results presented consider the utilization of the ILP-7 model, since they are not significantly impacted by the specific equipment reutilization policy adopted. Similarly, no results are shown for the EoL-P strategy, since it relies on provisioning optical channels with higher performance margins (a total of 3 dB) to ensure a viable quality-of-transmission up to the end-of-network operation.

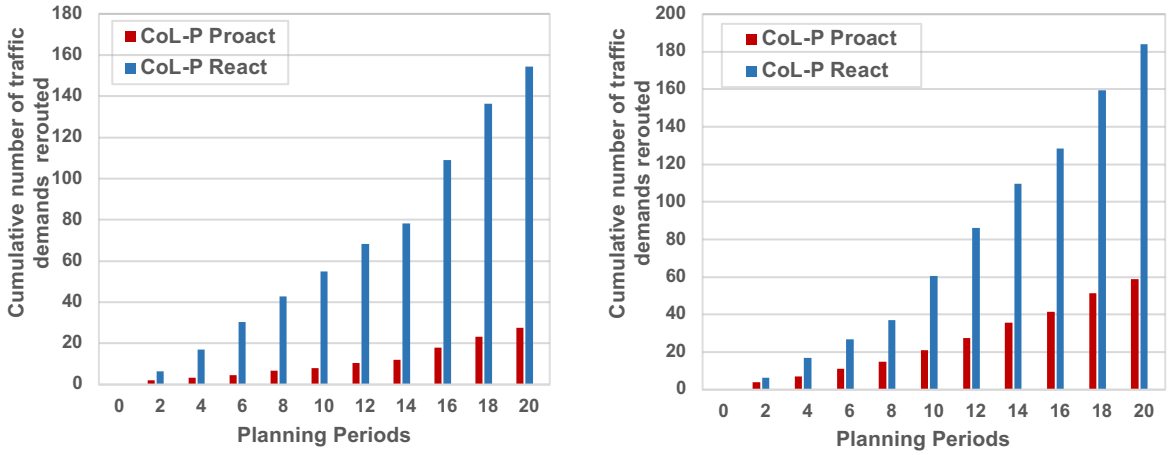

Figure 6.9 Cumulative number of traffic demands that have to be mandatory rerouted when reaching the minimum acceptable performance point for (a) SBN and (b) IBN topologies.

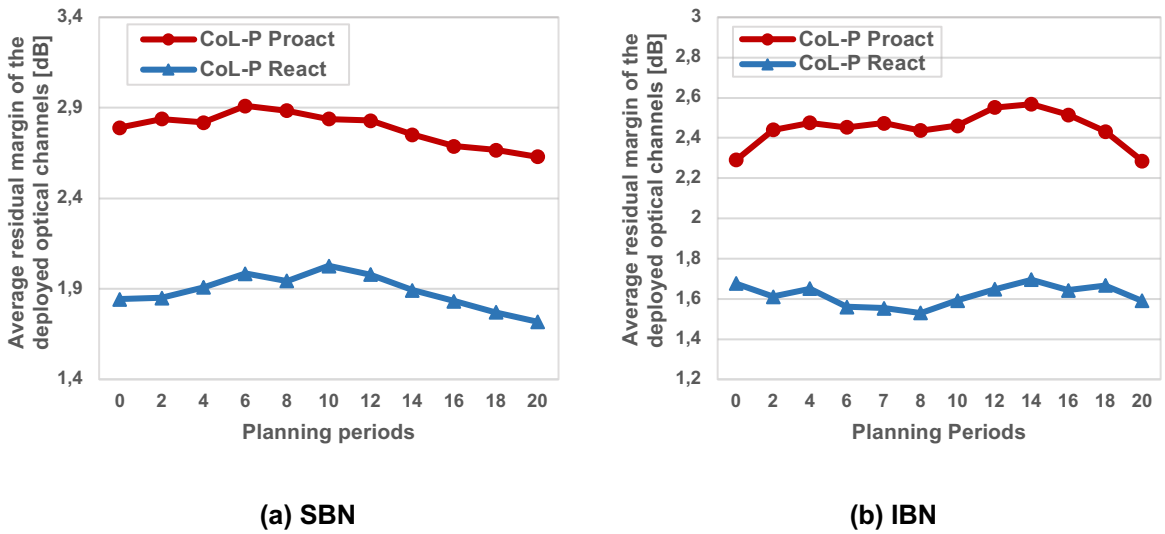

Figure 6.10 Average performance residual margin of the deployed optical channels for (a) SBN and (b) IBN topologies.

The results in Fig. 6.9 show that the proactive strategy to reroute in advance and in best-effort the traffic demands from optical channels that are between the performance threshold and the MAPP allows

the reduction of the number of traffic demands that have to be mandatorily rerouted by up to 82% for the SBN and 68% for the IBN. This observation confirms that the proposed proactive approach is also advantageous, when compared to the known reactive one, in terms of mitigating rerouting events at the MAPP, which represent an additional risk of service disruption. Note that in contrast to best-effort rerouting, mandatory rerouting of traffic demands requires setting additional constraints to guarantee the hitless reconfiguration of all traffic carried through the OTN switches (see Fig. 6.6), so the reduction in the number of mandatorily rerouting events also reduces the complexity of the optimization process. Moreover, the fact that in the SBN there is a substantial smaller number of mandatorily rerouting events when using CoL-P Proact is due to a less pronounced impact of aging model on the different modulation formats since the optical channels are on average smaller than in IBN topology. This allows to increase the performance of the optical channels deployed, which grants an extended period of time to execute best-effort rerouting.

The proposed framework also maintains as much as possible the overall optical channels' residual margin (defined in Equation A.5 of Appendix A) at higher levels, when compared to the reactive low-margin approach. This aspect is shown in Fig. 6.10, which compares the average residual margin of the deployed optical channels for CoL-P Proact and React. It can be seen that the former strategy is able to operate the network with optical channels that have on average more than 0.90 dB of performance margin in the SBN and 0.83 dB in the IBN when compared to the CoL-P React scenario. This emphasizes that, on average, optical channels are more resilient to events that might cause a sudden and steeper degradation in performance.

Furthermore, the evolution of the average residual margin depicted in Fig. 6.10 highlights that there are positive and negative variations of the performance margin over the time, due to the fact that in some cases there are transitions from higher to lower order modulation formats resulting from the continuous impact of devices and fibre plant aging. Note that, the use of a lower modulation format between two network nodes is a possibility when an optical channel operating at a higher order modulation format has to be mandatorily torn-down due to performance limitations, which allows to increase the average residual margin since the lower modulation formats will have less impact in the optical impairments and aging model, justifying the variation of the average residual margin of the deployed optical channels. Moreover, it can also be seen that on average the residual margin of the deployed optical channels reduces towards the end of the network operation, which is a direct result of the progressive degradation of the performance assumed by the aging modelling described in 6.3.1.2.

Overall, it is clear that the joint effect of using the proposed framework with the availability of OTN switching technology allows the optimization of resource utilization through the use of smaller performance margins, enabling the use of higher order modulation formats that allows to increase the capacity per deployed optical channel, while ensuring a minimum risk of traffic disruption by maintaining the overall performance margins at reasonably stable levels

6.3.1.5 Discussion of Proactive Service-Provisioning Framework

This section has proposed a service-provisioning framework that benefits from the availability of real-time performance monitoring platforms and OTN switching technology to cost-effectively shrink performance margins, allowing to increase the capacity per optical channel and reduce capital expenditures. The proposed multi-period planning framework optimizes the long-term resource utilization, while simultaneously acting to reduce the number of rerouting events involving the already provisioned traffic demands when the optical channels carrying them are reaching the minimum performance point. It accomplishes this by enforcing a best-effort rerouting of traffic demands when the optical channel's performance is within a given region above the MAPP. The optimization procedure is based on an ILP model that aims to minimize the hardware cost associated with the number of line interfaces acquired throughout the entire network lifetime, while also favouring to operate the optical channels not too close to the MAPP. Two variants of the ILP model are presented in order to comply with different network operator policies regarding line interface node reallocation.

The network simulation results, obtained over two reference transport networks, show that the use of CoL performance information makes it possible to delay, or in some cases avoid, line interface acquisitions. Note that delaying these acquisitions makes it possible to benefit from the usual cost depreciation of the line interfaces' cost. The proposed proactive strategy is shown to be more effective than the reactive approach in terms of line interface savings. This observation validates the relevance of being able to best-effort reroute traffic demands in advance of reaching the MAPP, instead of acting only when this limit is about to be reached. Notably, these savings are possible while reducing the amount of traffic demands that are rerouted when reaching the MAPP and keeping optical channels with higher performance margins, making the overall network operation more resilient [168, 169, 171, 170]. The main drawback of this approach resides in the additional cost of having an OTN switch at each network node, but its use is crucial to mitigate the service disruption inherent of operating the network with smaller performance margins that is ensured by the OTN switch capability of switching traffic demands between optical channels before the channels must be torn-down due to insufficient QoT.

6.3.2 Service-Provisioning Framework Exploiting Low-Margin for Preplanned Optical Shared Restoration Paths

The second service-provisioning framework proposed in the context of this chapter focuses on exploiting the benefits provided by deploying channels with smaller performance margins while reducing the network costs associated with the use of sophisticated reconfiguration mechanisms and network equipment to quickly detect and react to a faster than expected degradation of performance in order to avoid traffic disruption [171]. These sophisticated reconfiguration mechanisms can rely on, for example, OTN switching technology (the strategy adopted in the previous framework described in 6.3.1) or utilizing an already scheduled or dedicated maintenance window defined by the network operators to reroute the traffic from optical channels reaching the performance limit. Note that, these additional network costs (e.g., the cost associated with the OTN switching technology) may not be desirable, or

even acceptable, by the network operator, limiting the prospects of adopting service-provisioning strategies exploiting reduced margins.

In this context, larger margin reductions are only acceptable for traditional working channels (given their long time-to-live) if an advanced, and more expensive, network architecture that is prepared to proactively handle rapid deterioration of performance is deployed, otherwise fairly large margins still need to be considered. Conversely, low-margin provisioning can easily be exploited for most of the protection/restoration channels when utilizing survivability mechanisms as the ones described in Subsection 2.1.3.2, since these channels remain idle most of the time of the network operation, i.e., not carrying traffic, in the absence of failures. This property is advantageous due to the combination of two factors. Firstly, while the protection/restoration optical channels are not in use, reconfiguring it (e.g., via using a lower-order modulation format in some protection/restoration scenarios or adding extra 3R regenerators at intermediate network nodes of the channel) can be executed in a non-traffic affecting manner [185]. This could even enable to be more aggressive with respect to the margins used (e.g., discarding the system margins described in Fig. 2.7) in those paths. Secondly, because the network is expected to operate without failures almost all the time, there is a negligible risk that the protection/restoration optical channels would be reaching the performance limit at the same time that a failure in the network would trigger the need to divert traffic to it.

In order to illustrate the aforementioned properties of the protection/restoration channels, a network operation is described in Fig. 6.11 considering two optical channels (one for working and another for protection/restoration) and the occurrence of a link failure during the network operation and assuming that the protection/restoration channels are only utilized by traffic demands for protection or restoration. Additionally, this illustration also shows the active time and the residual margin for both channels. It can be seen that the active time of the protection/restoration channel (the time required to repair the failure)

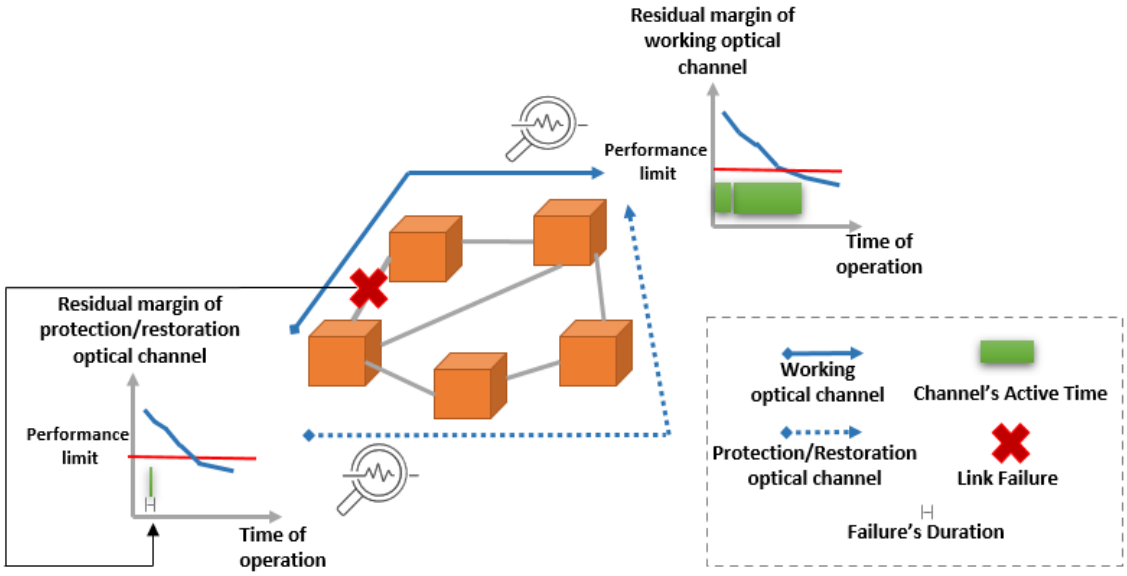

Figure 6.11 Network operation with working and protection/restoration channels in the presence of a network link failure.

is so short that the degradation of performance (residual margin of protection/restoration optical channel) during this period can be neglected. Therefore, adopting smaller margins only for protection/restoration paths can enable the deployment of fewer network resources (line interfaces or regenerators) over the typically longer paths by using higher order modulation formats, allowing to minimize the overall CAPEX without increasing the risk of traffic disruption or having to support sophisticated reconfiguration mechanisms.

6.3.2.1 Multi-period Framework

Given the aforementioned background, the proposed service-provisioning framework adopts an incremental multi-period scenario similar to the one described in 6.3.1.1 and assumes the use of preplanned shared restoration at OCh layer (see Subsection 2.1.3.2), due to its ability to share backup resources among several connections, which allows to reduce to the minimum the number of backup resources utilized, but the proposed multi-period framework can be adapted to use different types of survivability schemes. Moreover, it provisions the working optical channels with conventional additional performance margins detailed in 2.1.2.3 where the optical channels are always set up with 3 dB margins, whereas the restoration channels are provisioned with CoL margins. As mentioned in the description of Fig. 6.11, a more aggressive reduction of performance margins can be adopted for these channels since they are idle the vast majority of the time.

By assuming the preplanned shared restoration at OCh layer, it is necessary to constrain both working and restoration channels to use the same modulation format, since they share the same line interfaces deployed at the end-nodes, as described in Fig. 2.10 (b). In order to guarantee a residual margin of the restoration optical channels that allows the correct detection of the signal at the receiver (typically longer than the working channel), additional shared 3R regenerators are added to the restoration channel. From the example given in Fig. 6.12 one can see that the performance of the working channel allows the use of the 32 QAM even assuming a total of 3 dB margins, whereas the utilization of the same modulation format for the restoration channel is only possible if a 3R regenerator is placed at the network node D, due to the accumulation of optical impairments over the restoration

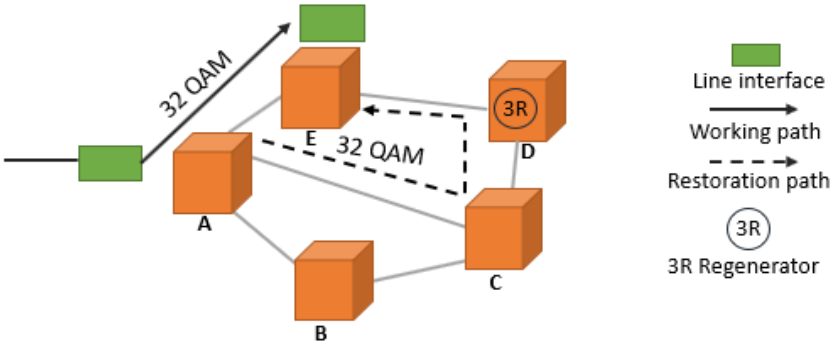

Figure 6.12 Network operation using the preplanned shared restoration at OCh layer with 3R regenerators.

channel. The placement of a 3R regenerator at node D allows to recover the signal that has already traversed the links A-C-D in order to successful transmit it over the last network link (D-E).

The location of the 3R regenerators is defined by the calculation of the performance of optical channel in the modulation format of the working path, i.e., if the performance is not sufficient to transmit the signal until the end of the channel (A-C-D-E), additional 3R regenerators are placed at the intermediate network nodes until the performance is enough to correctly detect the signal at the receiver. Note that, the placement of a 3R regenerator enables to "reset" the optical impairments accumulated until that node. In the example of Fig. 6.12, the performance of the restoration channel in the presence of 3R regenerator at node D is based on the performance between (A-C-D) and the performance between the network nodes (D-E). If both have the residual margin in the modulation format of the working path superior to zero then the global restoration path is considered to be feasible, as described in Appendix A. Moreover, the fact that the proposed framework considers the optical shared restoration will allow sharing the 3R regenerators among different connections under the assumption that the corresponding working paths do not share any network links, as depicted in Fig. 2.10 (b).

The complete flowchart of the multi-period framework is introduced in Fig. 6.13 considering as the input the network topology. The optimization is carried out per planning period receiving, i.e., knowing the set of traffic demands of the current planning period and the network state but not knowing the parameters of the next planning periods. For each traffic demand, a set of candidate routing paths is first computed based on the *k*-shortest path algorithm. Based on each routing path, the most spectrally

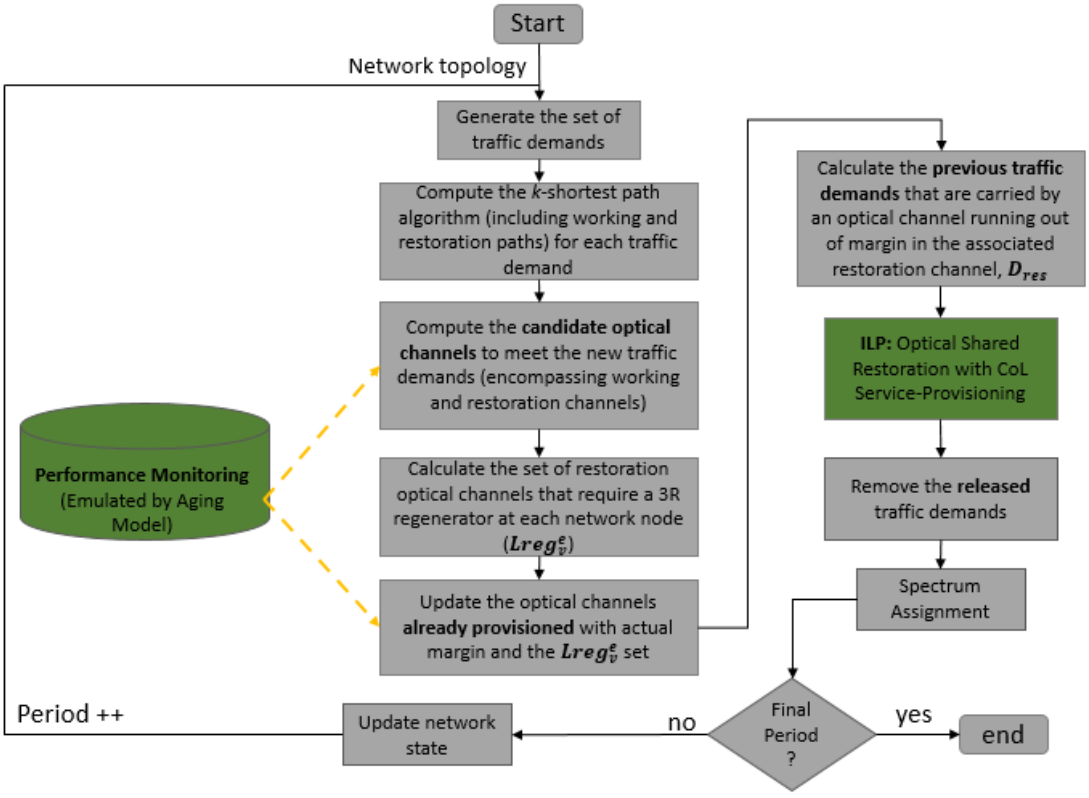

Figure 6.13 Multi-period framework using the optical shared restoration with CoL service-provisioning.

efficient modulation format with at least 3 dB of residual margin between two nodes of the path is assessed for working channel and afterwards the k-shortest path algorithm is again computed between those two network nodes of the routing path (without the network links utilized for the working channel) in order to compute a new path disjoint from the one already calculated that will be utilized for restoration. This step will allow to compute the set of candidate optical channels to meet the traffic demands, encompassing the working and restoration channels.

According to the current estimation of the performance of restoration channels (emulated by the aging model described in 6.3.1.2), the set of 3R regenerators required to ensure a sufficient residual margin for the restoration channels in the modulation format defined for the corresponding working channels is computed that enables to calculate the set of optical channels $l \in L$ that require a regenerator at network node $v \in V$ in their restoration channel using the network link $e \in E$ ($Lreg_v^e$) that will be utilized subsequently in the ILP model. Afterwards, the performance of the already provisioned optical channels utilized for optical shared restoration and the set of 3R regenerators required are also updated according to the aging performance model. Based on this information, the set of traffic demands carried over the restoration channels running out of margin (D_{res}) are computed in order to be properly rerouted within the ILP model.

Particularly, a novel Integer Linear Programming model is executed to route the new traffic demands, so that the available capacity of deployed optical channels is utilized and the number of line interfaces and 3R regenerators that have to be acquired is minimized. Simultaneously, the model also reroutes the traffic demands running out of margin in their restoration paths and gives priority to obtain a solution occupying the minimum number of frequency slots. In order to reduce the complexity of the ILP model, spectrum assignment is performed afterwards, using the first-fit algorithm and taking into account the restoration channels that share the same 3R regenerator within a network link also share the frequency slots in that link, as described in Fig. 2.10 (b).

6.3.2.2 ILP Model

This subsection introduces the ILP model referred to in Fig. 6.13. The ILP formulation requires the following variables and input parameters:

Parameters:

V	Set of network nodes
E	Set of network links
L	Generic set of candidate optical channels.
L_e	Set of optical channels that traverse the network link $e \in E$

$Lreg_v^e$ Set of optical channels $l \in L$ that require a regenerator at network node $v \in V$ in their restoration channel using the network link $e \in E$

$Lreg_v$ Set of optical channels $l \in L$ that require a regenerator at network node $v \in V$ in their restoration channel

$L_{i,j}$ Generic set of available optical channels between source node i and destination node j

D Set of traffic demands

D_T Set of traffic demands already allocated in the previous planning periods

D_n Set of new traffic demands in the current planning period

D_{res} Set of traffic demands that are carried by an optical channel running out of margin in the associated restoration channel

S_d Number of 1.25 Gbit/s slots used to aggregate $d \in D$ into an optical channel

X_l Total number of 1.25 Gbit/s slots chunks required available by per the optical channel $l \in L$, which depends on the bit-rate of the channel

N_d Total number of traffic demands from type $d \in D$

W_d^l Total number of traffic demands from type $d \in D_T$ that use the optical channel $l \in L_T$ in the previous planning periods

F Number of available (12.5 GHz) frequency slots per network link

F_l Number of 12.5 GHz frequency slots allocated to optical channels $l \in L$

Variables:

$\lambda_{d_{(o,t)}}^{l_{(i,j)}} \in \mathbb{N}^0$ Number of traffic demands from type $d \in D$ between source node o and destination node t using optical channel $l \in L$ with source node i and destination node j

$\theta_l \in \mathbb{N}^0$ Number of optical channels (encompassing the working and restoration channels) required from type $l \in L$

σ_v^e	Total number of backup 3R regenerators required at network node $v \in V$ in the event of a failure at network link $e \in E$
$\psi_v \in \mathbb{N}^0$	Maximum number of 3R regenerators that will be required at network node $v \in V$ in the event of any single link failure
$\eta \in \mathbb{N}^0$	Total number of network resources (line interfaces and regenerators) that have to be acquired
$\Gamma \in \mathbb{N}^0$	Amount of spectrum occupied

The following formulation describes ILP-9 model, which is responsible for provisioning working paths with conventional additional performance margins at the BoL and restoration paths with CoL margins:

$$min\ (\eta + \frac{\Gamma}{|E| \times F}) \tag{6.26}$$

subject to

$$\lambda_d^l = W_d^l \quad \forall d \in D_T \backslash (D_{res}), \forall l \in L_T \tag{6.27}$$

$$\sum_{l \in L_{i,j=v}} \lambda_{d_{(o,t)}}^{l_{(i,j)}} - \sum_{l \in L_{i=v,j}} \lambda_{d_{(o,t)}}^{l_{(i,j)}} = \begin{cases} -N_d, & v = o \\ N_d, & v = t \\ 0, & \forall v \in V \backslash \{o,t\} \end{cases} \quad \forall d \in D_n, D_{res} \tag{6.28}$$

$$\sum_{d \in D} S_d \times \lambda_d^l \leq X_l \times \theta_l \quad \forall l \in L \tag{6.29}$$

$$\sum_{l \in L_e} F_l \times \theta_l \leq F \qquad \forall e \in E \tag{6.30}$$

$$\sum_{l \in Lreg_v^e} \theta_l = \sigma_v^e \qquad \forall e \in E, \forall v \in V \tag{6.31}$$

$$\psi_v \geq \sigma_v^e \qquad \forall e \in E, \forall v \in V \tag{6.32}$$

$$\sum_{l \in L} 2 \times \theta_l + \sum_{v \in V} \psi_v = \eta \tag{6.33}$$

$$\sum_{e \in E} \sum_{l \in L_e} F_l \times \theta_l = \Gamma \tag{6.34}$$

The objective function (6.26) consists of minimizing the hardware resources (line interfaces and 3R regenerators) that have to be acquired and also gives priority to obtain a solution with the minimum number of frequency slots used. Note that, the secondary objective is only minimized as long as the following this preference does not translate into additional capital expenditures (line interfaces and 3R regenerators acquired). To do so, the secondary objective is normalized by the maximum number of

frequency slots that can be used in the optical network ($|E| \times F$). Constraints (6.27) impose that the traffic demands, already deployed in previous planning periods and that do not need to be rerouted, are kept in the same optical channels and (6.28) select the path of the optical channels to meet each traffic demand, ensuring the general flow conservation along the routing path for the new set of traffic demands and the ones that need to rerouted in their restoration channel (D_{res}) due to reaching the performance limit estimated by the aging model.

The optical channel capacity restrictions are set by constraints (6.29) and (6.30) guarantee that the total number of frequency slots used does not exceed the link capacity. Constraints (6.31) compute the number of shared 3R regenerators required at each network node in case a specific network link fails based on the variable $Lreg_v^e$, whereas (6.32) indicates that the total amount of backup 3R regenerators required at each network node must be above the total number of backup 3R regenerators needed in the event of any single link failure. Finally, constraints (6.33) and (6.34) compute the total number of hardware resources that have to be acquired and the total amount of spectrum utilized in the optical network, respectively. In case of ILP-9, the number of variables is defined by $|D| \times |L| + |L| + |V| \times |E| + |V| + 2$, whereas the number of constraints is given by $|D_T| \times |L_T| + \left|D_{n,res}\right| \times |V| + |L| + |E| + 2 \times |E| \times |V| + 2$.

6.3.2.3 Network Scenario, Results and Discussion

In order to gain insight into the potential benefits of adopting the proposed framework described in Fig. 6.13, it is necessary to emulate the performance degradation of the restoration channels through the progressive aging of the network elements, which is the same aging modelling utilized for the framework presented in 6.3.1. The study assumes three design scenarios: (i) the proposed framework with provisioning of EoL and CoL margins for working and restoration paths, respectively (SR-CoL); (ii) the conventional provisioning with EoL margins for both working and restoration paths (SR-EoL); and (iii) also assumes EoL margins but dedicated protection at OCh layer (the same protection scheme utilized in Chapter 4) instead of shared restoration (DP-EoL) aiming at highlighting the benefits of adopting the shared restoration scheme.

Moreover, the DP-EoL scenario assumes the use of ILP-9 with the constraints (6.31) and (6.32) being replaced by (6.35) that utilizes the parameter $Lreg_v$ already presented in the description of ILP-9. These constraints compute the total number of dedicated 3R regenerators required at each network node.

$$\sum_{l \in L_v} \theta_l = \psi_v \qquad \forall v \in V \tag{6.35}$$

The study is conducted over the 30- and 44- node transport networks covering Spain (SBN) and Italy (IBN) defined in Appendix A, using line interfaces operating at 64 Gbaud and supporting modulation formats from QPSK to 64 QAM over 75 GHz of frequency slots. The simulation assumes 10-year network lifecycle with 6 months between planning periods, 100/200/400 Gbit/s traffic demands randomly generated between 20% of the node-pairs and a 20% traffic increase per planning period, assuming the same percentage of the traffic rates at each planning period. At the end of each planning period, 10%

of the traffic is removed from the network. Moreover, this study assumes the same input scenario utilized for the proposed proactive service-provisioning framework described in 6.3.1.

The simulation results are averaged over 20 independent simulation runs. The ILP model was solved using the CPLEX solver platform [147] running on a PC with an Intel® Xeon® E5-2690 v2 3 GHz processor and 48GB of RAM. Nevertheless, on average the simulation run, for 20 planning periods, takes approximately 15 minutes for SBN topology and 45 minutes for IBN, although it depends on the traffic growth profile.

The set of results focuses on the CAPEX implications of using the three different provisioning strategies throughout the network lifetime. The obtained results are depicted in Fig. 6.14, where (a-b) show the evolution of the number of 3R regenerators deployed in the backup paths, whereas the Fig. 6.14 (c-d) plot the total number of interfaces (line interfaces at end-nodes and 3R regenerators) that have to be acquired throughout the network operation for both network topologies.

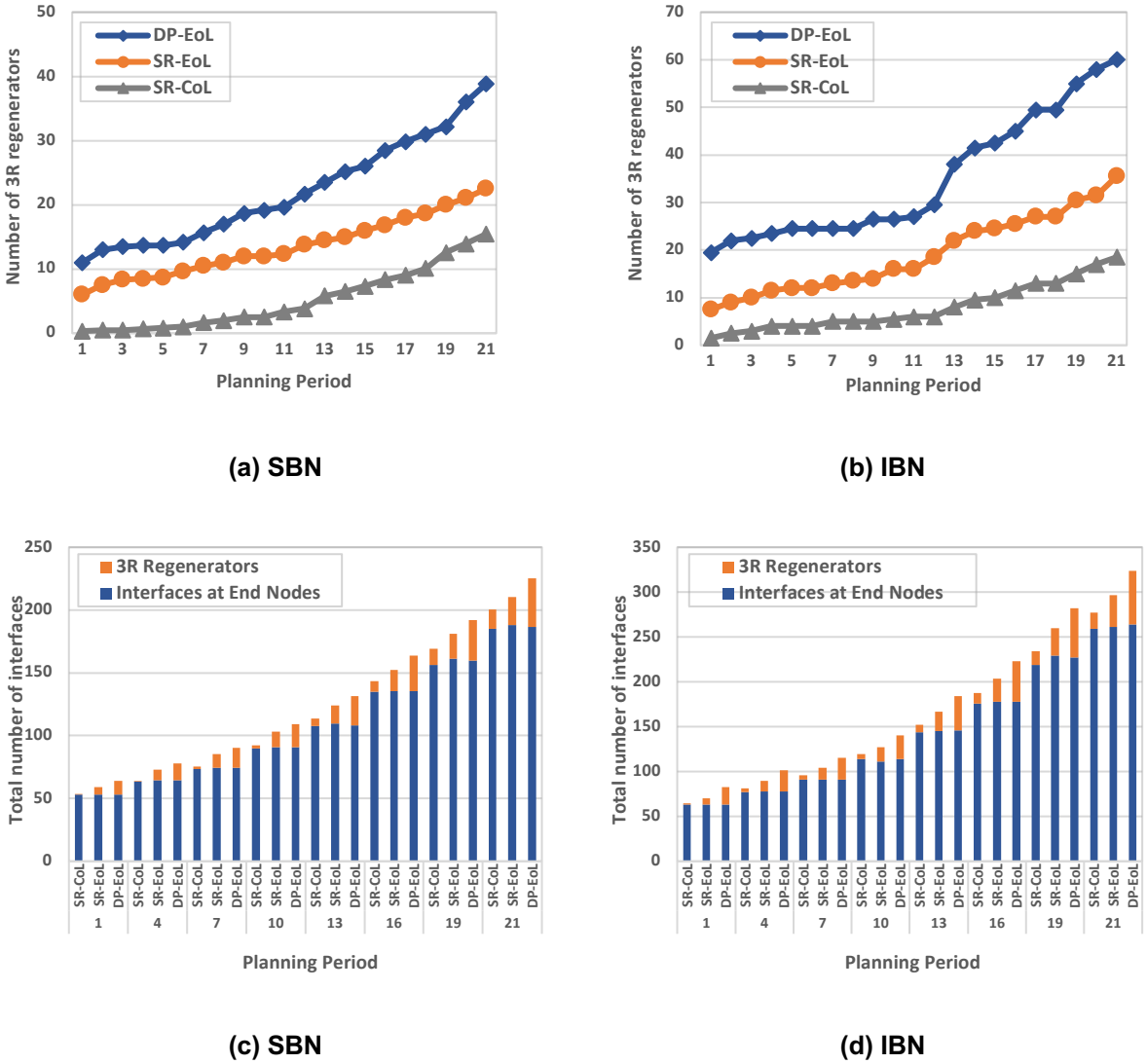

Figure 6.14 (a-b) Evolution of the number of 3R regenerators that have to be deployed for regeneration in the backup paths and (c-d) evolution of the total number of interfaces that have to be acquired throughout network operation for both network topologies.

Firstly, it can be seen that there is a clear benefit from using shared restoration instead of dedicated protection, since for the same provisioning margins (EoL) it allows to reduce the number of regenerator resources by up to 42% in both network topologies. This is due to the fact that the preplanned shared restoration allows to share the 3R regenerators between different connections, enabling to reduce the overall network costs. Secondly, using CoL instead of EoL margins in the restoration paths results in additional savings in the number of regenerators deployed of around 31% for SBN and 48% for IBN in the last planning period. The larger savings obtained with IBN, when compared to SBN, are a consequence of the fact that paths are on average longer in IBN, impacting not only the number of 3R regenerators required but also the evolution of the performance of restoration channels emulated by the aging model, which are usually a function of the path fibre length and the number of network elements traversed.

Importantly, the reported savings in both networks are attained while also reducing the total number of line interfaces required at the end-nodes to transport all traffic demands. As shown in Fig. 6.14 (c-d), the SR-CoL strategy always leads to the lowest total interfaces count. Interestingly, it can also be observed that in some cases there is a slight increase in the number of line interfaces used at the end-nodes due to the fact that the provisioning algorithm enforces a global optimization, minimizing the total number of interfaces irrespective of whether they are deployed at the paths' end-nodes or used for 3R regenerators at intermediate nodes of the backup paths. On the other hand, it can also be seen that the number of line interfaces at end-nodes is quite similar for the different design scenarios, which can be explained by the fact that all scenarios assume the use of EoL margins for the working channels and since the modulation format of the channel (composed by the working and survivability channels) is defined by the working one leads to a similar number of line interfaces utilized that is only different due to the use of a global optimization mentioned before.

6.3.2.4 Discussion of Service-Provisioning Framework Exploiting Low-Margin for Optical Shared Restoration Paths

This study proposes a service-provisioning framework that exploits the availability of real-time performance data to provision optical restoration paths with low-margins, while assuming a conservative margin stacking for working paths. Since, unlike working optical channels, which are active during the entire duration of the services they carry, restoration channels are idle most of the time, only being active for the time required to fix eventual failures. Therefore, a more aggressive reduction of performance margins can be adopted for these channels, reducing at minimum the risk of traffic disruption with respect to faster than expected performance degradation.

Simulation results over two reference transport networks highlight the benefits in terms of reducing the number of 3R regenerators required to provision the optical restoration paths while maintaining the number of line interfaces utilized at end-nodes of the channels, which enable to reduce the overall network CAPEX without increasing the risk of traffic disruption or having to support sophisticated reconfiguration mechanisms [172].

6.4 Comparison of Reduced Margins Provisioning Strategies

As described in the previous subsections, different innovative architectures and network design applications [45, 171, 172] have been proposed with the aim of provisioning channels with reduced margins, while minimizing the probability of traffic disruption due to any channel reaching the minimum acceptable quality-of-transmission. Therefore, this section overviews and compares the foreseeable network design frameworks for provisioning optical channels with reduced margins in an optical transport network, accounting for aspects such as the node architecture, the protection/restoration mechanism, and the flexibility by the network operators to schedule maintenance windows (i.e., periodical times that the network is down for maintenance). Firstly, the possible operational strategies utilized to manage the optical channels' performance and act upon approaching the performance limit are described. Secondly, a network simulation setup is introduced and utilized to compare the expected performance of the service-provisioning strategies in two reference network topologies.

6.4.1 Reduced Margins Provisioning Strategies

As explained in the previous sections, an optical transport network can only exploit the benefits of provisioning optical channels with (significantly) reduced margins, while complying with agreed service level agreements, if there is an efficient operational model to support the cases where an optical channel's performance is reaching the limit and the traffic demands being routed over them have a longer time to live. In this context, three different provisioning strategies are described and compared in this subsection.

The first provisioning strategy consists of exploiting already scheduled or dedicated maintenance windows (MW) to conduct specific sequences of actions (CoL-P MW) [45, 168], such as (1) temporarily halt the transport of traffic demands being routed over optical channels that are tagged as in critical condition; (2) tear down or reconfigure (e.g. to a lower-order modulation format) these optical channels; (3) set up new optical channels if required and (4) re-establish the affected traffic demands. This operational model is the most flexible and potentially more resource efficient one, particularly if the maintenance windows are/can be frequently scheduled. Importantly, it does not impose specific requirements on the traffic aggregation and switching node architecture, being compliant with the use of simple muxponders, as well as with the utilization of OTN switches. Nevertheless, this operational model is only viable when the SLA of the traffic demands being routed over optical channels with reduced margins allows the disruption required during the maintenance window (e.g., low-priority traffic).

The second scenario is the one proposed in Subsection 6.3.1 and assumes that OTN switching is present in the network nodes (CoL-P OS). Originally, this feature allows not only to optimize the fill ratio of optical channels but also to remotely request that a given traffic demand is rerouted from one optical channel to another in dozens or hundreds of milliseconds without traffic disruption, which is exploited to support advanced shared restoration schemes [99]. This operational model utilizes the capability provided by the OTN switches to reroute traffic demands from an optical channel reaching a critical condition to alternative ones. This has the advantage that any such event causes a hitless rerouting of

traffic, unlike the previous model. However, a key limitation of this model is that it can only be used in optical networks where the nodes are equipped with OTN switches. Furthermore, accomplishing an almost hitless rerouting requires that both the current and the next optical channel are active during a brief period of time, which may result in a slight increase in the total number of line interfaces required [171].

The previous two planning frameworks assume that provisioning with reduced margins is applicable to any optical channel type (e.g., working, protection, restoration). The third strategy exploits the nature of shared restoration optical channels to provision them with smaller margins, which remain idle, i.e., not carrying traffic, in the absence of failures (CoL-P SR), as described in Subsection 6.3.2. This property is advantageous due to the combination of two factors. Firstly, it exploits the fact that the restoration paths are usually active only during the time strictly necessary to fix the source of failures and, consequently, margins such as the ones used to account for devices or fibre plant aging are not required. Secondly, because the network is expected to operate without failures almost all the time, there is a negligible risk that the restoration optical channel would be reaching the performance limit at the same time that a failure in the network would trigger the need to divert traffic to it [172]. The main drawback of this operational model is that it only applies the reduced margins to a fraction of the optical channels (protection/restoration channels) being set up in the network.

The different planning frameworks described above have different advantages and limitations. Thus, Table 6.3 presents their main characteristics in order to facilitate a comparison of the network and traffic scenarios where each one is more suitable. When the network nodes are equipped with OTN switches, the operational model based on reconfiguration via OTN switch (CoL-P OS) is likely the most efficient one, since the reduced-margin provisioning can be applied for all types of optical channels while being quasi-hitless. On the other hand, if OTN switches are not present and muxponder-based aggregation is used instead, but maintenance windows can be scheduled by the network operators without violating the SLAs agreed upon, the planning framework based on reconfiguration during a maintenance window

Table 6.3 Main characteristics of the reduced margins service-provisioning strategies

Provisioning Strategy	**CoL-P MW**	**CoL-P OS**	**CoL-P SR**
Network Requirements	Any network architecture	With OTN switching	Any network architecture
Traffic Impact	Traffic affecting	Quasi-hitless	Hitless
Reduced Margin Channel Types	All channels	All channels	Restoration channels

(CoL-P MW) should be preferred, since it also applies reduced-margin provisioning to all types of optical channels. Finally, in case strict SLAs do not allow scheduling a maintenance window and restoration can be used as a mechanism to survive failures, the natural operational model to use is the one that restricts reduced-margin provisioning to restoration optical channels.

The support of the described service-provisioning frameworks must be considered at the planning stage, in order to capture their specific aspects and efficiently exploit the reduction in margins. Figure 6.15 provides a high-level view of the main steps of a multi-period planning workflow that can be used to enforce provisioning with reduced margins in a transport network. At the core of this workflow is the utilization of ILP models that are executed at each planning period to simultaneously determine (1) the allocation of the new traffic demands and the traffic demands that must be rerouted to other optical channels and (2) the new optical channels that have to be set up with the main objective to minimize the number of new line interfaces that need to be installed. Further details on the ILP models for CoL-P OS and SR can be found in Subsections 6.3.1 and 6.3.2, respectively. On the other hand, the CoL-P MW assumes the use of the ILP-7 defined for CoL-P OS (Subsection 6.3.1.3) without the constraints that ensure a non-disruptive reconfiguration of the traffic via the OTN switches, i.e., the constraints (6.6-6.16) of ILP-7.

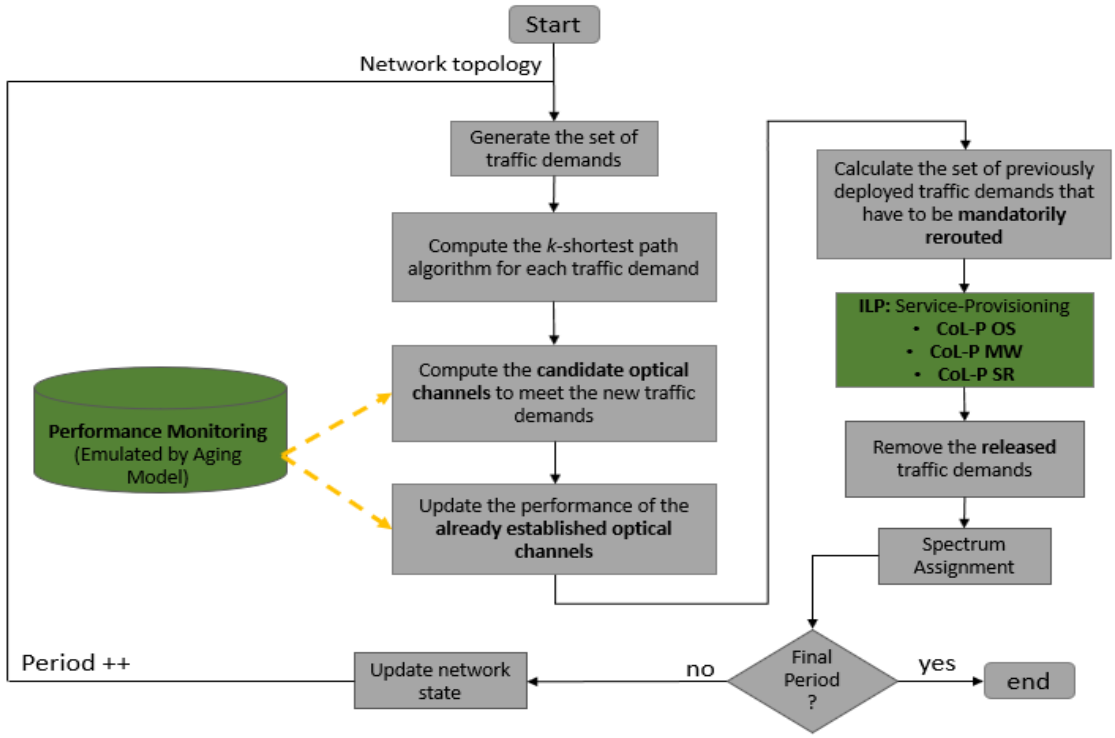

Figure 6.15 Multi-period planning workflow for provisioning with reduced margins.

Noteworthy, in the case of the CoL-P OS service-provisioning framework presented in Subsection 6.3.1.3, the ILP model embeds additional constraints (6.6-6.16) to ensure that traffic demands are rerouted between two active optical channels. Moreover, in the CoL-P SR operational model described in Subsection 6.3.2.2, it is assumed that EoL margins are enforced for the working optical channels (i.e., they are not expected to be torn down due to long-term performance degradation) and that shared 3R

regenerators can be used at intermediate nodes to guarantee that restoration optical channels provide the same capacity as the working optical channels they are associated with. Hence, in this model the objective function (6.26) needs to account for both the end-nodes line interfaces and shared 3R regenerators to be deployed. Lastly, the CoL-P MW is similar to the CoL-P OS but it assumes the use of a maintenance window to reroute the traffic carried over channels running out of margin instead of the utilization of OTN switching technology and therefore the constraints that ensure a hitless reconfiguration of the traffic via the OTN switches are not required (the constraints 6.6-6.16 of the ILP-7 presented in Subsection 6.3.1.3).

6.4.2 Simulation Results and Discussion

The effectiveness of three network planning frameworks for optical channels provisioning with reduced margins is compared in two reference topologies (SBN and IBN). The same network topologies that have been utilized in the simulation results of this chapter (Subsections 6.3.1.4 and 6.3.2.3), representative of large regional networks. In both networks, the 4.8 THz of the C-band are exploited. Moreover, the ROADM nodes are assumed to have CDC properties described in 2.1.3.3 [186]. Line interfaces operating at a symbol rate of 64 Gbaud and supporting modulation formats from QPSK up to 64 QAM are considered, where each optical channel is assumed to be assigned over a 75 GHz frequency slot. The performance degradation of the optical channels is emulated by the progressive impact of the aging in the network elements, the same utilized for the frameworks presented in 6.3.

The simulation considers a 10-year lifespan of the network, with six months between planning periods. Traffic demands of 100, 200 and 400 Gbit/s are assumed and randomly generated between 13% of the node-pairs of each network. Moreover, a 20% increase of traffic between consecutive periods is considered to mimic traffic growth, assuming the same percentage of the traffic rates at each period. At the end of each planning period, 10% of the traffic is removed from the network. Traffic demands are routed over one of the available routing possibilities along the three shortest routing paths.

The simulation of routing new traffic demands and setting up new optical channels, as well as continuously managing the optical channels' performance and triggering reconfiguration actions as a result of an optical channel reaching a critical condition, is performed using the three service-provisioning strategies presented in Subsection 6.4.1. The provisioning of optical channels with EoL margins is utilized for the different network planning approaches to set a baseline against which the percentage of line interfaces savings with CoL can be computed. In this context, Figure 6.16 shows the cumulative savings in number of line interfaces as a function of the planning period when using optical channels' provisioning with reduced margins (CoL) instead of provisioning with EoL margins for the different service-provisioning strategies. Results are shown for both the SBN and the IBN topologies.

The first observation is that all three network planning frameworks enable to reduce the number of line interfaces required to satisfy all traffic demands. Secondly, as expected, the extent of interface savings depends on the operational model adopted. The CoL-P SR operational model grants the smallest savings, which range between 6 and 11% in SBN and between 6 and 12% in IBN, depending

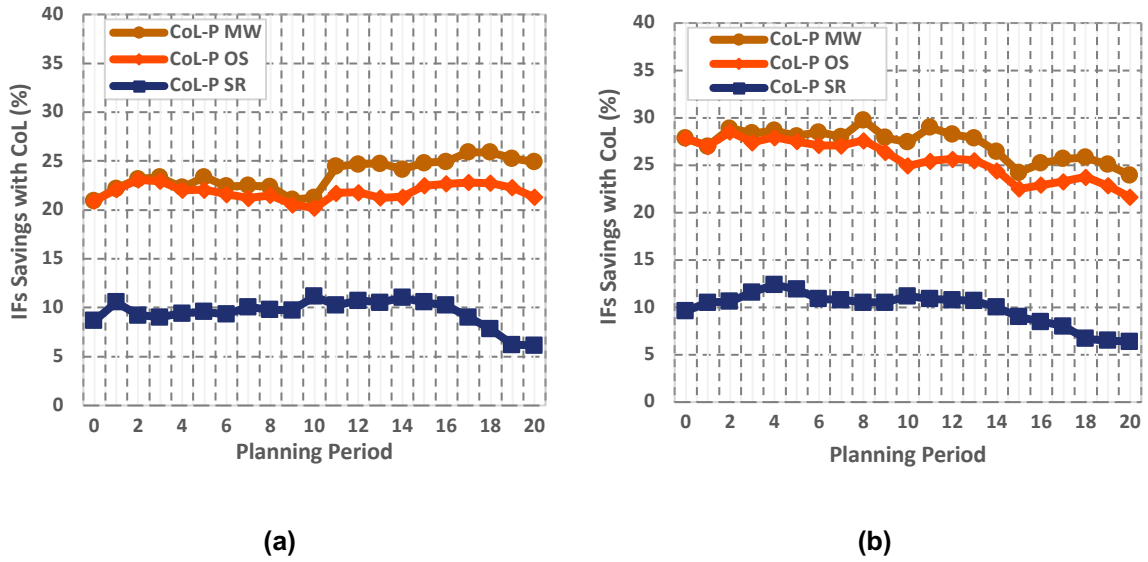

Figure 6.16 Line interface savings with respect to conventional EoL planning for both (a) SBN and (b) IBN network topologies.

on the planning period. This is due to the fact that the CoL-P SR model only exploits the reduced margins to save 3R regenerators in the restoration channels. Conversely, the CoL-P MW and OS approaches more than double these savings by applying reduced-margin provisioning for all optical channels. The CoL-P MW operational model maximizes the line interface savings, which range between 21 and 26% in SBN and between 24 and 30% in IBN. The CoL-P OS operational model provides only slighter smaller savings than CoL-P MW, with between 21 and 23% in SBN and between 22 and 28% in IBN, due to imposing additional constraints when switching traffic demands between optical channels in order to guarantee a quasi-hitless operation. Thirdly, when comparing the savings obtained in both network topologies, these are shown to be marginally larger in IBN than in SBN. The reason for this is the fact that, on average, optical channels are longer in IBN, both in terms of length and number of traversed filters and amplifiers. As a result, the optical channels set up in IBN are, on average, more impacted by performance degradation due to aging effects. Therefore, there is a larger scope in this network topology to capitalize the benefits of adopting a reduced-margin provisioning strategy.

With the aim to quantify the possible impact in terms of traffic interruption and risk of violating SLAs, Table 6.4 shows the percentage of traffic disrupted when using the CoL-P MW model and the number of mandatorily rerouting events, as a consequence of a channel reaching the performance limit, when using the CoL-P OS and SR scenarios during the network lifecycle. Note that, this mandatorily rerouting events do not translate into traffic disruption since both models ensure reconfiguration mechanisms capable of avoiding the traffic interruption. The results highlight that the CoL-P SR operational model is the least disruptive one, since there is a smaller number of rerouting events and these are traffic hitless (i.e., only impact the restoration optical channels). Moreover, it is also evident that the CoL-P OS operational model relies on enforcing more mandatorily rerouting events that can also be materialized into larger line interface savings. On the other hand, it is also necessary to highlight that the CoL-P OS is the slowest strategy in terms of computational time due to the use of challenging constraints to ensure that the traffic demands are rerouted without disruption.

In summary, this section overviews and compares the effectiveness of three main network planning strategies to support reduced-margin provisioning in two reference transport networks. The simulation results highlight that savings in the number of line interfaces are possible with all three service-provisioning scenarios. Importantly, the results also provide evidence that these models feature different trade-offs between the extent of line interface savings and the amount of traffic affected/rerouted as a result of optical channels' performance becoming close to the limit [173, 174].

Table 6.4 Total traffic interrupted and number of rerouting events

Provisioning Strategy	SBN		IBN	
	Percentage of traffic disrupted (%)	Number of Rerouting Events	Percentage of traffic disrupted (%)	Number of Rerouting Events
CoL-P MW	20.1	0	34.1	0
CoL-P OS	0	82.8	0	155.3
CoL-P SR	0	27.5	0	51.7

6.5 Chapter Summary

Recent trends in optical transport networks emphasize the need of adopting a self-driving network in order to operate autonomously and adaptatively to the actual network environment. In this context, advances in real-time telemetry platforms allow to continuously monitor the current performance of an optical channel, which can avoid the traditional provisioning with end-of-life margins that is characterized by imposing large enough margins to account for worst-case performance degradation profiles (e.g., due to aging) during all network operation. Reducing these margins when provisioning an optical channel, can enable to operate it at higher capacity, thereby decreasing capital expenditures. However, effectively adopting a more aggressive provisioning strategy requires a sophisticated service-provisioning framework that can properly address the fact that optical channels provisioned with reduced margins can have a time-to-live shorter than of some of the traffic demands they carry, resulting in traffic disruption.

Hence, this chapter has presented different network planning strategies to exploit reduced-margin provisioning in optical transport networks with the aim of operating them more cost-effectively. The first operational model proposed exploits the use of OTN switching technology in order to proactively divert the traffic from optical channels that are approaching the performance limit, enabling to manage how both existing and new traffic are rerouted/routed with the objective of optimizing the number of network resources that have to be acquired while guaranteeing a minimum risk of traffic disruption. On the other hand, the second approach restricts the utilization of reduced margins to shared restoration paths, assuming a more conservative margin stacking for working paths. This framework exploits the fact that

restoration paths are idle most of the time, only being active for the time required to fix eventual failures, which allows to reduce the performance margins for those channels without impacting the running traffic.

Finally, the work developed in this chapter also overviews and compares the foreseeable service-provisioning frameworks that have been proposed in the context of networks operating with reduced margins. The comparative analysis reveals the benefits and drawbacks of each strategy in terms of CAPEX savings and the amount of traffic affected/rerouted as a result of the performance of optical channels becoming close to the limit.

Chapter 7: Conclusions and Future Work

This chapter overviews the main topics and challenges addressed throughout this work with the aim of cost- and spectral-effectively designing the next-generation of core transport networks. Specifically, it will highlight the different network dimensioning methods proposed and the main contributions achieved to the progress of knowledge in the respective field of study, focusing on how the optical transport network can scale to provide higher capacity while reducing the cost per bit transported.

The final part of this Thesis (Subsection 7.2) provides a critical assessment of the work developed throughout this Thesis, identifying potential research avenues for the future based on either unexplored or only briefly explored subjects and analysing alternatives to the network design frameworks that have been proposed in this Thesis. These aspects can help forthcoming research efforts in the context of capacity planning optimization.

7.1 Conclusions

The stated objective of this Thesis resided in the definition of tools for designing and optimizing optical transport networks, while simultaneously provide the means to operate these networks closer to optimality in terms of capital expenditures and spectral efficiency. In this context, different frameworks were proposed, through Integer Linear Programming models and/or heuristic algorithm, that were responsible for providing a routing, grooming and resource allocation solution to transport all the traffic in the predefined optical transport architecture according to the different goals of optimization.

In detail, it investigated the impact of developing a network planning framework that aims at minimizing both transmission and switching capital expenditures exploiting the evolution of the optical switching architectures (Chapter 3), the exploitation of the full potential of a flexible DWDM grid and the next-generation of optical line interfaces, which enable the utilization of higher order modulation formats and symbol-rates (Chapter 4). Furthermore, it also addressed future-looking and disruptive scenarios, such as the utilization of more spectral bands of the single-mode optical fibre and/or parallel single-mode fibres to transport more capacity (Chapter 5) and the adoption of a self-driving optical transport network in order to operate it autonomously and adaptively to the actual network environment (Chapter 6).

Firstly, Chapter 2 overviews the main concepts that have been defined in the literature to design an optical transport network, ranging from architectural and technological subjects to future optical trends. By the fact that designing an optical transport network involves different types of problems and concepts (e.g., transport, routing, multiplexing, management and survivability of optical channels carrying traffic), the main goal of this chapter was to clearly clarify the different concepts involved before analysing the optimization procedures proposed in this Thesis.

The motivation of Chapter 3 was to develop a network planning framework that minimizes the network resources utilized in the transmission and switching components that are presented when considering the incorporation of an OTN (electrical) switch within the network nodes. This planning and dimensioning process encompasses two key resources that can affect the overall network costs, line interfaces used to carry the traffic and OTN switches, which number needs to be minimized. In this

context, the deployment of OTN switching technology may enable savings on the amount of transmission resources required to accommodate the traffic (line interfaces). However, deploying this flexible architecture entails an additional network cost, leading to conflicting minimization problem (the minimization of transmission CAPEX versus switching CAPEX).

In order to exploit different solutions with diverse trade-offs, a multi-objective genetic optimization framework modelling these possibly conflicting goals was proposed in the context of Chapter 3, more precisely a modified implementation of the NSGA-II. The proposed modified variant of this algorithm embedded in the mutation and crossover operations prior knowledge about the multi-objective problem defined in this study with the aim of increasing the convergence rate. In detail, the knowledge was focused towards the production of solutions more biased towards the minimization of one of the objectives: the number of line interfaces that have to be acquired. Noteworthy, this objective can take a wider range of values when compared to the number of OTN switches, which is upper bounded by the number of network nodes.

This novel sophisticated process contributed to generate new solutions which, to a given extent, prevented the algorithm from generating too many solutions that are far from optimality as for the number of line interfaces, leading to better convergence results when compared to the purely random genetic algorithm. Another important aspect of the proposed framework was the ability to provide planning insights regarding the range of potentially interesting trade-offs solutions between the number of line interfaces and OTN switches, in which the most appropriate result can be chosen according to the optimization scenario.

On the other hand, Chapter 4 exploits the use of OTN switching technology addressed in the previous chapter to properly leverage the advantages provided by the next-generation of coherent line interfaces. Particularly, this chapter considers one possibility to augment capacity in transport network, which relies on the deployment of consecutive generations of optical line interfaces to provide both higher capacity and higher spectral efficiency. The next-generation of line interfaces that are under development will be equipped with advanced technologies that allow to operate with higher order modulation formats and high-symbol rates. This deployment inevitably changes the design of an optical transport network, since the fixed DWDM grid used up to recently must be replaced by a flexible grid. Moreover, the expected co-existence of optical channels (current- and next-generation of line interfaces) that operate at different symbol-rates can lead to operational challenges, most notably in terms of managing the mismatch of frequency slots sizes in order to minimize the risk of spectrum fragmentation.

In order to mitigate the aforementioned limitations and still take advantage of the benefits provided by using high symbol rate line interfaces, a network design framework was proposed to be applied during the entire lifecycle of the transport network, considering the different types of line interfaces deployed and aiming at minimizing the CAPEX and optimizing the long-term usage of spectrum resources. Importantly, it comprised a novel customized virtual grid and a strategy to manage the spectrum resources from the beginning of the network operation with the aim of reducing complexity and proactively mitigating the spectrum fragmentation. This framework relied on a two-stage optimization procedure based on ILP models, where the first phase is responsible for minimizing the

hardware cost while the second model exploits the OTN switching technology to perform the hitless re-grooming process that allows to maintain the optical channel fill ratio at higher levels and release line interfaces that can be reused in the next planning periods.

The proposed optimization method considered a realistic temporal planning scenario where in the first planning periods of network operation only the current-generation of line interfaces are deployed, whereas at a latter period when the next-generation of line interfaces become readily available, the network operator only acquires these types of interfaces. The combined utilization of a virtual grid and hitless traffic re-grooming was essential to meet the long-term expectation of the network operator by sustaining more traffic load than the other spectrum management strategies with the same fibre infrastructure without having to incur into additional spending in terms of line interfaces and in some cases even enabling to slightly reduce this number. The ILP models were also extended to address survivability in the network operation through the support of 1+1 dedicated protection schemes at either the ODU and OCh layers, ensuring every service provisioned can survive any single link failure. The effectiveness of the proposed framework remained even when using more challenges network dimensioning scenarios.

As described before, the increase of capacity in optical networks was the central topic of this Thesis that started by exploring different switching architectures (Chapter 3) and consecutive generations of line interfaces (Chapter 4). However, fundamental physical limits dictate that only minor spectral efficiency improvements are to be expected in future when operating in the usual C-band of the single-mode optical fibres. Therefore, Chapter 5 focused on providing alternative strategies to increase capacity in OTN via exploiting the use of more spectrum and detailing their implications regarding the capacity planning algorithms.

Moreover, the recent optical developments and commercial solutions that will be available in the short- to medium-term indicate that the utilization of multi-band and multi-fibre transmission systems are the strategies to be taken into account to increase capacity in optical networks. In this context, the first part of Chapter 5 detailed the effectiveness of the deployment of a multi-band DWDM transmission system in postponing the acquisition of new fibres between two network nodes. Thus, a comparative study with C+L-bands was conducted with different optical line interfaces technologies aiming at determining the most effective design strategy when deploying a multi-band scenario, which revealed to be the next-generation of line interfaces. The benefits of adopting this strategy were analysed in terms of both number of line interfaces and fibres deployed to meet the traffic requirements, following the same conclusions provided in Chapter 4.

The final part of Chapter 5 proposed a robust network planning framework that addresses the different effects that impact the total cost of ownership in a C+L-band and multi-fibre transmission system. In detail, the solution provided by the proposed algorithm can be achieved by optimally selecting in which links it will be useful to add extra fibres based on geographically-depend specific costs and on fine-tuning the outcome, so that a minimum number of L-band systems has to be deployed in both existing and new fibres in order to avoid amplifiers costs in L-band. Importantly, this scenario also assumed a realistic planning approach where the expenditures associated with the use additional fibres

can vary significantly within the same network (geographically-dependent), for instance due to lease of fibres in some regions, licensing processes and/or shortage of dark fibres in specific ducts.

In order to balance these costs, the proposed network-planning framework was customizable in terms of giving preference to use additional fibres versus line interfaces through an ILP model that obtains a routing, grooming and fibre assignment solution combined with a heuristic algorithm that assigns spectrum to the optical channels used, so that the deployment of L-band systems is minimized. Simulation results highlighted the savings that can be realized by optimizing the usage of L-band and carefully selecting the fibre links to be upgraded. This analysis also provided a global understanding that the usual approach of focusing primarily on minimizing line interface count is ill-suited for future transport network scenarios where more optimization goals needed to be taken into account within the network design framework.

Finally, Chapter 6 expanded the concept of autonomous network in order to transform margins into capacity in optical transport networks (i.e., trading off margins for capacity in the sense that by reducing the margins one can use modulation format schemes with higher spectral efficiency) based on the incorporation of new building blocks within the design process, such as real-time performance monitoring and trend analysis platforms that can be properly managed by an advanced control plane architecture. In this context, real-time telemetry platforms allow to continuously monitor the current performance of an optical channel that allows to avoid the traditional provisioning with end-of-life margins, which is characterized by imposing large margins to account for worst-case performance degradation profiles (e.g., due to aging) during network operation. Reducing these margins when provisioning an optical channel, can enable to operate it at higher capacity (e.g., using a higher order modulation format), thereby decreasing the capital expenditures. However, effectively adopting a more aggressive provisioning strategy requires a sophisticated network design framework to address the higher probability of traffic having a longer time to live than that of the optical channel carrying them, leading to traffic disruption.

Hence, the aim of this chapter was to develop different frameworks to provision services with reduced margins while minimizing the utilization of optical channels reaching the performance limit, preventing traffic disruption. The first routing and architectural design proposed aimed to increase capacity per provisioned optical channel through the use of smaller margins and to efficiently and timely reroute traffic demands carried over channels approaching the performance limit. The rerouting of traffic was ensured through the use of OTN switches in addition to ROADM within the network nodes, enabling to shift traffic between optical channels with minimum disruption. The novel multi-period planning framework included an ILP model that manages how both existing and new traffic demands are rerouted/routed with the objective of optimizing the number of network resources that have to be acquired while guaranteeing a minimum risk of traffic disruption. The simulation results analysis showed that the use of the proposed framework to provision services enables to reduce the overall network cost with savings in the number of line interfaces while triggering fewer rerouting events due to optical channels being torn-down as a result of insufficient quality-of-transmission. Importantly, the results also highlighted that adopting the network design proposal enables to operate the transport network in a safer region concerning the

optical channels' performance while still retaining the benefits from squeezing margins to increase the total capacity and reduce the network costs.

The second framework proposed in the context of reduced-margins provisioning strategies restricted the utilization of smaller margins to shared restoration paths, assuming a more conservative margin stacking for working paths. It exploited the fact that restoration paths are usually active only during the time strictly necessary to fix the source of failures and, consequently, margins such as the ones used to account for device or fibre plant aging are not required. On the other hand, the fact that the network is expected to operate without failures almost all the time, there is a negligible risk that the restoration optical channel would be reaching the performance limit at the same time that a failure in the network would trigger the need to divert traffic to it. Therefore, this approach avoided the need of adopting a more complex network architecture and management/control system that are prepared to proactively handle a rapid deterioration of performance and still obtained a significant reduction in the number of network resources deployed to ensure network survivability.

The final part of Chapter 6 presented a comparative analysis of the different network planning frameworks proposed by the author of this Thesis and by other authors in literature to efficiently exploit low margin provisioning in optical transport networks, revealing the benefits and drawbacks of each strategy in terms of node architecture, network resilience and flexibility to schedule maintenance windows. Hence, a network simulation setup was introduced to compare the expected performance of these strategies concerning key metrics such as the extent of hardware savings and the total traffic interrupted or number of rerouting events.

7.2 Future Work

From the work developed throughout this Thesis, there are some topics that can be further investigated in the different chapters, which can have potential for future developments. The study conducted in Chapter 3 was based on the use of current state-of-life line interfaces but with the recent deployment of the next-generation of line interfaces. It is important to analyse the difference in the simulation results of the multi-objective genetic framework when addressing this line interfaces evolution. On the other hand, the survivability of network was also not taken into account in this study due to the fact that it will not have a direct impact on the minimizing of conflicting objectives, i.e., number of line interfaces and OTN switches. However, the resilience of the optical network is essential since a single channel failure can cause a substantial impact in network operation and therefore this framework should also be adapted to model this subject. In this case, the multi-objective framework should consider the increase of the genome size by comprising both working and protection paths for each traffic demand.

As for Chapter 4, the key novelty of the proposed study resides in the definition of a strategy to manage the spectrum resources from the beginning of network operation with the aim of reducing the hardware costs, complexity and proactively mitigating the spectrum fragmentation related to provision services using higher symbol rate line interfaces. In turn, this proposal also requires the introduction of OTN switches to improve optical channel fill ratio and adopt a more aggressive provisioning strategies

by relying on its electrical switching capabilities to reroute traffic. These capabilities may enable savings in the number of line interfaces required and the amount of spectrum utilized, eventually offsetting the cost of the OTN switches. However, this expenditure should be properly addressed within the network optimization process, even though the accurately characterization of the OTN switch's cost might not be an easy job as it is kept as company confidential material. Even so, it could be a subject analysed in the future.

In the context of Chapter 5, the first topic that needs to be clarified consists in the global optimization goal when deploying the multi-band and multi-fibre transmission system, since it involves different components that increase the total cost of ownership, such as the number of line interfaces, fibre-pairs and amplifiers that have to be deployed in the network to meet the high-capacity traffic. In this Thesis, a customized ILP model was proposed using additional fibres versus line interfaces complemented by a heuristic algorithm that minimizes the number of L-band subsystems required. Nevertheless, even with the inherent difficulty of considering the minimization of network costs as the whole goal of the network planning, when possible, it should be the adopted strategy in order to obtain an optimum solution. Furthermore, the future transport networks will inevitably change the resource allocation in order to account for both the spectral domain (e.g., optical channel formats with different sizes) and the spatial domain (e.g., multiple fibres/cores), as well as possible restrictions introduced by specific ROADM architectures deployed and physical impairments arising in those particular scenarios. As a result, the larger number of dimensions to be considered and the associated architecture and optical performance constraints will demand more complex routing and resource (spectrum, fibre, core) assignment algorithms. Thus, it is paramount to adapt the network design framework to address this challenging environment.

Finally, the proposed proactive service-provisioning framework with smaller margins presented in Chapter 6 assumed the definition of a performance threshold that was considered to be static throughout the entire network operation. However, the results can be optimized if the thresholds that define the rerouting policy of the optical channels are dynamically adapted according to the network topology, current optical channel performance and its forecasted evolution.

Appendixes

Appendix A. Optical Performance Model

The Gaussian noise (GN) approach is utilized in this Thesis for calculating the performance of a given optical channel based on the estimation of the impact of nonlinear interference (NLI) originated in the optical fibre transmission [29]. The GN model assumes a fully loaded system, i.e., considers the impact of potentially having all channels present in every fibre span, thereby giving a conservative estimation of the impact of nonlinear impairments. In this context, the performance of each optical channel, measured in residual margin, is estimated using the following formulas:

$$\frac{1}{OSNR_{tot}} = \frac{1}{OSNR_{add}} + \sum_{i_{span}=1}^{N_{spans}} \frac{1}{OSNR(i_{span})} + \frac{N_{ROADM} - 1}{OSNR_{int}} + \frac{1}{OSNR_{drop}} \quad \text{(A.1)}$$

The first formula (A.1) calculates the equivalent $OSNR$ of an optical channel at the end of the path ($OSNR_{tot}$), where $OSNR_{add}$, $OSNR_{int}$ and $OSNR_{drop}$ represent the $OSNR$ at the add, intermediate and drop ROADMs along the path, respectively, in linear units, N_{spans} is the number of fibre spans, N_{ROADM} is the total number of ROADMs traversed and $OSNR(i_{span})$ is the $OSNR$ after transmission along the fibre span i_{span}.

The $OSNR(i_{span})$ can be calculated by the Equation (A.2), where $P_{RX}(i_{span})$ and $P_{ASE}(i_{span})$ are the average optical signal and amplified spontaneous emission noise power levels in fibre span i_{span}, respectively. The $P_{NLI}(i_{span})$ is the NLI contribution to noise in fibre span i_{span}. All details of the computation of the noise level of the NLI for each fibre span i_{span} is presented in [29, 75]. Moreover, the calculation of the $P_{ASE}(i_{span})$ is given by the Equation (A.3), which depends on the noise figure of the amplifier at the end of each fibre span (NF), the amplifier gain represented by the span loss since this loss is compensated by the amplifier at the end of the span (S_{loss}), the reference optical bandwidth (B_{ref}) which is assumed to be equal to 0.1 nm , the Planck's constant (h) and the optical channel's frequency (f). The calculation of the span loss is presented in formula (A.4), where the S_{length} represents the span length and α_{atte} is the fibre attenuation coefficient, measured in dB/km whose values are presented in Table 5.1. Furthermore, the span loss also depends on the traversed number of connectors ($N_{connectors}$) and splices ($N_{splices}$) and their associated $Connector_{loss}$ and $Splice_{loss}$ values that are measured in dB. Note that, the splices are permanent joints between two optical fibres which could be degraded over the time, whereas the connectors allow the two fibres to be disconnected at the joint. In this context, it is considered an additional loss of 1 dB at the input and output of the optical fibres, as well as an extra attenuation of 0.01 dB/km due to splice losses proposed in [29] in order to achieve a more realistic modelling of the optical fibre plant.

$$OSNR(i_{span}) = \frac{P_{RX}(i_{span})}{P_{ASE}(i_{span}) + P_{NLI}(i_{span})} \quad \text{(A.2)}$$

$$\mathrm{P_{ASE}}(i_{span}) = NF \cdot 10^{\frac{S_{loss}(i_{span})}{10}} \cdot B_{ref} \cdot hf \quad \text{(A.3)}$$

$$S_{loss}(i_{span}) = S_{length}\alpha_{atte} + Splice_{loss}N_{splices} + Connector_{loss}N_{connectors}\ (dB) \quad \text{(A.4)}$$

Given the aforementioned formulas, the feasibility of an optical channel with format *fm*, shown in Equation (A.5), can be assessed by comparing the estimated equivalent OSNR (calculated by Equation (A.1)) with the required OSNR in back-to-back operation defined in the Table 2 of the study presented in [29], $OSNR_{B2B}$. A system margin, SM_{fm}, is also set to guarantee the correct system operation for the network lifecycle considering the impact of effects, such as aging, power ripple along the transmission bandwidth, polarization-dependent losses and power transients caused by channel add/drop, which are not considered by the GN model. To keep the performance evaluation complexity reduced, the system margin is defined as a function that depends on the number of network elements that the optical channels traversed (N_{OLAs} and N_{ROADMs}), as shown in Equation (A.6), where N_{OLAs} and N_{ROADMs} are the number of optical line amplifiers and ROADMs, respectively. Moreover, this equation also considers a filtering power penalty, $P_{filt,fm}$, due to the cascade of WSSs traversed by the optical signal using format *fm.* The impact of optical filtering considers the spectral modelling of WSSs described in [187] and estimates the resulting OSNR based on the values shown in [188], but with the symbol rate scaled to the values considered in the work of this Thesis. A minimum system margin of 2 dB is enforced to set the safety margins (design, system and transmission) defined in Fig. 2.7 in order to guarantee that the channel is feasible up to the end of the network operation. Therefore, the feasibility of a channel is essentially measured through the value of residual margin defined in Equation (A.5), if the residual margin is superior to zero then the channel is feasible otherwise it is unfeasible.

$$Residual\ Margin = OSNR_{tot} - (OSNR_{B2B} + SM_{fm})\ \text{(dB)} \quad \text{(A.5)}$$

$$SM_{fm} = 2 + 0.05 \times (N_{OLAs} + N_{ROADMs}) + P_{filt,fm}\ \text{(dB)}. \quad \text{(A.6)}$$

Appendix B. Network Topologies

This appendix shows the physical layouts of the network topologies used throughout this work. These include the following networks: Deutsch Telecom (DT) (Fig. B.1), Advanced Research Projects Agency Network (ARPANET) (Fig. B.2), Spanish Backbone Network (SBN) (Fig. B.3), Italian Backbone Network (IBN) (Fig. B.4). The main attributes of each topology are summarized in Table B.1.

Figure B.1 DT topology.

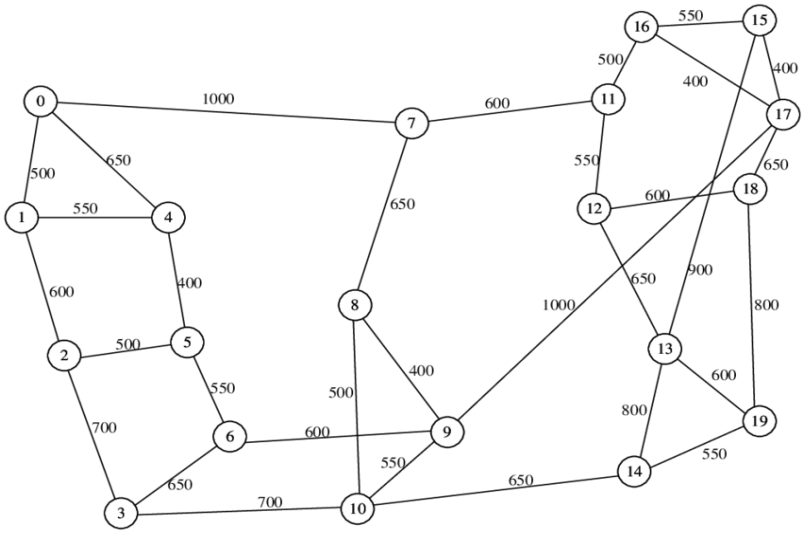

Figure B.2 ARPANET topology (link distances in km).

Figure B.3 SBN topology.

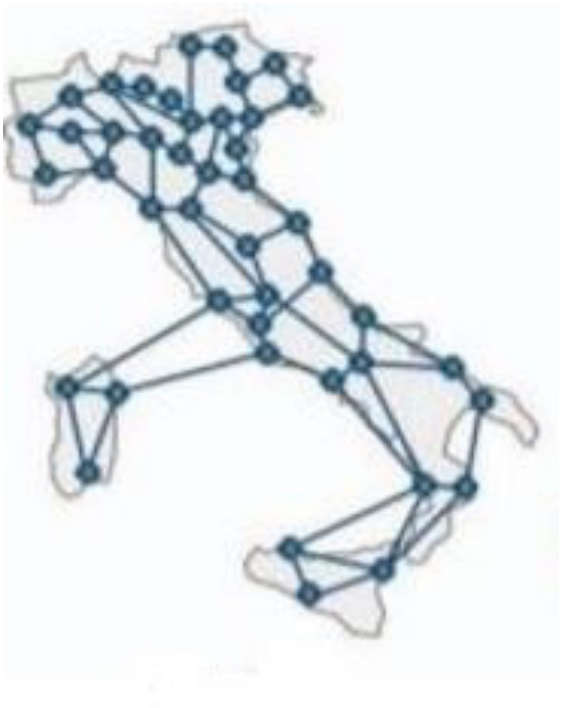

Figure B.4 IBN topology.

Table B.1 Topological characteristics of the reference networks.

Network Topology	Nodes	Links	Av. Nodal Degree	Av. Link Length (km)
DT	12	20	3.3	243
ARPANET	20	32	3.2	839.14
SBN	30	56	3.7	148
IBN	44	71	3.2	174

References

[1] N. Ghani, "Regional-metro optical networks," *Emerging optical network technologies,* pp. 75-108, 2005.

[2] B. Mikkelsen, "Challenges and key technologies for coherent metro 100G transceivers," Accacia, November 2012. [Online]. Available: https://www.lightwaveonline.com/optical-tech/transmission/article/16648259/challenges-and-key-technologies-for-coherent-metro-100g-transceivers.

[3] D. Kirk, "Transport networks shift from SDH to OTN," 2011. [Online]. Available: https://www.electronicdesign.com/technologies/communications/article/21759500/transport-networks-shift-from-sdh-to-otn.

[4] ITU-T Recommendation, "G.872 Architecture of optical transport networks," 2017. [Online]. Available: https://www.itu.int/rec/T-REC-G.872-201701-S/en.

[5] ITU-T Recommendation, "G.709 Interfaces for the optical transport network," June 2016. [Online]. Available: https://www.itu.int/rec/T-REC-G.709-201606-S/en.

[6] E. Desurvire, Erbium-doped fiber amplifiers: principles and applications, Willey, 1994.

[7] M. Taylor, "Coherent detection for optical communications using digital signal processing," in *Optical Fiber Communication Conference (OFC)*, Anaheim, CA, USA, 2007.

[8] T. Mizuochi, K. Kubo, H. Yoshida, H. Fujita, H. Tagami, M. Akita and K. Motoshima, "Next generation FEC for optical transmission systems," in *Optical Fiber Communication Conference (OFC)*, Atlanta, USA, 2003.

[9] K. Ho, "Exact evaluation of the capacity for intensity-modulated direct-detection channels with optical amplifier noises," *IEEE Photonics Technology,* vol. 17, pp. 858-860, 2005.

[10] E. Lp, A. Lau, D. Barros and J. Kahn, "Coherent detection in optical fiber systems," *Optics Express,* vol. 16, no. 2, pp. 753-791, 2008.

[11] P. Magill, "100G coherent trials and deployments: AT&T plans and perspective," in *European Conference and Exhibition on Optical Communication (ECOC)*, Torino, Italy, 2010.

[12] M. Kuschnerov, F. Hauske, K. Piyawanno, B. Spinnler, M. Alfiad, A. Napoli and B. Lankl, "DSP for coherent single-carrier receivers," *IEEE/OSA Journal of Lightwave Technology,* vol. 27, no. 16, pp. 3614-3622, 2009.

[13] X. Liu, S. Chandrasekhar and P. Winzer, "Digital signal processing techniques enabling multi-Tb/s superchannel transmission: an overview of recent advances in DSP-enabled superchannels," *IEEE Signal Processing Magazine,* vol. 31, no. 2, pp. 16-24, 2014.

[14] G. Bosco, V. Curri, A. Carena, P. Poggiolini and F. Forghieri, "On the performance of Nyquist-WDM terabit superchannels based on PM-BPSK, PM-QPSK, PM-8QAM or PM-16QAM subcarriers," *IEEE/OSA Journal of Lightwave Technology,* vol. 29, no. 1, pp. 53-61, 2011.

[15] M. Joindot and S. Gosselin, "Optical fiber transport systems and networks: fundamentals and prospects," *Comptes Rendus Physique,* vol. 9, no. 9-10, pp. 914-934, 2008.

[16] ITU-T Recommendation, "G.694.1 Spectral grids for WDM applications: DWDM frequency grid," June 2002. [Online]. Available: https://www.itu.int/rec/T-REC-G.694.1-200206-S/en.

[17] ITU-T Manual, Optical fibres, cables and systems, 2009.

[18] G. Bosco, A. Carena, V. Curri, P. Poggiolini and F. Forghieri, "Performance limits of Nyquist-WDM and CO-OFDM in high-speed PM-QPSK systems," *IEEE Photonics Technology Letters,* vol. 22, no. 15, pp. 1129-1131, 2010.

[19] J. Pan, C. Liu, T. Detwiler, A. Stark, Y. Hsueh and S. Ralph, "Inter-channel crosstalk cancellation for Nyquist-WDM superchannel applications," *IEEE/OSA Journal of Lightwave Technology,* vol. 30, no. 24, pp. 3993-3999, 2012.

[20] F. Zhang, D. Wang, R. Ding, T. Zhang, Z. Zheng and Z. Chen, "High spectral efficiency Nyquist optical superchannel transmission," in *23rd Wireless and Optical Communication Conference (WOCC)*, Newark, NJ, USA, 2014.

[21] ITU-T Recommendation, "G.694.1 Spectral grids for WDM applications: DWDM frequency grid," 2012. [Online]. Available: https://www.itu.int/rec/T-REC-G.694.1/en.

[22] Cisco, "Cisco visual networking index: forecast and methodology, 2017-2022," July 2019. [Online]. Available: https://www.cisco.com/c/en/us/solutions/collateral/serviceprovider/visual-networking-index-vni/white-paper-c11-741490.html.

[23] R. W. Tkach, "Scaling optical communications for the next decade and beyond," *Bell Labs Technical Journal,* vol. 14, no. 4, pp. 3-9, 2010.

[24] S. Korotky, "Traffic trends: Drivers and measures of cost-effective and energy-efficient technologies and architectures for backbone optical networks," in *Optical Fiber Communications Conference (OFC)*, Los Angeles, CA, 2012.

[25] J. Pedro, "Predeployment of regenerators for fast service provisioning in DWDM transport networks," *IEEE/OSA Journal of Optical Communications and Networking ,* vol. 8, no. 7, pp. A190-A199, 2015.

[26] B. Clouet, J. Pedro, N. Costa, M. Kuschnerov, A. Schex, J. Slovak, D. Rafique and A. Napoli, "Networking aspects for next-generation elastic optical interfaces," *IEEE/OSA Journal of Optical Communications and Networking,* vol. 8, no. 7, pp. A116-A125, 2016.

[27] A. Eira, J. Pedro and J. Pires, "Cost-optimized dimensioning of translucent WDM networks with mixed-line-rate spectrum-flexible channels," in *IEEE High Performance Switching and Routing (HPSR)*, Belgrade, Serbia, 2012.

[28] G. Agrawal, Fiber-optic communication systems, New York: John Wiley & Sons, 2002.

[29] J. Pedro and S. Pato, "Capacity increase and hardware savings in DWDM networks exploiting next-generation optical line interfaces," in *International Conference on Transparent Optical Networks (ICTON)*, Bucharest, Romania, 2018.

[30] T. Rahman, B. Spinnler, E. Pincemin, C. Le Bouetté, J. Jauffrit, S. Calabro, E. de Man, S. Bordais, U. Feiste, J. Slovak, A. Napoli, G. Khanna, N. Hanik, C. Andre, C. Okonkwo, M. Kuschnerov, A. Koonen, C. Dourthe, B. Raguénès , B. Sommerkorn-Krombholz, M. Bohn and H. de Waard, "Record field demostration of C-band multi-terabit 16QAM, 32 QAM, 64QAM over 762 km of SSMF," in *Opto-Electronics and Communications Conference (OECC)*, Shanghai, 2015.

[31] O. Vassilieva, I. Kim, T. Oyama, S. Oda, H. Nakashima, T. Hoshida and T. Ikeuchi, "Reach extension with 32- and 64 Gbaud single carrier vs. multi-carrier signals," in *Optical Fiber Communications Conference (OFC)*, Los Angeles, California, 2017.

[32] A. Napoli, M. Mezghanni, D. Rafique, V. Sleiffer, T. Rahman, B. Spinnler, S. Calabrò and M. Bohn, "Novel DAC digital pre-emphasis algorithm for next-generation flexible optical

transponders," in *Optical Fiber Communications Conference (OFC)*, Los Angeles, California, 2015.

[33] X. Wang, Q. Zhang, I. Kim, P. Palacharla and M. Sekiya, "Blocking performance in dynamic flexible grid optical networks- What is the ideal spectrum granularity?," in *European Conference and Exhibition on Optical Communication (ECOC)*, Geneva, Switzerland, 2011.

[34] E. Tsardinakis, A. Lord, P. Wright, G. Liu and P. Bayvel, "Should like demands be grouped in mixed line rate networks?," in *Optical Fiber Communication Conference (OFC)*, Anaheim, California, 2013.

[35] D. Moniz, A. Eira, A. de Sousa and J. Pires, "On the comparative efficiency of non-disruptive defragmentation techniques in flexible-grid optical networks," *Optical Switching and Networking,* vol. 25, pp. 149-159, 2017.

[36] C. Shannon, "A mathematical theory of communication," *Bell System Technical Journal,* vol. 27, pp. 379-423, 623-656, 1948.

[37] P. P. Mitra and J. Stark, "Nonlinear limits to the information capacity of optical fibre communications," *Nature,* vol. 411, pp. 1027-1030, 2001.

[38] R. Essiambre, G. Kramer, P. Winzer, G. Foschini and B. Goebel, "Capacity limits of optical fiber networks," *IEEE/OSA Journal of Lightwave and Technology,* vol. 28, no. 4, pp. 662-701, 2010.

[39] J. Pedro and N. Costa, "Optical Network Design Towards Beyond 100 Gbaud," in *Optical Fiber Communications Conference and Exhibition (OFC)*, San Diego, CA, 2019.

[40] A. Napoli, N. Calabretta, J. K. Fischer, N. Costa, S. Abrate, J. Pedro, V. Lopez, V. Curri, D. Zibar, E. Pincemin, S. Grot, G. Roelkens, C. Matrakidis and W. Forysiak, "Perspectives of Multi-band Optical Communication Systems," in *23rd Opto-Electronics and Communications Conference (OECC)*, Jeju Island, 2018.

[41] L. Chuang, L. Dardis, P. Abolghasem, A. Diba, M. Lu, T. Frost, B. Ellis, X. Xu, M. Montazeri, S. Murthy, A. Dentai, F. Sedgwick, M. Kuntz, J. Zhang, D. Pavinski, T. Butrie, S. DeMars, J. Rahn, V. Dominic, S. Corzine, V. Lal, P. Evans, M. Ziari and F. Kish, "Demonstration of Fully Integrated 6labdaX200Gbps (1.2 Tbps) PICs and Transceivers in L-band," in *European Conference on Optical Communication (ECOC)*, Rome, 2018.

[42] P. Winzer, "Scaling Optical Networks with SDM Technologies," in *24th OptoElectronics and Communications Conference (OECC)*, Fukuoka, 2019.

[43] J. Pesic, T. Zami, P. Ramantanis and S. Bigo, "Faster return of investment in WDM networks when elastic transponders dynamically fit ageing of link margins," in *Optical Fiber Communication Conference (OFC)*, Anaheim, California, 2016.

[44] Y. Pointurier, "Design of low-margin optical networks," *IEEE/OSA Journal of Optical Communications amd Networking ,* vol. 9, no. 1, pp. A9-A17, 2017.

[45] P. Soumplis, K. Christodoulopoulos and M. Quagliotti, "Network planning with actual margins," *IEEE/OSA Journal of Lightwave Technology,* vol. 35, no. 23, pp. 5105-5120, 2017.

[46] J. Slovak, M. Herrmann, W. Schairer, E. Torrengo, K. Pulverer, A. Napoli and U. Habel, "Aware optical networks: leaving the lab," *IEEE/OSA Journal of Optical Communications and Networking,* vol. 11, no. 2, pp. A134-A143, 2019.

[47] N. Sambo, P. Castoldi, A. D'Errico, E. Riccardi, A. Pagano, M. Moreolo, J. Fabrega, D. Rafique, A. Napoli, S. Frigerio, E. Hugues-Salas, G. Zervas, M. Nolle, J. Fischer, A. Lord and J. Gimenez, "Next generation sliceable bandwidth variable transponders," *IEEE Communications Magazine,* vol. 53, no. 2, pp. 163-171, 2015.

[48] V. Eramo, M. Listanti, R. Sabella and F. Testa, "Integrated OTN/WDM switching architecture equipped with the minimum number of OTN switches," *IEEE/OSA Journal of Optical Communications and Networking,* vol. 6, no. 2, pp. 138-151, 2014.

[49] B. Gangopadhyay, J. Pedro and S. Spalter, "Cost-effective next-generation information highways leveraging universal OTN switching and flexible-rate," in *Optical Fiber Communications Conference (OFC)*, Los Angeles, California, 2017.

[50] W. Fawaz, B. Daheb, O. Audouin, M. Du-Pond and G. Pujolle, "Service Level Agreement and Provisioning in Optical Networks," *IEEE Communications Maganize,* vol. 42, no. 1, pp. 36-43, 2004.

[51] H. Mouftah and J. Zheng, "Optical WDM networks: Concepts and Design Principles," *Wiley-IEEE Press,* pp. 59-68, 2004.

[52] B. Mukherjee, D. Banerjee and S. Ramamurthy, "Some principles for designing a wide-area WDM optical network," *IEEE/ACM Transactions on Networking,* vol. 4, no. 5, pp. 684-696, 1996.

[53] A. Eira, J. Pedro and J. Pires, "Optimal multi-period provisioning of fixed and flex-rate modular line interfaces," *IEEE/OSA Journal of Optical Communications and Networking,* vol. 7, no. 4, pp. 223-234, 2015.

[54] J. Pires, "Redes de Telecomunicações," Instituto Superior Técnico, [Online]. Available: https://fenix.tecnico.ulisboa.pt/downloadFile/3779573650253/RT_Mersc_1.pdf .

[55] J. Santos, J. Pedro, P. Monteiro and J. Pires, "Optimized routing and buffer design for optical transport networks based on virtual concatenation," *IEEE/OSA Journal of Optical Communications and Networking,* vol. 3, no. 9, pp. 725-738, 2011.

[56] J. Justesen, K. J. Larsen and L. Pedersen, "Error correcting coding for OTN," *IEEE Communications Magazine,* vol. 48, no. 9, pp. 70-75, 2010.

[57] J. Cameron, L. Chen and X. Bao, "Impact of chromatic dispersion on the system limitation due to polarization mode dispersion," *IEEE Photonics Technology Letters,* vol. 12, no. 1, pp. 47-49, 2000.

[58] B. Fu and R. Hui, "Fiber chromatic dispersion and polarization-mode dispersion monitoring using coherent detection," *IEEE Photonics Technology Letters,* vol. 17, no. 7, pp. 1561-1563, 2005.

[59] G. Katz, D. Sadot and J. Tabrikian, "Electrical dispersion compensation equalizers in optical direct- and coherent- detection systems," *IEEE Transactions on Communications,* vol. 54, no. 11, pp. 2045-2050, 2006.

[60] N. Kikuchi, K. Sekine, S. Sasaki and T. Sugawara, "Study on cross-phase modulation (XPM) effect on amplitude and differentially phase-modulated multilevel signals in DWDM transmission," *IEEE Photonics Technology Letters,* vol. 17, no. 7, pp. 1549-1551, 2005.

[61] B. Batagelj, M. Vidmar and S. Tomazic, "Use of four-wave mixing in optical fibers for applications in transparent optical networks," in *6th International Conference on Transparent Optical Networks*, Wroclaw, Poland, 2004.

[62] A. Souza, N. Costa, J. Pedro and J. Pires, "Benefits of counterpropagating Raman amplification for multiband optical networks," *IEEE/OSA Journal of Optical Communications and Networking (JOCN),* vol. 14, no. 7, pp. 562-571, 2022.

[63] J. Simmons, Optical Network Design and Planning, Springer, 2014.

[64] P. Johannisson and M. Karlsson, "Characterization of a self-phase modulation based all-optical regeneration system," *IEEE Photonics Technology Letters,* vol. 17, no. 12, pp. 2667-2669, 2005.

[65] E. P. Silva, "Linear and Nonlinear impairment compensation in coherent optical transmission with digital signal processing," PhD Thesis, Porto, 2017.

[66] K. Kikuchi, "Fundamentals of Coherent Optical Fiber Communications," *IEEE/OSA Journal of Lightwave and Technology,* vol. 34, no. 1, pp. 157-179, 2016.

[67] Infinera, "The role of higher baud rates in evolving coherent transport," [Online]. Available: https://cdn.extranet.coriant.com/resources/White-Papers/WP_Role_of_Higher_Baud_Rates_74C0176.pdf?mtime=20180307013252.

[68] J. Pires, "Single-Channel Systems," [Online]. Available: Optical Fibre Telecommunication Systems Slides.

[69] J. Pedro, "Designing transparent flexible-grid optical networks for maximum spectral efficiency," *IEEE/OSA Journal of Optical Communication and Networking,* vol. 9, no. 4, pp. C35-C44, 2017.

[70] R. Going, M. Lauermann, R. Maher, H. Tsai, M. Lu, N. Kim, S. Corzine, P. Studenkov, J. Summers, A. Hosseini, J. Zhang, B. Behnia, J. Tang, S. Buggaveeti, T. Vallaitis, J. Osenbach, M. Kuntz, X. Xu, K. Croussore, V. Lal, P. Evans, J. Rahn, T. Butrie, A. Karanicolas, K.-T. Wu, M. Mitchell, M. Ziari, D. Welch and F. Kish, "Multi-channel In-P-based coherent PICs with hybrid integrated SiGe electronics operating up to 100 Gbd," in *European Conference on Optical Communication (ECOC)*, Gothenburg, Sweden, 2017.

[71] Infinera, "Infinera breaks industry record with 800G transmission over 950 kilimeters in a live network trial," 2020. [Online]. Available: https://www.infinera.com/press-release/Infinera-Breaks-Industry-Record-with-800G-Transmission-over-950-Kilometers-in-a-Live-Network-Trial.

[72] I. Sartzetakis, K. Christodoulopoulos, C. Tsekrekos, D. Syvridis and E. Varvarigos, "Quality of transmission estimation in WDM and elastic optical networks accounting for space-spectrum dependencies," *IEEE/OSA Journal of Optical Communication Networking,* vol. 8, no. 9, pp. 676-688, 2016.

[73] O. Sinkin, R. Holzlohner, J. Zweck and C. Menyuk, "Optimization of the split-step fourier method in modeling optical-fiber communications systems," *IEEE/OSA Journal of Lightwave Technology,* vol. 21, no. 1, pp. 61-68, 2003.

[74] P. Poggiolini, "The GN model of non-linear propagation in uncompensated coherent optical systems," *IEEE/OSA Journal of Lightwave Technology,* vol. 30, no. 24, pp. 3857-3879, 2012.

[75] P. Poggiolini, G. Bosco, A. Carena, V. Curri, Y. Jiang and F. Forghieri, "A detailed analytical derivation of the GN model of non-linear interference in coherent optical transmission systems," Technical Report, 2012.

[76] P. Poggiolini, G. Bosco, A. Carena, V. Curri, Y. Jiang and F. Forghieri, "The GN-model of fiber non-linear propogation and its applications," *IEEE/OSA Journal of Lightwave Technology,* vol. 32, no. 4, pp. 694-721, 2014.

[77] R. Morais, C. Pavan, A. Pinto and C. Requeijo, "Genetic algorithm fot the topological design of survivable optical transport networks," *IEEE/OSA Journal of Optical Communications and Networking,* vol. 3, no. 1, pp. 17-26, 2011.

[78] M. Garnot and P. Perrier, "Planning of WDM networks: methods, routing node modelling and applications," in *IEEE Global Telecomunications Conference*, Sydney, 1998.

[79] A. Eira, J. Pedro and J. Pires, "Optimized design of multistage passive optical networks," *IEEE/OSA Journal of Optical Communication and Networking,* vol. 4, no. 5, pp. 402-411, 2012.

[80] J. Santos, "Evaluating the potential for spectrally-efficient super-channel formats in brownfield networks with legacy services," in *Optical Fiber Communication Conference (OFC)*, Los Angeles, CA, USA, 2014.

[81] R. Morais, J. Pedro and A. Pinto, "Planning and dimensioning of multilayer optical transport networks," in *International Conference on Transparent Optical Networks (ICTON)*, Budapest, Hungary, 2015.

[82] J. Q. Hu and B. Leida, "Traffic grooming, routing and wavelength assignment in optical WDM mesh networks," in *Twenty-thrid Annual Joint Conference on IEEE Computer and Communications Societies (INFOCOM)*, Hong Kong, China, 2004.

[83] S. Straub, A. Kirstadter and D. Schupke, "Multi-period planning of WDM-networks: comparison of incremental and EoL approaches," in *2nd IEEE/IFIP International Conference in Center Asia on Internet*, Tashkent, Uzbekistan, 2006.

[84] J. Yen, "Finding the k shortest loopless paths in a network," *Management Science,* vol. 17, no. 11, pp. 712-716, 1971.

[85] R. Dutta, A. Kamal and G. Rouskas, Traffic grooming for optical networks, Springer, 2008.

[86] R. Ramaswami and K. Sivarajan, "Routing and wavelength assignment in all-optical networks," *IEEE/ACM Transactions on Networking,* vol. 3, no. 5, pp. 489-500, 1995.

[87] J. Zheng and H. Mouftah, Optical WDM networks: concepts and design principles, Wiley, 2004.

[88] K. Walkowiak and M. Klinkowski, "Routing and spectrum assignment in spectrum sliced elastic optical path network," *IEEE Communication Letters,* vol. 15, pp. 884-886, 2011.

[89] R. Ahuja, T. Magnanti and J. Orlin, Network flows: theory, algorithms, and applications, Prentice Hall, 1993.

[90] K. Christodoulopoulos, K. Manousakis and E. Varvarigos, "Comparison of routing and wavelength assignment algorithms in WDM networks," in *IEEE Global Telecommunications Conference (GLOBECOM)*, New Orleans, LA, USA, 2008.

[91] D. Kirovski and M. Potkonjak, "Efficient coloring of a large spectrum of graphs," in *35th Design and Automation Conference (DAC)*, San Francisco, CA, USA, 1998.

[92] J. Santos and J. Pedro, "Support of superchannel formats in optical networks with legacy services and traffic churn," *IEEE/OSA Journal of Optical Communications and Networking,* vol. 7, no. 12, pp. B122-B130, 2015.

[93] D. Moniz, A. Eira and J. Pires, "On the effect of spectrum assignment policies in the efficiency of non-disruptive defragmentation techniques," in *European Conference on Network and Optical Communications (NOC)*, Lisbon, Portugal, 2016.

[94] B. Mukherjee, Y. Huang and J. Heritage, "Impairment-aware routing in wavelength-routed optical networks," in *The 17th Annual Meeting of the IEEE Lasers and Electro-Optics Society*, Rio Grande, Puerto Rico, 2004.

[95] R. Pandya, V. Chandra and D. Chadha, "Impairment aware routing and wavelength assignment algorithms for optical WDM networks and experimental validation of impairment aware automatic light-path switching," *Optical Switching and Networking,* vol. 11, no. A, pp. 16-28, 2014.

[96] M. Xia, M. Tornatore, C. Martel and B. Mukherjee, "Risk-aware provisioning for optical WDM mesh networks," *IEEE/ACM Transactions on Networking,* vol. 19, no. 3, pp. 921-931, 2011.

[97] S. Ramamurthy, L. Sahasrabuddhe and B. Mukherjee, "Survivable WDM mesh networks," *IEEE/OSA Journal of Ligthtwave Technology,* vol. 21, no. 4, pp. 870-883, 2003.

[98] M. To and P. Neusy, "Unavailability analysis of long-haul networks," *IEEE Journal on Selected Areas in Communications,* vol. 12, no. 1, 1994.

[99] J. Pedro and B. Gangopadhyay, "On the trade-offs between ODU and OCh preplanned shared restoration in transport networks," in *16th International Telecommunications Network Strategy and Planning Symposium* , Funchal, Portugal, 2014.

[100] C. Rocha and B. Jaumard, "A unified framework for shared protection schemes in optical mesh network," *Pesquisa Operacional,* vol. 29, no. 3, 2009.

[101] ITU-T Recommendation, "G.808.3 Generic protection switching- shared mesh protection," 2012. [Online]. Available: https://www.itu.int/rec/T-REC-G.808.3-201210-I/en.

[102] J. Vasseur, M. Pickavet and P. Demeester, Network recovery: Protection and restoration of optical, SONET-SDH, IP, and MPLS, Elsevier, 2004.

[103] A. Eira, "Optimized Design of Flexible Grid DWDM Networks," PhD Thesis, Lisbon, 2018.

[104] J. L. Wagener and T. Strasser, "Wavelength-Selective Switches for ROADM Applications," *IEEE Journal of Selected Topics in Quantum Electronics,* vol. 16, no. 5, pp. 1150-1157, 2010.

[105] G. Notarnicola, G. Rizzelli, G. Maier and A. Pattavina, "Scalability analysis of WSS-based ROADMs," in *17th European Conference on Networks and Optical Communications*, Vilanova i la Geltru, Spain, 2012.

[106] M. Filer and S. Tibuleac, "N-degree ROADM architecture comparision: Broadcast-and-select versus route-and-select in 120 Gb/s DP-QPSK transmission systems," in *Optical Fiber Communication (OFC) Conference*, San Francisco, CA, USA, 2014.

[107] R. Morais, J. Pedro and A. Pinto, "Impact of node architecture in the power consumption and footprint requirements of optical transport network," *IEEE/OSA Journal of Optical Communications and Networking,* vol. 5, no. 5, pp. 421-436, 2013.

[108] R. Morais, J. Pedro, P. Monteiro and A. Pinto, "Benefits of node architecture flexibility and hitless re-grooming in transport networks," *IEEE/OSA Journal of Lightwave Technology,* vol. 33, no. 21, pp. 4424-4436, 2015.

[109] Infinera, "The role of OTN switching in 100G & beyond transport networks," 2016. [Online]. Available: https://www.ofcconference.org/getattachment/90c0e6a4-08c1-45fb-a7f2-2957d444dc7d/The-Role-of-OTN-Switching-in-100G-Beyond-Transpo.aspx.

[110] B. Gangopadhyay, J. Pedro and S. Spaelter, "Next-generation transport networks leveraging universal traffic switching and flexible optical transponders," in *Optical Fiber and Wireless Communications*, 2017, pp. 211-232.

[111] Microsemi, "Making 100G OTN Economical: OTN switching & Packet-Optical Transport," White Paper, [Online]. Available: https://docplayer.net/47565304-White-paper-making-100g-otn-economical-otn-switching-packet-optical-transport.html.

[112] V. Lopez, L. Contreras, O. Gonzalez de Dios and J. Fernandez-Palacios, "Towards a transport SDN for carriers networks: an evolutionary perspective," in *European Conference on Optical Communications (NOC)*, Lisbon, 2016.

[113] R. Borkowski, R. Duran, C. Kachris, D. Siracusa, A. Caballero, N. Fernandez, D. Klonidis, A. Francescon, T. Jimenez, J. Aguado, I. Miguel, E. Salvadori, I. Tomkos, R. Lorenzo and I. Monroy, "Cognitive optical network testbed: EU project CHRON," *IEEE/OSA Journal of Optical Communications and Networking,* vol. 7, no. 2, pp. A344-A355, 2015.

[114] K. Christodoulopoulos, C. Delezoide, N. Sambo, A. Kretsis, I. Sartzetakis, A. Sgambelluri, N. Argyris, G. Kanakis, P. Giardina, G. Bernini, D. Roccato, A. Percelsi, R. Morro, H. Avramopoulos, P. Castoldi, P. Layec and S. Bigo, "Toward efficient, reliable, and autonomous optical networks: the ORCHESTRA solution," *IEEE/OSA Journal of Optical Communications and Networking,* vol. 11, no. 9, pp. C10-C24, 2019.

[115] R. M. Morais and J. Pedro, "Machine learning models for estimating quality of transmission in DWDM networks," *IEEE/OSA Journal of Optical Communications and Networking,* vol. 10, no. 10, pp. D84-D99, 2018.

[116] J. Pedro, N. Costa and S. Pato, "Optical transport network design beyond 100 Gbaud," *IEEE/OSA Journal of Optical Communications and Networking,* vol. 12, pp. A123-A134, 2020.

[117] P. J. Winzer, "Optical networking beyond WDM," *IEEE Photonics Journal,* vol. 4, no. 2, pp. 647-651, 2012.

[118] L. Yan, X. Liu and W. Shieh, "Toward the shannon limit of spectral efficiency," *IEEE Photonics Journal,* vol. 3, no. 2, pp. 325-330, 2011.

[119] B. Shariati, J. Rivas-Moscoso, D. Klonidis, I. Tomkos, S. Ben-Ezra, F. Jiménez, D. M. Marom, P. S. Khodashenas, J. Comellas and L. Velasco, "Options for cost-effective capacity upgrades in backbone optical networks," in *21st European Conference on Networks and Optical Communications (NOC)*, Lisbon, 2016.

[120] T. Matsui, Y. Sagae, T. Sakamoto and K. Nakajima, "Design and applicability of multi-core fibers with standard cladding diameter," *IEEE/OSA Journal of Lighwave Technology,* vol. 38, no. 21, pp. 6065-6070, 2020.

[121] D. J. DiGiovanni, "Optical fibers: Challenges and opportunities in SDM," in *Conference on Lasers and Electro-Optics (CLEO)*, San Jose, CA, USA, 2020.

[122] M. Klinkowski, P. Lechowicz and K. Walkowiak, "A study on the impact of inter-core crosstalk on SDM network performance," in *International Conference on Computing, Networking and Communications (ICNC)*, Maui, Hawaii, USA, 2018.

[123] ITU-T Recommendation, "G.652 : Characteristics of a single-mode optical fibre and cable," 2016. [Online]. Available: https://www.itu.int/rec/T-REC-G.652-201611-I/en.

[124] A. Ferrari, A. Napoli, J. K. Fischer, N. Costa, A. D'Amico, J. Pedro, W. Forysiak, E. Pincemin, A. Lord, A. Stavdas, J. Gimenez, G. Roelkens, N. Calabretta, S. Abrate, B. Sommerkorn-Krombholz and V. Curri, "Assessment on the achievable throughput of multi-band ITU-T G.652.D fiber transmission systems," *IEEE/OSA Journal of Lightwave Technology,* vol. 38, no. 16, pp. 4279-4291, 2020.

[125] A. Napoli, N. Costa, J. Fischer, J. Pedro, S. Abrate, N. Calabretta, W. Forysiak, E. Pincemin, J. Gimenez, C. Matrakidis, G. Roelkens and V. Curri, "Towards multiband optical systems," in *Photonic Networks and Devices*, Zurich, Switzerland, 2018.

[126] A. Ferrari, A. Napoli, J. K. Fischer, N. Costa, J. Pedro, N. Sambo, E. Pincemin, B. Sommerkohrn-Krombholz and V. Curri, "Upgrade capacity scenarios enabled by multiband

optical systems," in *International Conference on Transparent Optical Networks (ICTON)*, Angers, France, 2019.

[127] S. Okamoto, K. Horikoshi, F. Hamaoka, K. Minoguchi and A. Hirano, "5-band (O, E, S, C and L) WDM transmission with wavelegth adaptive modulation format allocation," in *42nd European Conference and Exhibition on Optical Communications*, Dusseldorf, 2016.

[128] A. Ferrari, D. Pilori, E. Virgillito and V. Curri, "Power control strategies in C+L optical line systems," in *Optical Fiber Communications Conference (OFC)*, San Diego, USA , 2019.

[129] E. Virgillito, R. Sadeghi, A. Ferrari, G. Borraccini and V. Curri, "Network performance assessment of C+L upgrades vs. fiber doubling SDM solutions," in *Optical Fiber Communication Conference (OFC)*, San Diego, USA, 2020.

[130] N. Correia, R. Sadeghi, E. Virgillito, A. Napoli, N. Costa, J. Pedro and V. Curri, "Power control strategies and network performance assessment for C+L+S multiband optical transport," *IEEE/OSA Journal of Optical Communications and Networking,* vol. 13, no. 7, pp. 147-157, 2021.

[131] D. Moniz, J. Pedro, N. Horta and J. Pires, "Multi-objective framework for cost-effective OTN switch placement using NSGA-II with embedded domain knowledge," *Applied Soft Computing,* vol. 83, 2019.

[132] M. Emmerich and A. Deutz, "A tutorial on multiobjective optimization: fundamentals and evolutionary methods," *Natural Computing,* vol. 17, no. 3, pp. 585-609, 2018.

[133] C. Fonseca and P. Fleming, "An overview of evolutionary algorithms in multiobjective optimization," *Evolutionary Computation,* vol. 3, no. 1, pp. 1-16, 1995.

[134] K. Deb, Multi-objective optimization using evolutionary algorithms, New York: John Wiley and sons ltd., 2001.

[135] C. Coello, G. Lamont and D. Van Veldhuizen, Evolutionary algorithms for solving multi-objective problems, Springer, 2002.

[136] M. Bertolini, O. Rocher, A. Bisson, P. Pecci and G. Bellotti, "Benefits of OTN switching introduction in 100Gb/s optical transport networks," in *Optical Fiber Communication Conference (OFC)* , Los Angeles, CA, USA, 2012.

[137] S. Roy, O. Turkcu, S. Hand and S. Melle, "Variation of OTN switching benefits in real-world networks based on network and traffic connectivity," in *Optical Fiber Communication Conference (OFC)*, San Francisco, CA, USA, 2014.

[138] A. Deore, O. Turkcu, S. Ahuja, S. Hand and S. Melle, "Total cost of ownership of WDM and switching architectures for next-generation 100Gb/s networks," *IEEE Communications Maganize,* vol. 50, no. 11, pp. 179-187, 2012.

[139] P. Leesutthipornchai, C. Charnsripninyo and N. Wattanapongsakom, "Multi-objective traffic grooming in WDM network using NSGA-II," in *6th International Conference on Networked Computing (INC)*, Gyeongju, South Korea, 2010.

[140] P. Leesutthipornchai, C. Charnsripninyo and N. Wattanapongsakom, "Multi-objective traffic grooming for survivable network design," in *IEEE International Conference on Quality and Reliability* , Bangkok, Thailand, 2011.

[141] P. Prathombutr, J. Stach and E. Park, "An algorithm for traffic grooming in WDM optical mesh networks with multiple objectives," in *12th International Conference on Computer Communications and Networks (ICCCN)*, Dallas, USA, 2003.

[142] A. Eira, J. Santos, J. Pedro and J. Pires, "Multi-objective design of survivable flexible-grid DWDM networks," *IEEE/OSA Journal of Optical Communications and Networking,* vol. 6, no. 3, pp. 326-339, 2014.

[143] K. Deb, A. Pratap, S. Agarwal and T. Meyarivan, "A fast and elitism multiobjective genetic algorithm: NSGA-II," *IEEE Transactions on Evolutionary Computation,* vol. 6, no. 2, pp. 182-197, 2002.

[144] E. Zitzler and L. Thiele, "Multiobjective evolutionary algorithms: A comparative case study and the strength Pareto approach," *IEEE Transactions on Evolutionary Computation,* vol. 3, no. 4, pp. 257-271, 1999.

[145] J. Knowles and D. Corne, "The Pareto archived evolution strategy: a new baseline algorithm for multiobjective optimisation," in *Congress on Evolutionary Computation*, Washington D.C., USA, 1999.

[146] T. Back, Evolutionary algorithms in theory and practice: Evolution strategies, evolutionary programming, genetic algorithms, New York: Oxford University Press, Inc, 1996.

[147] CPLEX Optimizer. [Online]. Available: https://www.ibm.com/analytics/cplex-optimizer.

[148] D. Whitley, R. Heckendorn and S. Rana, "The island model genetic algorithm: On separability, population size and convergence," *Journal of Computing and Information Technology,* vol. 7, no. 1, pp. 33-47, 1998.

[149] D. Moniz, J. Pedro and J. Pires, "Network design framework to spectral- and cost-efficiently exploit next-generation line interfaces," in *Optical Fiber Communications Conference and Exposition (OFC)*, San Diego, California, 2018.

[150] D. Moniz, J. Pedro and J. Pires, "Spectral-efficient provisioning of protected services over DWDM networks exploiting high-symbol rate line interfaces," in *European Conference on Optical Communication (ECOC)*, Rome, 2018.

[151] D. Moniz, J. Pedro and J. Pires, "Network design framework to optimally provision services using higher-symbol line interfaces," *IEEE/OSA Journal of Optical Communications and Networking ,* vol. 11, no. 2, pp. A174-A185, 2019.

[152] T. Zami, B. Lavigne and M. Bertolini, "How 64 GBaud optical carriers maximize the capacity in core elastic WDM networks with fewer transponders per Gb/s," *IEEE/OSA Journal of Optical Communications and Networking,* vol. 11, no. 1, pp. A20-A32, 2019.

[153] T. Zami, A. Morea, G. Bellotti and B. Lavigne, "Is Mixing 50 GHz-Spaced 32 Gbaud Channels and 75 GHz-Spaced 64 Gbaud Ones Useful in a WDM Elastic Network?," in *European Conference on Optical Communication (ECOC)*, Rome, Italy, 2018.

[154] S. Gringeri, B. Basch, V. Shukla, R. Ergorov and T. Xia, "Flexible architectures for optical transport nodes and networks," *IEEE Communication Magazine ,* vol. 48, no. 7, pp. 40-50, 2010.

[155] FP7 IDEALIST Project Deliverable, "D1.1 Elastic optical network architecture: reference scenario, cost and planning," [Online]. Available: https://cordis.europa.eu/project/id/317999/reporting.

[156] P. Winzer, D. Neilson and A. Chraplyvy, "Fiber-optic transmission and networking: the previous 20 and the next 20 years," *Optics Express,* vol. 26, no. 18, pp. 24190-24239, 2018.

[157] K. Kim, K. Doo, H. Lee, S. Kim, H. Park, J. Oh and H. Chung, "High speed and low latency passive optical network for 5G wireless systems," *IEEE/OSA Journal of Lightwave Technology,* vol. 37, pp. 2873-2882, 2019.

[158] V. Lopez, B. Zhu, D. Moniz, N. Costa, J. Pedro, X. Xu, A. Kumpera, L. Dardis, J. Rahn and S. Sanders, "Optimized Design and Challenges for C&L Band Optical Line Systems," *IEEE/OSA Journal of Lightwave Technology,* vol. 38, no. 5, pp. 1080-1091, 2020.

[159] D. Moniz, V. Lopez and J. Pedro, "Design strategies exploiting C+L-band in networks with geographically-dependent fiber upgrade expenditures," in *Optical Fiber Communications Conference and Exhibition (OFC)*, San Diego, CA, USA, 2020.

[160] P. Winzer and D. Neilson, "From scaling disparities to integrated parallelism: A decathlon for a decade," *IEEE/OSA Journal of Lightwave and Technology,* vol. 35, no. 5, pp. 1099-1115, 2017.

[161] C. Doerr, L. Chen, T. Nielsen, R. Aroca, L. Chen, M. Banaee, S. Azemati, G. McBrien, S. Park, J. Geyer, B. Guan, B. Mikkelsen, C. Rasmussen, M. Givehchi, Z. Wang, B. Potsaid, H. Lee, E. Swanson and J. Fujimoto, "O, E, S, C and L band silicon photonics coherent modulator/receiver," in *Optical Fiber Communications Conference (OFC)*, Anaheim, CA, USA, 2016.

[162] M. C. Parker, P. Wright and A. Lord, "Multiple fiber, flexgrid elastic optical network design using maxnet optimization," *IEEE/OSA Journal of Optical Communications and Networking,* vol. 7, no. 12, pp. B194-B201, 2015.

[163] K. Nakajima, P. Sillard, D. Richardson, M. J. Li, R. J. Essiambre and S. Matsuo, "Transmission media for an SDM-based optical communication systems," *IEEE Communications Magazine ,* vol. 53, no. 2, pp. 44-51, 2015.

[164] T. Jimenez, V. López, F. Jimenez, O. Gonzalez and J. Fernandez, "Techno-economic analysis of transmission technologies in low aggregation rings of metropolitan networks," in *Optical Fiber Conference (OFC)*, Los Angeles, CA USA, 2017.

[165] Corning, "Duct Cables," [Online]. Available: https://www.corning.com/optical-communications/worldwide/en/home/products/fiber-optic-cable/outdoor-cables/duct-cable.html.

[166] Reuters, 2021. [Online]. Available: https://www.reuters.com/article/uk-bt-group-outlook-idUSKBN2A40TX.

[167] Istituto Nazionale di Statistica, "Map of population density in Italy (2011 census)," [Online]. Available: https://www.istat.it/.

[168] D. Moniz, J. Pedro and J. Pires, "Service provisioning framework with dynamic margin management for optical transport networks," in *Optical Fiber Communications Conference and Exhibition*, San Diego, California, 2019.

[169] J. Pedro, D. Moniz and J. Pires, "Multi-layer optimization framework for optical transport networks with dynamic margin management," in *21st International Conference on Transparent Optical Networks*, Angers, 2019.

[170] D. Moniz, J. Pedro and J. Pires , "Multi-layer network optimization efficiently exploiting real-time performance monitoring," in *IEEE Global Communications Conference*, Waikoloa, Hawaii, 2019.

[171] D. Moniz, J. Pedro and J. Pires, "Dynamic multi-layer service provisioning framework operating with reduced performance margins," *IEEE/OSA Journal of Optical Communications and Networking,* vol. 11, no. 9, pp. C35-C47, 2019.

[172] D. Moniz, J. Pedro and J. Pires, "Network design framework exploiting low-margin provisioning of optical shared restoration resources," in *Optical Fiber Communications Conference and Exhibition (OFC)*, San Diego, CA, USA, 2020.

[173] D. Moniz, J. Pedro and J. Pires, "Design and operation strategies for optical transport networks with reduced margins service-provisioning," in *Optical Fiber Communications Conference and Exhibition (OFC)*, San Diego CA, USA, 2020.

[174] J. Pedro, D. Moniz and J. Pires, "Operational strategies for MCh provisioning with reduced margins," in *22nd International Conference on Transparent Optical Networks (ICTON)*, Bari, Italy, 2020.

[175] I. T. Monroy, D. Zibar, N. G. Gonzalez and R. Borkowski, "Cognitive heterogeneous reconfigurable optical networks (CHRON): Enabling technologies and techniques," in *International Conference on Transparent Optical Networks*, Stockholm, Sweden, 2011.

[176] P. Imai, P. Harvey and T. Amin, "Towards A Truly Autonomous Network," Rakuten Mobile Innovation Studio, 2020.

[177] Infinera, "The infinite network," 2019. [Online]. Available: https://www.infinera.com/the-infinite-network/Infinera_The_Infinite_Network_Brochure.pdf.

[178] HUAWEI, "Autonomous driving networks," 2020. [Online]. Available: https://e.huawei.com/en/material/MaterialDownload?materialid=a74e9d79a7e4404e8303a0d27bd9d1e7.

[179] Juniper, "Unleash experience-first networking with Juniper Paragon Automation," 2021. [Online]. Available: https://blogs.juniper.net/en-us/service-provider-transformation/unleash-experience-first-networking-with-juniper-paragon-automation.

[180] Ciena, "Manage, control and plan," 2020. [Online]. Available: https://media.ciena.com/documents/Manage_Control_and_Plan_DS.pdf.

[181] J. Pesic, N. Rossi and T. Zami, "Impact of margins evolution along ageing in elastic optical networks," *IEEE/OSA Journal of Lightwave and Technology,* vol. 37, no. 16, pp. 4081-4089, 2019.

[182] M. Sheikh and S. Asselin, "Capacity enhancement in optical networks using margin extraction," in *Optical Fiber Communication Conference (OFC)*, San Diego, CA, USA, 2018.

[183] B. Spinnler, A. X. Lindgren, U. Andersen, S. Melin, J. Slovak, W. Schairer, K. Pulverer, J. Martensson, E. De Man, G. Khanna, R. H. Derksen, J. Steinmayer, R. Jozapovics, J. Blume, T. Lemstrom, J. Christensen, U. Habel, U. Bauer, A. Napoli and B. Sommerkorn-Krombholz, "Autonomous intelligent transponder enabling adaptive network optimization in a live network field trial," *IEEE/OSA Journal of Optical Communications and Networking,* vol. 11, no. 9, pp. C1-C9, 2019.

[184] L. Binh, Optical Fiber Communications Systems, CRC Press, 2011.

[185] B. Gangopadhyay, J. Pedro and S. Pato, "Exploiting Real-Time Performance Awareness for Cost-Effective Restoration in Optical Transport Networks," in *21st International Conference on Transparent Optical Networks*, Angers, France, 2019.

[186] J. Pedro and S. Pato, "Impact of add/drop port utilization flexibility in DWDM networks," *IEEE/OSA Journal of Optical Communications and Networking,* vol. 4, no. 11, pp. B142-B150, 2012.

[187] C. Pulikkaseril, L. Stewart, M. Roelens, G. Baxter, S. Poole and S. Frisken, "Spectral modeling of channel band shapes in wavelength selective switches," *Optics Express,* vol. 19, no. 9, pp. 8458-8470, 2011.

[188] T. Rahman, A. Napoli, D. Rafique, B. Spinnler, M. Kuschnerov, I. Lobato, B. Clouet, M. Bohn, C. Okonkwo and H. Waardt, "On the mitigation of optical filtering penalties originating from ROADM cascade," *IEEE Photonics Technology Letters,* vol. 26, no. 2, pp. 154-157, 2014.